COMPARATIVE PHYSICOCHEMICAL CHANGES OF HUMAN AND BOVINE ENAMEL FOLLOWING A SHORT DURATION ACID EXPOSURE.

Paul Laurance-Young

A dissertation submitted to University College London in accordance with the requirements of the degree of Doctor of Philosophy in the Department of Biomaterials and Tissue Engineering, Faculty of Life Sciences.

JANUARY 2011

Department of Biomaterials & Tissue Engineering

University College London

256 Grays Inn Road

London WC1X 8LD

CONTENTS

AUTHOR'S DECLARATION

I, Paul Laurance-Young, confirm that the work presented in this thesis is my own. Where information has been derived from other sources, I confirm this has been indicated in the thesis. Work submitted for publication or presented at conferences is included at the rear of this work in the appendices.

Signed…… Date……..

Paul Laurance-Young

ABSTRACT

The principle aims of this work were two-fold: to investigate the effects of a short duration acid exposure on enamel and to evaluate the suitability of bovine material as a substitute for human enamel at these early stages. The former has largely been overlooked in the literature and has potential for clinical care and remineralisation strategies, while the latter has become an increasing issue manifesting as a lack of human research material neccessitating the substitution of an alternative species.

Two models of erosion commonly employed in the literature were evaluated against each other. Greater bulk tissue loss was observed in the model with a repeated exposure of acid to enamel compared to the alternative single immersion model. Quantitative optical profilometry (OP) assessment of bulk tissue loss in both human and bovine enamel using 1 $mol.L^{-1}$ acetic, citric and phosphoric acid solutions was not significant, a finding supported by alternative quantitative light fluorescence (QLF). This early data provided information regarding the expected shape of subsequent, more commercially applicable experimental data.

The next series of experiments mirrored those mentioned previously but using commercially applicable 0.05% solutions. OP assessed bulk tissue loss was significantly different from that of 1 $mol.L^{-1}$ solutions but direct comparison of the two species at 0.05% remained not significant.

Both 1M and 0.05% acid solution datasets revealed a biphasic trend during the early erosion challenge. The erosion rate between 10-60 seconds was significantly different from the later 60-600 seconds, irrespective of acid type or species. Further analysis of the erosion lesions using atomic force microscopy (force vs distance measurements) suggested lesion morphology was more varied than previously thought.

This led to an examination of lesion ultrastructure using micro-computed tomography and confocal microscopy. Potential subsurface softening was observed, together with areas of apparent acid resistance standing proud of the lesion base. The latter were probed using EDX, AFM and focussed-ion beam SEM, which confirmed the uneroded nature of these resistant areas. As far as we are aware, this is the first time such erosion trends and morphology have been reported.

ACKNOWLEDGEMENTS

So many people have helped me, both directly and indirectly, to produce this work over the last three years. My special thanks must first go to my academic supervisors Prof Jonathan C Knowles and Dr Laurent Bozec and my industrial supervisors (past and present) Drs Gareth D Rees, Frank Lippert, Louise Gracia and Richard JM Lynch, whose guidance, instruction and unflagging support were indispensible.

My colleagues at UCL and the Eastman Dental Institute, Drs Graham Palmer (a special thank you, especially for your help with the temperamental ion chromatography), George Georgiou, Nicky Mordan, Ensanya Abou-Neel, Anne Young, Peter Brett and Vehid Salih and my fellow PhD students Xin Zhao, Idris Mehdawi, Azadeh Kiani, Kirsty Main and Claire Raison for constructive advice and direction and, more importantly, good friendship. To Dr Isabelle Orriss for her help with the μCT and Dr Suguo Huo for his assistance in obtaining FIB SEM images.

Special thanks are reserved for my parents, who despite all the horrible events of the last year, still managed to remain interested every step of the way. Lastly, to my long suffering wife who kept the coffee coming and forcibly removed me from my office when necessary and who will no doubt be glad to have a return to normality.

CHAPTER 1

INTRODUCTION

1.1. HISTORICAL PERSPECTIVE

Interest in human dental health stretches back into antiquity. The Egyptian Djedmaatesankh mummy, dating from the 9th century BC, exhibits extensive oral disease and tooth substrate loss (Melcher *et al.*, 1997). The observed abrasive wear has been attributed to the coarsely ground flour used to make bread, the staple diet of ancient Egypt, which was often contaminated with rock flour and sand (Hoffman & Hudgens, 2001). The Egyptians were aware of the link between wear of dentition and flour milling but, despite their relatively advanced medical practices, did not routinely extract diseased teeth, including those as a result of excessive wear (Melcher *et al.*, 1997).

More recently a set of well used, 18th century porcelain dentures, belonging to Archbishop Dillon (of Narbonne, 1721-1806), was discovered during the exhumation of the burial grounds of St. Pancras Old Church in London (Powers, 2006). At that time, porcelain dentures were both rare and relatively expensive, as such people tended to favour ivory or human teeth set in precious metals. The progression of denture development illustrates how the population was becoming more aware of dental hygiene (Powers, 2006). A further illustration of this trend is epitomised by Pierre Fauchard, an 18th century surgeon-dentist, who made great advances in the teaching and understanding of dentistry. In 1728 he published his seminal work "*Le Chirurgien Dentiste ou Traité des Dents*' ('The Surgeon Dentist or Treatise on the Teeth'), a compilation of dental knowledge backed by many influential medical practitioners (Spielman, 2007). In this book he advocated many revolutionary techniques, among them: recorded observations, seating of the patient on a chair as opposed to laying them

on the floor and became the first to employ the term "dental caries" (Lynch *et al.*, 2006). The 19th century saw the establishment of the world's first dedicated dental college in Baltimore, USA and the subsequent spreading of dental schools around the globe with the aim of entrenching dentistry as a recognised medical profession. Amalgam was first employed in 1826 by Auguste Taveau in France but its use was contentious owing to the presence of comparatively high levels of mercury to lower the material boiling point. In 1903 Charles Land developed the porcelain crown. Dental anaesthesia was also implemented in the early 1900s but was restricted to inhalation of nitrous oxide, ether, ethyl chloride or chloroform and surgery remained difficult until the synthesis of intravenous anaesthetics such as hexobarbitone in 1931 (Gopakumar & Gopakumar, 2009). By the mid-20th century it was found that certain compounds, most notably fluoride in the form of sodium monofluoride, posses an ability to limit dental bulk tissue loss through remineralisation (Norén *et al*, 1983) but, despite experimental and clinical studies during the 1960s, the natural repair of incipient enamel damage did not become common knowledge among dental practitioners until the 1990s (ten Cate, 1999).

The progressive change from a high fibre diet, exemplified by the 18th century rise in refined sugar consumption and its observed association with caries, continues today but is now complicated further by emerging pathologies such as erosion, all of which bring new challenges to the dental profession.

1.2. THE ORAL ENVIRONMENT

The oral cavity is comprised of the teeth (accounting for approximately 20% of the surface area), gingiva, hard and soft palate and tongue. It is a partially anaerobic environment, inhabited by approximately 700 species of bacteria. Salivary glands are located in the upper maxilla and lower mandible.

Histologically, the cells of the oral mucosal environment can be classified into three groups, depending on their functionality: "masticatory", "lining" and "specialised". "Masticatory" mucosal cells are keratinised and cover the gingiva and hard palate. "Lining" cells are not keratinised and allow for distortion of the oral morphology, while maintaining a protective effect. "Specialised" cells are found on the tongue and enclose papillae and taste buds, while maintaining the essential muscular flexibility of the tongue (Nanci, 2003).

In healthy individuals, the enamel is the only part of the tooth exposed to the oral environment. The onset of advanced age usually leads to the exposure of root surfaces and cementum as a result of chronic periodontal disease (Boehm & Scannapieco, 2007). The exposed surfaces are coated with saliva (pH 5.7 – 6.2) consisting of proteins and glycoproteins (such as lysozyme, defensins, lactoferrins, immunoglobulins and mucin) and which serve in a microbial protective capacity (van Nieuw Amerongen *et al.*, 2004) and as an acid diffusion barrier in the form of an acquired pellicle.

The oral cavity is colonised from a very early age: while an infant lacks any teeth the bacterial emphasis is toward facultatively aerobic species such as streptococci and lactobacilli. The emergence of teeth in the oral cavity results in a pronounced shift

toward anaerobic species and those specially adapted for growth on the enamel surface. Teeth colonisation by bacteria is initially the result of a single cell layer of highly specific primary colonising species (i.e.: *Streptococcus sanguinis*, *S. sobrinus and S. mutans*) onto the thin proteinaceous film of acidic glycoproteins present on the enamel which is naturally deposited by saliva. The continued growth of these species forms a thick mat of bacteria which may be populated by secondary colonising species such as filamentous *Fusobacterium* spp and *Actinomyces* spp and spirochete *Borelia* spp (Madigan *et al*., 1997). Thus far more than 700 species or phyla of bacteria have been found in the healthy oral cavity with 34-72 different bacterial species, which are site and individual specific, found at each analysed site (Aas *et al*., 2005).

1.3. ODONTOGENESIS AND ANATOMY OF THE TOOTH

The development of the tooth, like all tissue development, is a highly organised process involving not only epithelial tissue secretions producing dentine and enamel but also tissue specific interactions. The process of enamel development and maturation, metabolically speaking, takes a very long time. Maturation alone, the final step in the process, may take between 950-1187 days to complete, two thirds of the total duration of tooth formation (Smith, 1998).

It is thought that it is the thickened embryonic dental lamina that initiates dental development. Epithelial ectodermal cells, lining the primitive oral cavity, grow down into the proliferating gingival mesenchyme and secrete lymphoid enhancer factor-1 (LEF-1), which in turn stimulates the production of bone morphogenetic protein (BMP-4), fibroblast growth factor-8 (FGF-8) and sonic hedgehog (SHH) protein (Carlson, 1994; Miletich & Sharpe, 2003).

These signal transduction molecules act on the mesenchyme and stimulate the expression of homeobox genes *msx-1*, *msx-2* as well as Early Growth Response-1 (EGR-1), BMP-4 and the extracellular matrix proteins tenascin and syndecan. The latter two glycoproteins promote the cohesion of mesenchymal cells when forming the precursor tooth bud and are associated with extracellular matrix (ECM) structure and the influencing of cell physiology in contact with the ECM (ten Cate, 1995). Extracellular BMP-4 signalling is vital in promoting the differentiation of the mesenchyme into a tooth, with its associated expression of the molecules listed above. However, experiments have determined that BMP-4 alone does not induce the expression of tenascin and syndecan. It is thought the dental mesenchyme, now more

organised and called the dental papilla, determines the shape of the developing tooth, i.e: molar, incisor or canine and later the premolar by means of controlling cellular division (ten Cate, 1995). The enamel knot, a cell signalling centre derived from the overlying ectoderm, secretes several signalling molecules, including BMP-2, 4 & 7, SHH and FGF-4, which promotes the differentiation and proliferation of ameloblastic and odontoblastic epithelia. The origins of this enamel knot are not known but, once the tooth development reaches a certain phase, it will undergo apoptosis. This is regulated by BMP-4 secreted by the dental epithelium, resulting in cessation of the cell signalling at the late-cap to early-bell stage of tooth development (Kim *et al*, 2006). Two cell types exist in the generation of a tooth: odontoblasts, responsible for dentine production and ameloblasts, derived from stratified oral epithelial cells and responsible for the generation of enamel (Smith & Nanci, 1995). Odontoblasts withdraw from the cell cycle late in their differentiation and begin to elongate and secrete predentin, a predominantly type I collagen but also containing other molecules such as dentin phosphoprotein and dentine osteocalcin. These are released from the enamel organ-facing apical surface and will form the apex of the budding tooth. Further accumulated dentin deposition causes the separation of the odontoblast-ameloblast interface. Under direction from the odontoblasts, ameloblasts withdraw from the cell cycle and commence synthesis of two classes of protein: amelogenins* and enamelins (Carlson, 1994). Odontoblasts migrate to the centre of the tooth, the pulp chamber, and continue to secrete dentine until development of the tooth is complete (Aiello & Dean, 1990). During this secretory phase of amelogenesis, enamel crystallites elongate to produce evenly spaced, parallel long, thin ribbons. It is this ribbon length which determines the overall depth of enamel (Caterina *et al*, 2002). This elongation continues until the full

* Amelogenins will comprise 90% of the total protein matrix of formed hydroxyapatite.

thickness of the enamel is achieved, at which point the ameloblasts reduce in size and undergo apoptosis. It is thought that amelogenin self-assembles into a scaffold-like matrix, together with other proteins in order to facilitate enamel nucleation and crystallisation (Iijima & Moradian-Oldak, 2004). As the tissue matures, these proteins will disassemble (Margolis *et al*, 2006).

Hypothetical ideas have been previously suggested in papers which highlight the presumed necessity for an underlying 3-dimensional organisational structure during odontogenesis. Such a structure could conceivably include proteins such as amelogenin, whose folded and charged nature would theoretically permit charge interactions which would lower molecular activation energy and promote hydroxyapatite nucleation. The element of enamel directional elongation and expansion would then be protein thus genetically regulated (Simmer & Fincham, 1995; Robinson et al., 1998), however, this hypothesis has not yet been proved.

Individual teeth are seated in sockets (alveolar process, *pl.* alveoli) within an arch of bone on the upper (maxilla) and lower (mandible) jaw and held in place by the periodontal ligament. Should the tooth be removed the alveolar process is absorbed and the arch disappears. Deciduous teeth can begin to appear between six months until two years of age and consist of four sets of two incisors, one canine and two molars; a total of 20 teeth. These are gradually replaced by adult teeth commencing at approximately six years and continuing until adulthood: four sets of two incisors, one canine, two premolars and three molars giving a total of 32 teeth in total.

The basic structures of all teeth are comparatively uniform consisting of a crown - projecting above the gum line - and root embedded in the alveolar arch and enclosing the pulp cavity. Differences in the morphology are explained by the individual tooth

function. Incisors are designed to "bite" and are flat and spade shaped. Canines are designed to "hold" or "grip". Molars and premolars are for grinding, the additional shear stress placed upon them necessitating three and two roots respectively compared to the single root of incisors and canines. Figure 1.3-1 shows how the enamel and subsurface dentine serve to protect the vascularised and enervated pulp tissue, which is accessed via the apical foramen. The irregularly organised cementum, a hard tissue conglomerate, is situated at the enamel-gingival junction and aids ligament attachment.

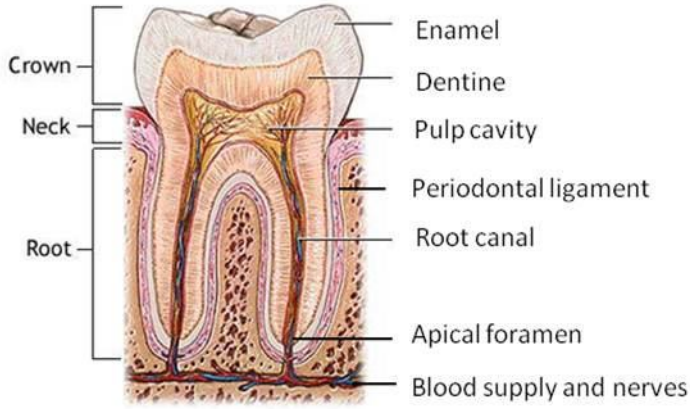

Figure 1.3-1: Diagrammatic representation of a human molar in relation to the jaw showing the internal morphology, vasculature and nerves.

1.3.1. GINGIVA

Surrounding the alveolar bone and roots of the teeth is the gingiva (gum), a specialised oral mucosa. The gingiva is anatomically subdivided into marginal gingiva (forming the collar surrounding each tooth as well as the gingival sulcus), the attached gingiva (forming the interface between the alveolar bone and the tooth) and the interdental gingiva. Disease or pathology arising in the gingiva can have an

impact on the entire oral cavity. Gingivitis (inflammation of the gum) may often progress to more serious conditions such as periodontal disease, resulting in subsequent loss of teeth. Healthy gingivae are a pale pink colour with some stippling. It is continuous with the smooth oral mucosa at the mucogingival junction (Standring, 2005).

1.3.2. CEMENTUM AND PERIODONTAL LIGAMENT

The tooth root is held in place within the alveolar socket by a combination of cementum and the periodontal ligament. The former is an agglomerate of hydroxyapatite mineral (HA) and amorphous calcium phosphate. The latter separates the cementum from the alveolar bone and is approximately 0.2mm thick. Coarse bundles of collagen fibres transect the cementum and periodontal ligament to implant in the alveolar bone, which is affected in advanced periodontal disease (Standring, 2005).

1.3.3. DENTINE

Dentine is an avascular, mineralised material made up of approximately 70% by weight mineral (largely hydroxyapatite and fluoroapatite with some calcium carbonate) with a 20% organic component (type I collagen fibres, phosphoproteins and glycosaminoglycans). Dentinal tubules are approximately 1-2μm in diameter and extend from the pulpal surface to the dentine-enamel junction. Some of these tubules bifurcate at this junction and may penetrate a short way into the enamel. Each of these

tubules contains a cytoplasmic process of an odontoblast. The cell bodies reside in a pseudostratified layer at the periphery of the pulpal surface (Standring, 2005).

1.4.COMPOSITION, STRUCTURE AND FUNCTION OF HUMAN ENAMEL

Enamel covers the crown portion of the tooth, the area appearing above the gingiva. It is a highly mineralised tissue composed of prismatic crystals of calcium-deficient, carbonated hydroxyapatite (Featherstone & Lussi, 2006). These enamel prisms are hexagonal and approximately 3-6μm in diameter; the HA crystallites being approximately 68nm in diameter. Enamel has also been shown to contain microscopic HA crystal inclusions at the surface, which do not form part of any particular prism but may add strength to the overall structure. Enamels chemical composition and function will be further discussed in the next subsection

1.4.1. STRUCTURE OF ENAMEL

Enamel is considered to comprise ca. 87% hydroxyapatite by volume in the form of small, tightly packed crystal prisms which comprise ca. 95% of the total enamel mass (Risnes, 1997) of the tooth. The remaining 13% volume consists of water and organic fractions, such as the protein amelogenin, which is thought to be responsible for the embryonic organisation of enamel rods, about which more will be said later. Enamel crystal prisms are composed of an ordered arrangement of hydroxyapatite crystals, which are in turn large, uniform and regularly dispersed within the tissue matrix (Braley et al, 2007).

Morphologically, enamel consists of solid, interwoven, rod-like structures, approximately 4-8 μm in diameter (as depicted in Figure 1.4-1), extending from the enamel-dentine interface to the tooth surface (Zhang et al., 2000). The shape of the enamel rod is dependent on the plane of sectioning, which explains the variation in morphological descriptions in the literature. Radlanski *et al.* generated a 3D representation of enamel rods from the dentine-enamel junction to the external surface for both foetal and adult samples. The only morphological difference was found to be the smaller size of foetal enamel rods. It was further observed that the rods are not static in their path but merge, twist and bend in relation to other rods. Thus it is hypothesised that each enamel rod is the product of a single ameloblast (Radlanski et al., 2001; Skobe, 2006), which in addition to secreted mineral produces an organic, proteinaceous fraction and water.

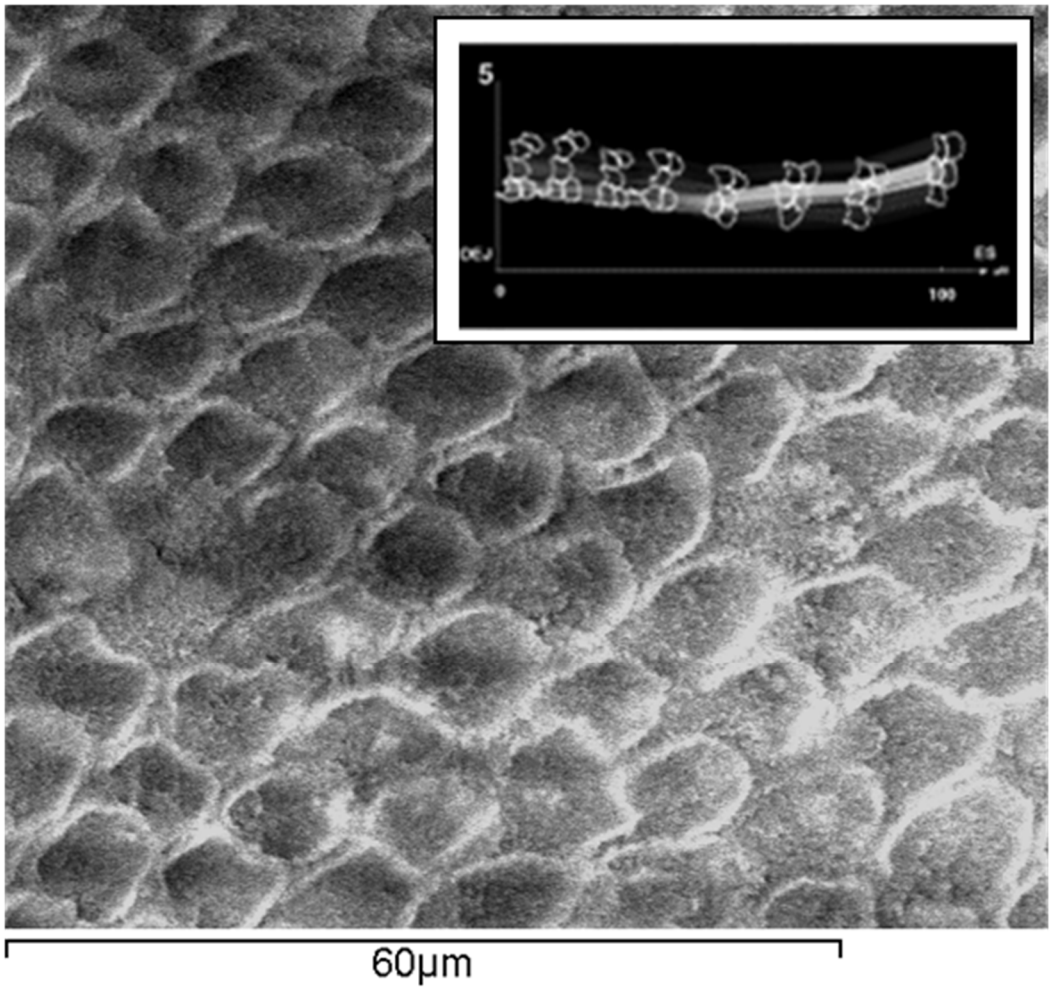

Figure 1.4-1: Uncoated human enamel rod etched with 37% phosphoric acid. The rods extend perpendicular to the surface toward the dentine. At the dentine-enamel junction, the arcade form of enamel rods dominate but changes to favour the keyhole form closer to the surface. Inset: 3D reconstruction of confocal microscopic image detailing five enamel rods *in situ*. (Radlanski *et al*, 2001).

1.4.2. CHEMICAL COMPOSITION

Hydroxyapatite is a naturally occurring mineral in biology and in geochemistry, whose stoichiometric formula is $Ca_{10}(PO_4)_6(OH)$. An example of a single hydroxyapatite crystal is shown in Figure 1.4-2 showing the organisation of hydroxyl, calcium and phosphates within the crystal lattice and the resulting differential charge. Hydroxyapatite in geochemistry is primarily, but not wholly, limited to igneous rocks

(Deer *et al.*, 1993). Substitution in the mineral matrix from impurities, such as fluoride, chloride, magnesium or sodium are depicted below:

$$Ca10 - xNax - (PO_4)6 - y(CO_3) - z(OH)2 - uFu$$

The mineral is also the inorganic component of bone, enamel, dentine and cementum.

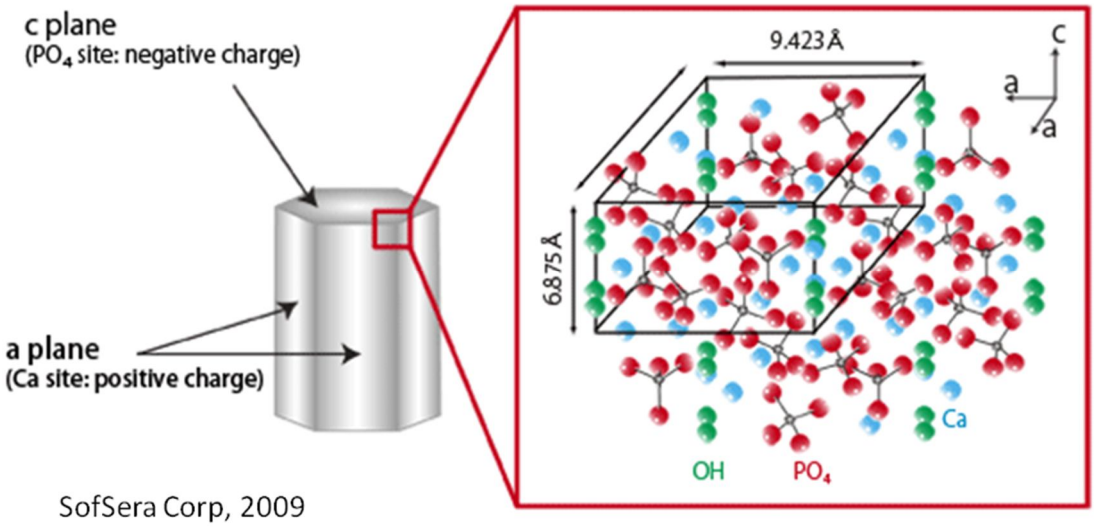

Figure 1.4-2: Schematic representation of a single hydroxyapatite crystal with its associated charge (shown on the left) and the molecular lattice structure(shown on the right)

Embryological development of enamel often results in the incorporation of numerous trace elements, including magnesium, iron, zinc, strontium, fluoride and carbonate (Curzon & Crocker, 1978; Lee *et al.*, 2006; Sydney-Zax *et al.*, 1991). The incorporation of such ions into the mineral affects crystal structure and lattice stability (Sydney-Zax *et al.*, 1991; Featherstone & Lussi, 2006). This in turn impacts on the susceptibility of the mineral to demineralisation by acids of bacterial and dietary origin and are thus relevant to the dental caries and dental erosion. Levels of potassium, magnesium, chlorine and sodium (ions common in tap water and biological fluids) were

reportedly slightly increased in hypomineralised enamel versus sound enamel (Jälevik *et al.*, 2001).

Secondary ion mass spectrometry (SIMS) has been used to monitor a number of elements believed to be important in HA formation. The carbon present in sound human enamel can be attributed to the presence of carbonate and proteins laid down during tooth development, and its concentration is effectively constant in the bulk of the tissue (Jälevik *et al.*, 2001). Hypomineralised enamel, a result of local, systemic or hereditary factors (Suckling, 1989), has more variability in carbon content but it is generally present in greater quantity than that found in sound human enamel, although the reason for this remains unclear. The concentration of metal ions such as Na^{+}, K^{+} and Mg^{2+} is higher in the sound enamel interior compared to the external surfaces whilst hypomineralised enamel have been found to have overall slightly raised quantities than sound enamel (Jälevik *et al.*, 2001). In the case of the aforementioned cations, the skewed distribution, particularly in sound enamel, may relate to the preferential dissolution of sodium, potassium and magnesium phosphates during periods of demineralisation.

F^{-} and Cl^{-} ions are more predominant at the surface of sound enamel, in the case of F^{-} this is presumably related to assimilation by the tooth mineral of exogenous sources of fluoride, such as that provided by fluoridated toothpastes. Strontium is reportedly to be fairly uniformly distributed through the tissue, with some enhancement of concentration observed in the cervical region of the tooth (Norén *et al.*, 1983).

1.5. TOOTH PATHOLOGY

1.5.1. CARIES

Caries, often referred to as cavities or "tooth decay", is attributed to the build up of bacterial plaques, typically *Streptococcus mutans* and lactobacilli but these are by no means a definitive population, on the enamel surface of susceptible teeth (Van Houte, 1994).

Caries-driven enamel dissolution occurs over time as a result of the organic acid by-products of bacterial metabolism. The bacterial utilisation of dietary carbohydrate as an energy source results in the formation of an organic acid by-product, which in turn dissolves calcium and phosphates out of the enamel matrix and into solution, thus resulting in gradual bulk tissue loss. This acid shift in the local environment pH also allows for the perpetuation of acidophilic bacteria, in turn promoting colonisation of the enamel surface and furthering the formation of caries. The formation of caries requiring medical intervention is a process taking months to years (Featherstone, 2008).

1.5.2. EROSION

The definition of the term "dental erosion" has been debated since 1890 (Zipkin *et al*, 1949). Consensus today is that dental erosion may be defined as the loss of surface enamel through acids of non-bacterial origin (such as citric acid from citrus fruit) or chelation (Amaechi *et al*, 2005, Bartlett *et al*, 1996; Imfeld *et al*, 1996). Furthermore, the term has been subdivided to distinguish between intrinsic or extrinsic

erosion, according to the acid origin. A summary of the origin for these are provided in Table 1.5-1. Intrinsic acids include gastric juices - the principal erosive component being hydrochloric acid - from patients with pathological conditions including bulimia, chronic alcoholism or gastro-oesophageal reflux disease (Bartlett *et al*, 1996). Extrinsic acids are derived from diet (carbonated drinks), medication, which are the most commonly encountered sources of acid but environment (such as acid fumes from heavy industry) and lifestyle, such as professional swimming in pools with a very low pH (Zero, 1996) are also documented.

Intrinsic factors		
Origin	Aetiology	Reference
Only endogenous acids originating from the gastric tract (e.g.: hydrochloric acid)	Recurrent vomiting (eating disorders, drug and alcohol abuse) Regurgitation (gastro-oesophogeal reflux disorder) Rumination syndrome	Zero, 2000
Extrinsic factors		
Origin	Example	Reference
Diet Behaviour Medication Industrial	Food and drink containing acids (e.g.: citric acid) Repeated exposure to excessively chlorinated swimming pools Gastric irritation attributed to asprin Sulphuric acid mist present in battery manufacture	Bartlett, 2005 Imfeld, 1996 Zero, 2000 Malcolm & Paul, 1961

Table 1.5-1: Origin of extrinsic and intrinsic acids with a known dental erosion aetiology

1.5.3. ABRASION

The abrasion of dental enamel involves the loss of dental substrate as a result of exogenous force, such as tooth brushing or tooth-to-food contact (Barbour & Rees, 2006; Grippo et al., 2004). It is commonly observed in synergy with the effects of enamel softening (the progressive loss of calcium and phosphates from the mineral matrix), such as dental erosion or caries formation. Furthermore, some authors have linked the use of particularly abrasive dentifrices (Joiner et al., 2004) or excessive force

when brushing (particularly when coupled to a toothbrush of high stiffness bristles and large quantity of toothpaste) to substrate loss (Imfeld, 1996b). However, this quantity of substrate loss is limited to less than 1 μm and its clinical significance remains debated (Bartlett & Shah, 2006).

With the advent of the electric (and sonic) toothbrush, concerns have been raised that the very rapid brushing action of this implement may speed the loss of tooth enamel, particularly when coupled to previous enamel softening and poor brushing technique (Weigand *et al.*, 2006, Bergström & Lavstedt, 1978). Mantokoudis found a statistically significance difference between the quantities of plaque removed using an electric brush compared to manual brushing (Mantokoudis *et al.*, 2001). However, the group felt this to be of questionable clinical relevance and the benefits gained from plaque removal may be offset by the damage attributed to abrasion resulting from inappropriate use (Addy & Hunter, 2003).

1.5.4. ABFRACTION AND ATTRITION

Abfraction and attrition relate to high occlusal loads placed on the teeth through actions such as chewing or habits such as bruxism and clenching (Grippo *et al.*, 2004). The conditions result in progressive wear of enamel at the cemento-enamel junction, cervical surfaces and occlusal surfaces and can become significant in the presence of exacerbating circumstances.

In abfraction these loads comprise of biomechanical axial loads in the vertical plane and lateral loading from natural jaw motion during chewing (Rees, 2006) but have been predominantly linked to bruxism (McCoy, 1982; Grippo, 1991). These compressive, tension and flexural forces concentrate in the cervical region of the tooth,

eventually resulting in material fatigue characterised by wedge shaped microfracture lesions (Bartlett & Shah, 2006).

Attrition has been defined as substrate loss arising from tooth-to-tooth contact as a result of normal and/or abnormal masticatory function, usually on the occlusal or incisal surface and in the absence of foreign substance intervention (Seligman *et al*, 1988; Grippo, 1991; Addy & Shellis, 2006). Abfraction and attrition differ from abrasion in that the loss of substrate is a direct result of excessive loads originating from conscious and unconscious behavioural action while abrasion typically occurs following a softening event and is related to biomechanical friction (Addy & Shellis, 2006).

Tooth pathology encompasses these four principle means by which dental enamel (and dentine) may be lost from the oral cavity. However, dental hard tissue loss is not uniformly ascribed to a single pathology, but is an accumulation of multiple factors, for example: abrasion in conjunction with erosion (Ashcroft & Joiner, 2010).

1.6. PHYSICOCHEMISTRY OF HYDROXYAPATITE

1.6.1. HYDROXYAPATITE DISSOLUTION

Hydroxyapatite is sparingly soluble in acid* and dissolves as follows:

$Ca_{10}(PO_4)_6(OH)_2 + 8H^+ \leftrightarrow 10Ca^{2+} + 6(HPO_4)^{2-} + 2H_2$ (Hannig *et al.*, 2005).

The formula given above implies a linear relationship between apatite and its dissolution products, suggesting that the reaction progresses in a linear manner, while the experimental curve (Figure 1.6-1) is logarithmic in appearance with respect to pH, meaning the lower the pH the more dissolution product is generated (Hannig *et al.*, 2005).

*See Section 1.6.2, the solubility of hydroxyapatite.

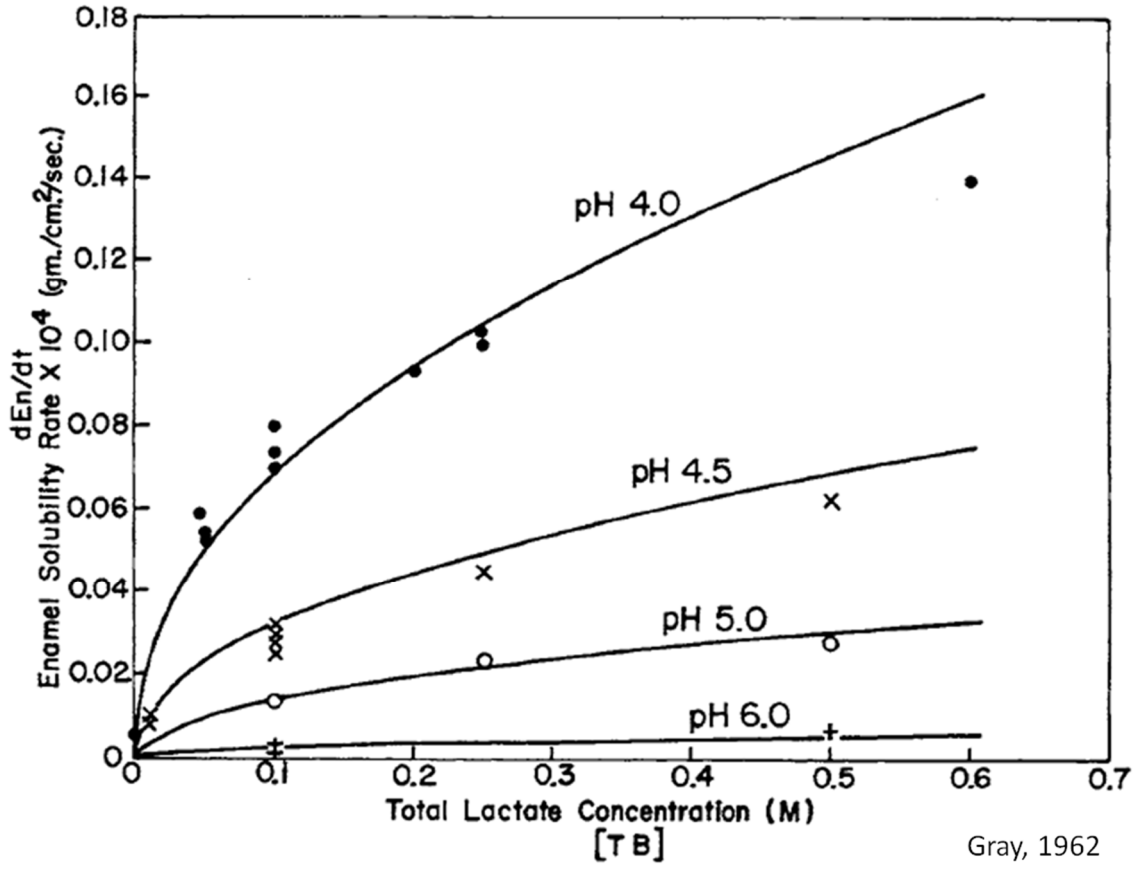

Figure 1.6-1: Dissolution curves of human enamel in acidified lactate buffer showing the effect of increased pH on dissolution product generation.

Successful dissolution of a hydroxyapatite crystal involves the transportation from a solid (crystalline) phase into a solution adjacent to the crystal surface. The dissolution of hydroxyapatite, with respect to a dental perspective, consists of two phases. The first phase relates to the dissolution of the hydroxyapatite crystal surface into solution; the second deals with the action of subsurface dissolution, whereby dissolved subsurface must be transferred to the external fluid environment (Christoffersen, 1981). Dissolution rates are also affected by the experimental medium, e.g.: a pelletised or powdered form of HAP. Experimental data has shown that dissolution of hydroxyapatite in pellet form is diffusion controlled (White & Nancollas, 1977). There is less evidence for this in hydroxyapatite powder but it becomes more evident as the experiment duration continues (Wong *et al* 1987). This data may be explained by work

showing that dissolution of hydroxyapatite requires the formation of nanoscale pits on the crystal surface as precursors to dissolution progression.

It has been postulated that apatite crystal surface dissolution is controlled by the initial and continuing formation and subsequent growth of nanoscale pits. Upon exposure to an acid environment, these pits begin to form and the critical radius within the crystalline matrix is the primary determinant of the rate of crystal dissolution (Tang *et al.*, 2003). The critical radius of these pits can be calculated as follows:

$$r^* = {\gamma\Omega}/{|kT \ln S|} \qquad \text{(Wang \& Nancollas, 2009)}$$

where r is the radius of the crystal nanopit, r^* is the critical radius (for the formation of a two-dimensional pit, which must be exceeded for active dissolution to occur), γ is the surface free energy, Ω is the molecular volume, k is Boltzman's constant, T is the temperature and S is the degree of saturation.

Furthermore, these pits are critical to determining the rate of crystal dissolution according to:

$$R(r) = R_\infty \left[1 - \frac{e^{(1-S)r^*/r} - 1}{e^{1-S} - 1}\right] \qquad \text{(Wang \& Nancollas, 2009)}$$

where R(r) is the rate of spread outward from the radius, r and R_∞ is the dissolution velocity when r approaches infinity. In pits where r approaches r^*, the rate of dissolution approaches zero. This may be linked to the size of the hydroxyapatite nanocrystalline needle-like particles (the shape a result of the molecular structure of hydroxyapatite), which play an important role in dissolution kinetics. When these mineral particles approach a critical size of between 20-50 nm, the strength of a perfect

hydroxyapatite crystal is preserved and, as a result, dissolution becomes progressively more difficult (Wang & Nancollas, 2009).

1.6.2. SOLUBILITY PRODUCT OF HYDROXYAPATITE

The above subsection described the formation and progression of nanopits on the surface of hydroxyapatite crystals and its solubility. Solubility describes the movement of a solute within a saturated solution; the amount of solute being transferred into solution (or dissolving) *versus* the amount of solute returning into a solid phase. When both these rates are equal, the reaction is at equilibrium and the quantity of substrate lost is equal to that being precipitated out of solution (Wu & Nancollas, 1998).

The accepted solubility of HA is $K = 5.5 \times 10^{-55}$ $mol.dm^{-3}$ (Margolis & Moreno, 1985), although enamel has been found to have an increased value: The solubility product of powdered human enamel HA has been experimentally shown to follow a linear trend between $1 \times 10^{-56.9}$ $mol.dm^{-3}$ at pH 4.6 and $1 \times 10^{-52.8}$ $mol.dm^{-3}$ at pH 7.6 assuming all reactants are kept above saturation level (Gray, 1966; Larsen & Jensen, 1989).

Larsen & Jensen (1989) also found that the solution was undersaturated with respect to octacalcium phosphate (OCP, with the chemical formula $Ca_8H_2(PO_4)_6$) and tricalcium phosphate (TCP with the chemical formula $Ca_3(PO_4)_2$), both reactive products of HA, suggestive that these salts would be unlikely to form under unsaturated conditions at low pH. By contrast, the solution was saturated with respect to brushite

($CaHPO_4$) and fluoroapatite ($Ca_5(PO_4)3F$, where applicable fluoride is available) at low pH (Larsen, 1973; Larsen & Jensen, 1989).

1.6.3. ENAMEL DISSOLUTION

Biological apatites, with their inclusion of extraneous elements such as fluoride, carbonate, sodium, potassium and chloride ions (Norén *et al*, 1983), will not behave in a similar manner to the dissolution kinetics described above. This is because the dissolution kinetics described above relate to pure hydroxyapatite, while biological inclusions (arising from extraneous sources such as diet) will alter the crystal lattice in the *a*- and *c*-axis, due to differences in atomic size (Legeros *et al*., 1976). In the case of fluoridated hydroxyapatite, this will result in a softer, preferentially eroded mineral matrix (Sydney-Zax *et al.*, 1991; Featherstone & Lussi, 2006). In addition to this, extraneous factors, such as the presence of a bacterial biofilm, salivary flow and salivary pellicle will further alter the kinetics of dissolution.

An appropriate acid (such as phosphoric acid, present in certain carbonated beverages) contacting the pellicle-covered tooth surface overwhelms the buffering capacity of salivary HPO_4^{2-} (Edgar & O'Mullane, 1990) resulting in reactions with enamel phosphate (PO_4^{3-}), which in turn nullifies the effect of salivary buffers. The initial stages of dissolution, as alluded to previously, involve a process of mineral softening – the diffusion of an acid solution into the enamel results in the loss of calcium and phosphate ions from the hard tissue matrix (Eisenburger *et al*, 2004). Prolonged exposure to acidic solutions will eventually lead to large quantities of enamel dissolving

into solution and the resultant irreversible loss of surface material severely compromising overall dental health (Smith *et al.*, 2001).

The initial softening of the local area to a depth of several micrometers, as a result of erosion for example, will also render enamel more susceptible to abrasive action (Barbour & Shellis, 2007). In clinical terms, such softening is almost impossible to detect at the early stages (superficial, involving only the enamel) and, when correctly identified, is often at a late stage (more than a third of the tooth is involved, including the dentine) which then requires intervention (Imfeld, 1996; Pretty, 2006). Prolonged exposure to acidic solutions will eventually lead to large quantities of enamel dissolving into solution and the resultant irreversible loss of surface material severely compromising overall dental health (Smith *et al.*, 2001).

into solution and the resultant irreversible loss of surface material severely compromising overall dental health (Smith *et al.*, 2001).

pH

pH is an inverse logarithmic scale related to the concentration of free protons in solution available to interact with any substance (Atkins & Jones, 1997); thus the higher the molarity of H^+ ions the lower the pH value will be, as the formula depicts:

$$pH = -log[H^+]$$

In terms of acid solutions this means that strong acids, with a ready availability of protons (H^+), sufficient to exceed the alkali (*R*-OH) concentration, will have a lower pH compared to a weakly dissociated acid with fewer protons available. This scale does not reflect the kinetics of acid:base interactions, which are more accurately represented by the acid dissociation constant (pKa) and thought by some to more effectively

represent erosion dynamics (Yoshida *et al.*, 2001), about which more will be discussed later.

Meurman and ten Cate suggested that any solution with a pH lower than 5.5 will cause erosion, particularly if the duration of exposure is long and/or repeated over time (Meurman & ten Cate, 1996). Theoretically, solutions of pH 4 or below will exponentially dissolve apatite. However this cannot be confirmed experimentally as competing brushite formation, precipitating at the same time as apatite is dissolved, prevents apatite saturation of the solution (Larsen & Nyvad, 1999) and thus masks the results. This effectively prevents a clear empirical understanding of the kinetics of enamel erosion and the interplay of hydroxyapatite; brushite and the solvent.

TITRATABLE ACIDITY

Acid titration relates to the negation of acid using an appropriate alkali, thereby gradually increasing the pH of an acid solution to physiological or neutral. This process aims to halt acid etching without any negative side effects such as apatite precipitation attributed to a rapid increase in pH from washing in pH neutral water (Eisenburger *et al.*, 2004). It is regarded by some researchers as a more accurate tool for the evaluation of potentially erosive acidic drinks (Edwards *et al.*, 1999) as initial pH measurements often fail to factor in underlying buffering capacity, which is related to the pKa, and a known problem when exclusively considering pH. Thus acids with a greater acid titration value require more alkali to neutralise.

pKA

pKa defines the logarithmic rate at which an acid will dissociate into a proton donor and proton acceptor component; for example ethanoic acid (CH_2COOH) in water (H_2O) dissociates into a proton donating hydroxonium ion (H_30^+) and proton accepting ion (CH_2COO^-), in accordance with Brønsted/Lowry theory (Atkins & Jones, 1997):

$$pKa = -log\frac{[H_3O^+][CH_2CO_2^-]}{[CH_2COOH]}$$

The higher the pKa value, the more the acid will readily dissociate and the greater the potential proton availability, thus the more effective the acid. This is in contrast to the pH values, which only determine the concentration of protons and may not provide an accurate representation of the true chemical kinetics. Thus, while pH pertains to the concentration of H^+ in solution, which may change with the addition of further solutions, pKa relates to the ability of an acid to generate H^+ ions and may better reflect the efficacy of certain acids to dissolve enamel. Some examples of naturally occurring chelating acids, about which more will be discussed in the next subsection, are listed in Table 1.6-1, which shows the variation of pKa among these compounds.

Acid	Product	pKa
Lactic	Diary products	3.86
Citric	Citrus drinks	3.13
Tartaric	Grapes, bananas	3.04
Oxalic	Spinach, rhubarb	1.25

Table 1.6-1: Table showing some common chelating acids in context of their consumable products and pKa.

An investigation by Yoshida *et al* of some commonly employed clinical carboxylic acids: malic, citric, lactic, polyacrylic and polyalkenoic acid found that the case for acidity as the primary driving force behind dissolution kinetics may have been overstated. It was found that these acids either decalcified or adhered to hydroxyapatite irrespective of the effects of pH or acid concentration, but was dependent on the dissolution rate of the resulting acid-determined calcium salts. As such, this group hypothesised that the pKa value, not the pH, of individual acids was the more determining factor (Yoshida *et al.*, 2001).

CHELATION

Chelation describes the preferential binding affinity of one molecule for another. It has been shown that certain naturally occurring acids for example citric acid, have an affinity for the calcium component of hydroxyapatite and will induce greater mineral loss as a result of reduced saturation and so may increase bulk tissue loss (Amaechi *et al*, 1999). However, at low pH values, such as below 2.2, the effects of chelation are reduced or irrelevant (Attin *et al.*, 2003).

DEGREE OF SATURATION

The degree of saturation (DS) relates to the ratio of mean ionic interactions between one substrate and another, in the case of dental erosion, the interaction between hydroxyapatite and its dissolution products. A high degree of saturation will therefore refer to a greater concentration of dissolved substrate in the acid solution. Barbour *et al* investigated enamel erosion with respect to degree of saturation and

found that adding calcium could reduce the erosive effect of acidic beverages by increasing in DS of the acid solution. The formation of acidic calcium phosphates, as well as additional compounds formed as a result of enamel inclusions, also plays a role in dissolution (Barbour *et al.*, 2005a).

TEMPERATURE

Temperature has long been known as a catalyst for chemical kinetics (Atkins & Jones, 1997). Amaechi *et al*. found that samples of enamel exposed to constant pH orange juice at 4, 20 and 37°C over a cumulative total of 30 minutes a day were significantly different from each other in terms of both bulk tissue loss and lesion depth (Amaechi *et al*., 1999). Thus the group concluded that acid drinks consumed at higher temperatures are likely to cause the greater erosive effect than those consumed chilled.

FLOW RATE AND DURATION OF EXPOSURE

Eisenburger & Addy, attempting to mimic fluid flow during drinking behaviour using a straw found a significant increase in enamel erosion as a result of increased flow rate of an acid solution (Eisenburger & Addy, 2003). Slower stirring speeds permit greater diffusion into the wider solution column, taking advantage of local variations in porosity and solubility to greatly increase bulk tissue loss rather than relying on the energy of the liquid flow as would occur in fast flowing systems (Shellis *et al*, 2005). By contrast, a static solution will result in diffusion of calcium and phosphate dissolution products into the opposing liquid phase, which will in turn become partially saturated with respect to the local enamel.

Prolonged exposure to acidic solutions will eventually lead to large quantities of enamel dissolution and irreversible bulk tissue loss from the surface (Smith *et al.*, 2001). Clinically, the early phase where the damage is reversible is almost impossible to detect, and it is generally not until the point that bulk tissue loss becomes evident that pathological levels of erosive wear can be identified (Pretty, 2006).

1.7. MORPHOLOGY OF ERODED ENAMEL

The electron microscope has been extensively employed in dental research using both scanning (Rios *et al.*, 2008, Eisenburger *et al.*, 2004, Schilke *et al.*, 2000) and transmission electron microscopy (Daculsi *et al.*, 1984; Nelson *et al.*, 1984). The method permits high resolution imaging of surface topography (Transmission EM more so than scanning EM but the former technique is limited by small sample dimensions of approximately 3 mm^2 and 100 nm thick). Figure 1.7-1 shows a backscattered electron scanning electron micrograph† of a transverse section of human enamel, which has been minimally polished and coated with gold palladium. The effect of backscatter electron microscopy serves to highlight differences in enamel resulting from the close compaction of inter-rod enamel, showing up as darker honeycomb lines, against that of intra-enamel rods.

† See section 1.12.5

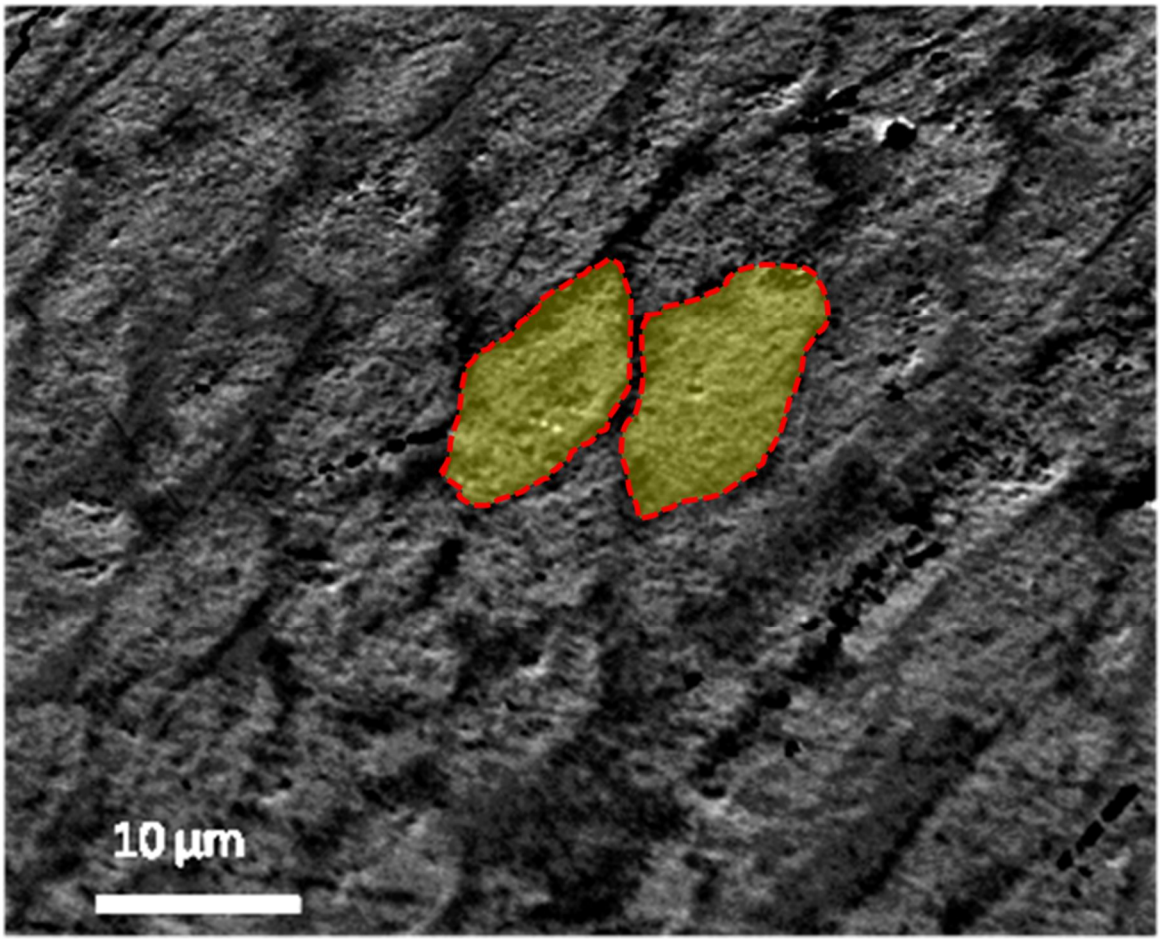

Figure 1.7-1: Backscatter scanning electron microscope image of uneroded, polished human enamel. The inter-rod enamel shows as darker honey-comb hexagonal lines (red dashed lines), while the enamel rods are observed as brighter hexagonal shapes (translucent yellow areas).

Eroded enamel has a structure which usually mirrors that observed from backscatter SEM studies. This is exemplified by the appearance of enamel rods standing proud of the erosion lesion (Eisenburger *et al.,* 2004) as seen in Figure 1.7-2, although different acids have been shown to have a different erosive effect on enamel: e.g.: EDTA has been found to preferentially dissolve the inter-rod enamel as the molecular size does not readily permit penetration between the densely packed core prisms compared to citric acid, which is a comparatively smaller molecule and preferentially erodes rod core enamel (Simmelink *et al*., 1974).

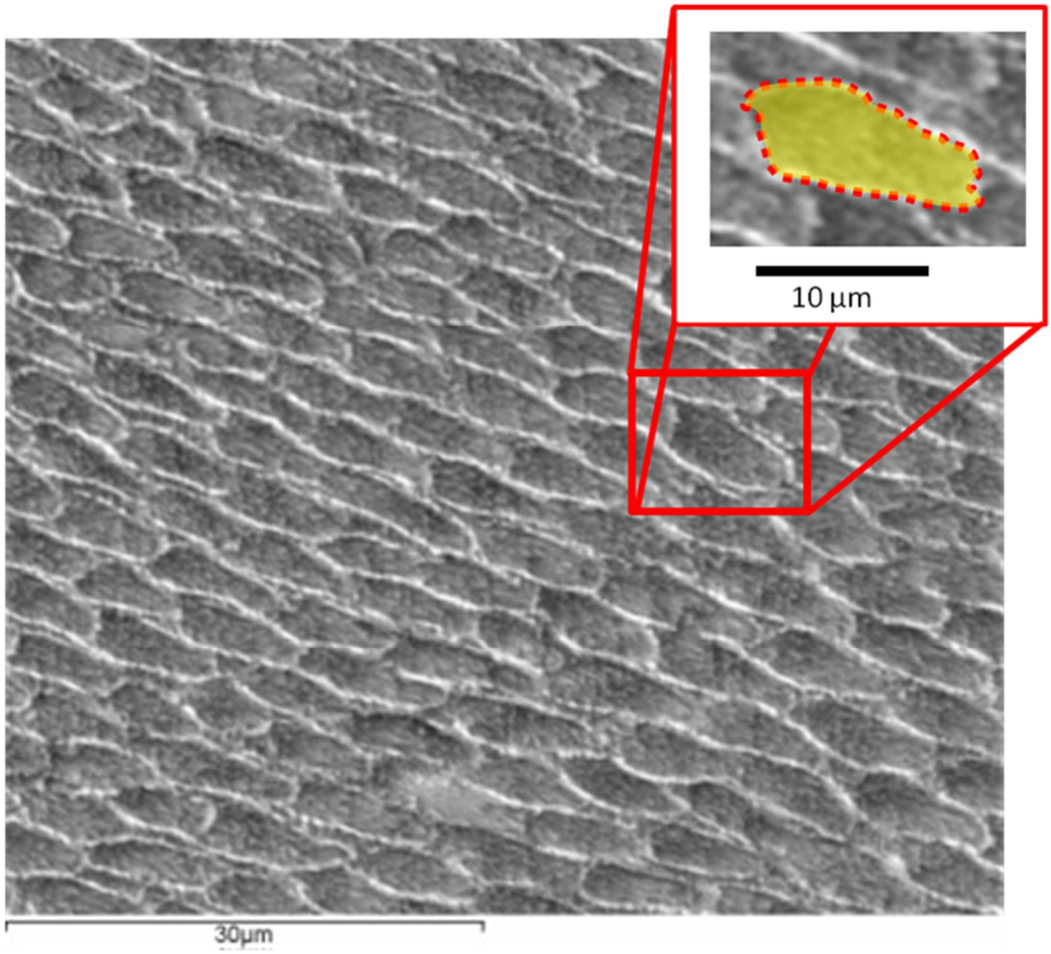

Figure 1.7-2: Scanning electron microscopy image of bovine enamel etched with 37% phosphoric acid for 20 seconds. The inter-rod enamel (dashed red line) stands proud of the surface, while intra-rod enamel (opaque yellow fill) is more deeply eroded.

Enamel erosion also reveals the asymmetrical layout of enamel rods in relation to each other: the rods do not follow identical tracks through the matrix but twist and weave in relation to their neighbours (Radlanski *et al*, 2001), although distinct changes in direction of groups of rods are also seen (Figure 1.7-3). It should be noted that such changes in direction (seen from Figure 1.7-3) for an entire section of enamel rods with respect to the surrounding rods was not commonly observed during this work. As such, this may represent an unusual orientation.

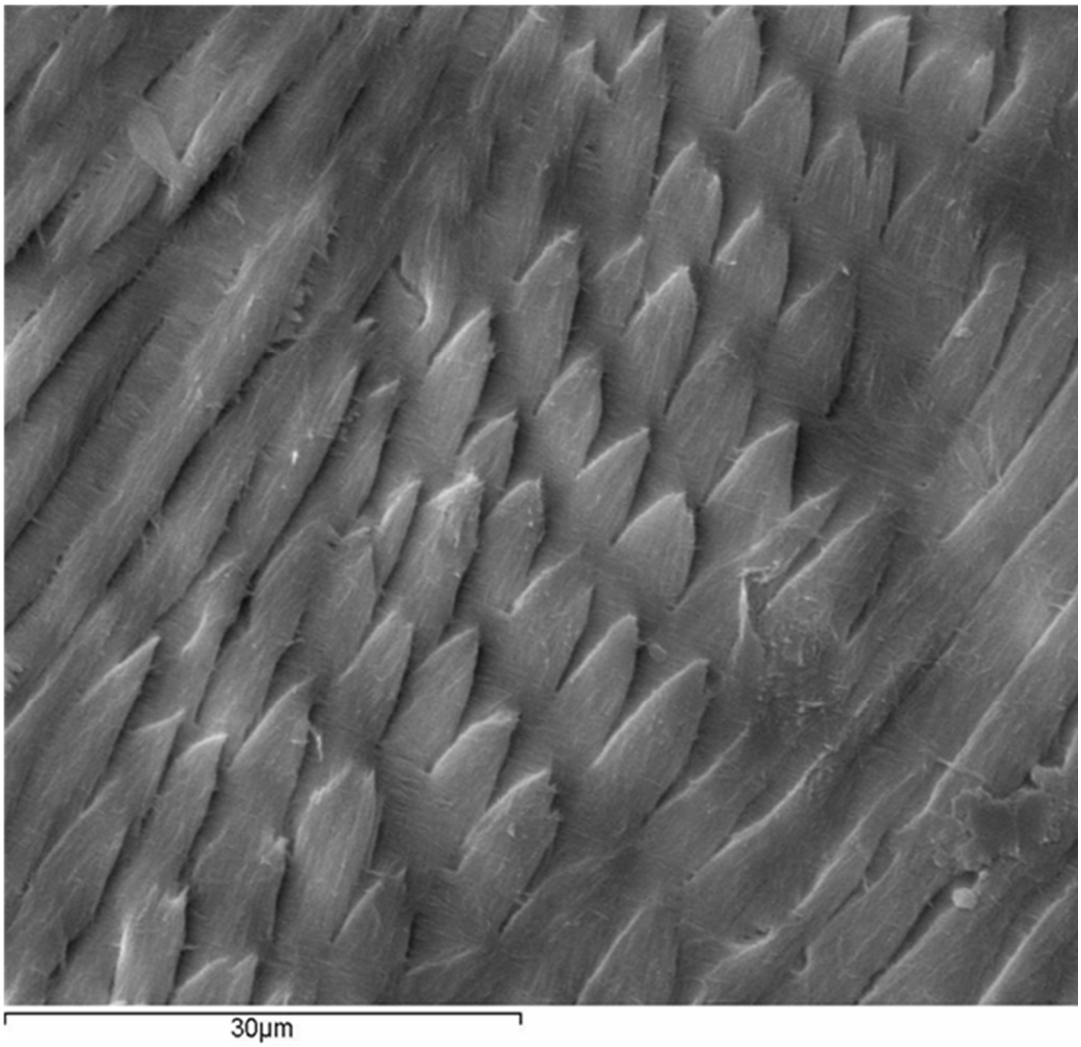

Figure 1.7-3: Change in orientation of enamel rods showing rod heterogeneity in terms of directionality. The group of rods in the centre of the image appear to be "coming out" of the image, while surrounding rods are running parallel to the image plane.

1.8. REMINERALISATION OF ENAMEL

Enamel cannot be replaced as the cellular component of this material is absent from the mature product. However, natural processes in physiology aim to minimise continual bulk tissue loss through diet and extraneous factors. This is achieved through the rehardening of previously softened enamel (Arends & ten Cate, 1981), resulting from exposure to acid elements such as acidic beverages, which progressively removes the interprismatic enamel.

Previous studies have shown that hydroxyapatite precipitates out of saliva or remineralising solutions onto nucleation points on the surface of the enamel (originating as a result of an acid challenge) only when the appropriate conditions are satisfied (Feagin, 1971). These typically include the saturation of the local area solution with calcium, phosphate and, typically in remineralising solutions, fluoride ions as well as increased pH. Experiments involving the remineralisation of previously eroded enamel remineralised with radioisotopes of calcium, followed by serial grinding to determine its location, found large quantities of precipitated calcium radioisotopes on the superficial surface of the enamel, as well as an accumulation of radioisotopes at deeper depths of the lesion. These data supported the previous observations regarding surface precipitation but also suggested a chromatography-like adsorption and dissolution mechanism resulting from changes in enamel porosity (Arends & ten Cate, 1981).

One of the most effective, naturally occurring means of enamel remineralisation is that of saliva in the oral cavity.

1.8.1. SALIVA AND SALIVARY COMPOSITION

Saliva is produced by small glands embedded in the mucosa and submucosa and draining into the oral cavity. In addition to these small glands are three large paired glands: the parotid (which sits outside the boundary of the oral cavity), submandibular and sublingual glands all of which drain into the oral cavity via salivary ducts (Drake *et al*, 2005). In addition to its role in minimising enamel loss, saliva is responsible for buffering incipient acid challenges, maintaining and controlling oral flora and lubricating the oral cavity to assist swallowing and vocalisation (Randall *et al*, 2000). Stimulation of the saliva flow is notably achieved prior and during mastication but is also under autonomic nervous control, particularly during night time when circadian rhythms much reduce the salivary flow.

	Resting (µL.min)	**Stimulated** (µL.min)
Whole saliva	0.32 (0.1-0.5)	1.7 (1.1-3.0)
Parotid saliva	0.04 (00.1-0.07)	1.5 (0.7-2.3)
Submandibular/sublingual saliva	0.10 (00.2-0.20)	0.8 (0.4-1.3)

Edgar, 1998

Table 1.8-1: Table to show the differences between stimulated and resting whole and glandular saliva. The data range is supplied in parenthesis.

The composition of saliva varies greatly between individuals and within the person alone (as seen in Table 1.8-1) but generally consists of water (~99% of the volume) and an amalgamation of proteins - 200 mg per 100 mL comprising immunoglobulins A, M and G, enzymes (α-amylase being the most notable digestive enzyme), mucus glycoproteins and albumin, for example - and inorganic ions. Resting

saliva originates from the submandibular and sublingual glands, while stimulated saliva has a greater flow rate and is predominantly from the larger parotid gland and has reduced calcium content but increased phosphate content than resting saliva (Dawes & Jenkins, 1964; Drake *et al*, 2005).

Studies have been conducted concerning the effects of saliva on the mitigation of dental erosion. Paice *et al*. investigated the erosive effects of expectorated saliva following the use of two brands of acidic chewing gum and found no significant enamel loss resulting from this, which was attributed to increased salivary flow, clearance of the acid media and buffering capacity (Paice *et al*., 2011).

Saliva has also been investigated as a means of directly mediating erosion, for example the retention of anti-erosive compounds, such as fluoride. Work has been performed to investigate the salivary retention of fluoride in mouth rinses and found that the post treatment retention of high levels of fluoride (450 ppm, compared to samples containing 0, 100 and 225 ppm) is significant after 120 minutes post erosive challenge (Mason *et al*., 2010). This finding was supported by Austin *et al*. who found significant protective effects against cyclic, increasing duration erosive and abrasive challenges using 5000 and 19 000 ppm fluoride (Austin *et al*., 2010).

1.8.2. SALIVARY PELLICLE

The salivary pellicle predominantly consists of a layer of mucins deposited on the tooth surface, which slows or inhibits mineral loss through diffusion during an erosive challenge (Meurman *et al*, 1996). The pellicle mucins provide an anchor point for bacterial colonisation and, as mentioned before, has a role in minimising the effects

of erosion *in vivo* and *in vitro*, whether it is natural, clarified or artificial in origin (Meurman & Frank, 1991; Amaechi *et al*, 2001). Amaechi *et al* (1999) found the average *in situ* pellicle had a thickness of 0.3 to 1.06 μm at the upper anterior palatal and lower posterior lingual surfaces respectively but noted there was a significant difference between the mean pellicle thicknesses of individuals. By contrast, Hannig & Balz found the thickness of the pellicle to be between 50 – 170 nm for a pellicle generated over 24 hours and 60 – 300 nm for a pellicle generated over seven days (Hannig & Balz, 1999).

The thickness of the pellicle has been linked to a reduction in erosive tissue loss of enamel, providing the pellicle has satisfactory time to form, typically a minimum of one hour for maximum protection (Wetton *et al*., 2006) but significant protection is afforded following a three minute pellicle acquisition (Hannig *et al*., 2004). This has been substantiated by previous work which also found that the acquired pellicle is not completely lost from the enamel, even after one minute of continuous exposure to a citric acid media (Hannig *et al*., 2003; Hannig *et al*., 2004).

The presence of mucins as a constituent of the salivary pellicle has also been shown to help reduce the severity of erosive lesions – by as much as 30% (Amerongen *et al*., 1987). This has recently been questioned by Cheaib & Lussi, who found no significant additional protective effect from the pellicle when pig mucin was added to pooled saliva, but a significant effect was noted when this was combined with casein. This has been hypothesised as resulting from the formation of micellar structures of mucin and casein, which bind to the enamel surface and increase the thickness and density of the salivary pellicle (Cheaib & Lussi, 2011).

1.9. EROSION PREVENTION

1.9.1. MODIFICATION OF BEHAVIOUR

A reduction in the frequency of exposure to erosive agents may be brought about by a change in subject behaviour, such as avoidance or reduction of erosive beverage consumption. In addition, certain foods have been found to minimise demineralisation or promote the remineralisation of softened enamel.

Sela *et al.* advocated the consumption of soft cheeses following a meal to increase dental rehardening of softened enamel based on the increased availability of calcium (Sela *et al.*, 1994), while chewing a sugar-free gum stimulates salivary flow, which in turn promotes the constant supply of calcium and phosphate ions to the tooth surface as well as providing a buffer to pH change (Imfeld, 1996b).

Drinking carbonated beverages though a straw is a further example of modification of behaviour, providing the straw is placed correctly in the oral cavity lest the increased flow in labial surfaces promote instead of reduce erosion (Eisenburger & Addy, 2003; Bassiouny & Yang, 2005), while a fluoride mouthrinse, lozenge or varnish has been shown to stimulate salivary flow as well as provide additional fluoride to aid remineralisation (Amaechi & Higham, 2005).

1.9.2. MODIFICATION OF PRODUCT

Modification of a product may be done in order to reduce the impact of an erosive challenge on dentition. Such additives may include xanthan gum, which adhere to the enamel surface (West *et al*., 2004); ovalbumin and casein, which interact with calcium on the surface of enamel (Hemingway, 2008) and polyphosphates reduce the solubility of hydroxyapatite (Hooper *et al*., 2007).

A major component in the remineralisation of enamel, now routinely added to most toothpaste, is fluoride. This highly electronegative charged ion reacts with enamel to form fluoroapatite, a compound less soluble than HAP. Consequently this renders enamel more resistant to erosion and caries formation. In addition, fluoride in the presence of phosphate ions has been shown to preferentially bind acids (Murray *et al*, 1991) thus neutralising the effects of the acid on enamel.

There is well documented evidence demonstrating the effectiveness of fluoride in remineralisation strategies (Hughes *et* al., 2004; Extercate *et* al, 2005; Fowler *et al*, 2009) but it should be remembered that excessive fluoride uptake (in excess of the optimal 0.7ppm and 1.2ppm per day), particularly between the ages of two months and five years has been shown to have a detrimental effect on dental development – a condition known as dental fluorosis (Fluoridation Facts, 2005). This condition manifests as a continuum of effects ranging from fine opaque lines within the enamel to entirely opaque teeth and is associated with increased surface and subsurface porosity attributed to incomplete crystal growth and a subsequent failure of the close proximity of enamel prisms to each other. In extreme fluorosis at the post eruptive stage, large chunks of enamel may crumble from the tooth (Fejerskov *et al.*, 1990; Robinson *et al.*,

2004). However, the benefits of fluoride in correct dosage to minimise tooth erosion far outweigh these uncommon drawbacks.

1.10. DIFFERENCES BETWEEN ENAMEL SUBSTRATES

1.10.1. HUMAN ENAMEL

Human enamel is the more clinically relevant substrate to use when evaluating dental erosion both *in vitro* and *in vivo.* Typically the third molars (wisdom teeth) are utilised owing to the common removal of these teeth for orthodontic purposes and of these it is preferred if these teeth are unerupted owing to the constant surface composition and absence of extraneous effects on the surface. The longer teeth have been exposed to the oral cavity the greater the impact of extraneous factors such as dietary intake and salivary composition have on modifying the compositional make up (Hemingway, 2008).

Differences have been identified between human mature and deciduous enamel, the latter having been shown to have chemical and morphological differences compared to mature enamel, which manifests as increased matrix porosity (Lindén *et al*., 1986. Koutsi *et al.,* 1994; Meurman & ten Cate, 1996). In addition, the grinding and polishing of samples removes the outermost enamel layer, that which contains the highest proportion of fluoride (Norén *et al*., 1983), in order to obtain a flat, polished surface thus introducing an element of bias into the study. This bias is exacerbated because of the natural variation of individual samples, a problem which may be bypassed by the use of powdered pooled enamel. However, this potentially reduces the efficacy of a study by removing influencing morphology and therefore may not be representative of the true kinetics of erosion (Campbell *et al*, 1991; Shellis *et al.*, 1993).

However, the principal problem of studying human material lies in obtaining sufficient quantities of healthy teeth. This is hampered by the prevalence of caries and advanced decay in a majority of clinical samples and the recent decline in retention of post-surgical specimens owing to the costs involved in establishing accredited tissue banks (HTA, 2010).

1.10.2. ANIMAL ENAMEL

For a number of years now there has been particular interest in the use of bovine dental hard tissue for *in vitro* dental models. Its ready availability coupled to its comparatively large surface makes it particularly suitable for research. Differences have been reported with respect to human *versus* various mammalian species, such as enamel rod configuration in human *versus* porcine (Reis *et al*, 2004) or human *versus* bovine enamel (Mellberg, 1992). Additional structural differences between forming and mature bovine and human enamel include thicker crystallites, lower fluoride concentration and increased porosity in bovine enamel compared to that of human enamel (Featherstone & Mellberg, 1981; Mellberg, 1992). As a result of such findings, it has been suggested that the properties of permanent bovine enamel most closely mirror those of deciduous human enamel (Attin *et al.*, 2007).

However, the identified differences in structure and chemistry have not stopped alternative sources, such as bovine enamel, being utilised in experimental work (Hannig *et al.*, 2005; Lynch & ten Cate, 2006; Wegehaupt *et al.,* 2008), the primary reasons for which are cited as bovine enamel being less variable in composition and having greater surface area with which to work (Mellberg, 1992).

Bovine dentine exhibits a similar collagen matrix to human dentine as well as similar structural details including the number density of dentine tubules (Carmago *et al.*, 2007). A number of workers have identified that dentine (and enamel) structure varies according to location and depth within the tooth (Koutsi *et al,* 1994; Radlanski *et al*, 2001; Wegehaupt *et al*, 2008). Schilke, investigating the number of dentine tubules in human and bovine samples, demonstrated no significant difference between deciduous and permanent dentition (Schilke *et al.*, 2000). However, Koutsi reported significantly lower numbers of tubules in primary dentine compared to permanent dentition when examined using SEM but acknowledges this may be an artefact attributed to the specimen preparation during sectioning (Koutsi *et al.*, 1994).

Employing an erosion treatment regime on bovine dentine samples yielded significantly less erosion of the deciduous incisors and molars compared to their mature counterparts (Wegehaupt *et al.*, 2008). This observation was partly corroborated by Hunter, who found a similar trend but no significant difference (Hunter *et al.*, 2000) between mature and deciduous dentine erosion. Both these results contrast with the accepted observation that deciduous human and bovine enamel is found to be significantly more susceptible to acid erosion when compared to permanent human and bovine enamel (Wang *et al.*, 2006; Melberg, 1992). It has been suggested that the increased susceptibility of deciduous dentition may be linked to the different hydroxyapatite crystal and enamel matrix compositional structure of forming teeth compared to mature teeth (Shellis, 1984; Sydney-Zax *et al.*, 1991). Extrapolating this suggests that this may be due to increased permeability of deciduous enamel compared to permanent enamel (Featherstone & Mellberg, 1981; Lindén *et al.*, 1986).

1.10.3. SYNTHETIC HYDROXYAPATITE

Synthetic hydroxyapatite (HA) has been employed for the use of dental research in three principal forms: either pellets (Bollet-Quivogne *et al*., 2005), tablets (Kosoric *et al*, 2007) or in powdered form (Kosoric *et al*, 2010).

Synthetic HA is commonly produced using a precipitation method and relies on the formation of intermediate salts to produce the final product. It can be created using continuously stirred solutions of calcium nitrate, calcium chloride and orthophosphoric acid at pH 9 or above. Continued stirring promotes the slow integration of calcium into the apatite structure and allows for the gradual increase to desired stoichiometric Ca:P ratio (Hemingway, 2008).

The principal distinction between synthetic HA and enamel lies in the comparative purity of the former, permitting a more homogenous substrate and greater control over any experimental procedure than would be encountered using enamel. However, the absence of any organic fraction from synthetic HA and the lack of order in the crystalline matrix to mimic the formation of enamel rods make any system using synthetic HA artificial, by depriving the sample of remineralisation nucleation points for example, and thus the results may not reflect the actuality (Hemingway, 2008).

1.11. ACIDS PRESENT IN COMMON SOFT DRINKS

Some of the common "soft drink" beverages sold in the UK include colas, lemonade, orange juice and fruit concentrates which are diluted at home. Soft drink sales - particularly among younger generations - continue to rise. Britvic plc, a leading UK branded soft drinks manufacturer, posted sales of £8.5bn in 2009 (of which £6.2bn were drinks to "take home" sales), an increase of 2% profit on the previous year and 1% on volume of goods sold (Britvic, 2010). The increasing trend in soft drink sales, particularly carbonated beverages among younger people, runs concomitant to an increase in dental erosion observed in clinics (Taras *et al*, 2004).

The basic composition of a carbonated beverage is water, sugars, flavour enhancers and carbon dioxide. Such flavour enhancers can include aspartame, caffeine as well as preservatives such as benzoic acid (Walker *et al*, 1997) and phosphoric acid (Coca Cola company, 2009‡), the latter particularly in colas, although mineral acids are not as widely used as organic acids in this industry. These organic fruit acids often retain their low pH for a prolonged period of time owing to their buffering effects (Larsen & Nyvad, 1999). Examples include citric acid as a common component of citrus fruits and drinks, such as orange juice, malic acid in apple and cherry drinks and tartaric acid in wine and grape drinks.

‡ Personal communication

1.12. EXPERIMENTAL DESIGN IN EROSION STUDIES

Studies of the effects of dental erosion may be carried out in three different manners: *in vitro*, *in vivo* and *in situ.* The controlled study of erosion in a completely artificial setting, while attempting to closely mimic natural effects, such as the effects of acidic solutions, remineralising compounds or fluid dynamics, are termed *in vitro* studies. While variables may be closely controlled (e.g.: the quantity of fluoride in remineralisation work) the work is by its nature artificial and, therefore, may not be an accurate reflection of the multi-factorial oral cavity. The use of a highly controlled laboratory environment - while often exaggerating the effects of the experiment - is useful for determining potential effects of an experimental protocol during *in vivo/in situ* studies.

In situ work refers to better mimicking of the oral cavity than *in vitro* work by the application of a medical device, typically containing enamel slabs, into the oral cavity of a volunteer. This allows for better control over the experimental variables, such as sample exposure time, than would be achieved *in vivo* but retains the inherent population variability exemplified by salivary flow rate, which would impact on the study. Measurement can be better performed by the removal of the samples from the oral cavity compared to *in vivo* work, whereby the samples are observed in their natural state and subject to conditions specific to each individual.

A number of techniques are available for the qualitative and quantitative analysis of dental erosion and these are briefly summarised below.

1.12.1. CHEMICAL ANALYSIS

Ion chromatography allows for obtaining quantifiable data regarding the presence of specific ions relating to enamel chemistry. Aoba and Moreno used ion chromatography to show the prevalent presence of calcium, magnesium, potassium and sodium in enamel fluid during amelogenesis (Aoba and Moreno, 1987) but the technique is more commonly employed to determine the quantities of specific ions in reagents rather than reaction products as was the case for this work.

A specimen of enamel may be subjected to an acid solution challenge and a sample of the fluid taken at defined intervals. This fluid may then be introduced into the ion chromatograph whereupon the desired ions present in solution will be separated out according to their charge and retained on a stationary phase prior to being quantified using computer software.

A more detailed explanation of ion chromatography is found in Section 0

1.12.2. SPECTROSCOPY

A broad definition of spectroscopy is the use of radiation to study matter by means of absorption or emission of light from the sample as a function of its wavelength. Vibrational spectroscopy refers to the analysis of chemical bonds as a result of changes to the vibration state of molecular bonds. Changes in molecular vibrations present within a sample are detected using optical detection methods. The changes in emitted light from excited molecules are analysed to provide a variety of information such as the vibrational and rotational molecular interactions, in the case of Raman analysis, or to analyse the changes in surface chemistry by measuring the

wavelength of scattered light absorbed by the sample, as performed using infrared spectroscopy. Both of these techniques are examined in more detail below.

Infrared spectroscopy (IR) provides information regarding molecular structures and their interactions using measurable changes in the molecular vibrations. These vibrations are attributed to energy absorption of molecular polarisation changes, or vibrating dipoles, at specific wavelengths. Therefore, every chemical bond has a specific frequency and absorption within its local environment and, as IR is particularly sensitive to the vibrational dipole, this technique can detect changes in molecular structure, conformation or physical state (Alben, 1996). A commonly used form of infrared spectroscopy is that of Fourier Transformed Infrared (FTIR) spectroscopy, which has previously been employed to examine the effects of fluoride on hydroxyapatite morphology (Fan *et al.*, 2009). Light is passed through an interferometer then the sample (although the reverse is also possible) and the resulting output is recorded as a function of a movable mirror, which alters the distribution of the outgoing signal. Fourier transformation of the raw data provides a result in terms of light output resulting from defined infrared wavelength.

IR has also been used to investigate the surface chemical changes of enamel remineralisation *in situ* (Krutchkoff & Rowe, 1971) although this has been increasingly replaced in recent years by the emerging spectroscopic technique of quantitative light fluorescence (QLF).

QLF indirectly measures changes in enamel autofluorescence brought about by mineral loss and/or remineralisation when viewed with a blue (370 nm wavelength) laser. It is not clearly understood what drives the change in enamel autofluorescence of human and bovine enamel. Human enamel has a maximum absorption peak of 270 (±5) nm, while bovine has a maximum absorption peak of 260 (±5) nm (Spitzer & Ten Bosch,

1976). Evidence of three distinct autofluorescence spectra at 350–360 nm, 405–410 nm, 440–450 nm has also been found and attributed to the organic fraction of enamel, in particular the amino acid tryptophan (for emission spectra between 405 -450 nm). It was also found that an erosive challenge will cause a shift in autofluorescence, particularly at the 450 nm emission band. This was attributed to light scattering and wavelength dependent upon the resulting scattering (Spitzer & Ten Bosch, 1976). Pretty *et al*. added an alternative hypothesis for this suggesting the prevention of light entry and exit into underlying fluorescent tissue by light scattering and a change in the chromophore's molecular environment resulted in fluorescence decrease (Pretty *et al.*, 2004). Thus, enamel autofluorescence continues to be poorly understood; As a result the accuracy and application of QLF remains debated when evaluating enamel erosion. However, the technique can be used either in the laboratory setting or *in vivo*, making it an extremely useful technique for clinical trials (Stookey, 2004).

Raman analysis is the spectroscopic measure, by means of measuring inelastic scattered light from the sample, of the molecular vibrational and rotational pattern of a structure under monochromatic (laser) light. When the laser encounters a target molecule the photon excites the molecule from its ground state to a virtual higher excitation state (thereby distinguishing this technique from fluorescence, by which the elevation to an excited state is a result of absorption). When the target molecule returns from its virtual excitation state a photon is emitted. The difference between the ground state and the virtual excitation state induces a shift in the emitted photon frequency and is known as Raman scattering. This inelastic scatter yields vibrational information regarding chemical bonds, each specific for a particular molecule. This technique is complementary to IR and can be useful when investigating chemical

changes to the enamel structure such as changes in carbonate content (Nishino *et al*, 1981).

1.12.3. MICRORADIOGRAPHY

Microradiography, in particular transverse microradiography (TMR) is a method used to assess quantitative morphological changes in the mineral content of dental materials using x-rays (Amaechi *et al.*, 1998). Small, thin sections (approximately 80 μm thick) are cut from the sample, which permit partial absorbance of x-rays, such as from a 20 minute exposure to a Cu(Kα) source. These are imaged on high resolution film prior to digitisation using a photomultiplier and analysis by computer software. More recently TMR imaging has become digitised and has been shown to provide accurate results for samples between 50-350 μm with a resolution of 2.0 μm (Darling *et al*., 2009). Software analysis allows for quantification of the amount of mineral lost and the depth of the lesion created (Elton *et al*., 2009) but the resolution is not suitable, especially when small erosion lesions, such as those created for this work, are examined.

1.12.4. PROFILOMETRY

Profilometry employs a physical stylus or optical tool (such as a laser) to scan the surface of a material, thereby providing information regarding the topography. A major drawback to optical and physical profilometry is the prerequisite that the surface be as flat as possible prior to scanning as some machines lack the detection range necessary to image large variations in height. Changes in surface height typically arise

from changes in surface morphology, such as curvature of the tooth, for example, a human canine. In order to avoid such changes in height or to remove the external cementum layer occasionally present on bovine enamel, samples are often ground flat and polished to remove scratches. In the case of human enamel samples this may result in the loss of the potentially highest concentration of fluoridated enamel, found at the surface of the enamel rod (Frostell *et al*., 1977), and as a result lead to inaccuracies of the true representation of the fluoride content of enamel. Furthermore, although computer software can mediate the effects of surface curvature, the erosion lesion depth result may be distorted.

Usually control measurements (baseline lesions) are initially obtained of the uneroded surface prior to exposure of the sample to an acid medium providing the sample may be accurately repositioned. The test surface is usually demarcated into a test area and one or two control areas using acrylic varnish or adhesive tape and subjected to an acid challenge. The sample is then rescanned and may then be compared to baseline lesion data for a direct comparison of treated and untreated samples.

Optical profilometry often lacks the resolving power of stylus profilometry (Hemingway, 2008). It has been suggested that lesions smaller than 2 μm are difficult to measure owing to this lack of resolving power (Stenhagen *et al*, 2010). However, contact profilometry has been found to be comparable with non-contact profilometry, for example: in acid exposures of dentine lasting 120 minutes (Ganss *et al*., 2009).

CONTACT PROFILOMETRY

Contact profilometry employs a physical stylus of varying dimensions (dependent on the experimental requirements) to raster scan across a section of a sample. Scanned sample areas may vary between nanometres up to millimetres, the former scan areas typically obtained using atomic force microscopy.

As mentioned previously, contact profilometry employs a physical stylus or tip attached to a cantilever with a reflective surface on the reverse side. A typical contact profilometry stylus can range between approximately 10 -20 μm in diameter and scans at a rate of 10 $mm.min^{-1}$ (Barbour & Rees, 2004; Schlueter *et al*., 2005). Stylus profilometers can image to a vertical resolution of 15 μm but may inaccurately report surface topography owing to the size of the stylus (Schlueter *et al*, 2005), as depicted in Figure 1.11.1:

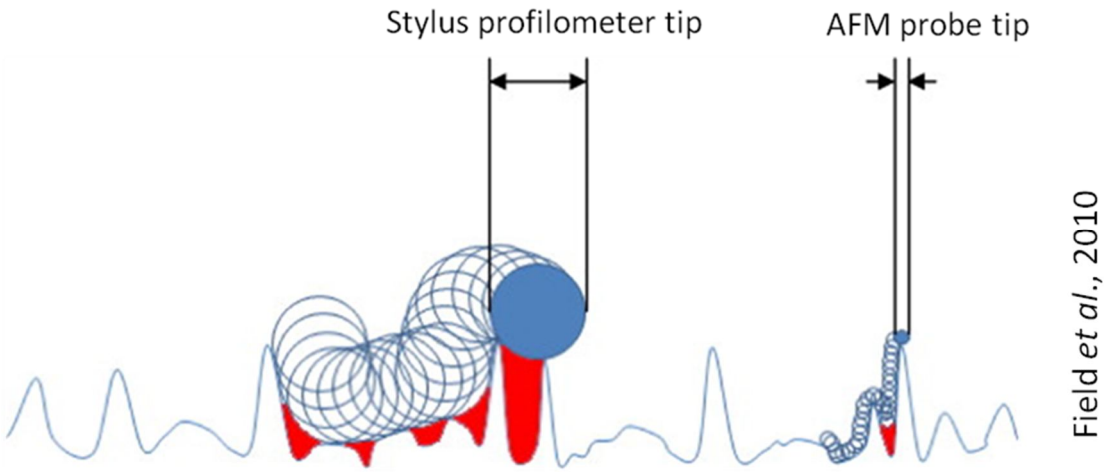

Figure 1.12-1: A stylistic comparison between the radius of a stylus (contact) profilometer and that of an AFM probe. While the stylus profilometer permits greater vertical movement, allowing for rougher samples to be images, fine detail of the surface topography is missed (highlighted in red areas underneath the stylus track) as the larger probe size does not permit these areas to be imaged.

An issue with stylus profilometry is the deformation of surface architecture by the stylus, particularly on previously softened enamel, as a result of contact loads of

~0.8 mN (Attin *et* al., 2009; Heurich *et al*., 2010). This may damage or distort the superficial surface of the sample, e.g.: scratching or by knocking off the peak of a projecting surface feature, and provide an erroneous result (Azzopardi *et al.*, 2001; Zhang *et al,* 2000; Field *et al.,* 2010). In order to minimise this potential risk, casts of the sample may be taken and scanned in lieu of the original (Rugg-Gunn *et al.*, 1998). Thus, should any distortion occur, the damaged imprint may be discarded while the original remains an accurate representation. This has a further benefit in that multiple copies may be made for evaluation but detail may be lost during the imprinting process.

NON-CONTACT PROFILOMETRY

Non-contact profilometry employs a light source, such as a blue laser with a wavelength of 470 nm (Stenhagen *et al*., 2010), as a substitute for a physical contact stylus to determine changes in topography (Hemingway, 2008). As with a fixed dimension stylus profilometer, the use of a single wavelength of light restricts the step height of the sample. One advantage of optical profilometry is the ability to switch scanning heads on the machine in order to vary the measurement dimensions of a particular sample (Imfeld, 1996). Alternatively, certain machines utilise a white light source, such as from a halogen lamp, meaning the measurement range is not restricted to one wavelength (Cross, *et al*., 2009).

Using the example of white light machines, the emitted beam is reflected through a beam splitter before being focussed on the sample. The separated wavelengths passing through the beam splitter corresponds to different heights, thus only one wavelength of the emitted light will be in focus for a given height. Reflected light from the sample passes back though an interferometer, for example a Mireau interferometer,

before passing through the beam splitter and is projected through a pinhole onto the sensor or camera. A surface map is generated by interferometry, the comparison of light wavelength reflected from the sample (Cross, *et al*., 2009).

The reproducibility of optical profilometry has been found to be not normally distributed but not significant from confocal microscopy and micrometre screw gauge measurements when evaluating both step height, roughness, as well as reflectivity from impression materials (Azzopardi *et al*., 2001; Rodriquez *et al*., 2009). However, particularly reflective samples may interfere with data interpretation (Barbour & Rees, 2004). Furthermore, transparent impression material samples, or those coloured similar to the emitted wavelength of the light source, have been shown to interfere with measurement dimensions (Rodriquez *et al*., 2009).

WHITE LIGHT INTERFEROMETRY

Like optical profilometry white light interferometry employs a confocal white light source but, unlike the former, the interference pattern of light generated by an interferometer (such as a Michelson interferometer, which splits the light into two or more paths) is independent of the light wavelength. Measurements rely on two or more wavelengths being analysed and the sample is in focus only when the maximum difference in light fringe coherence (or comparative similarities of wavelength properties) has been obtained, thus reducing focus error and making for a more precise measurement. The drawback to this method is that only one light frequency may be analysed at one time, thus powerful computers are required in order to deal with the data flow accurately and speedily (Wyant, 2010). Recently, machines have been produced with a vertical resolution of 0.01 nm but are not as effective at measuring in

the lateral plane as AFM, only having a lateral resolution of 0.35 μm (Blunt, 2006). The technique is therefore becoming more widely used in dental research owing to its increased speed and accuracy compared to other optical methods and the ability to image greater surface areas compared to AFM (Holme *et al*., 2005).

1.12.5. ELECTRON MICROSCOPY

Transmission- and scanning electron microscopy have been extensively used in dental research for imaging of thin section and surface topography respectively (Marshall & Lawless, 1981; Rios *et al*, 2007; Viera *et al*, 2006; Wang *et al*, 2006). These two techniques allow for high resolution imaging but in most instances are destructive to the sample.

In Transmission Electron Microscopy (TEM), a beam of high voltage electrons, generated at 300kV within a vacuum environment, are focussed by means of electromagnets and passed through a thin section of a sample (60-90 nm thick) onto a fluorescent viewing screen (Bodier-Houllé *et al*, 2000). The sample is coated with an electron dense medium, such as osmium tetroxide (OsO_4) and the final image product is a function of electron density within the sample and may have a Scherzer resolution (point resolution) up to 0.19 nm , which can permit the study of crystal interrelationships at the dentino-enamel junction (Bodier-Houllé *et al*, 2000).

Scanning Electron Microscopy (SEM) functions in a similar manner to TEM but does not have the resolving power of the latter. However, SEM is able to image larger samples as this technique employs raster scanning of the electron beam across the surface of the sample (Goldstein *et al*., 2003). By contrast to TEM, in which electrons

penetrate through the sample surface, the beam raster scanning of SEM results in the effects of the electron beam interactions with target molecules being measured, such as secondary electron release (the most common mode of imaging), backscatter electrons and x-rays, in order to generate an image (Goldstein *et al*., 2003). Furthermore, the large optical depth of field of SEM enables 3-dimensional representative images, a feature not available using TEM, which result from the different contrast between various structures when viewed on the monitor; This contrast arises from the varying quantities of secondary electrons generated from different parts of the specimen when contacted by the electron beam (Bozzola & Russell, 1998).

The analysis of backscattered electrons, which originate as high powered electrons reflected (backscattered) from the target surface provide information regarding different chemical compositions. This is a result of atoms with a high atomic number reflecting electrons (from the sample surface) back with greater intensity compared to atoms with a low molecular weight. The secondary release of x-rays from target molecules within a sample allows for quantitative identification of elements present within the substrate, such as enamel, in a non-destructive manner while obtaining images of the targeted area (Goldstein *et al*, 2003), a process termed x-ray dispersive spectroscopy.

1.12.6. FOCUSSED ION BEAM SEM

The focussed ion beam is a component which may be added onto the SEM module for purposes of milling target areas but also permits the deposition of heavy ions, such as tungsten, on the surface of a designated target. In contrast to the SEM

module, which employs a non-destructive electron source to visualise the target sample, the FIB module employs heavier, liquid ion sources, such as high energy gallium ions, which may be controlled with nanometre precision by controlling the intensity and energy of the ion beam. Gallium ions displace neutral surface atoms or ions, which results in a clean, minimal residue milling process. The positioning of the electron and focussed ion beams, at a 54° angle from each other but both focussing on a coincident point, permits immediate imaging of the effects of ion beam milling and/or deposition.

1.12.7. ATOMIC FORCE MICROSCOPY

The atomic force microscope employs a flexible cantilevered probe to obtain image and hardness data of a sample. The basic unit consists of a monochromatic laser, which is reflected back from the cantilever to a photosensitive diode linked to a computer.

The cantilever is a dual construction of microfabricated Si or Si_3N_4 probe, with a tip radius between 10-60 μm, attached to the underside of a flexible, reflective cantilever with a defined spring constant. Dependant on the scan requirements, different tip aspect ratios may be employed, for example to permit greater depth of field a high aspect ratio tip is employed. However, sample roughness should not exceed the height of the tip as this will make imaging impossible (Morris *et al.*, 1999).

The scanning mechanism consists of a piezo-electric ceramic holding either the sample of the tip-cantilever complex. The ceramic expands when a potential difference is applied (in the x+, x-, y+, y- and z direction) resulting in highly controlled *x,y,z*-axis

motion. As such, this controlled motion of the scanner means that the tip may be positioned either in contact or relative proximity to the sample before scanning commences (Morris *et al*., 1999).

Vertical and lateral flexion of the tip-cantilever complex is detected using a position sensitive photodiode, which also has the benefit of amplifying the incoming signal. A laser, reflected from the reverse of the cantilever, is directed into the diode, which is subdivided into four segments (A,B,C and D), illustrated below.

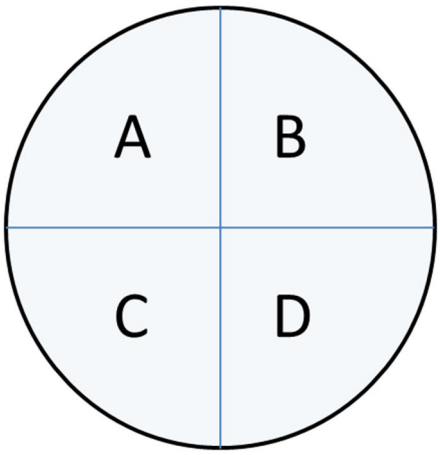

Figure 1.12-2: Schematic representation of AFM photodiode to show the relationship between the four segments and how this relates to tip motion detection.

Changes in the angle of laser deflection, resulting from changes in topography, result in a change in the spot intensity of different segments. The difference of light intensity between the top two segments (A+B) and the lower two segments (C+D) determines the direction of vertical flexion in the tip. Likewise, changes in intensity between the lateral segments (A+D) and (B+D) determines lateral motion of the tip. This also permits the distinguishing between friction forces during scanning and

topography (Morris *et al.*, 1999). The information from the photodiode is modulated by a computer feedback loop which controls the distance of the tip to the sample. Computer software is used to translate this signal deflection into an image map (Lippert, 2003). An example of how the AFM functions is depicted in Figure 1.12-3:

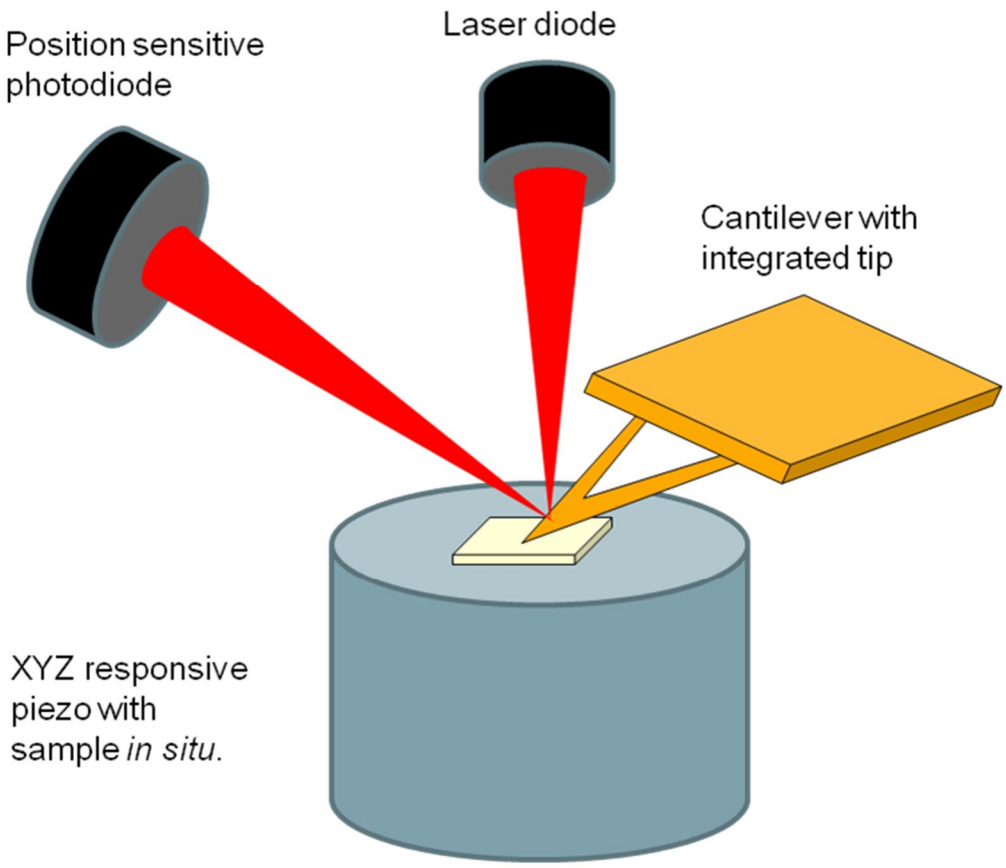

Figure 1.12-3: Schematic representation of the function of an AFM.

There are significant differences in the resolution between AFM and other stylus profilometers[§]: Carbon nanotube tips have been used to image inorganic substrates, such as gold nanoparticles, down to a resolution of 3 nm, while biological substrates, such as DNA, have been imaged to a resolution of 3.5-5 nm (Hafner *et al.*, 2001)

[§] See section "1.11.4: Profilometry"

Three modes of AFM are commonly employed in obtaining images of a sample: contact mode, non contact and tapping mode: Contact mode images are obtained by a similar principle as stylus profilometry: a flexible probe in direct contact with the surface, under controlled applied load, is raster scanned over the surface of a sample. The flexion of the tip in response to topographical changes results in a deflection of the reflected laser. However, the high frictional forces generated by the cantilever moving over the surface make this technique suitable for hard surfaces (such as enamel) only (Lippert, 2003).

Dynamic mode (non-contact) images are obtained by raster scanning the oscillating probe close to its resonant frequency along the topography and, in the case of tapping mode AFM, intermittently contacting the surface. This method removes any shear stress damage which may result on soft samples and reduce image quality.

Tapping AFM has the tip oscillating at a higher frequency than non-contact AFM, typically an order of magnitude greater. The tip is kept at a constant oscillation from the surface, and gradually brought closer to the sample surface. Intermittent contact of the tip to the sample results in a loss of energy manifesting as a significant reduction of the tip amplitude (Jandt, 2001), which is then recorded by the photodiode and compared with the initial set value to provide information regarding the surface topography (Lippert, 2003). This technique has the advantage of being able to image samples submerged in fluid, making it useful for work involving the salivary pellicle (Jandt, 2001).

Non-contact AFM employs even less force than that utilised by tapping mode AFM. The tip is placed approximately 1-10 nm away from the sample surface (Jandt, 2003) and the results of this type of scan are determined by intermolecular forces. Van der Waals forces acting close to a sample surface, the dominant force at this distance,

attract the tip toward the sample, thereby decreasing the tip oscillation. The AFM records changes in topography by recording the distance changes required by the AFM in order to maintain a constant tip oscillation (Lipert, 2003).

1.12.8. HARDNESS

The evaluation of enamel softening utilising surface indentation to evaluate the hardness of a material and is still regularly used in a number of experimental protocols (Devlin *et al.*, 2006, Jaeggi & Lussi, 1999; Preston *et al.*, 2007). Hardness testing measures the resistance of a material to plastic, or permanent deformation by a sharp object under a constant load. Two units are most commonly used in classic bulk indentation studies: Knoop and Vickers hardness numbers. Each method is suited to a particular type of measurement required, as a result of which, each possess distinct pyramid geometries. The hardness number is calculated for a specific hardness test and is derived from the depth of penetration of the indenter (the length of the indenter arm, measured microscopically) and applied force (Lippert, 2003; British standards, 2005). These measurement values, relating to enamel as a bioceramic (as opposed to metallic substances, which form the basis of the equations) are not readily convertible between various hardness numbers, i.e.: Knoop to Vickers and *vice versa*, relying as they do on different measurement variables (the length of the pyramid arm) in order to obtain the final result (British standards, 2005). Vickers hardness is calculated using the formula:

$$VH = \frac{1854.4F}{d^2}$$

VH represents the Vickers hardness number, *F* represents the load applied (g), d^2 represents the average impression length (μm) and 1854.4 is a constant representing

the relationship between the indenter geometry, the load applied and the diagonal (Blau, 1983; Instron, 2010). By comparison, Knoop hardness is calculated using the formula:

$$KHN = \frac{14229F}{D^2}$$

KHN represents the Knoop hardness number, F represents the load applied (g), D^2 represents the length of the major impression diagonal (μm) and 14229 a correction factor (Blau, 1983).

Thus, problems may arise when comparing work which utilises a particular method, for example Knoop, against other work employing Vickers hardness.

Micro-indentation and atomic force microscope nano-indentation continue to be widely used in the literature (Lussi *et* al., 2000; Lippert, 2003; Hara & Zero, 2008). These techniques employ indentation over small areas, sometimes to individual prisms, and to increasingly smaller depths, micrometre to tens of micrometres and nanometre (up to <100nm) scale, respectively (Arends & Ten Bosch, 1992; Lippert *et al.*, 2004a). AFM nano-indentation carries the additional benefit of being able to image samples before and after indentation (Lippert *et al.*, 2004b). Microhardness measurements are fast and reproducible (Lippert, 2003) and capable of investigating the early effects of dental erosion but more limited with respect to more advanced lesions, such as those in excess of 30 minutes acid exposure (Hara & Zero, 2008).

This list has provided a brief overview of some of the more common techniques used to evaluate dental erosion. However, the study of the effects of dental erosion is only one aspect of overall dental health; the prevention of erosion can be brought about

by modifications of behaviour or in consumable product composition and will be discussed in the next section.

1.13. EXPERIMENTAL EROSION MODELS

Two laboratory models have been principally employed in the investigation of enamel erosion.

In the first example, a single sample may be used for a single exposure to erosive media. Such use of samples is most prevalent in work employing chemical analysis of dissolved enamel ions using both powdered enamel (Buzalaf *et al*., 2006) or individual samples (Eisenburger, 2009). In addition, this method has been employed when subjecting test samples to certain techniques which require direct interference with the sample. Such interference makes further use of the sample difficult, such as gold/palladium coating in scanning electron microscopy (Eisenburger *et al*., 2004).

An alternative to this is the use of a single sample, which is repeatedly exposed to acid media for as many times as is required (Attin *et al*., 2007; White *et al*., 2010). The purpose of this is often to determine the effects of repeated exposure of enamel to acid challenges. However, unless baseline measurements have been taken prior to the experiment, which may be used as a reference for the erosive challenge, this method requires a realignment of the tape demarking the erosion lesion, which may adversely affect the result (White *et al*., 2010; Hughes *et al*., 2004).

A direct comparison of theses protocols will be undertaken in a later chapter, in order to evaluate differences between these protocols.

1.14. AIMS AND OBJECTIVES OF THIS WORK

With the increasing prevalence of dental erosion, particularly among younger people, there is an increasing need to be able to accurately model this pathology. Bovine enamel is commonly employed in enamel erosion studies owing to the paucity of human dentition available for research purposes and recent legislation governing human tissue. Despite bovine enamel's comparative ultrastructural similarities to human enamel[**], it has been shown to differ in its chemical composition, which impacts on its behaviour when exposed to an acid erosion challenge.

The literature contains numerous publications evaluating a number of factors all linked to dental erosion but no consensus is apparent, most likely attributed to the variety of protocols individual groups use to generate their results (Laurance-Young, 2011). Furthermore, it was identified that most of the models used to emulate dental erosion attributed to acidic beverage consumption involved durations of acid exposure to substrate which are not commensurate with the repeated intake behaviour associated with systematic drinking (Amaechi *et al.*, 1999; West *et al.*, 2005; White *et al.*, 2010).

This work has a two-fold aim: **First, we aim to explore the effect of a short term acid exposure on enamel, with special emphasis on the first 60 seconds**. We hypothesise that there should be no significant difference between the early and later durations (for example, a 10 minute exposure) of an acid challenge but the relative paucity of literature exploring this would benefit from additional work (White *et al.*,

[**] Reviewed in Section 1.10.

2010). Bulk tissue loss will be assessed using optical profilometry, hardness measurements and scanning electron microscopy.

Second, we will investigate the suitability of bovine enamel as a substitute for human enamel during short term acid exposure experiments as expounded by Mellberg (1992) using the same techniques as those above. Again, we anticipate there will be no statistically significant difference between these two substrates, thus providing further support for the acceptance of bovine material in dental hard tissue studies.

In addition to this, we will also explore some secondary questions, for example: the effects of minimal doses of fluoride on the remineralisation of enamel. This will be done with the aim of determining at which minimum concentration the efficacy of fluoride begins to decline. Finally, we would examine the effect of alternative compounds suggested in the literature to have remineralising properties and compare them to a fluoride dose often employed in erosion research.

The number of human samples to be used in this study is largely reliant on the ready supply of clinical material, which owing to the nature of a majority of the extracted teeth, are unsuitable for use. Thus sample numbers will, of necessity, have to be quite low. A power analysis performed by Attin showed a satisfactory sample size of n = 5 (Attin *et* al., 2009) while other works have employed a range of sample sizes from n = 6 to n =18 (Rios *et al.*, 2008; Ganss *et al.*, 2000; Amaechi *et al.*, 1999; Eisenburger *et al.,* 2000; Attin *et al.*, 2003; White *et al.*, 2010). Therefore, our use of sample sizes of n = 8 fits well with published work.

CHAPTER 2

MATERIALS & METHODS

2.1.COLLECTION OF DENTAL MATERIAL

2.1.1. TISSUE BANK & HTA

The tissue bank for this body of work was established on the premises of the Eastman Dental Institute, 256 Gray's Inn Road, London, WC1X 8LD, under the license of University College London and supervision of the HTA representative Dr Vehid Salih. All samples, together with signed, informed consent, were received from Oral Surgery as routine surgical waste, annonymised by the principal investigator and stored in a locked refrigerator on the premises. The only access to this fridge was by the principal investigator (Paul Laurance-Young). An ethical review was not required following an enquiry to the National Research Ethics Service.

2.1.2. HUMAN ENAMEL

Human molars were obtained as surgical waste from patients aged 18 – 45 years, attending the department of Oral Surgery at the Eastman Dental Hospital, Gray's Inn Road, London.

Individual, resealable packs containing a plastic container (Sterilin, UK) filled with ethanol and standard consent forms (Appendix A) were supplied to the clinic. Samples were removed as part of routine surgery and placed into the ethanol-filled container for a minimum of 48 hours in order to minimise potential risk from pathogenic organisms, e.g.: bacteria, HIV, Hep B & C. All samples were received with signed informed patient consent.

After 48 hours the samples were removed from the ethanol and allocated an individual, unique numerical identifier *in lieu* of name in order to anonymise them. The samples were then debrided of any residual soft tissues using a scalpel blade and running water and examined for evidence of caries and cracks. Unsuitable samples were disposed of by incineration. The remaining samples were then returned to their individually numerically identifiable sample container, now filled with tap water and thymol (BDH, UK), and refrigerated in a secure, specially designated fridge. Hard copy consent forms were stored in a locked, limited access room separate from the sample store.

2.1.3. BOVINE ENAMEL

Samples of bovine incisors were obtained from slaughtered beef cattle less than 30 months (F. Conisbee & Son, Surrey, UK), stored in tap water and thymol (BDH, UK), courtesy of GlaxoSmithKline Oral Healthcare Research Laboratories, Weybridge.

These samples were received as a batch and stored as such in a secure, specially designated fridge.

2.2.MEASUREMENT OF BULK TISSUE LOSS

2.2.1. OPTICAL PROFILOMETRY

Optical profilometry permits the non-destructive investigation of surface topography when investigating bulk tissue loss, such as occurs in dental erosion. A schematic representation of an optical profilometer is shown in Figure 2.2-1. The machine employed for this work was a Proscan 1000 (Scantron, Taunton, UK)

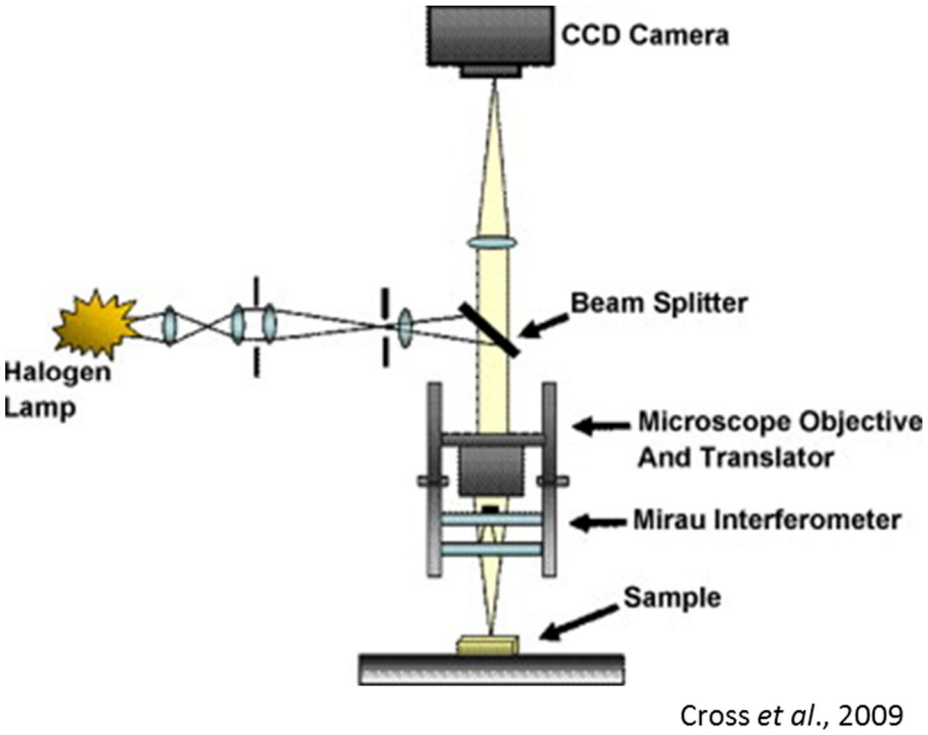

Figure 2.2-1: Generalised schematic representation of an optical profilometer.

The stage is motorised using ball bearings permitting a smooth movement in the *x-y* axis with a straight line accuracy of ±1.0 µm. A sample was aligned on the stage and a 780 nm wavelength laser optimised for height to 120 µm above the sample using a

monochromic sensor and adjusted by means of a dial at the top of the height adjustable rack. The laser had a spot size of 12 μm and a resolution of 0.02 μm, taking samples every 5 μm along the raster scan. A video camera permitted visualisation of the sample to confirm alignment and observe the progress of scanning. The scan dimensions were input into the software, typically a 3 x 5 mm^2 area, along with the scan co-ordinates, light intensity gain and reading average. Calibration was performed using specially made standards using 30, 10, 5 and 1 μm grooves. The results from these calibration scans were not significant from the standard. Eight samples from each species were investigated for each acid (n = 8).

Equipment restrictions meant that the entire scanned image could not be imported for analysis, owing to the size of the original file. Therefore the image had to be cropped prior to export, which was done by removing the borders of areas of uneroded enamel from the image. The scan was auto levelled to correct for any incline of the sample (e.g.: during embedding) and exported as a **.txt* file using the system software (Scantron Software v2.1.0).

The resulting file was imported to Microsoft Excel™ as a spread sheet[††]. Each line of data represented a single raster scan from the Proscan. The data was copied to a new sheet where the data corresponding to the erosion lesion was manually removed line by line. From the remaining data it was possible to calculate the individual sample slope and intercept, which would be imported into the preceding spread sheet. The average lesion depth, including tape height, could then be calculated using these values on a line-by-line basis. The average was then taken of all the individual lesion depths from each sample.

[††] See Appendix C – Examples of raw data

This technique also permitted the calculation of the mean tape height. This was then subtracted from the sample data result to provide the mean lesion depth, which in turn was statistically analysed using Origin 8.1.

2.2.2. WHITE LIGHT INTERFEROMETRY

Samples consisted of five specimens of human enamel embedded in epoxy resin. The samples were fixed to an aluminium mount on the stage. Images were obtained using a confocal white light sensor (XYRIS 4000 WL, TaiCaan Technologies Ltd., Southampton, UK) with a resolution of 0.01 μm, a spot size of 7 μm. The area scanned was 5 x 3 mm^2 with a 10 μm step distance. Images were viewed and analysed using surface analysis software (Boddies 2D v1.4, TaiCaan Technologies Ltd, Southampton, UK), which enabled analysis of the images to be performed following levelling of the reference areas, with an accuracy and resolution of 0.068 μm and a 0.016 μm, respectively. The experimental area was then identified and demarked and height measurements from the top of the reference area to the base of the lesion were taken, as shown in Appendix C – Examples of raw data. Eight samples from each species were investigated for each acid (n = 8)

2.2.3. QUANTITATIVE LIGHT FLUORESCENCE

Eight samples of human or bovine enamel were examined using the protocol described in section 2.9.2. Once the protocol was complete, the tape was removed and

the sample was ready for QLF analysis. The QLF was calibrated using a colour grid corresponding to defined depths. This calibration grid was placed into a darkened scanning area, the grid correctly aligned and an image obtained under blue light (peak wavelength of 370 nm) captured through a yellow light filter (peak wavelength of 570 nm). Once the calibration reference was acquired, a sample, free of adhesive tape and any surface residue, was placed in the capture area and an image obtained encompassing a defined area of interest. Backscattered and reflected light from the sample was removed using digital image grabbing software. The area of interest, usually consisting of the entire lesion, was demarcated into two using supplied software with one area representing the uneroded control and the other the erosion lesion as depicted in Figure 2.2-2. Eight samples from each species were investigated for each acid (n = 8)

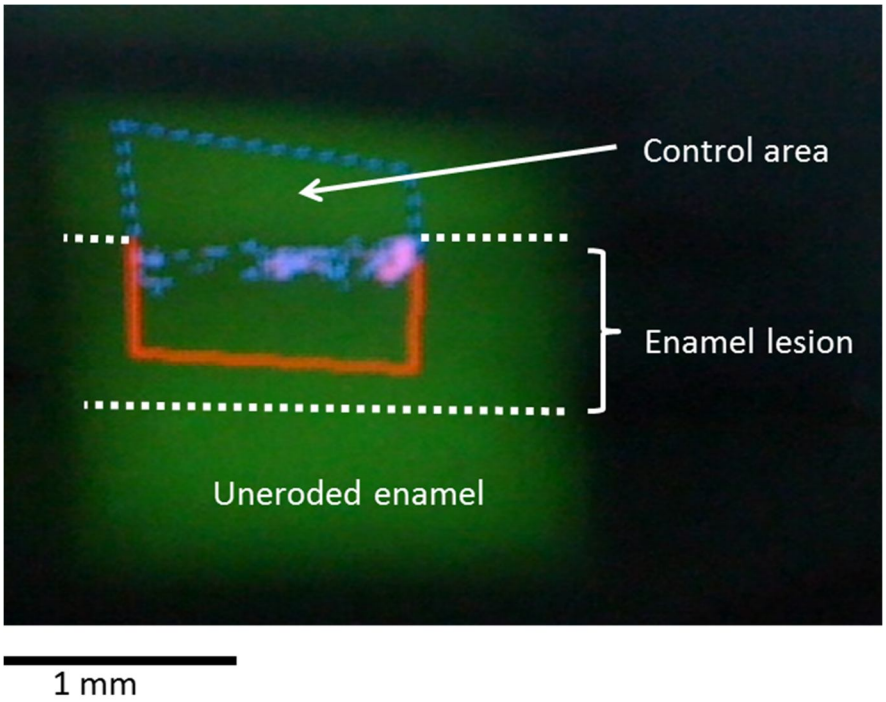

Figure 2.2-2: Image of a bovine enamel sample imaged using QLF, showing the demarcation of control and erosion lesion areas.

The software calculated differences in reflected light and supplied the data as lesion area (mm^2), lesion depth (DF in %) and lesion volume (DQ in mm^2.%). The results were tabulated and statistically analysed using Origin statistical software.

2.2.4. ATOMIC FORCE MICROSCOPY

Two atomic force instruments were utilised during this work; a Park XE-100 (Park Systems Corp, Suwon, Korea), while force *versus* distance measurements were obtained using a Dimension 3100 (Veeco, Santa Barbara, CA).

Eight samples from each species were investigated for each acid (n = 8). The samples of polished human and bovine enamel were mounted to a metal disc using thin double sided tape. The sample was then placed onto the magnetised stage, which held the sample securely in place. For imaging purposes Si_3N_4 tips with a spring constant of 0.6 $N.m^{-1}$ were employed (µMasch, Talinn, Estonia) to scan an area up to 40 μm^2 at a resolution of 512 x 512 pixels with a typical set point of 2 nN and a z-servo gain of 5. Images were analysed using supplied software (XEP, Park Systems, Suwon, Korea).

Unlike the imaging protocol, force *versus* distance curves were obtained using cantilevers with a spring constant of 40 $N.m^{-1}$ (µMasch, Talinn, Estonia). The spring constant was manufacturer calibrated prior to delivery, as this was an affordable commodity. The tip was replaced after eight specimens had been tested in order to maintain sharpness. Areas of the erosion lesion were selected and quickly imaged at low resolution (using the 40 $N.m^{-1}$ cantilever) to determine whether or not they appropriate (free from debris or scratches caused by grinding) before an indentation was performed. Eight indentations were performed at random locations along the

erosion window for each sample using a 60 $nm.V^{-1}$ sensitivity deflection. The data was then analysed using Nanoscope 6.14 software (Veeco, Santa Barbara, USA) and results further anaylsed using Origin statistical software.

2.2.5. SCANNING ELECTRON MICROSCOPY

Two scanning electron microscopes were employed during this work. The first, a Jeol JSM-5410LV SEM, was used for imaging and energy dispersive x-ray spectroscopy (EDX), while the latter, a Carl Zeiss XB1540 Cross Beam (Figure 2.2-4), was used for imaging and focussed ion beam SEM. The Jeol SEM employed 15 kV for imaging, while the Carl Zeiss SEM employed 5 kV owing to the improved image quality of this more advanced instrument.

Eight samples from each species were investigated for each acid (n = 8). The samples were sputter-coated with either gold or gold palladium for 1 or 2 minutes prior to visualisation, dependent on final surface covering. Both scanning electron microscopes were field emission SEM instruments. The EDX spectroscope, attached to the Jeol SEM, used 25 keV and an average of 500-12000 counts. The focussed ion beam attachment (Orsay Physics Canion 31) for the Carl Zeiss XB1540 SEM functioned using 30kV and 200 pA and could be rotated to 54° relative to the SEM field of view, permitting later observations of the interior of the milled area (represented schematically below).

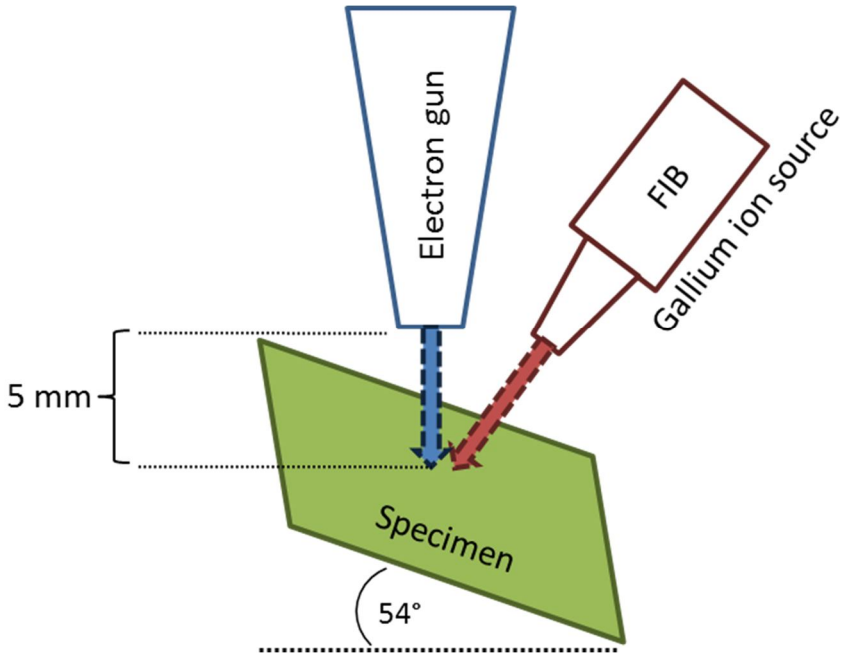

Figure 2.2-3: Schematic representation of the FIB and electron gun configuration in relation to the movable stage.

Milling of the sample was achieved using a liquid metal ion source (Gallium), which was focussed through apertures onto a designated target area using an electromagnetic field.

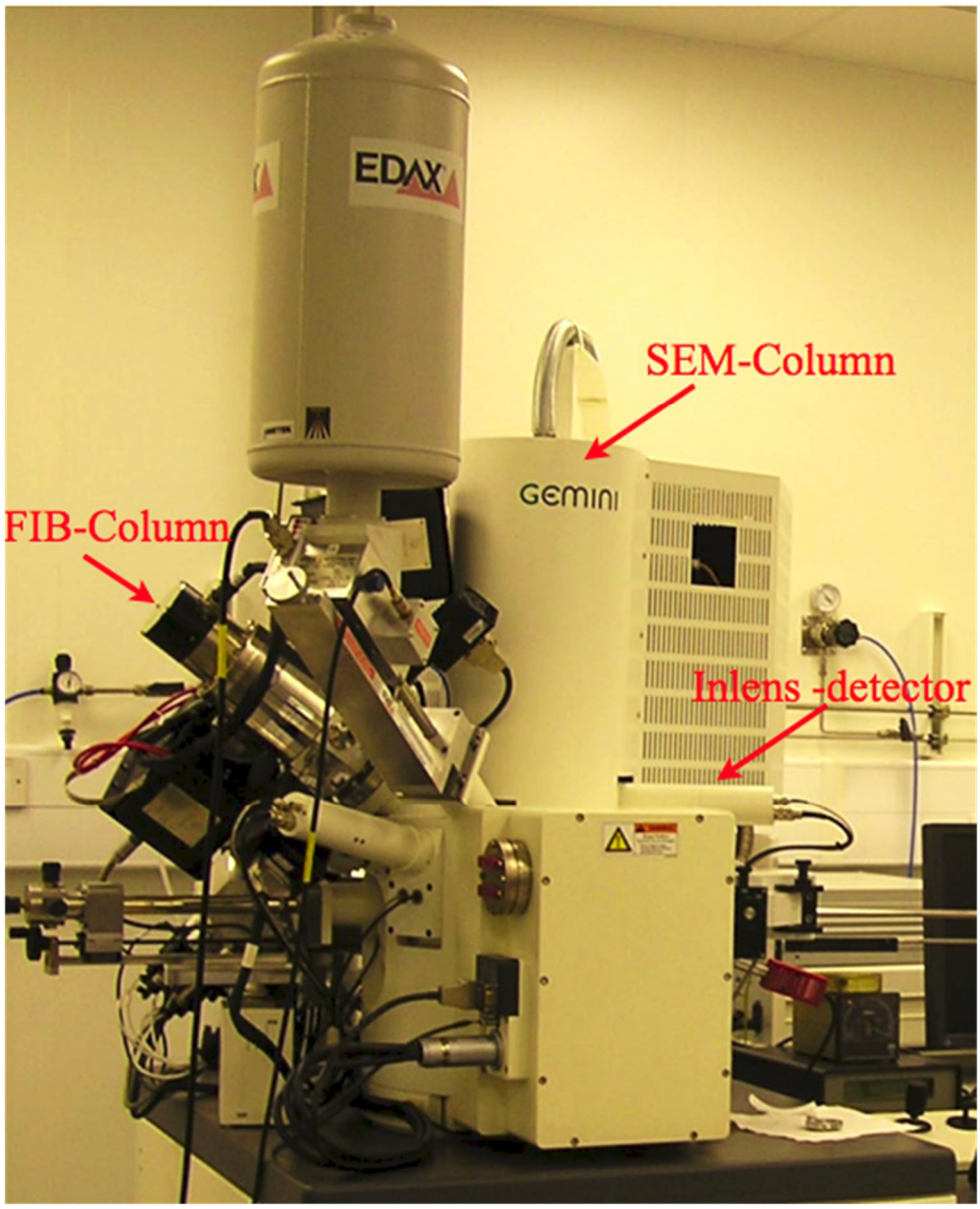

Figure 2.2-4: Carl Zeiss XB1540 Cross Beam scanning electron microscope with focussed ion beam attachment.

2.3. SAMPLE PREPARATION

2.3.1. SECTIONING

Attempts were made to minimise any deviation of protocol with respect to species. However, given the morphological differences between the samples, it was not possible to cut and trim bovine and human enamel samples in an identical manner.

Non-carious bovine teeth, free of cracks and surface cementum layer were selected for experimental use. The samples were bisected using a rotary saw with twin-mounted, diamond-tipped copper blades (Testbourne, UK - as shown in Figure 2.3-1), removing a 3 mm cross-section from the middle of the tooth. This was done to minimise any potential error which would result from material degradation attributed to wear on the occlusal surface and damage during extraction.

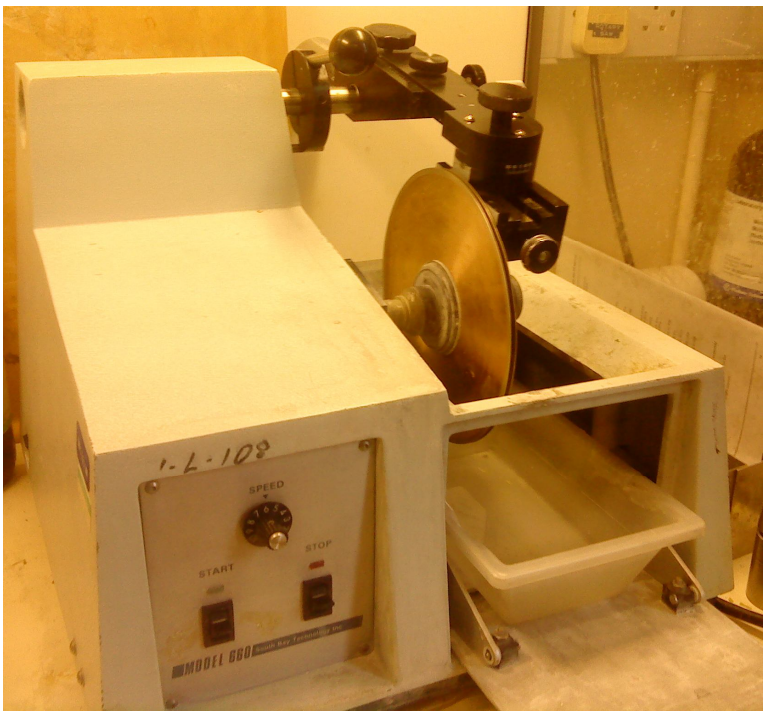

Figure 2.3-1: Testbourne Rotary saw with twin mounted diamond tipped copper blades.

The cross section then had the lingual surface removed and was then bisected again, producing a matched pair each approximately 3 mm^2. These were separated for research purposes so that no two test samples originated from the same animal, which could potentially interfere with the statistics.

Figure 2.3-2 shows the process of creating the human test samples. Non-carious, debrided human samples had the crown separated from the root using a rotary saw fitted with a single diamond-tipped copper blade (Testbourne, UK). The crown was then bisected along the vertical plane, maximising available flat surfaces on the lingual plane using a hand-held rotary saw (Dremel, UK) to provide a matched pair with the maximum flat surface area.

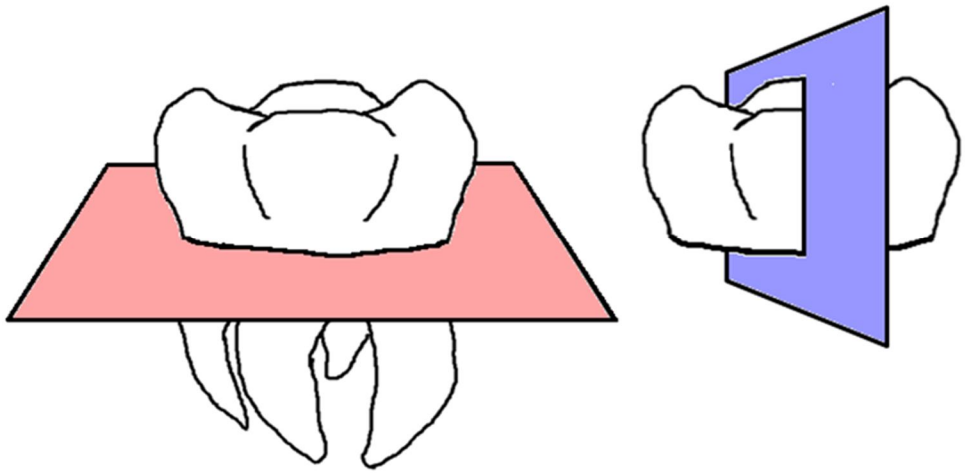

Figure 2.3-2: Sectioning of a human tooth. The left image shows how the crown is resected from the root along the horizontal plane. The image on the right shows how the crown is then bisected along the vertical plane to produce matched sample pairs.

Matched pairs were separated from each other to ensure that no two test samples originated from the same patient, which could potentially interfere with the statistical analysis.

2.3.2. EMBEDDING, GRINDING AND POLISHING

Samples of hard dental material, be it bovine or human, were placed enamel side down in hard polypropylene moulds and embedded using an ultra-low shrinkage, dry-curing epoxy resin (Epoxy-20, Struers, UK) for 24 hours.

Grinding of the embedded enamel samples removed any superficial debris present (or cementum layer, in the case of bovine enamel) as well as levelling the surface from potential tooth curvature. Polishing removed scratches present on the enamel surface following grinding.

Minimal grinding and polishing was used, only exposing as much surface area as was required, in order to limit the loss of enamel from the surface and so restrict potential error. This error may occur as a result of reduced hardness occurring at greater depth, as reported by Meredith *et al.* (1996), attributed to the change in enamel chemical composition (Cuy *et al.*, 2002). The samples were initially ground using an orbital grinder (LaboForce 5/LabPol1, Struers, UK) and 1200- followed by 2400 grade silicon-carbide grit paper. Samples having been excessively ground or polished and showing a potential for dentine exposure, illustrated by a change in enamel colour from pearlescent to opaque yellow, were discarded. Once polishing was complete the samples were subjected to ultrasonication in deionised water for 30 seconds to remove any extraneous grinding and polishing debris, a finding which was confirmed using electron microscopy. Once ultrasonication was complete, the samples were then left to air dry. Samples for which the underlying dentine was likely to be exposed, or which were too thinly polished were removed from the study.

2.4. STATISTICAL ANALYSIS

The data were analysed using Origin (versions 7.5 and 8.1) statistical and graphing software. Variation was expressed as either standard error of the mean (SE) or standard deviation, both provided in parenthesis.

Data was initially analysed using Levene's test to assess the quality of the data distribution in order to select the appropriate parametric or non-parametric test.

Where comparative data were normally distributed it was analysed using a parametric two sample or paired T-test (the latter if the n values for comparative data were equal) as well as ANOVA. Where data was skewed (or non-parametric) Mann-Whitney U-tests were performed, together with multiple sample Kruskall-Wallis analysis of variance. A table summarising these tests is provided in Table 2.4-1:

	Parametric test	Non-parametric tests
Comparing two means	Paired T-test	Mann-Whitney U test
	2 sample T-test	
Comparing multiple means	ANOVA	Kruskall-Wallis test

Table 2.4-1: Statistical tests employed during this work

Box-and-whisker plots were a useful method of demonstrating a large quantity of statistical data in one graph, including the mean, median and variance, as depicted in Figure 2.4-1.

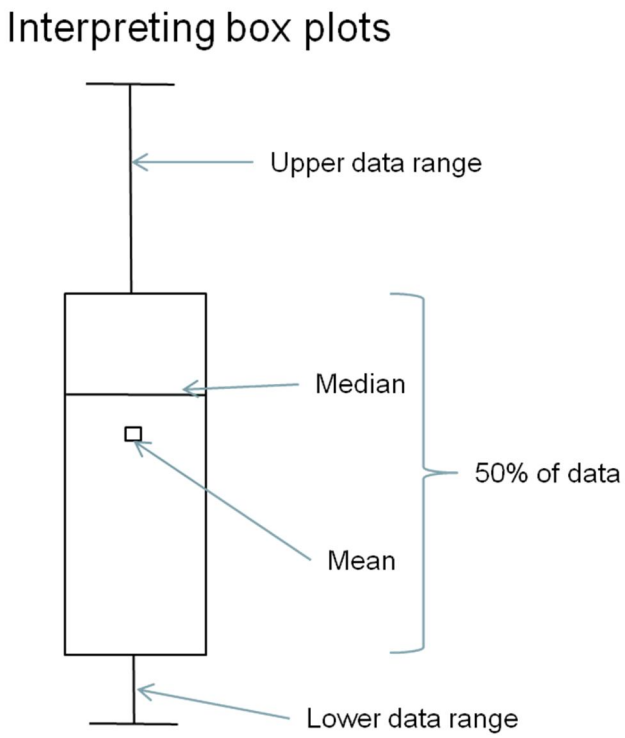

Figure 2.4-1: Interpretation of box-and-whisker plot showing the median and interquartile range (Q1-Q3), represented as 50% of the data.

The small, hollow square, inside the larger rectangle, denotes the sample mean, while the horizontal line within the rectangle denotes median values. The hollow rectangle denotes 50% of the data surrounding the mean, corresponding to the interquartile range (Q1-Q3). The whiskers at either end of the rectangle represent the maximum and minimum data values.

Where applicable correlation of the data was performed using an adjusted R^2 test (R^2_a). R^2_a only increases if additional terms, added to the equation, improve the model more than may be encountered by chance. Thus, if additional terms improve the model more than will be encountered by chance, R^2_a will increase.

2.5. EROSION WINDOW

A number of works in the literature employ epoxy varnish to create an erosion window by applying the varnish to either side of the desired test area prior to acid exposure (Attin *et al*., 2007; Elton *et al*., 2009; Venasakulchai *et al*., 2010). The removal of this varnish layer following the acid exposure is usually achieved by gentle rubbing with cotton wool dipped in acetone or ethyl acetate. We hypothesised that this motion could impinge on the erosion lesion and potentially interfere with the experimental results by removing previously softened enamel, in a manner similar to abrasion.

An alternative to this method is the application of an adhesive tape, usually one that is cellulose based (White *et al.,* 2010). Given the expected small lesion depths anticipated using low acid concentrations for a short duration the appropriate selection of an adhesive tape media was important. The tape had to remain adherent to both enamel and epoxy resin in acidified aqueous conditions with minimal water absorption. This brief work set out to examine the effectiveness of commercially available cellulose tape (Scotch®, 3M, UK) against biaxially-oriented polyethylene terephthalate – commercially known as mylar – tape. Mylar is known for its thermostability and resistance to swelling in aqueous media but has not been evaluated against the more commonly used cellulose tape.

EVALUATION OF TAPE MEDIA

Two samples of epoxy resin (Epoxy-20, Struers, UK) were generated using hard polypropylene moulds. One sample was allocated to each tape type. Two strips of mylar

and Scotch® tape were then applied in parallel as would be used experimentally‡‡. The samples were then scanned using an optical profilometer to obtain base-line results before being immersed in deionised water for 10 minutes on an orbital shaker (Stuart SSM1, Bibby Scientific, Staffs, UK) at 100 rpm. The samples were then removed from the water and allowed to air dry before being scanned again to determine by how much the tape had swollen. Statistical analysis was performed using Origin 8.1 statistical software and the results presented in Figure 2.5-1.

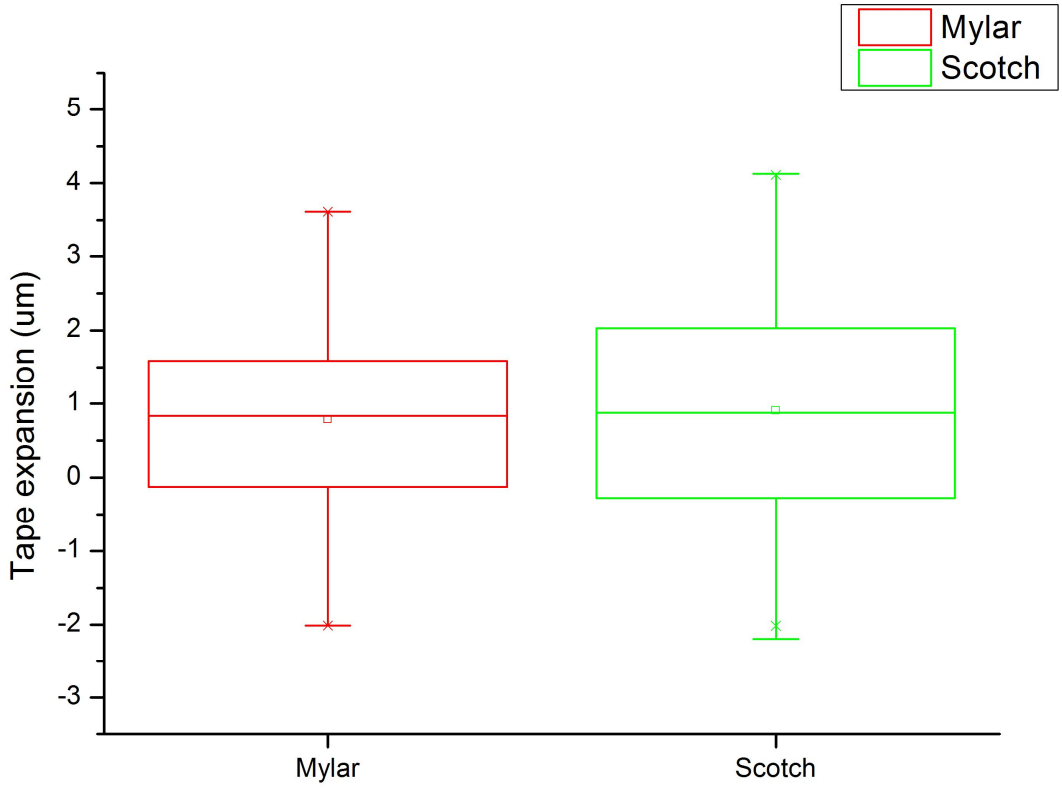

Figure 2.5-1: Comparison of the difference between the control and expanded Mylar and Scotch® tapes.

Mylar had a pre-test mean height of 63.72 μm (±0.14) and Scotch® tape had a pre-test mean height of 57.57 μm (±0.17). Following a 10 minute exposure to an aqueous medium Mylar tape had a mean height of 63.24 μm (±0.33) and an adjusted

‡‡ See section 2.4: Demarcation of erosion window

Chi-squared value of 0.38, while Scotch® tape had a mean height of 59.21 μm (±0.16) an adjusted Chi-squared value of 0.53. The data were not normally distributed for both sets of intra-sample data, showing greater numbers of low values. A non-parametric Mann-Whitney U-test showed there were significant differences between the pre-test and post-test samples regardless of the type of tape used ($p = 0.03$). However, when the differences between expanded Mylar and control Mylar tape was directly compared to expanded Scotch® tape and control Scotch® tape, no significant difference was found between the two ($p = 0.62$). Given the lack of significant difference between the two tape types, it was decided that the cellulose based Scotch® would be appropriate for the experimental purposes.

2.6. DEMARCATION OF EROSION WINDOW

A previously established protocol by GSK was employed to demark the erosion window using cellulose tape (Scotch®, 3M, UK). Two 5 mm strips of tape were laid parallel to each other approximately 1 mm apart as shown in Figure 2.6-1. This provided a control area present either side of the erosion window with the central exposed area running the length of the exposed enamel surface.

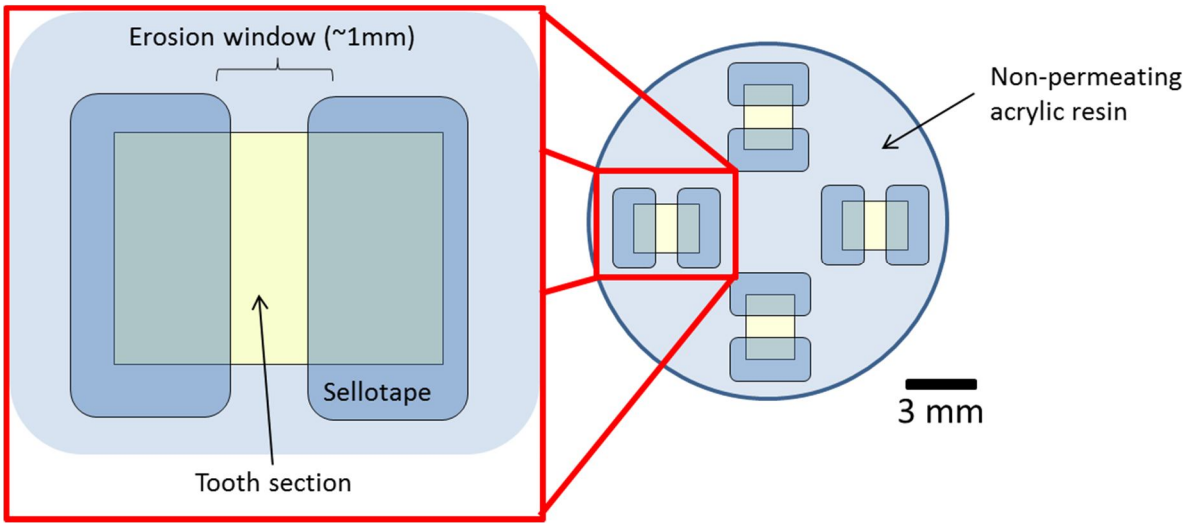

Figure 2.6-1: Schematic representation of resin-embedded samples of ground and polished enamel, arranged in a circular formation as used throughout this work. The inset shows the final orientation of the tape to generate an erosion window.

2.7.COMPARISON OF TAPE VERSUS IMPRESSION METHOD

In addition to determining which tape medium would be most appropriate for this work, a suitable method representative of short duration repeated acid exposure had to be determined. As the optical profilometer would be employed as the primary lesion depth measurement instrument (for reasons cited in the introduction), there was potential for sample reflectivity to adversely affect the data. Polyvinyl siloxane impression material (siloxane) has been suggested as an alternative to direct enamel scanning owing to its reproducibility of topographical features and minimal reflectivity (German *et al*., 2008). However, the use of polyvinyl siloxane prior to scanning the topography may represent an unnecessary additional step in the protocol. Furthermore, the impression material may not adequately provide an accurate representation of early stage erosion lesions. Thus, this method was compared with the more common method in the literature of directly scanning the tooth sample.

Two alternatives were explored as part of determining the differences between samples alone and siloxane: one involved leaving the tape *in situ* on the sample during scanning and mathematically correcting for this later, the other involved removal of the tape after dissolution was complete (at 600 seconds) and prior to scanning. Both these tests would be evaluated against siloxane.

A light-body polyvinyl siloxane (President jet, Calténe, Switzerland) was ejected onto the surface of the samples with the tape *in situ* – the process of ejection also serving to mix the polymer together, until the enamel sample was completely covered. A plastic cap was placed inverted onto the siloxane in order to provide a level backing. The impression material was then left to polymerise overnight. Once polymerised, the

impression material was removed from the sample, thereby providing a mirror image and both samples scanned using optical profilometry.

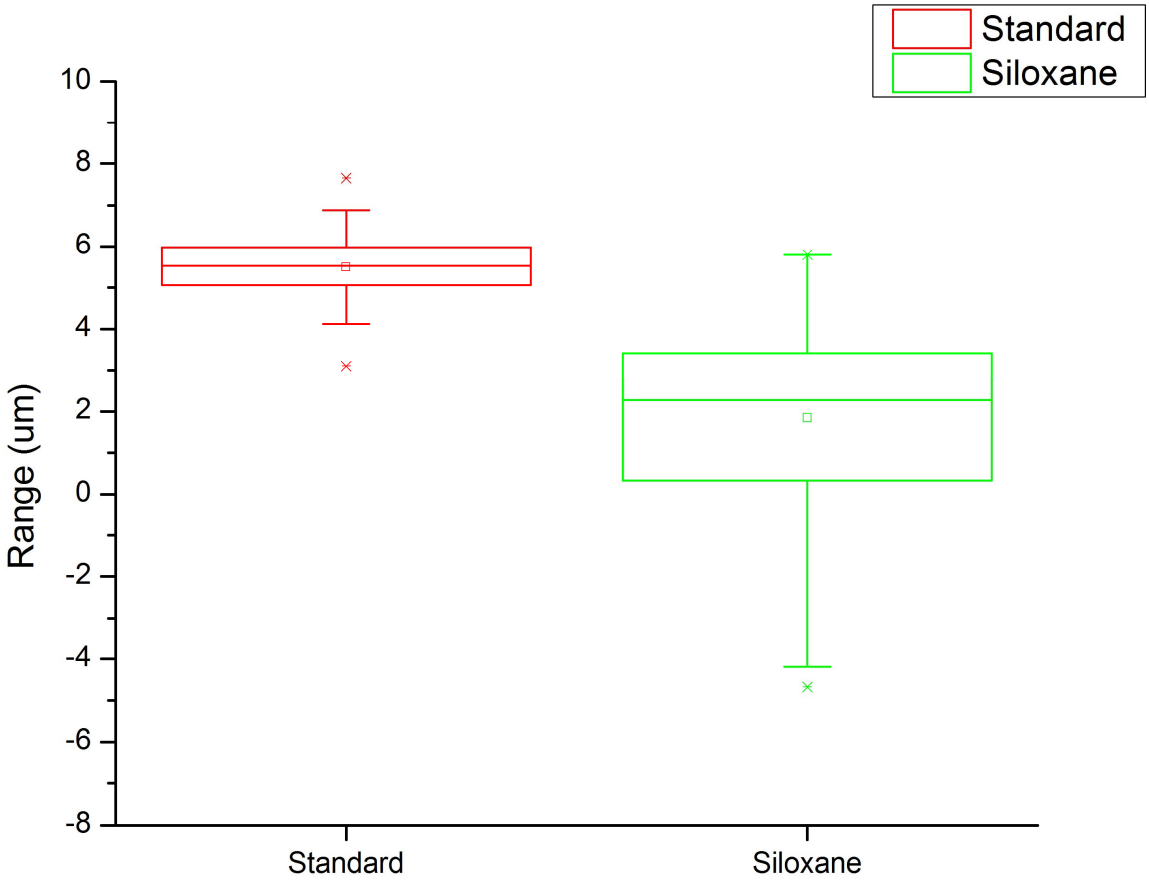

Figure 2.7-1: Box plot of enamel alone, following removal of erosion window demarking tape, and a siloxane impression of enamel following removal of erosion window demarking tape to show the data variation between the two methods (n = 8).

Removal of the tape prior to scanning was shown to be significantly different from leaving the tape in situ and correcting for the additional height of the tape. Scanning the sample without tape *in situ* produced a median value of 5.53 μm (0.93 Q1-Q3), while the siloxane impression material yielded a value of 2.27 μm (3.03 Q1-Q3). However, as may be seen from the box plots above (Figure 2.7-1), the data scattering of the siloxane material is greater than that of the sample without the tape *in situ*, which is reflected in the adjusted Chi-squared values of 0.90 and 0.44 for the sample alone and siloxane impression material, respectively. Furthermore, certain readings from the

siloxane impression material appeared to indicate the enamel lesion stood proud of the uneroded surface, a finding that was not supported by scanning of the enamel alone. This may potentially be explained by the effects of the optical profilometer laser, with a wavelength of 780 nm, interacting with the siloxane impression material and providing an artificial indication of a rougher surface of the impression (Field *et al*., 2010).

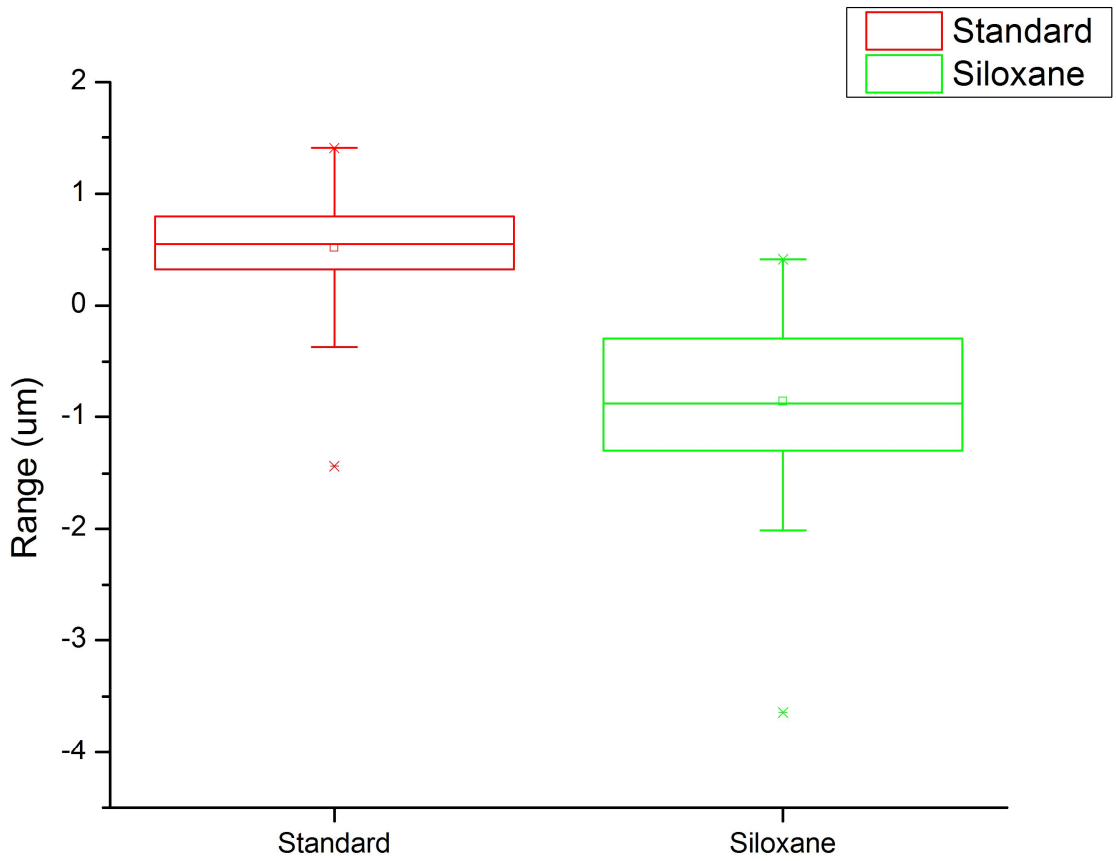

Figure 2.7-2: Box plot of taped enamel alone and a siloxane impression of taped enamel to show the data variation between the two methods (n = 8).

Leaving the tape in place (including while taking an impression) and correcting for the mean tape height at a later duration produced a significantly different result (p = <0.01) when the samples were compared with median values of 0.56 μm (0.48 Q1-Q3) for the tape alone and -0.88 μm (1.00 Q1-Q3) for siloxane once adjustment for the tape had been completed. Again the variation for the siloxane impression material is greater

than that of the sample with the tape *in situ*, with adjusted Chi-squared values of 0.85 and 1.42 for the sample with adherent tape and siloxane impression, respectively. Siloxane impression material again gave an indication that the shape of the erosion lesion was the inverse to that which would be expected.

An unpredictable effect of using siloxane impression material was that it showed the presence of trapped air in some parts, which would negatively impact the results. It was therefore suggestive that the fine detail present within the samples could be lost because of the higher viscosity, despite using a light body compound. Furthermore, the samples had to be completely dry or there was a risk the material would either swell or retain moisture at the surface owing to its inherent hydrophobicity (German *et al*., 2008). The better data correlation of the enamel with adhesive tape suggested this method was more appropriate to the study than using an impression material. Furthermore, the small differences noted when evaluating samples with no tape *in situ*, whether of an impression material or not, would increase the difficulty in data interpretation and differentiation from intrasample variation.

2.8. SOLUTION PREPARATION

2.8.1. 1 MOL.L^{-1} SOLUTIONS

Initial solutions were prepared at 1 mol.L^{-1} owing to the anticipated low bulk tissue loss at low concentrations. This would permit the identification of potential patterns of erosion by exaggerating the acid challenge. The volume/mass of reagent required to create 1mol.L^{-1} was calculated using the following equation:

$$Required\ mass = \frac{\rho(wt\%)}{RMM}$$

where P is the reagent density, wt%, the purity of the solution and RMM the relative molecular mass.

The following amounts of reagent were used to create a 1 mol.L^{-1} solution:

57.3 mL of glacial acetic acid (VWR BDH, Leicestershire, UK) per 1000 mL, pH 2.2.

192g of citric acid granules (VWR BDH, Leicestershire, UK) per 1000 mL, pH 1.85.

68.45 mL of 85% phosphoric acid (Sigma Aldrich, Dorset, UK) per 1000 mL, pH 1.75.

The solutions were normalised to pH 3.2, in accordance with GSKs previous protocols, using 1 mol.L^{-1} of NaOH (Riedel-de-Haan, Germany).

2.8.2. 0.05% SOLUTIONS

The selection of 0.05% v/v acid solutions was taken under advisement from the Coca-Cola Company following an enquiry regarding the concentration of phosphoric acid used in Coca-Cola®. As branded colas are consistently the bestselling carbonated beverages sold in the UK (BSDA, 2010), this concentration was used as the benchmark for standardising acid concentrations for physiologically better tolerated acids to be explored during this work. The use of a percent solution, in contrast to the previous section which employed a single defined molar value solution, was employed as the original molar concentration of phosphoric acid used by Coca-Cola® was unspecified. 0.05% solutions were therefore created using 50 µL per 1000 mL of the stock solutions listed above. The calculation for determining molar concentration was derived from:

$$mole = \frac{mass}{molar\ ratio}$$

Acetic acid has a molar ratio of 60.05 $g.mol^{-1}$ resulting in a 0.05% solution containing 8.33×10^{-4} moles.

Citric acid has a molar ratio of 192 $g.mol^{-1}$ resulting in a 0.05% solution containing 2.60×10^{-4} moles.

Phosphoric acid has a molar ratio of 98 $g.mol^{-1}$ resulting in a 0.05% solution containing 5.10×10^{-4} moles.

For ease of reading during this work and to alleviate any confusion arising from the use of four apparently different acid concentrations, any referral to a 0.05 % acid solution undertaken for this work will relate to the above concentrations.

2.8.4. SYNTHETIC HYDROXYAPATITE SYNTHESIS

Sintered synthetic hydroxyapatite was utilised for the comparative EDX analysis of eroded enamel. 4 g of powdered, synthetic hydroxyapatite (BDH, UK) was placed into a steel mould, together with a shape retaining U-spacer. Initial compaction of the disk was achieved at five tons pressure, following which the U-spacer was removed. The sample was then compressed using 20 tons weight/force.

The compressed sample was then sintered at 1300 °C for 60 minutes before being removed from the oven and allowed to cool overnight.

2.8.5. FLUORIDE SOLUTIONS

Different concentrations of fluoride for the first remineralisation work were created using sodium fluoride (VWR BDH, Leicestershire, UK) in deionised water. The required concentrations were calculated using the formula below:

$$\frac{M}{E} \text{ x } c$$

where M represents the molecular weight (g mol^{-1}), E the element weight (g mol^{-1}) and c represents the concentration required (ppm).

Sodium fluoride (BDH, UK) was used in the following quantities per 200 mL: 10ppm = 0.04g; 50ppm = 0.022g; 100ppm = .044g; 200ppm = 0.088g 300ppm = 1.32g; 500ppm = 2.21g and 1000ppm = 4.42g.

2.8.6. ADDITIONAL REMINERALISATION COMPOUNDS

Solutions for the second remineralisation work were generated as follows per 200 mL:

Sodium fluoride (BDH, UK) at 1200 ppm = 0.663 g

Sodium Phosphate (BDH, UK) at 30 mmol.L^{-1} = 0.89 g

Calcium carbonate (BDH, UK) at 40 mmol.L^{-1} = 0.75 g

2.9. EXPERIMENTAL PROCEDURES

A number of analyses were performed to evaluate the early patterns of enamel erosion. However, some of these techniques were operating at the limit of the machine sensitivity and were therefore of limited use or superceded by additional methods once the findings had been analysed. Further details of these techniques may be found in Appendix E - Additional evaluation techniques.

2.9.1. MULTIPLE SAMPLES FOR INDIVIDUAL TIME POINTS

Two principal techniques are often employed in the literature to explore dental hard tissue erosion. The first to be examined involves investigating the effects of erosion using multiple samples for each individual time point (MSIT) to be investigated (Eisenburger & Addy, 2001; Hughes *et al.*, 2004; Lussi *et al.*, 1995, Wiegand *et al.*, 2007). These samples are not carried over to following time points for reasons such as use of electron microscopy coating, which makes repeat use impossible. While this protocol permits the assessment of the effects of a single extended erosion on enamel, it does not model the effects of repeated short duration intakes.

Individual test solutions of 200 mL 1 $mol.L^{-1}$ phosphoric acid were generated for defined time points under investigation at 10; 20; 30; 40; 50; 60; 300 and 600 seconds. A sample, consisting of 8 specimens, was then created to correspond to one of these defined time points. Thus multiple samples for each individual time point were generated for a single experiment.

Each sample (n = 8) was then submerged in the erosive medium corresponding to its defined duration on an orbital shaker (100 rpm in order to ensure a constant composition) and, at the end of each experimental duration, the sample was removed from the solution, washed in deionised water, allowed to air dry and scanned using optical profilometry. The resulting datasets were analysed using Origin statistical software.

This protocol requires a cumulative total of 64 samples. In addition to this, the protocol employed here does not accurately reflect true drinking behaviour as short term repetitive intake behaviour is not modelled. However, this technique does serve to reduce potential error attributed to intrasample variation as any potential error will not be magnified through repeated use but rather be restricted to one sample category.

2.9.2. SINGLE SAMPLE, REPEATED EXPOSURE

The second most predominant protocol employed in the literature is that of the single sample, consisting of a number of specimens, which is used repeatedly for the duration of the work (Amaechi *et al.*, 1999; West *et al.*, 2005; White *et al.*, 2010). As with the above protocol described in 2.9.1, individual 200 mL test solutions of phosphoric acid were generated for defined time points under investigation: 10; 20; 30; 40; 50; 60; 300 and 600 seconds. However, for this protocol a single sample, containing eight specimens (n = 8), was created for use with all the solutions pertaining to each acid.

The sample was submerged in the first solution, removed after 10 seconds and washed in deionised water and allowed to air dry, before being scanned using an optical

profilometer[§§]. Following scanning, the sample was submerged again in the acid solution for a further 10 seconds, making a cumulative total of 20 seconds, before being removed, washed in deionised water, allowed to air dry and scanned using an optical profilometer. This process was repeated for four additional intervals of 10 seconds, making a cumulative total of 60 seconds. From then an extended interval of 240 seconds (to bring total cumulative exposure to 300 seconds) was employed, followed by further extended intervals to bring the cumulative exposure to 450 and 600 seconds, until all experimental categories had been fulfilled and corresponded to those tested in the previous subsection. The data was then analysed using Origin statistical software.

Later iterations of this model, such as that evaluating the effects of acids on short duration enamel physicochemical behaviour, included an additional time point at 450 seconds to increase statistical analysis capabilities when reviewing potential erosion trends and employed Origin statistical software.

2.9.3. ANALYSIS OF THE PUBLISHED PROTOCOLS

As mentioned previously, a number of studies in the literature employ a single acid exposure protocol for the duration of the experimental procedure (Eisenburger & Addy, 2001; Hughes *et al.*, 2004; Lussi *et al.*, 1995, Wiegand *et al.*, 2007). Although this attempts to model mid- to long-term dental erosion, it is not representative of true drinking behaviour such as sipping, in which a mouthful of liquid is usually consumed within a matter of seconds. This subsection will compare the two most commonly

[§§] The tape demarcating the control areas from the lesion was left *in situ* and the height difference corrected for mathematically.

employed models to determine the differences in bulk tissue loss arising from these different protocols.

Figure 2.9-1 shows the results of the two common protocols investigated, presented as box plots.

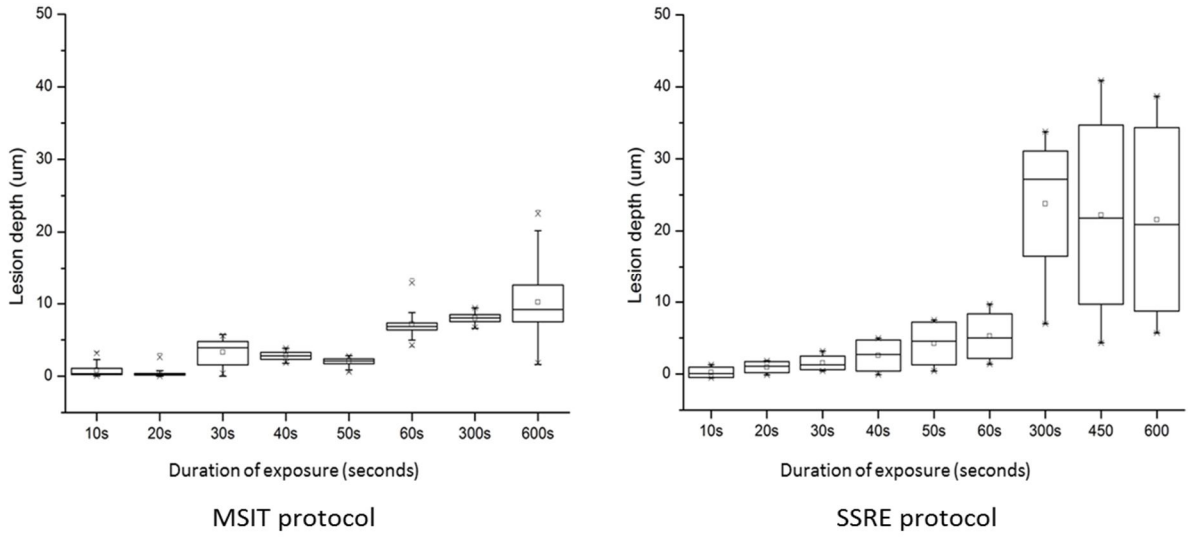

Figure 2.9-1: A comparison of the results of multiple sample-individual time point (MSIT) protocol (displayed on the left) and single sample-repeated exposure (SSRE) protocol samples (displayed on the right) using bovine enamel exposed to 1 mol.L^{-1} phosphoric acid over a cumulative 600 second exposure (n = 8).

After 10 seconds Multiple Samples for Individual Time point (MSIT) samples recorded a median depth of 0.34 µm (0.88 Q1-Q3) and SSRE samples recorded a mean depth of 0.08 µm (1.41 Q1-Q3). At 50 seconds the mean depth of erosion of the Single Sample and Repeated Exposure (SSRE) samples was 4.56 µm (5.94 Q1-Q3) and had surpassed that of MSIT, with mean values of 2.11 µm (0.66 Q1-Q3), although this was not a significant difference. At 60 seconds the MSIT sample recorded a mean value 6.87 µm (0.97 Q1-Q3) and SSRE samples recorded a mean value of 5.02 µm (6.19 Q1-Q3). As previously this difference was not significant but the divergence of results suggests an underlying erosion effect not adequately modelling by MSIT.

At 300 seconds of erosion the MSIT samples had a mean lesion depth of 8.04 μm (0.98 Q1-Q3), which was significantly different ($p = 0.01$) from SSRE samples with a mean lesion depth of 27.16 μm (14.60 Q1-Q3). This significant divergence was maintained at 600 seconds with MSIT lesion depths of 9.17 μm (5.08 Q1-Q3) compared to SSRE lesion depths of 20.90 μm (25.59 Q1-Q3).

Although both these techniques are employed in the literature, these results clearly show an increased bulk tissue arising from a repeated submersion of an enamel sample in an acid media. Such an effect appears to be comparatively absent from samples immersed just once in an acid medium, which suggests surface or subsurface activities have a role to play. As such, the SSRE protocol will be followed throughout this work as it most closely models the effect of erosion under observation.

COMPARING EROSION PROTOCOLS

Section 2.9 compared two models commonly employed in the literature but was crucial in determining the appropriate protocol to follow for this work. The first to be evaluated was termed the multiple sample-individual time point (MSIT) and involved the use of multiple samples allocated to specific experimental durations (Millward *et al*, 1995; Edwards *et al*, 1999, Larsen & Nyvad, 1999). A direct comparison of the results from this preliminary investigation with published data was hampered owing to the absence of any previous work in the literature employing acids of this high concentration. Thus measurements obtained from this work of the effect of acid exposure at very early time points (a central theme to this thesis) had no resources with which to compare it.

A problem with the MSIT model lies in that it does not factor in behavioural aspects such as repeated exposure of the same enamel area to the fluid in question into its design. Recently Eisenburger *et al.* (2004) using the MSIT model published work demonstrating the effects of acid on subsurface demineralisation and showed that it extended 9-12 μm below the surface.

It is therefore hypothesised that subjecting this softened surface (resulting from a single acid challenge) to a repeat exposure (exemplified by behaviour whereby repeated exposure of acidic fluid to the same enamel surface occurs) would increase the bulk tissue loss greater than would be observed in an experimental system that subjected samples to an acid exposure just once. This was the second protocol to be evaluated: a single sample subjected to a repeated acid exposure at short intervals (SSRE), which better emulates the erosive effect of repeated exposures on enamel (Amaechi *et al*., 1999; West *et al*., 2005; White *et al*., 2010). The use of high acid concentrations (relative to more commercially relevant ones) enabled the determination of the trends of the data prior to investigating this early exposure at more commercially exploited concentrations. However, both these protocols do not model the motion of fluid in the oral cavity, nor are the effects of saliva considered, thus these protocols are suitable exclusively as *in vitro* models rather than representative of physiological behaviour.

As may be seen from Figure 2.9-1, the MSIT experiment carried out and presented in section 2.9.1 showed relatively comparable quantities of erosion lesion depth when compared with data in the literature. Rios *et al* (Rios *et al.*, 2008) recorded an average lesion depth of 4.24 μm (±0.44 SEM) using a commercial brand of acidic beverage for a single 60 second long exposure compared to our work where a 1 $mol.L^{-1}$ concentration of phosphoric acid produced a lesion of 7.20 μm (±1.70). The SSRE protocol appears to substantiate previous authors regarding additional bulk tissue loss resulting from

subsurface softening (Amaechi *et al*., 1999; Eisenburger *et* al., 2004; West *et al*., 2005). Bovine SSRE samples showed an average 47% increase in enamel lesion depth when treated with 1 mol.L^{-1} phosphoric acid compared to the MSIT model by the end of a very long 600 second exposure. Therefore it is possible to conclude that repeated exposure of enamel to an acid environment enhances bulk tissue loss. As was mentioned previously, it should be noted that this work focussed on the effects of acids on enamel as a material and did not employ any erosion mitigating factors, such as remineralisation protocol (Ganss *et al*, 2004) or salivary pellicle (Amaechi & Higham, 2001) at this stage. As such, extrapolation of this data as representative of behaviour of enamel in the oral cavity should be treated with caution.

2.10. ADDITIONAL EXPERIMENTAL PROCEDURES

2.10.1. CALCIUM ION RELEASE IN ACID SOLUTION

Samples of human and of bovine enamel, embedded in epoxy resin were employed for this experiment. The samples were minimally ground and polished to expose an area of 1 mm^2 of enamel as no adhesive tape could be utilised in this work.

A single 200 mL solution of 0.05% phosphoric acid was made for each of the human and bovine samples. The sample of each was immersed in its respective solution according to the protocol described above, however, at each time interval the enamel sample was removed from the solution and washed in deionised water. A 1 mL sample, containing dissolved Ca^{2+}, was taken from the acid solution using a syringe prior to the enamel sample being returned to the solution. The samples were then run through the chromatograph using a calcium ion selective electrode. At the completion of the experiment the sequential sample solutions of acid containing dissolved Ca^{2+} were analysed using ion chromatography software and statistically analysed.

2.10.2. ASSESSMENT OF THE EFFECT OF FLUORIDE ON ENAMEL REMINERALISATION

For ease of reading and better comparison with published data, the approved SI notation of $mg.L^{-1}$ has been replaced with the more popular parts per million (ppm) when referring to fluoride concentrations (Lussi *et al.*, 2004; ten Cate, 1999). Each fluoride treatment (control, 10, 50; 100; 200; 300; 500 & 1000 ppm) utilised eight

bovine enamel specimens embedded in a single epoxy resin sample. The samples were ground and polished with 1000, 1200 and 2400 grade grit paper before ultrasonication (five minutes duration) to remove the smear layer.

Erosion windows were created on the enamel surface using adhesive tape, which allowed for flanking areas under the tape of uneroded material to be used as a surface level control either side of the erosion window.

Fluoride was administered *via* the addition of defined quantities of NaF to a fluoride free placebo dentifrice (ProNamel, GSK, UK). Specimens were treated twice daily, morning and afternoon, in 200 mL of the relevant toothpaste slurry mixed with deionised water (1:3 v/v) slurry on an orbital shaker at 100 rpm for 120 s at room temperature. Once the fluoride treatment was complete, the samples were washed in deionised water. In the intervening periods between fluoride administration, the specimens were subject to a series of five demineralising/remineralisation cycles, in which the demineralising challenge involved immersion in 200 mL of 1.0 M citric acid (pH 3.2) for 5 minutes at 100 rpm at room temperature. The use of a 1 $mol.L^{-1}$ citric acid solution allowed for ready detection of potential remineralisation using optical profilometry due to the increased lesion depth. The remineralisation phase comprised 200 mL of artificial saliva (pH 7.0) for 60 minutes at 35°C, using the protocol established by Pretty (Pretty *et al*, 2004). Following the final slurry exposure, specimens were incubated overnight under mild agitation (20 rpm) in the artificial saliva at pH7.0 at room temperature. Once the five day protocol was complete, the samples were removed from the artificial saliva, washed in deionised water and allowed to air dry. Optical profilometry (Proscan 2000, Scantron, UK) was used to determine the final lesion depth.

2.10.3. ASSESSMENT OF THE EFFECT OF SODIUM PHOSPHATE, SODIUM FLUORIDE AND CALCIUM CARBONATE ON ENAMEL REMINERALISATION.

Each remineralising treatment category employed five human enamel specimens embedded in a single epoxy resin sample. The samples were ground and polished with 1000, 1200 and 2400 grade grit paper before ultrasonication (five minutes duration) to remove the smear layer.

Erosion windows (approximately 2mm x 4mm) were created on the enamel surface using adhesive tape, which allowed for flanking areas of un-eroded material to be used as a surface level control either side of the erosion window.

One sample was used as a tape height control and subjected to a 20 minute immersion in deionised water. A 0.05 % phosphoric acid solution was employed as the erosive media for this work. In order to ensure a comparatively deep erosion lesion was initially generated in the test samples they were immersed in the erosive media for 60 minutes, then washed in deionised water.

200 mL solutions of 30 $mmol.L^{-1}$ sodium phosphate (Larsen & Nyvad, 1999), 1200 ppm sodium fluoride (Buchalla *et al.*, 2007) and 40 $mmol.L^{-1}$ calcium carbonate (Larsen & Pearce, 2003) were created, as previously employed in the literature. The samples were then subjected to a single 10 minute remineralisation period in designated solutions on an orbital shaker (100 rpm at room temperature) and scanned using white light interferometry. The samples were then demineralised again (20 minutes at 100 rpm at room temperature) before being remineralised for a further 10

minutes (100 rpm at room temperature). White light interferometry was used to obtain a second set of results before all results were analysed using Origin statistical software.

CHAPTER 3

CHARACTERISING EARLY EROSION TRENDS.

3.1. THE EARLY PATTERNS OF EROSION

Comparing multiple samples allocated for individual acid exposures (MSIT) against a single sample used during the entire experimental duration (SSRE) showed a difference in erosive bulk tissue loss as a consequence of the treatment regimen. Furthermore it was observed that two distinct trends in lesion creation were apparent: an initial more rapid trend of erosion from 0-60 seconds and a second, less rapid trend from 60 – 600 seconds. Using the single sample-repeated exposure (SSRE) model, this phenomenon was investigated using standardised 1 $mol.L^{-1}$ acetic, citric and phosphoric acid, in order to determine if such a pattern of erosion was a reflection of one particular acid type or indicative of a previously unrecorded physicochemical behaviour.

3.1.1. EFFECT OF THREE COMMON ACIDS IN DIETARY CONSUMPTION

3.1.1.1. 1 MOL.L^{-1} ACETIC ACID

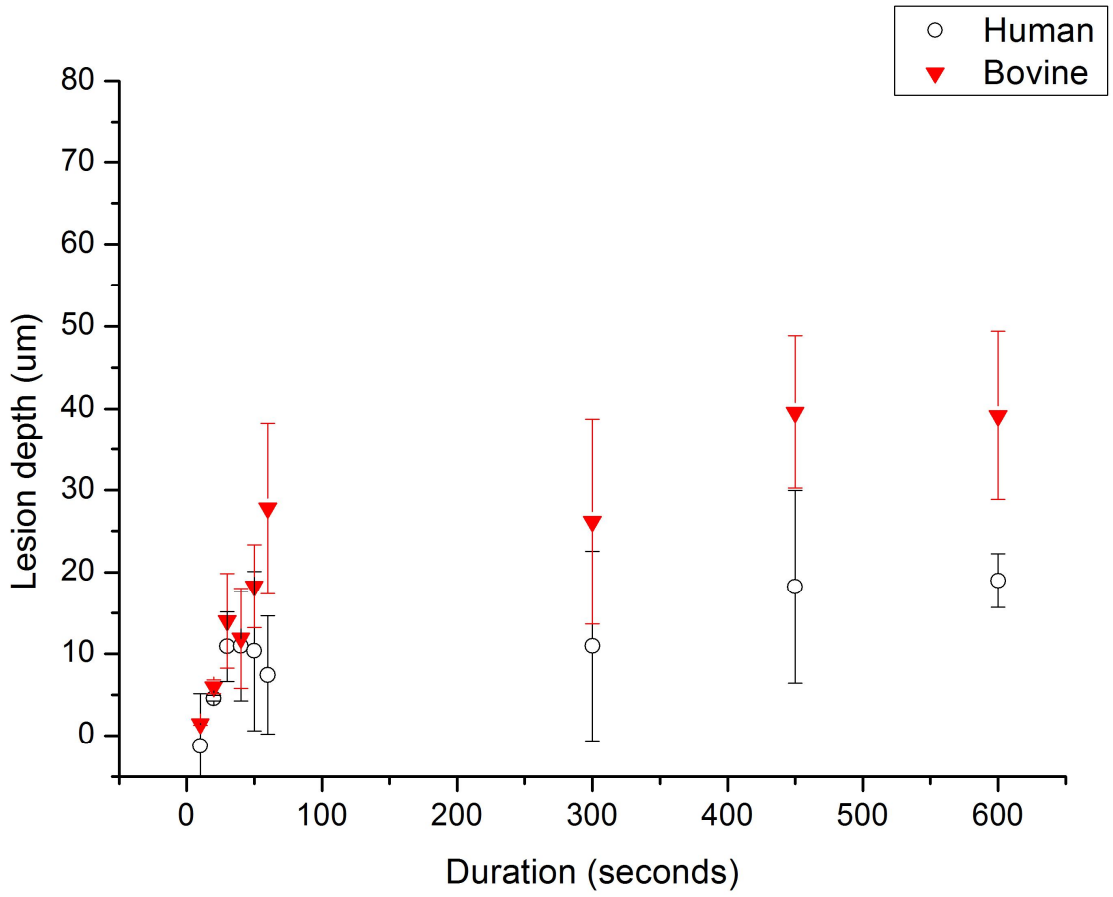

Figure 3.1-1: The effect of 1 mol.L^{-1} acetic acid on human and bovine enamel during a 600 second erosion challenge, represented by the median and IQR (n = 8).

Figure 3.1-1 shows the effects of a 600 second 1mol.L^{-1} acetic acid challenge on eight human and bovine enamel samples. At 10 seconds erosion duration bovine enamel records a median lesion depth of 3.59 µm (±11.18 SE) and human enamel 4.01 µm (±0.09 SE). These interspecies results were not significantly different from each other.

After 60 seconds there was no significance difference between the species samples (p = 0.06); bovine enamel had a median lesion depth of 34.56 µm (±5.21 SE)

and human enamel 9.27 μm (±5.89 SE). The bovine enamel lesion depth had increased by an average of 13.98% on the 10 second data, while human enamel had increased in depth by 15.05% but these increases in depth were not significant. There was a significant difference between the bovine enamel sample eroded for 10 seconds compared to a cumulative erosion duration of 60 seconds ($p = 0.002$). By contrast, the 60 second human enamel lesion was not significantly different from its corresponding 10 second dataset.

After 600 seconds of immersion the interspecies samples remain not significantly different from each other ($p = 0.07$). Bovine enamel had a mean lesion depth of 39.14 μm (±5.11 SE) an increase of 71.07% from the erosion encountered at 60 seconds, however this was not found to be significant, most likely attributed to the increased standard deviation at the later duration exposures. Human enamel had a mean lesion depth of 20.55 μm (±7.14 SE), a significant increase of 46.86% on the recorded depth at 60 seconds ($p = 0.02$).

3.1.1.2. 1 MOL.L^{-1} CITRIC ACID

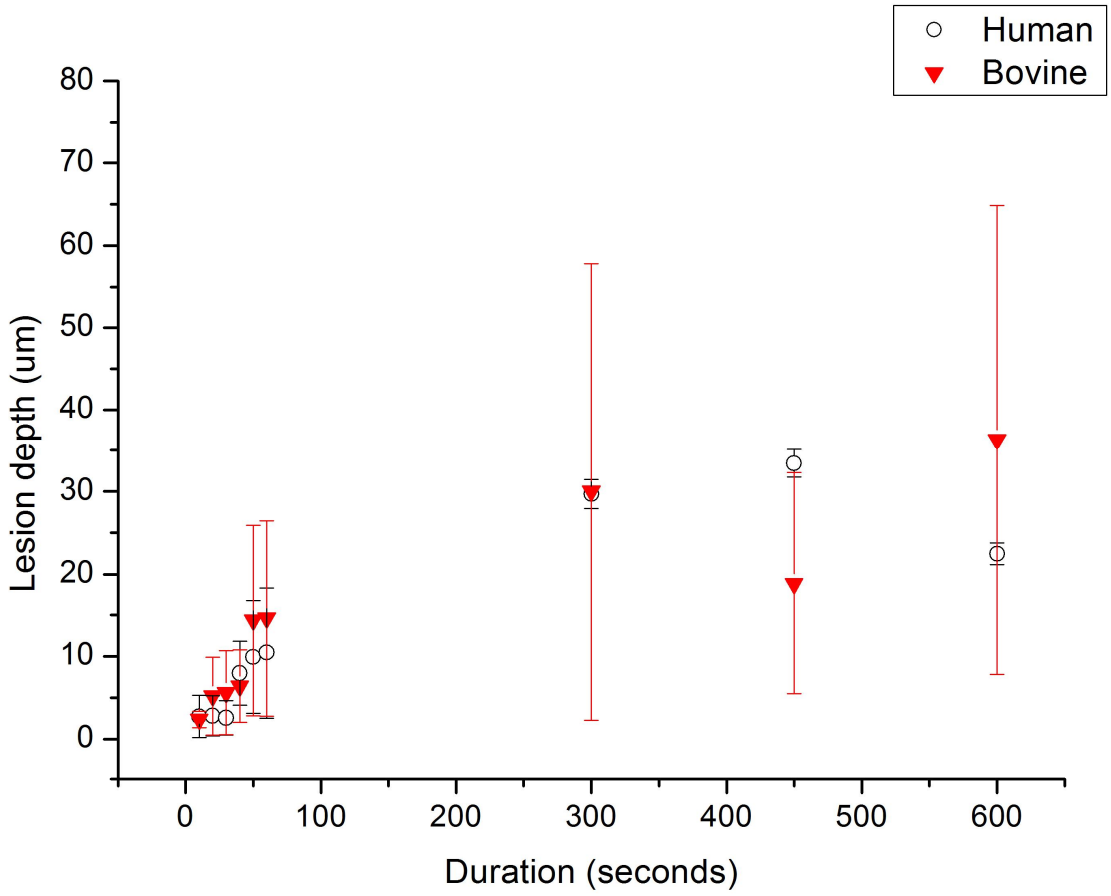

Figure 3.1-2: The effect of 1 mol.L^{-1} citric acid on human and bovine enamel during a 600 second erosion challenge, represented by the median and IQR (n = 8).

Figure 3.1-2 shows the effects of a 600 second 1mol.L^{-1} citric acid challenge on eight samples of bovine and human enamel. At 10 seconds erosion duration bovine enamel records a median lesion depth of 1.49 µm (±0.37 SE) and human enamel 2.74 µm (±1.79 SE). These results were not significantly different from each other ($p = 0.41$).

After 60 seconds there was no significance difference between the median depth of individual species lesions ($p = 0.18$); bovine enamel had a median lesion depth of 20.26 µm (±4.48 SE) and human enamel 10.44 µm (±5.60 SE). Bovine samples were

significantly deeper in depth at 60 seconds compared to the lesion at 10 seconds ($p = 0.01$).

After 300 seconds no significant difference was apparent between the interspecies samples ($p = 0.98$); bovine enamel lesions had a median lesion depth of 59.41 µm (±10.49 SE) and human enamel 29.70 µm (±1.23 SE). Bovine enamel had increased by an average of 34.74% on the 60 second data, while human enamel had increased in depth by 35.15%. Furthermore, there was a significant difference between the bovine data at 300 seconds and that at 60 seconds ($p = 0.001$) but no significant difference was apparent for the human samples ($p = 0.07$).

At the end of this experiment (600 seconds of immersion) the interspecies samples remained not significantly different from each other ($p = 0.53$). Bovine enamel had a median lesion depth of 67.04 µm (±10.77 SE), a significant lesion depth increase in bovine enamel of 40.20% compared to the lesion depth at 60 seconds. Human enamel had a median lesion depth of 22.05 µm (±0.92 SE), which corresponded to an increase of 47.34% on the 60 second human enamel lesion depth but this was not significant.

3.1.1.3. 1 MOL.L^{-1} PHOSPHORIC ACID

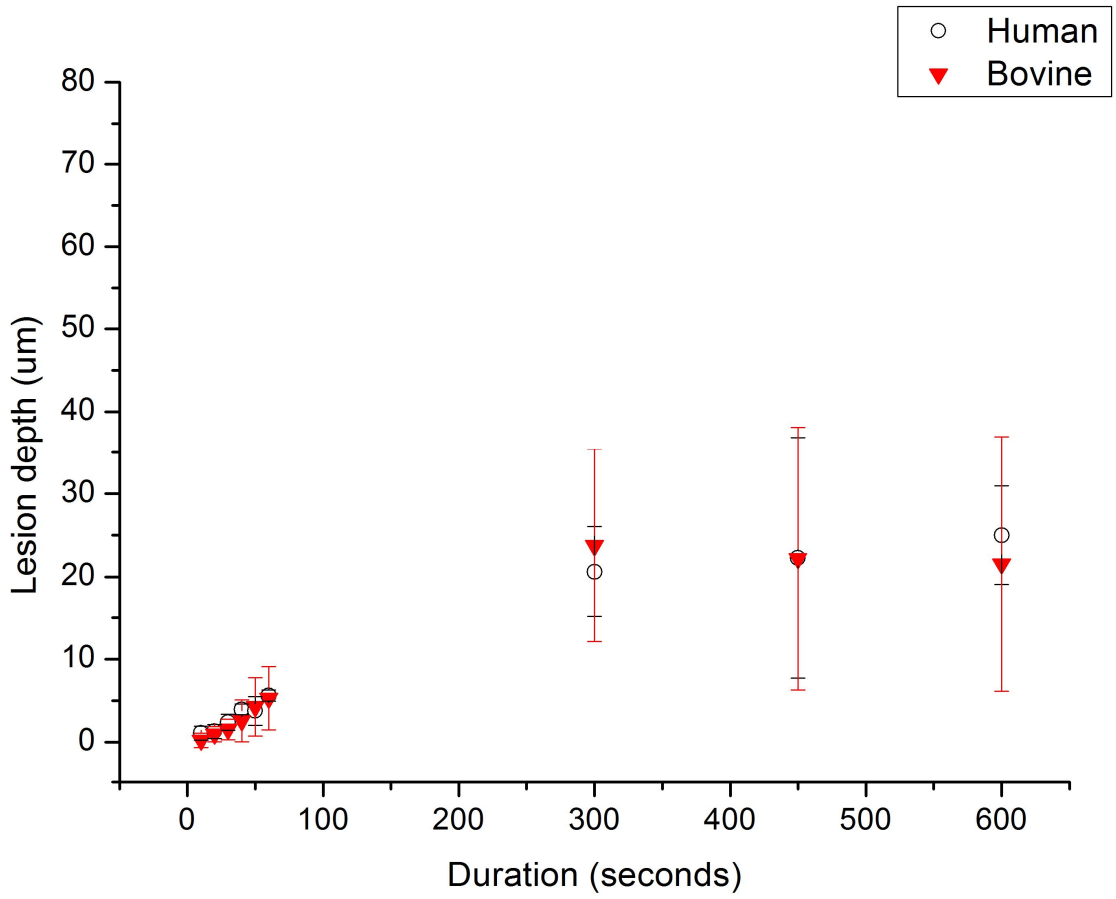

Figure 3.1-3: The effect of 1 mol.L^{-1} phosphoric acid on human and bovine enamel during a 600 second erosion challenge, represented by the median and IQR (n = 8).

Figure 3.1-3 shows the effects of a 600 second 1mol.L^{-1} phosphoric acid challenge on eight samples of human and bovine enamel. At 10 seconds erosion duration bovine enamel records a median lesion depth of 0.08 µm (±0.43 SE) and human enamel 1.55 µm (±0.48 SE). These results were not significantly different from each other (p = 0.24).

After 60 seconds there was no significance difference between the species samples (p = 0.86); bovine enamel had a median lesion depth of 5.02 µm (±1.89 SE),

which was significantly different from the bovine 10 second lesion depth (p = 0.04). Human enamel had a median lesion depth of 5.55 µm (±0.33 SE), which was significantly different from the human 10 second lesion data (p = >0.01).

After 300 seconds of immersion bovine enamel had a median lesion depth of 27.16 µm (±5.82 SE), a significant increase (p = 0.02) of 22.17% from the bovine lesion depth measured at 60 seconds. Human enamel had a median lesion depth of 21.81 µm (±2.73 SE), an increase of 27.23% on the recorded human lesion depth at 60 seconds but, unlike the bovine enamel, this was not significant from the 60 second lesion depth. Comparing the lesion depths at 300 seconds showed there was no significant difference between the means of bovine and human enamel (p = 0.64).

At 600 seconds bovine enamel yielded a median lesion depth of 20.90 µm (±7.69 SE), which was not significant from the bovine lesion depth at 300 seconds. The human enamel lesion recorded a median depth of 25.11 µm (±2.96 SE), which was not significant with respect to either the human enamel 300 second dataset (p = 0.31) or an interspecies comparison with bovine enamel after the same duration (p =0.68).

COMPARISON OF DATA

A Kruskall-Wallis ANOVA (significance value p = 0.05) of all optical profilometric data for both human and bovine material showed no significant difference between acetic -, citric - and phosphoric acid samples at 600 seconds (whether human or bovine). Thus, there appears to be good correlation between the species in terms of bulk tissue loss measured by optical profilometry.

An interesting observation between these samples was the behaviour of the individual species and the acid media. Previous authors have found bovine enamel to

erode more rapidly than human enamel when exposed to an acid solution (Attin *et al.,* 2007; White *et al*., 2010). However, these experiments showed that this was not the case with respect to 1 mol.L^{-1} phosphoric acid, which showed human enamel to be more resistant to the erosive challenge than its bovine counterpart. This may be an anomalous result attributed to the high acid concentration or possibly be related to the effects of acid type (Wegehaupt *et al*., 2008) or intrasample variability (Mellberg, 1992), all of which will be further discussed in section 3.5.

3.2. SUPERFICIAL EROSION OF HUMAN AND BOVINE ENAMEL

The effects of erosion may also manifest in topographical changes of the enamel surface. Scanning electron microscopy has been employed to examine such changes (Eisenburger *et al.*, 2004). Therefore it was decided to use this method to compare our results with that of the published literature, beginning with examining the effects of a clinical application of acid.

The clinical application of a 37% solution of phosphoric acid to superficial enamel for 30 seconds is undertaken to enhance the bonding properties of dental restorative materials by increasing the available surface area: volume ratio of enamel. The effects are more severe than would be encountered from a similar duration exposure using weaker acid solutions (which will be explored later) as more protons are available to interact with the enamel substrate and initiate bulk tissue loss. This discrepancy provides an initial basis from which to explore surface dissolution.

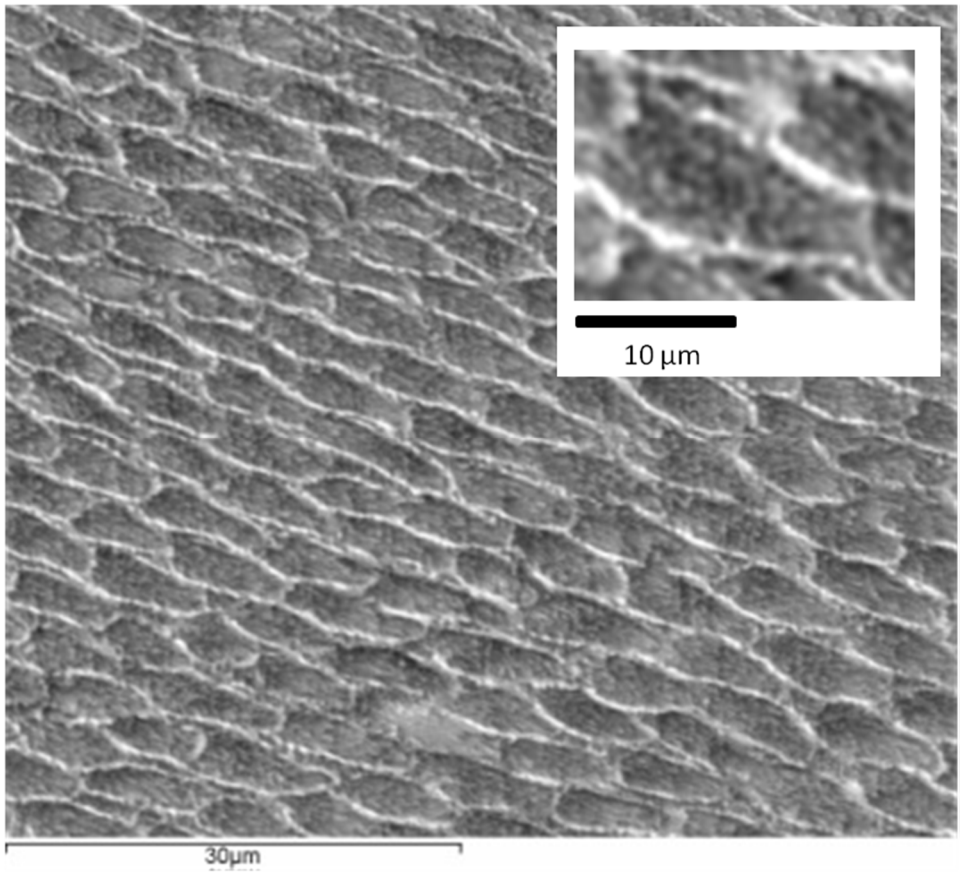

Figure 3.2-1: Human enamel treated with 37 % phosphoric acid for 20 seconds, as employed in the clinical environment. The insert shows an example of the rounded hydroxyapatite crystallites at the base of a single eroded enamel rod, which show up as paler areas against the darker background of the enamel rod basal surface.

Figure 3.2-1 shows the effect of a 30 second exposure of clinical strength acid (37 %) on a sample of human enamel. The inter-rod enamel is now very much more pronounced with the central enamel rod taking on a sunken appearance, the base of which is roughened with rounded hydroxyapatite crystals (Figure 3.2-1 image insert).

A characteristic that also appeared was the presence of feathering effect at the peripheral edges of the inter-rod enamel, as observed in Figure 3.2-2. This effect was most likely the result of rapid precipitation nucleating on the roughened peripheral edges of enamel crystals resulting from localised calcium and phosphate saturation. This feathering effect was particularly noticeable in samples treated with more

concentrated acid solutions such as the 37 % solutions than was observed later using the 0.05 % solutions.

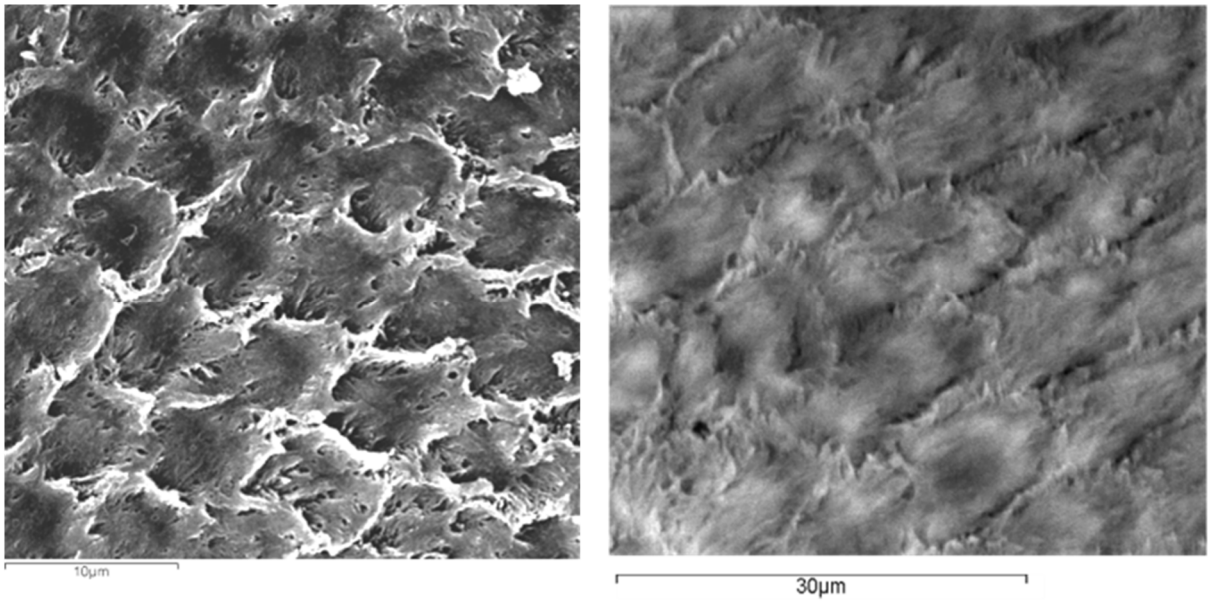

Figure 3.2-2: Bovine enamel (left) and human enamel (right) eroded using 37% phosphoric acid for 20 seconds. The inter-rod enamel is feathered, reflecting a directional erosive process, while the intra-rod enamel appears to erode faster resulting in a hollowed depression.

3.3. RAPID MEASUREMENTS FOR THE CLINICAL ENVIRONMENT

Quantitative Light-induced Fluorescence (QLF), as described in the Materials & Methods, is a technique shown to have good correlation between the change of reflected light intensity, ΔF, and the change in height, ΔQ, as less light is reflected from eroded enamel compared to sound enamel (Pretty *et al.*, 2004). Owing to the prevalence of investigation of *in situ* erosion at the clinic (Barbour & Rees, 2004; Meller *et al.*, 2006), this QLF data relates exclusively to the 600 second data for both human and bovine enamel.

ACID TYPE	ΔQ (μm)	SD	F STATISTIC
Acetic			
Bovine	7.20	0.51	**0.33**
Human	8.04	0.51	
Citric			
Bovine	7.06	0.79	**0.49**
Human	6.73	0.39	
Phosphoric			
Bovine	6.70	0.41	**0.64**
Human	6.95	0.97	

Table 3.3-1: Results of QLF analysis on bovine and human enamel following 600 seconds immersion in 1 mol.L^{-1} acetic, citric or phosphoric acid (n = 8).

As may be seen from Table 3.3-1, QLF shows no significant difference in topographic height (ΔQ) between the species with respect to acetic (p = 0.33), citric (p = 0.49) or phosphoric acid (p = 0.64). A one-way ANOVA (coupled to Levene's test for sample variance) to determine any potential significance between all the samples showed no significant difference (p = 0.05).

Comparing this data with the recorded optical profilometry, as seen in Table 3.3-2, showed significant differences in the mean lesion depth ($p = 0.003$ to > 0.001) with the exception of bovine enamel treated with phosphoric acid ($p = 0.10$).

Acid type	ΔQ (μm)	OP* (μm)	F statistic
Acetic			
Bovine	7.20	39.14	**>0.001**
Human	8.04	20.55	**0.003**
Citric			
Bovine	7.06	36.44	**>0.001**
Human	6.73	22.05	**>0.001**
Phosphoric			
Bovine	6.70	21.54	**0.1**
Human	6.95	25.01	**>0.001**
F statistic	**0.34**	**0.62**	

* Optical profilometry

Table 3.3-2: Comparison of the mean depth of lesions created in bovine and human enamel using 1 $mol.L^{-1}$ acetic, citric and phosphoric acid over 600 seconds, measured using QLF (ΔQ) and optical profilometry (OP).

Table 3.3-2 also shows the results of two one-way ANOVA analyses with respect to differences between the means of human and bovine enamel erosion measured by QLF and optical profilometry. Both these techniques show no significant difference for either species involved or acid type.

Figure 3.3-1 shows an alternative explanation of the results of 600 seconds cumulative erosion duration measured with optical profilometry and QLF. This chart shows the disparity between OP and QLF, particularly with regard to variation. Although neither technique yielded significant variation within samples (according to

Levene's test) it is evident that direct comparison between these two methods should be undertaken with caution.

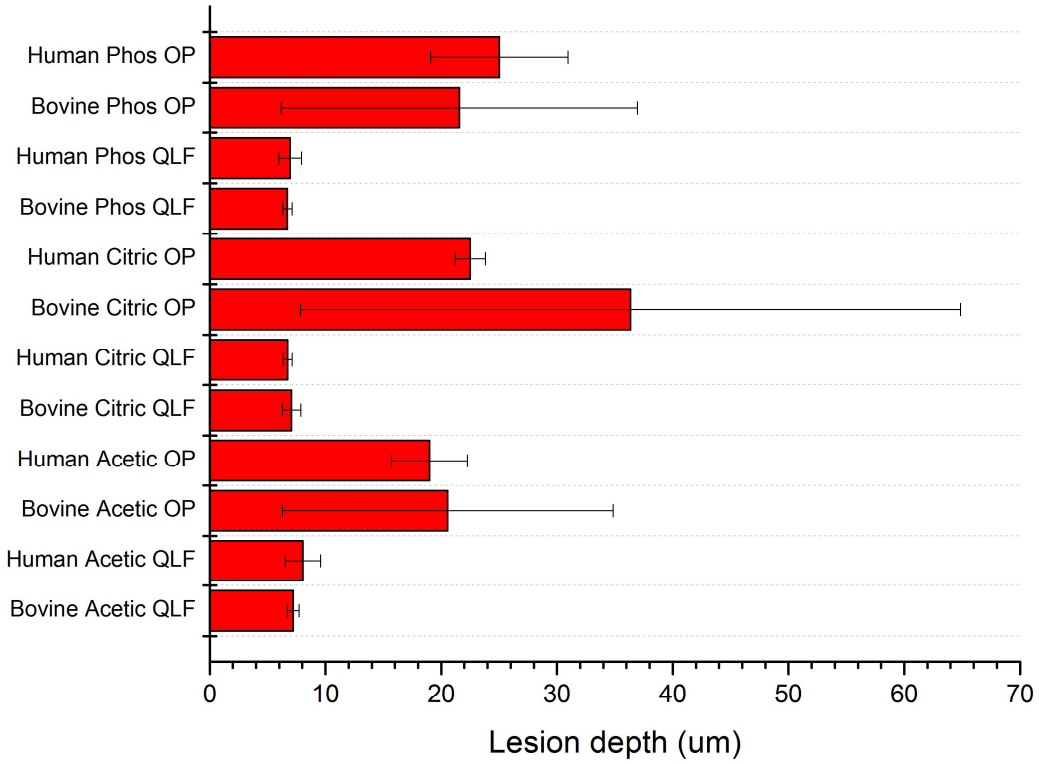

Figure 3.3-1: Bar chart to show the median and IQR relationship between human and bovine enamel samples eroded with 1 mol.L^{-1} acetic, citric and phosphoric acid analysed using QLF and Optical profilometry (OP).

OP and QLF demonstrated the bulk tissue loss of enamel following an erosive challenge, while SEM showed changes to the surface topography. This latter point has been linked to enamel softening (Eisenburger *et al.*, 2004) and was subsequently tested using Vickers microhardness. However, this technique was found to be unsuitable, particularly in light of later work. The limitations of microhardness will be discussed in a later chapter.

It was then decided to investigate the effects of fluoride as a remineralising compound, with a view to further expansion of this topic later.

3.4. POTENTIAL OF A BIPHASIC MODEL

Observations of the data trend relating to single sample-repeated exposure (SSRE) and multiple sample-individual time point (MSIT) were suggestive that enamel erosion at the early stages did not progress in the expected linear manner as depicted in Figure 3.4-1 below:

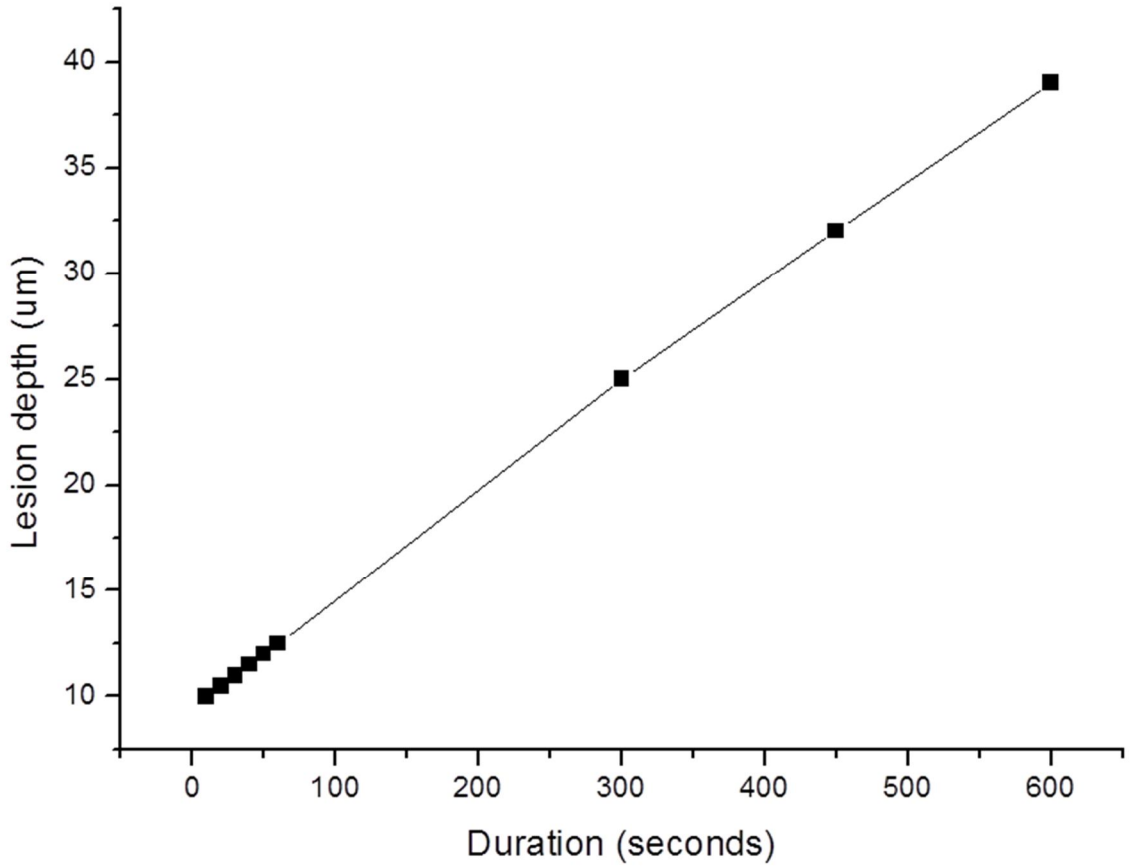

Figure 3.4-1: Representation of a hypothetical linear trend through the mean or median values of enamel samples following an erosion event.

This was corroborated by the 1 mol.L^{-1} acetic, citric and phosphoric acid data from both species, all of which appeared to provide empirical evidence for an acute

linear trend between 10 - 60 seconds followed by a reduction effect from 60 - 600 seconds.

CALCULATING THE 1 MOL.L^{-1} EROSION RATE

For ease of statistical use the data were subdivided into two respective categories at 10-60 seconds and 60-600 seconds (as illustrated below) and designated primary - and secondary erosion phase, respectively. This marked an apparent change in the continuous erosion trend but allowed for the approximate calculation of each using an oblique asymptote.

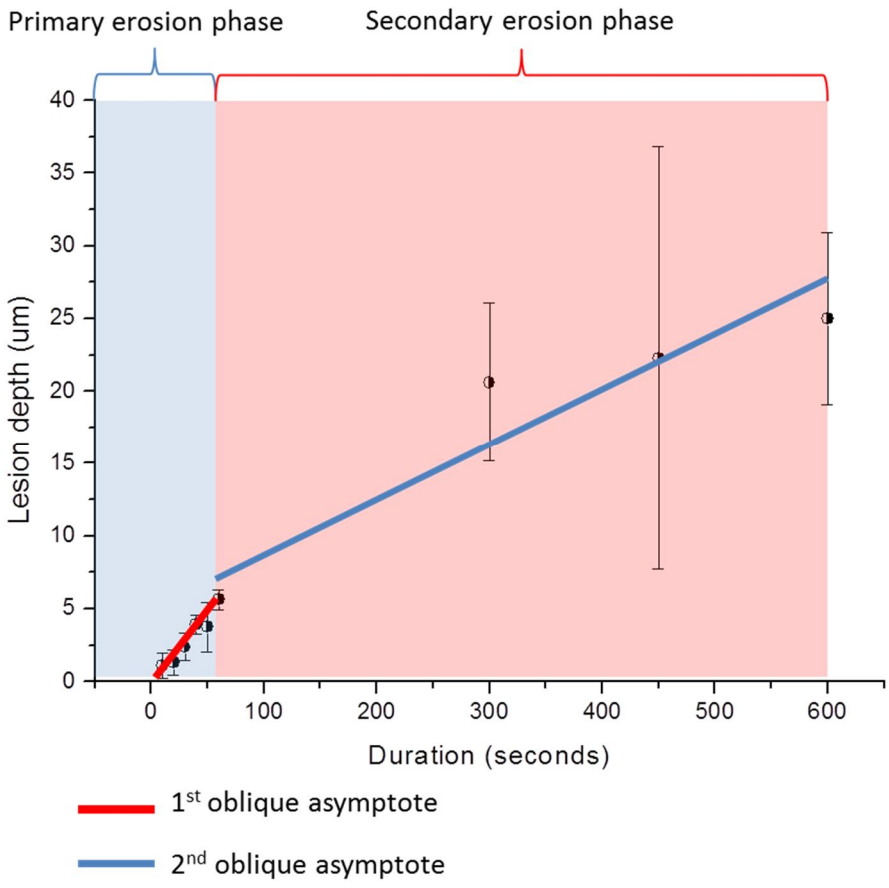

Figure 3.4-2: Schematic representation showing the division of the early erosion event into two distinct trends at 10-60 seconds and 60-600 seconds.

Oblique asymptotes were fitted to previously obtained profilometry data from 1 mol.L^{-1} acetic, citric and phosphoric acid and the results of this analysis are presented in Table 3.4-1:

ACID TYPE (1 mol.L^{-1})	10-60s µm.s^{-1}	Std Err	Adj R^2	60-600s µm.s^{-1}	Std Err	Adj R^2
Acetic						
Bovine	0.48	0.07	0.90	0.03	0.01	0.50
Human	0.17	0.10	0.32	0.02	0.00	0.88
Citric						
Bovine	0.19	0.03	0.86	0.02	0.02	0.19
Human	0.19	0.04	0.81	0.03	0.02	0.04
Phosphoric						
Bovine	0.10	0.01	0.96	0.03	0.02	0.43
Human	0.09	0.01	0.92	0.04	0.01	0.82

Table 3.4-1: A biphasic trend of erosion occurring during enamel dissolution using 1 mol.L^{-1} acetic, citric and phosphoric acids revealed by linear analysis of the rates of erosion at 10 -60 seconds and 60 – 600 seconds (n = 8 for each category).

1 mol.L^{-1} acetic acid eroded human enamel at a rate of 0.17 µm.s^{-1} (±0.01) between 10-60 seconds, while bovine enamel was eroded at a rate of 0.48 µm.s $^{-1}$ (±0.07). The later stages of erosion saw a reduction in the rates of tissue loss for both human and bovine enamel: Bovine enamel increased in depth at a rate of 0.02 µm.s^{-1} (±0.02) and human enamel increased at a rate of 0.02 µm.s^{-1} (±0.01). A one-way ANOVA of the rate means showed bovine erosion was significantly affected by this acid challenge ($p = 0.002$) at 10-60 seconds, while human enamel was significantly affected ($p = 0.04$) at 60-600 seconds.

Rates of erosion at 10-60 seconds for 1 mol.L^{-1} of citric acid were 0.19 µm.s^{-1} (±0.04) and 0.19 µm.s^{-1} (±0.03) for human and bovine respectively, with good conformity of the model. At later stages of the protocol, 60-600 seconds, the rate of erosion reduced to 0.03 µm.s^{-1} (±0.03) for human, and 0.02 µm.s^{-1} (±0.02) for bovine

samples, with concomitant reduction in goodness-of-fit (R^2_a) to 0.04 and 0.19 from 0.81 and 0.86 for human and bovine respectively. This reduction in R^2_a is further discussed in the summary of this data in section 3.5. A one-way ANOVA of the means showed that both human ($p = 0.004$) and bovine ($p = 0.005$) enamel were significantly affected by the acid during the 10-60 second period but not for the later 60-600 second duration.

The human enamel showed a reduced rate of erosion compared to bovine enamel when treated with 1 $mol.L^{-1}$ phosphoric acid during the 10-60 second phase. The human enamel rate was 0.09 $\mu m.s^{-1}$ (±0.01) compared to 0.10 $\mu m.s^{-1}$ (±0.01) for bovine enamel. Following the latter stages of the challenge, from 60-600 seconds, both bovine and human enamel recorded similar rates of erosion: 0.04 $\mu m.s^{-1}$ (±0.01) for human and 0.03 $\mu m.s^{-1}$ (±0.02) for bovine enamel. A one-way ANOVA showed that the average mean depth was significantly affected during the first phase ($p = 0.001$ for both human and bovine) but no significant difference was observed during the second phase of 60-600 seconds.

3.5. DISCUSSION OF CHAPTER 3

Two points should be considered before beginning a detailed discussion of the findings presented in this chapter: The first relates to data from this chapter and all subsequent chapters: These data relate exclusively to the *in vitro* physicochemical behaviour of enamel, without additional factors that would influence the result were this to be replicated *in vivo*. Such factors would include saliva, the biofilm and the fluid mechanics of the oral cavity, as well as synergistic pathological factors such as abrasion. Second, the comparative work performed in section 2.9 employed the two principal protocols of erosion in dental studies, which were evaluated against each other. A feature of this work which deserves special mention is the durations of acid exposure, which are not common in the literature. This was done in order to satisfy the approximation of short duration exposure of acidic fluids to enamel as occurs during beverage consumption. The consequences of this short duration acid exposure are that the erosion lesions are correspondingly smaller and distinguishing the mean lesion depths from background error could on occasion be difficult.

A number of studies in the literature employ multiple samples at defined, often excessively long time intervals in order to elucidate data regarding dental erosion (Eisenburger & Addy, 2001; West *et al*, 2000). The work in this thesis set out to explore the effects of acid erosion on dental enamel following repeated exposures of short duration, better physiologically tolerated acid solutions. The purpose of the initial protocol in section 3.1, involving an acid of 1 $mol.L^{-1}$, was to allow measurement methods to be established and validated. Furthermore, it permitted the determination of the potential shape of the data at these early durations of exposure, albeit at a high

acid concentration. This would provide guidance for later experimental work using more commercially applicable concentrations. It should also be noted that a significant amount of work was put into ensuring the assays and measurement methods could measure, repeatedly and reliably, the relatively small changes that occurred in the enamel.

Focussing the work on the first 60 seconds of erosion permits the *in vitro* assessment of the effects of repeated, short duration exposure of an acid media on enamel, as may be encountered when consuming a can of carbonated beverage. This has potential relevance for the clinical aspect, relating as it does to an increasing trend in the excessive consumption of such beverages (Hunter *et al.*, 1999; Barbour & Ress, 2004). However, the relative paucity of data with respect to these early durations would make a comparison with the literature difficult. Thus the study incudes three additional time points to increase the overall experimental duration to 10 minutes, which has been employed previously by other authors (Bartlett *et* al., 2003; White *et al*., 2010)

OPTICAL PROFILOMETRY AND QLF

The bar chart shown in Figure 3.3-1 serves to highlight the variation present within samples when using optical profilometry (OP), which is a well documented characteristic, particularly of bovine enamel (Moss, 1998; Iijima *et al*, 1999). This is much reduced in the QLF data, an observation also reported by Elton *et al* (2009). The increased variation of the OP data, particularly at the latter stages of the procedure may occur as a result of differential erosion trends based on genetically determined mineral content (Parkinson *et al*, 2010), the depth of grinding for individual samples thereby

exposing more readily dissolved material and the orientation of the enamel rods with respect to different samples (Boyd, 1984) or related to the absorbance of light, which will be discussed further in the next chapter.

Such large error within the OP data may be also explained by the restricted image sample size necessitated by equipment restrictions and the shape of the lesion, about which more will be discussed later. The data presented in this chapter does not compare well with that obtained from QLF, which may be a reflection of the current state of this relatively new technique compared to the more well established OP. The former technique remains contentious owing to the conflicting reports of lesion measurements present in the literature, which contrast to measurements from well established protocols employing alternative instrumentation such as transverse microradiography (Pretty *et al*, 2004; Stookey, 2004; Elton *et al*., 2005).

The research discussed in these previous subchapters has provided insight regarding the effect of a repeated short duration acid exposure to human and bovine enamel. The statistical analysis has shown that bovine material is a suitable substitute for human material regarding bulk tissue loss when investigating repeated short duration acid exposure. As such any subsequent investigative work may be considered valid with respect to both species.

POTENTIAL FOR A BIPHASIC TREND OF EROSION

There is a lack of literature to be found with which to compare the results regarding the exposure durations employed during this work. In particular, it was not possible to locate any previous work relating to the presence of a biphasic trend of bulk

tissue loss in early stage erosion. Therefore any conclusions that can be drawn will need to be substantiated by additional work in the future.

It was noted during this work that the very early stages of enamel erosion, between 10-60 seconds, appeared to progress significantly more rapidly than subsequent dissolution. Attempting to compensate for this by plotting the data as a function of the square root of time did not appear to alter the apparent overall trend shape.

A potential reason for the observed change in erosion trend (measured using optical profilometry) could be attributed to the shape of the erosion lesion. This was observed using μCT and will be further discussed in later chapters, when additional information may be utilised from samples treated with 0.05% acid solutions.

THE SURFACE EROSION OF ENAMEL

As explained in section 3.2, the clinical use of acids arose out of a need to enhance the binding properties of dental restorative materials with the native enamel or dentine. A 20 – 30 second topical application of a 37 % (v/v) solution of acids such as phosphoric acid etches the enamel, exposing the enamel rods and thereby increasing the available surface area: volume for dental material bonding (Buonocore, 1955; Kugel & Ferrari, 2000).

A feature of using such a high concentration of acid, is the comparatively more rapid and pronounced erosion of enamel when compared to more physiologically tolerable acids at concentrations of 0.05 %. The use of phosphoric acid in clinics is well documented (Sasaki *et al.*, 2008; Orellana *et al.*, 2008) and so provided a suitable

example with which to determine what potential effects of erosion might be observed during an early erosion event using weaker solutions. In contrast to the profilometry work which employed 1 mol.L^{-1} acid solutions as the basis for background work, this subsection of work employed a greater quantity of electron microscopy, which is more subjective than quantitative data. There is considerable work in the literature involving the use of acid etching to improve bonding (Hikata *et al*., 2007; Mehdawi *et al*., 2009; Øgaard & Fjeld, 2010) but very little relating to the use of organic acids and none at concentrations of 1 mol L^{-1}. As such, most of the work involving imaging has been done with these commonly used etching acids, one of the most popular being a 37 % (v/v) phosphoric acid solution, which in turn would provide a better comparative basis for our work with that previously published.

The principal observation, using clinically applicable 37% phosphoric acid solutions to erode human and bovine enamel, was the preferential erosion of the intra-rod enamel (or enamel rod core). This is a characteristic pattern of erosion associated with this acid. In addition to this, it was observed that there was an apparent thickening of the inter-rod enamel together with some peripheral mineral loss. This was supported by Poole & Johnson, who hypothesised that the effects of acid type dictated the preferential loss of the enamel rod core (Poole & Johnson, 1967). However, the group focussed exclusively on the type of acid employed and, unlike later authors such as Eisenburger *et al* and Orellana *et al*, did not anticipate different morphological changes of enamel occurring as a result of single acid exposure. (Eisenburger *et al.*, 2000; Orellana *et al*., 2008).

Orellana *et al*. found differential patterns of erosion following a single 30 second phosphoric acid etching of human enamel. 62% of the etch patterns examined were

classified as Type 4 - poorly etched, according to the Galil and Wright [1979] classification*** - rather than the desired preferential dissolution of the enamel core as was observed in our work (Orellana *et al*., 2008). The group attributed their observed differential etching to the effects of phosphoric acid on enamel and placed little emphasis on the role of enamel morphology on the etch pattern. The presence of thin crystals projecting from the intra-rod enamel following an erosion event (as seen in Figure 3.2-2) was observed by Eisenburger *et* al. (Eisenburger *et al*., 2004) and Boyde *et al* (Boyde *et al*., 1978), who attributed this to precipitation of calcium phosphates in solution following the rapid elevation in pH as the hydroxyapatite saturated acid solvent contacts water.

Thus, the etching patterns of human and bovine enamel achieved for this chapter using a 37 % phosphoric acid solution was supported by evidence from the literature thus it was hypothesised that this pattern would be present in eroded enamel using a more physiologically relevant solution.

SUMMARY OF CHAPTER 3

This chapter has set out to investigate the comparative behaviour of human and bovine enamel. An initial assessment of comparatively high concentration (1 mol.L^{-1}) commercially relevant acids found no significant difference between the species, a finding corroborated by quantitative light-induced fluorescence. However, a comparative analysis of the median values of lesion depth obtained using optical profilometry against QLF found significant differences, meaning there was significant

*** See Appendix D – Summary of Galil & Wright, 1979 classification

disparity in the lesion depth measurements recorded by these techniques. The reason for this remains unclear but may be attributed to the genetically determined mineral composition, the effect of sample preparation, light scattering or a combination of all of these.

Furthermore, during the analysis of optical profilometry data it was noted that a potential biphasic trend of erosion appeared to be present at the very early stages of erosion between 10-60 seconds and 60-600 seconds. Rates of erosion were calculated and these were found to be significantly different from each other.

The work thus far, whilst using physiologically more relevant time scales, now will move towards using physiologically more relevant acidity levels. It is hypothesised that the patterns observed in enamel erosion at relatively high concentrations of 1 $mol.L^{-1}$ will be mirrored in the more commercially applicable concentrations of 0.05%, albeit at a reduced level. One tool that shall be brought to this work in the next chapter will be the use of atomic force microscopy to allow the imaging of the surface in 3-dimensional resolution, but also to develop methods to measure the material stiffness at the surface in an attempt to overcome the inconclusive data obtained using the Vickers indenter. The presence of an apparent biphasic trend in erosion suggests that subsurface softening plays an integral role in early erosion events and this will also be further explored in later chapters.

CHAPTER 4.

THE EFFECTS OF ACID ON HUMAN AND BOVINE ENAMEL.

4.1. THE EROSION TREND AT PHYSIOLOGICALLY TOLERABLE CONCENTRATIONS

Chapter 2 described the differences between the two most commonly employed protocols when evaluating dental erosion. In particular it drew attention to the increased bulk tissue loss occurring on an enamel sample arising from a repeated exposure model of dental erosion. Chapter 3 employed this protocol but used exposure durations based on more realistic drinking times and commensurate with behaviour such as sipping. This was experimentally tested using 1 $mol.L^{-1}$ solutions of three commonly employed commercial acids. The results obtained using optical profilometry were cross-referenced with an emerging rapid quantitative technique of QLF and found to be significantly different. Furthermore, the shape of the plotted data were suggestive of a biphasic trend of erosion, for which no description could be found in the literature.

Chapter 4 sets out to further explore the physicochemical properties observed in the previous chapter using acid solutions which are of lower concentration and employed in the drinks industry. It will aim to determine if the biphasic trend is reproducible using lower concentrations of acids, whether or not QLF is suitable as a diagnostic technique and examine the microscopic changes at the acid:surface interface. The latter should provide evidence for the effect of enamel softening, the gradual dissolution of subsurface calcium and phosphates thought to result in progressive surface enamel bulk tissue loss (Eisenburger *et al*, 2004)

Chapter 3 described the finding that the erosion does not appear to progress in a single linear event but consists of two relatively discrete phases when subjected to 1 $mol.L^{-1}$ acid solutions. As mentioned previously, the use of such strong acids is not

physiologically tolerated, therefore we aimed to investigate whether this biphasic phenomenon would occur using more appropriate solutions. The work had to remain standardised, in accordance with the previous work, in order to minimise extraneous variables. As such a concentration mirroring that of a single acid beverage was selected using an independent commercial source[†††] detailing consumer drinking habits and a leading manufacturer[‡‡‡] provided the concentration of the selected acid at 0.05%. The table below shows the equivalent 0.05 % (v/v) expressed as moles:

Acid type	Molecular weight ($g.mol^{-1}$)	Moles used ($mol.L^{-1}$)
Acetic	60.05	8.33×10^{-4}
Citric	192	2.60×10^{-4}
Phosphoric	98	5.10×10^{-4}

Table 4.1-1: The molar equivalent of 0.05 % (v/v) acid solutions

In accordance with the work performed in Chapter 3, the initial results were obtained using optical profilometry.

[†††] Just-drinks.com is an independent, online resource for professionals in the beverage industry. The publication lists colas as having a 41% stake in the global soft drinks industry.
[‡‡‡] Coca-Cola Company, plc – personal communication.

4.1.1. EFFECT OF THREE COMMERCIALLY RELEVANT ACIDS ON EARLY STAGE ENAMEL EROSION AT LOW CONCENTRATIONS.

4.1.1.1. 0.05 % ACETIC ACID

Figure 4.1-1 shows the effect of a cumulative 600 second 0.05% acetic acid challenge on human and bovine enamel. After 10 seconds exposure the median human enamel lesion was 1.86 µm (1.50 Q1-Q3) in depth and the median bovine lesion depth was 0.0* µm (3.95 Q1-Q3) §§§. After 30 seconds exposure the median human enamel lesion was 1.59 µm (1.44 Q1-Q3) in depth and the median bovine lesion depth was 1.11 µm (6.45 Q1-Q3). A Mann-Whitney U-test of the intersample (bovine *versus* human) median values was not significant.

The median bovine enamel lesion depth at 60 seconds was 3.26 µm (6.03 Q1-Q3) and human lesion depth was 1.50 µm (0.94 Q1-Q3) and again the two results were not significant from each other. By 300 seconds, the median lesion depths had increased to 1.62 µm (0.92 Q1-Q3) for human and 2.12 µm (3.26 Q1-Q3) for bovine. By the end of the experiment at 600 seconds the median lesion depth of human enamel was 2.74 µm (2.04 Q1-Q3), while the mean bovine lesion depth was 4.68 µm (3.21 Q1-Q3). A Mann-Whitney U-test showed there was no significant difference between the means of the two species at 600 seconds and Kruskall-Walllis ANOVA of the intrasample data of both specimens was not significant.

§§§ The measurement of 0.0* indicates no net bulk tissue loss for the sample. This may potentially result from intersample variation.

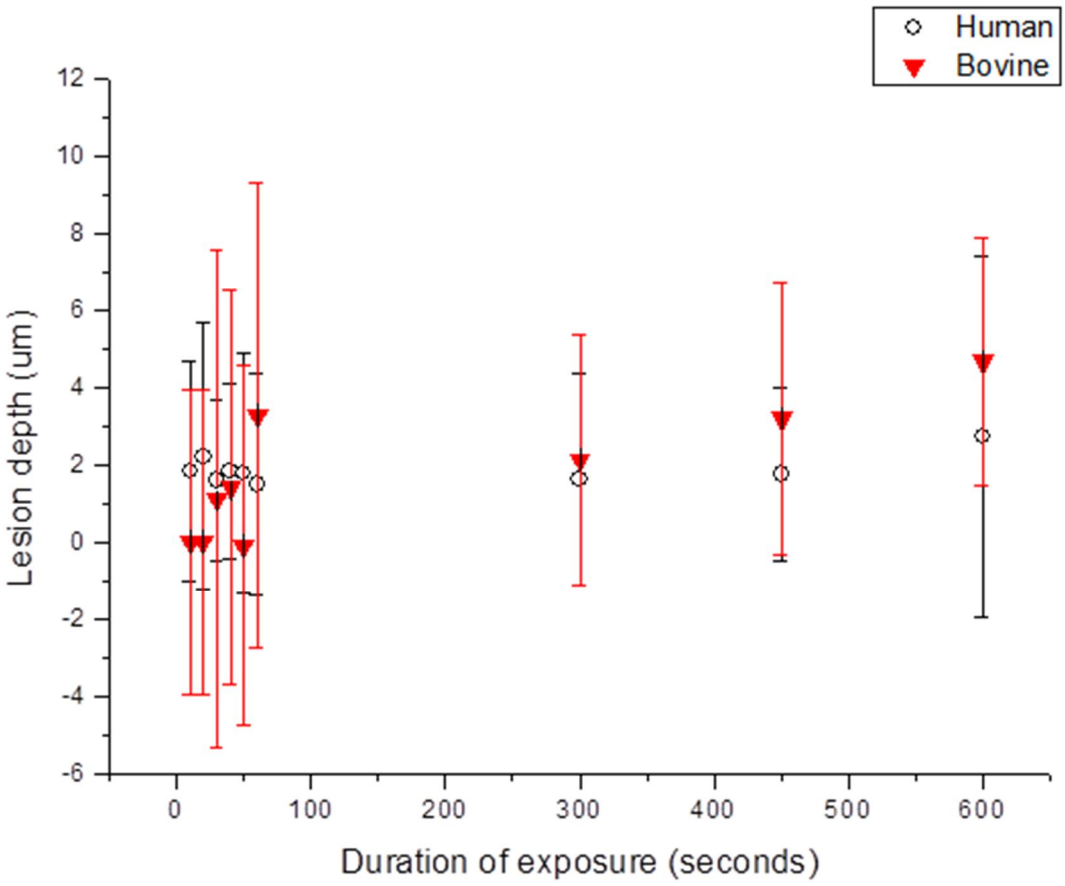

Figure 4.1-1: The median and IQR of samples of human and bovine enamel during a cumulative 600 second 0.05 % acetic acid erosion challenge (n = 8).

4.1.1.2. 0.05 % CITRIC ACID

Figure 4.1-2 shows the effect of a cumulative 600 second 0.05% citric acid challenge on human and bovine enamel. After 10 seconds erosion the median human enamel lesion was 0.56 µm (1.96 Q1-Q3) in depth and the median bovine lesion depth was 0.39 µm (0.46 Q1-Q3). After 30 seconds erosion the median human enamel lesion was 0.98 µm (1.60 Q1-Q3) in depth and the median bovine lesion depth was 0.02 µm (0.69 Q1-Q3). The human enamel lesion depth at 60 seconds was 1.14 µm (1.71 Q1-Q3) and bovine lesion depth was 0.0* µm (0.94 Q1-Q3). By 300 seconds, the median lesion depths had increased to 0.88 µm (1.13 Q1-Q3) for human and 0.0* µm (0.85 Q1-Q3) for

bovine lesion depth, which were not significantly different from each other (p = 0.08). At the end of the experiment at 600 seconds the median lesion depths for human enamel lesion depth was 1.46 µm (2.61 Q1-Q3), while mean bovine lesion depth was 0.28 µm (0.80 Q1-Q3). These values were not significant from each other and a Kruskall-Wallis ANOVA was not significant for either species intrasample variability.

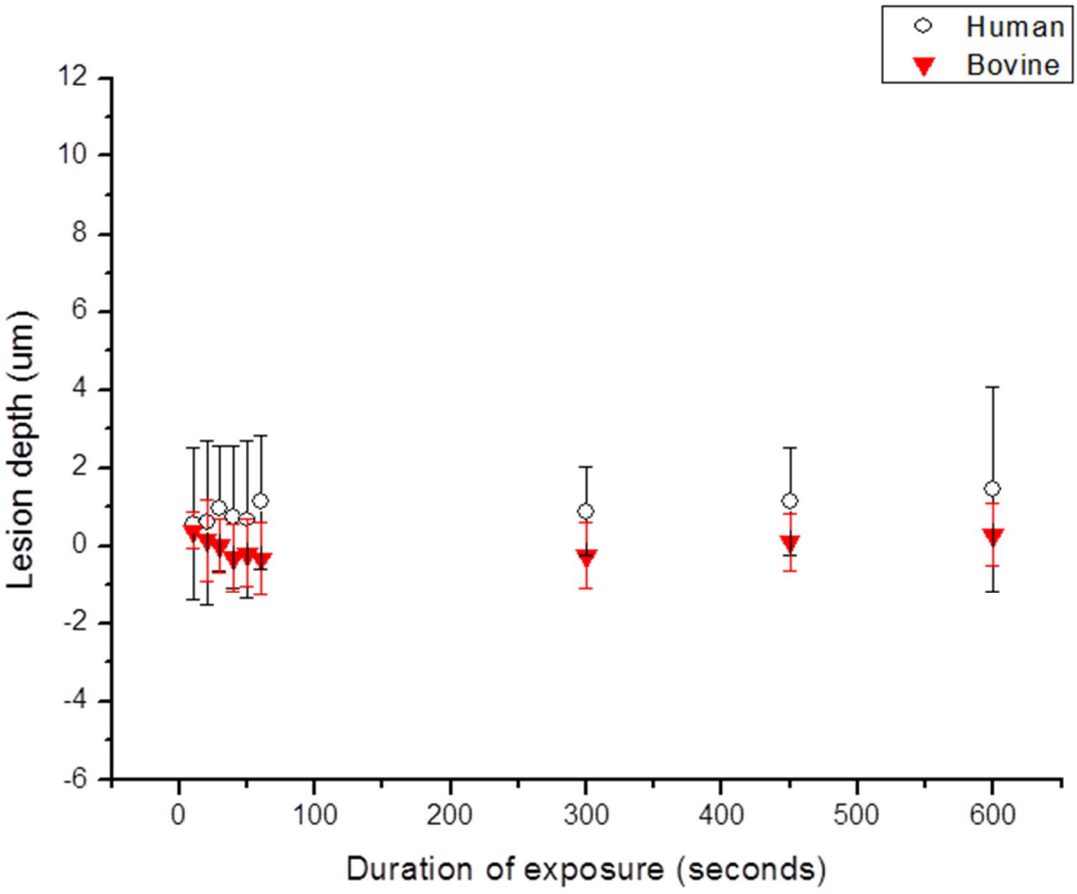

Figure 4.1-2: The median and IQR of samples of human and bovine enamel during a cumulative 600 second 0.05 % citric acid erosion challenge (n = 8).

In this particular dataset there is minimal change in enamel depth over the first 300 seconds for both human and bovine enamel but a gradual increase in lesion depth becomes apparent for human enamel as the experiment continues to 450 and 600 seconds. This gradual increase in lesion depth is less marked for bovine enamel but not significant.

4.1.1.3. 0.05 % PHOSPHORIC ACID

Figure 4.1-3 shows the effect of a cumulative 600 second 0.05% phosphoric acid challenge on human and bovine enamel. After 10 seconds erosion the median human enamel lesion was 0.20 µm (3.48 Q1-Q3) in depth and the median bovine lesion depth was 0.31 µm (1.57 Q1-Q3). After 30 seconds erosion the median human enamel lesion was 0.0* µm (0.60 Q1-Q3) in depth and the median bovine lesion depth was 1.33 µm (4.79 Q1-Q3). The human enamel lesion depth at 60 seconds was 0.77 µm (3.08 Q1-Q3) and bovine lesion depth was 2.15 µm (4.62 Q1-Q3); these were not significant from each other. By 300 seconds, the median lesion depths were 0.83 µm (3.37 Q1-Q3) for human and 3.13 µm (1.72 Q1-Q3) for bovine. At the end of the experiment at 600 seconds the human enamel lesion depth was 0.90 µm (2.52 Q1-Q3), while median bovine lesion depth was 5.40 µm (1.77 Q1-Q3).

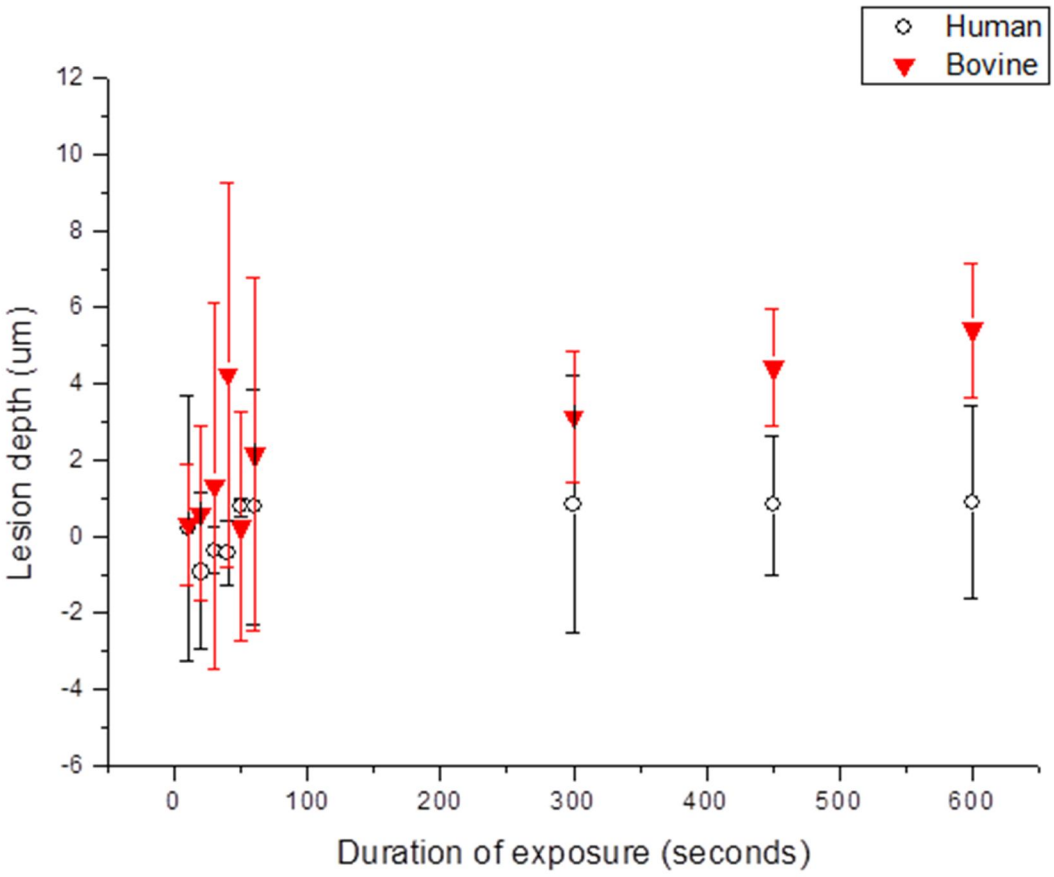

Figure 4.1-3: The median and IQR of samples of human and bovine enamel during a cumulative 600 second 0.05 % phosphoric acid erosion challenge (n = 8).

A comparison of the means (Mann-Whitney U-test) of bovine and human enamel is not significant until 600 seconds whereupon a significant difference becomes apparent ($p = 0.02$). A Kruskall-Wallis ANOVA of the intrasample data was significant for both human and bovine lesion depths ($p = 0.0.4$ and 0.001, respectively) and the variation for human lesion depths was also significant according to Levene's test ($p = >0.01$). The data for the phosphoric acid shows evidence for a similar two-stage erosion event as was seen with the higher concentration acids discussed in chapter 3.

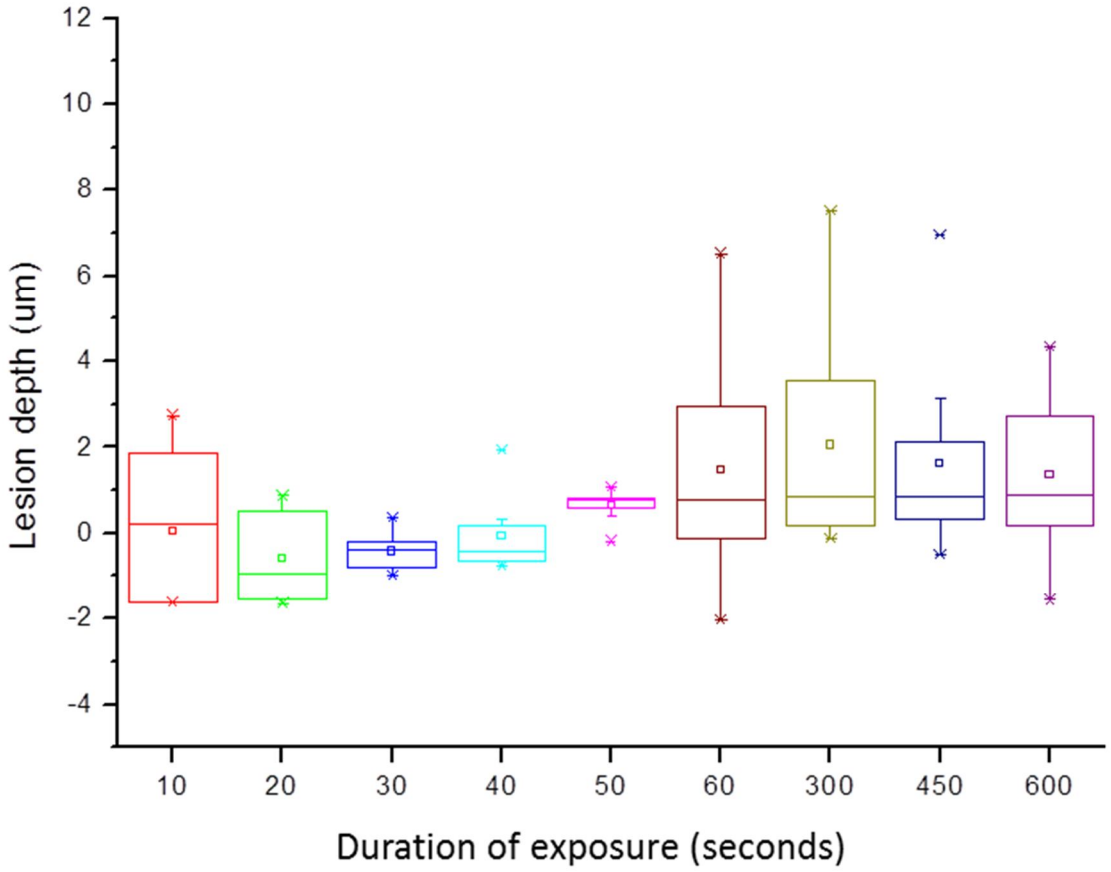

Figure 4.1-4: Box plot of human enamel data eroded with 0.05% phosphoric acid for a cumulative total of 600 seconds (n = 8).

It can be seen from Figure 4.1-4 that the data is skewed to the right - thus the data is not normally distributed but has comparatively few high values - in a number of categories, in particular those between 60 – 600 seconds. Having previously established the variance is significant between the samples, a non-parametric Kruskal-Wallis ANOVA for the human data was performed, which showed there was no significance between the data. The erosion behaviour for this acid appears to favour an initial rapid rate of erosion followed by a reduction in the rate for the later durations but the mean values were not significantly different from each other. However, this may be confirmed by examining the linear rates between 10 – 60 seconds and 60 – 600 seconds in the next section.

As with the previous chapter, the results for all three acids were divided into 10-60 second and 60-600 second categories to plot the rates of erosion pertaining to the most likely rate change observed in the graphical data.

4.1.2. BEHAVIOUR OF EROSION: 0.05 % RATES

There was no significant difference in the trend of lesion development of bovine enamel created using 1 mol.L^{-1} and 0.05 % acetic acid, irrespective of the acid used. By contrast, human enamel was significantly less affected by all the acids ($p = >0.001$).

The 1 mol.L^{-1} acid study revealed a biphasic trend in erosion (see Section 3.4) which, it is hypothesised, should still be present at these reduced concentrations, albeit a reduced rate.

ACID TYPE (0.05% solution)	10-60s µm/s	Std Err	R^2a	60-600s µm/s	Std Err	R^2a
Acetic						
Bovine	0.040	0.040	0.00	0.006	0.002	0.76
Human	0*	0.009	0.24	0.001	< 0.001	0.95
Citric						
Bovine	0*	0.001	0.95	0.001	0.000	1.00
Human	0*	0.002	0.03	0.003	0.001	0.79
Phosphoric						
Bovine	0.035	0.020	0.29	0.007	0.001	0.96
Human	0*	0.010	0.85	0*	0.001	0.88

Table 4.1-2: Biphasic trend of erosion occurring during enamel dissolution using 0.05% acids, revealed by linear calculation of the rates of erosion at 10-60 seconds and 60-600 seconds. Results of 0* indicate no apparent bulk tissue loss, most likely attributed to intrasample variation (n = 8 for each category).

Table 4.1-2 shows a mixed picture of the 0.05% data compared to the 1 mol.L^{-1} data presented in Table 3.4-1. The initial rate of erosion for bovine enamel exposed to 0.05% acetic acid was 40 x 10^{-3} µm.s^{-1} (±40 x 10^{-3} SE) and human enamel remained comparatively static, apparently showing no mineral loss at 0* µm.s^{-1} (±4 x 10^{-3} SE). At the later durations of exposure, between 60-600 seconds, this rate had decreased by a factor of 10 to 6 x 10^{-3} µm.s^{-1} (±2 x 10^{-3} SE) for bovine and marginally increased for human enamel at 2 x 10^{-3} µm.s^{-1} (±1 x 10^{-3} SE). The later stages of the erosion rate showed a greater R^2_a, indicating better conformity of this model to that encountered by chance or intrasample variability.

The initial 0.05% citric acid data showed a different rate pattern to the erosion rates of 0.05% acetic acid data: the variation in the data of bovine and human enamel gave the effect of no apparent mineral loss, recorded as an initial rate of 0* µm.s^{-1} (±1 x 10^{-3} SE) for bovine enamel and 0* µm.s^{-1} (±2 x 10^{-3} SE) for human enamel. As with the example of human enamel eroded using acetic acid, this may not be indicative of any absence of bulk tissue loss but a reflection of the data variation. The later stages of erosion (60-600 seconds) showed an increase in the rate of erosion for bovine enamel to 1 x 10^{-3} µm.s^{-1} (±1 x 10^{-3} SE), while human enamel increased to 3 x 10^{-3} µm.s^{-1} (±1 x 10^{-3} SE). With the exception of the 10-60 second rate for human enamel, all samples showed good conformity to the hypothesised model.

0.05% phosphoric acid showed bovine enamel eroded at a rate of 35 x 10^{-3} µm.s^{-1} (±20 x 10^{-3} SE) but human enamel appeared to remain static at a rate of 0* µm.s^{-1} (±2 x 10^{-3} SE). Data from the 60-600 seconds category showed a reduction in erosion for bovine enamel to a rate of 7 x 10^{-3} µm.s^{-1} (±1 x 10^{-3} SE) and human enamel showed an increase of erosion to 3 x 10^{-3} µm.s^{-1} (±1 x 10^{-3} SE).

4.2. RAPID MEASUREMENTS FOR THE CLINICAL SETTING

As seen in section 3.3, QLF is a rapid technique for determining mineral loss in dental tissues. No significant difference was observed in the results using 1 mol.L^{-1} acid solutions and it was hypothesised that no significant difference would again be apparent in this study.

ACID TYPE	ΔQ (μm)	SD	F STATISTIC
Acetic			
Bovine	7.09	1.37	**0.45**
Human	8.18	2.20	
Citric			
Bovine	7.76	1.71	**0.87**
Human	8.14	2.63	
Phosphoric			
Bovine	6.49	0.11	**0.03**
Human	8.29	1.33	

Table 4.2-1: Results of the mean values of QLF analysis on bovine and human enamel following a cumulative 600 second immersion in 0.05% acetic, citric and phosphoric acid (n = 8).

Table 4.2-1 shows the results of a QLF analysis of human and bovine enamel eroded using 0.05% solutions of acetic, citric or phosphoric acid. There was no statistical significant difference between human and bovine samples for both acetic (p = 0.45) and citric (p = 0.87) acids. However a significant difference in ΔQ (p = 0.03), correlated to a change in height, was found for human versus bovine material post 600 seconds erosion in phosphoric acid.

Acid type (0.05 % solution)	ΔQ (μm)	OP* (μm)	F statistic
Acetic			
Bovine	7.09	3.77	0.07
Human	8.18	3.01	0.04
Citric			
Bovine	7.76	0.30	> 0.001
Human	8.14	2.20	0.01
Phosphoric			
Bovine	6.49	5.52	0.17
Human	8.29	1.35	> 0.001
F statistic	0.56	0.03	

* Optical profilometry

Table 4.2-2: Comparison of the mean depth of lesions created in bovine and human enamel using 0.05% acetic, citric or phosphoric acid over 600 seconds measured using QLF (ΔQ) and optical profilometry (OP).

Table 4.2-2 shows the result of a direct comparison of these two techniques (QLF and optical profilometry) using Mann-Whitney U-tests. This showed no significant difference in results for bovine material using 0.05% acetic acid ($p = 0.07$) and phosphoric acid ($p = 0.17$). Statistical significance was found for human material using acetic acid ($p = 0.04$), both human and bovine material using citric acid ($p = 0.01$ and >0.001, respectively) and human material eroded with phosphoric acid ($p = >0.001$).

In terms of how the data relates to each other, Figure 4.2-1 shows 0.05% data plotted on the same axis as 1 mol.L^{-1} data.

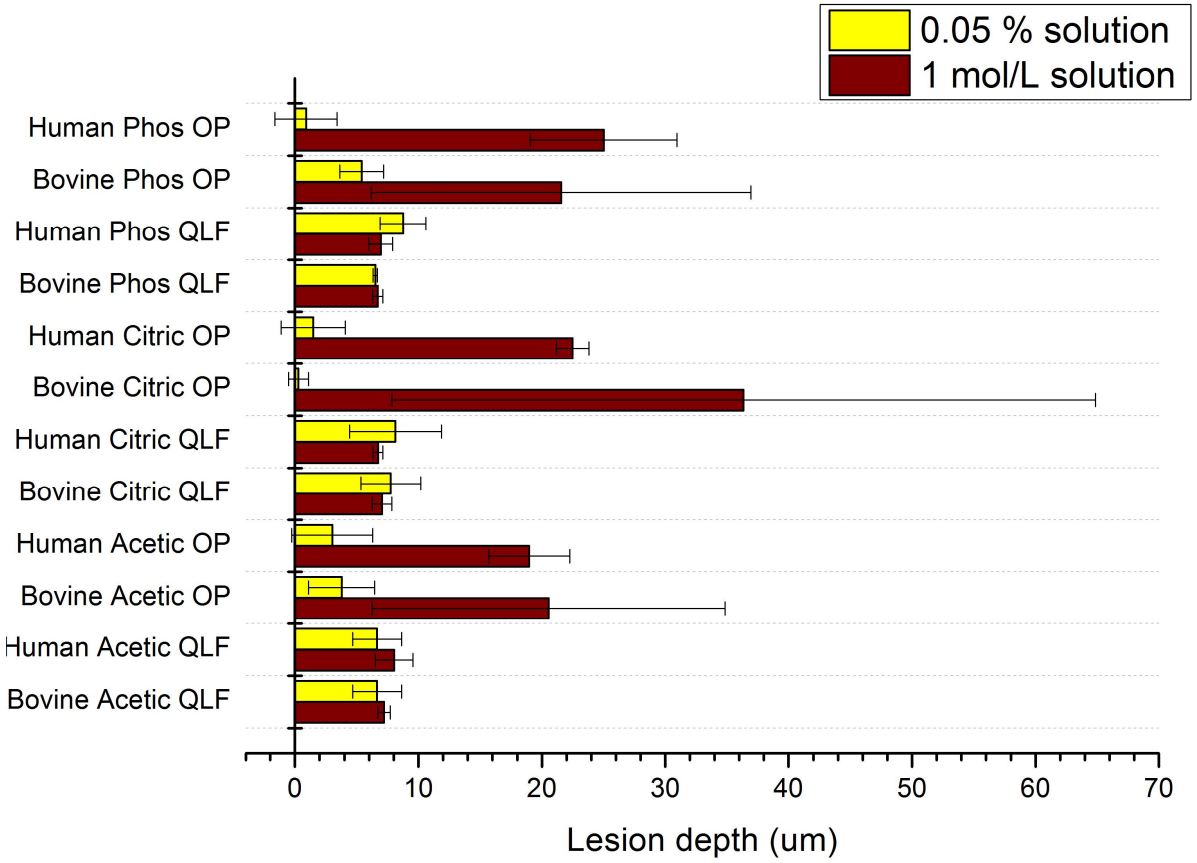

Figure 4.2-1: Bar chart to show the relationship between the median and IQR values of QLF and optical profilometry data for both human and bovine enamel eroded using 1 mol.L^{-1} and 0.05% acetic, citric & phosphoric acid solutions (n = 8).

A comparative analysis of all the QLF results (Kruskall-Wallis ANOVA) for both 1 mol.L-1 and 0.05% erosion of human and bovine material showed no significant difference ($p = 0.44$), while a Kruskall-Wallis ANOVA of optical profilometry showed these data were significantly different ($p = > 0.001$). Further analysis using multiple Mann-Whitney U-tests identified bovine enamel, treated with citric acid to be responsible for the significant impact on the human data – when this category was removed for example, the remaining datasets were not significant from each other ($p = 0.09$), indicating that this data is responsible for the significant skew in the data, most likely a result of anomalous intrasample variation.

4.3. THE MORPHOLOGY OF THE EARLY EROSION LESION.

The 0.05 % acid data yielded some interesting data with respect to the differences between human and bovine material. The absence of significance with respect to lesion depth for bovine enamel compared with the significant difference in human bulk tissue loss may potentially be explained by morphology. It was therefore decided to image a cross section of the lesion using micro-computed tomography (μCT) in order to determine if any surface morphology was affecting the samples.

In order to ensure a readily identifiable and measurable lesion could be formed and imaged with μCT, an extended acid exposure time of 24 hours was used on the samples. This was because the resolution of the imaging modality was not known, therefore it was decided to create an artificially deep lesion, which would be readily detectable.

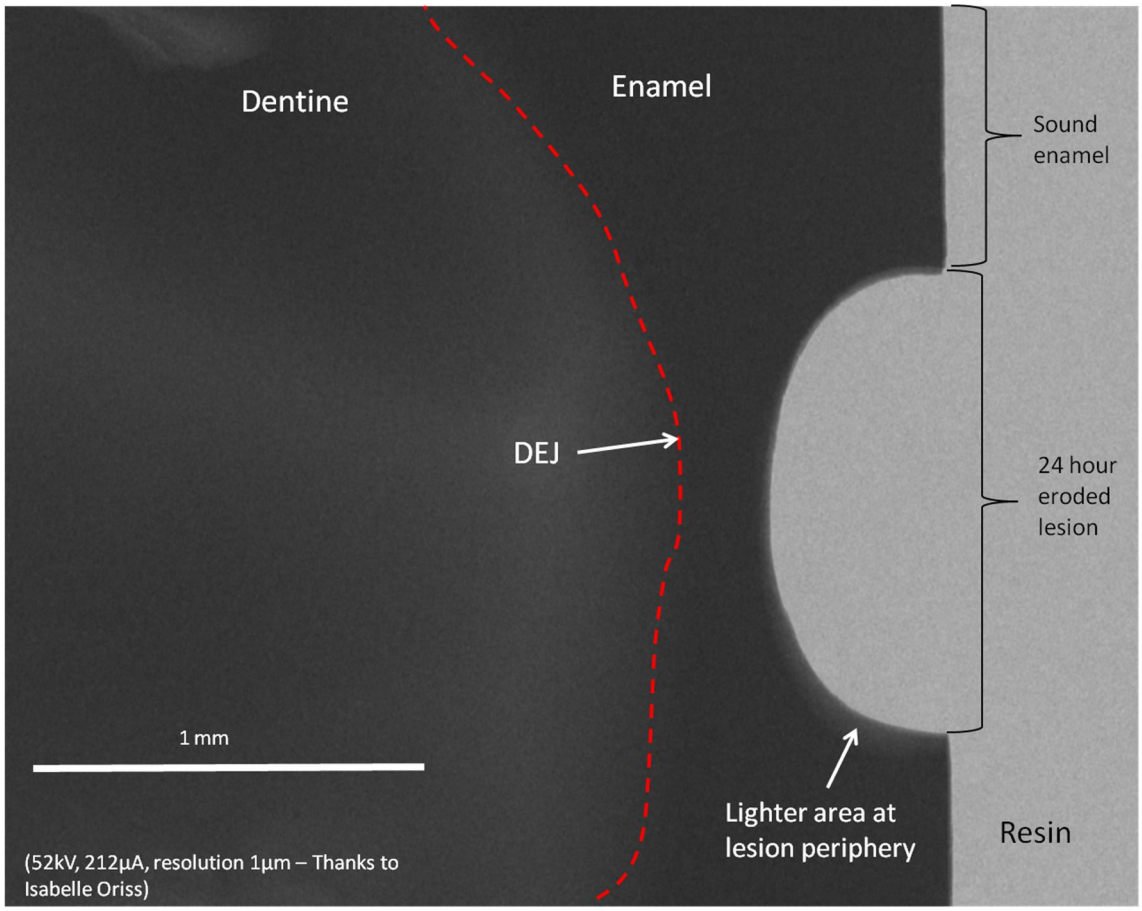

Figure 4.3-1: Cross section of human enamel eroded for 24 hours in 0.05 % phosphoric acid (n = 4).

µCT enabled the characterisation of the erosion lesion (treated with 0.05% phosphoric acid for 24 hours) in cross section without damaging the samples, as shown in Figure 4.3-1. 3-dimensional reconstruction showed the lesion to be bowl-shaped. Erosion progressed under the lip of the erosion window and was deepest at the centre. The lesion depth was measured at 500 µm, approximately 200 µm from the dentine-enamel junction (DEJ). It was possible to clearly define between dentine and enamel in the test sample but the instrument lacked the resolution (clearly imaging items in excess of 10 μm) to be an effective tool at viewing surface and subsurface softening, which would be anticipated to be in the region of 2-5 μm based on work by Eisenburger *et al* (2004).

Additional work to examine a cross section of a pre-prepared erosion lesion using confocal microscopy was also carried out. This would potentially provide details regarding the internal structure of these lesions not obtainable using μCT.

A previously eroded sample (10 minutes in 0.05% phosphoric acid) was cut in cross section through the erosion lesion before being re-embedded in epoxy resin as depicted in Figure 4.3-2:

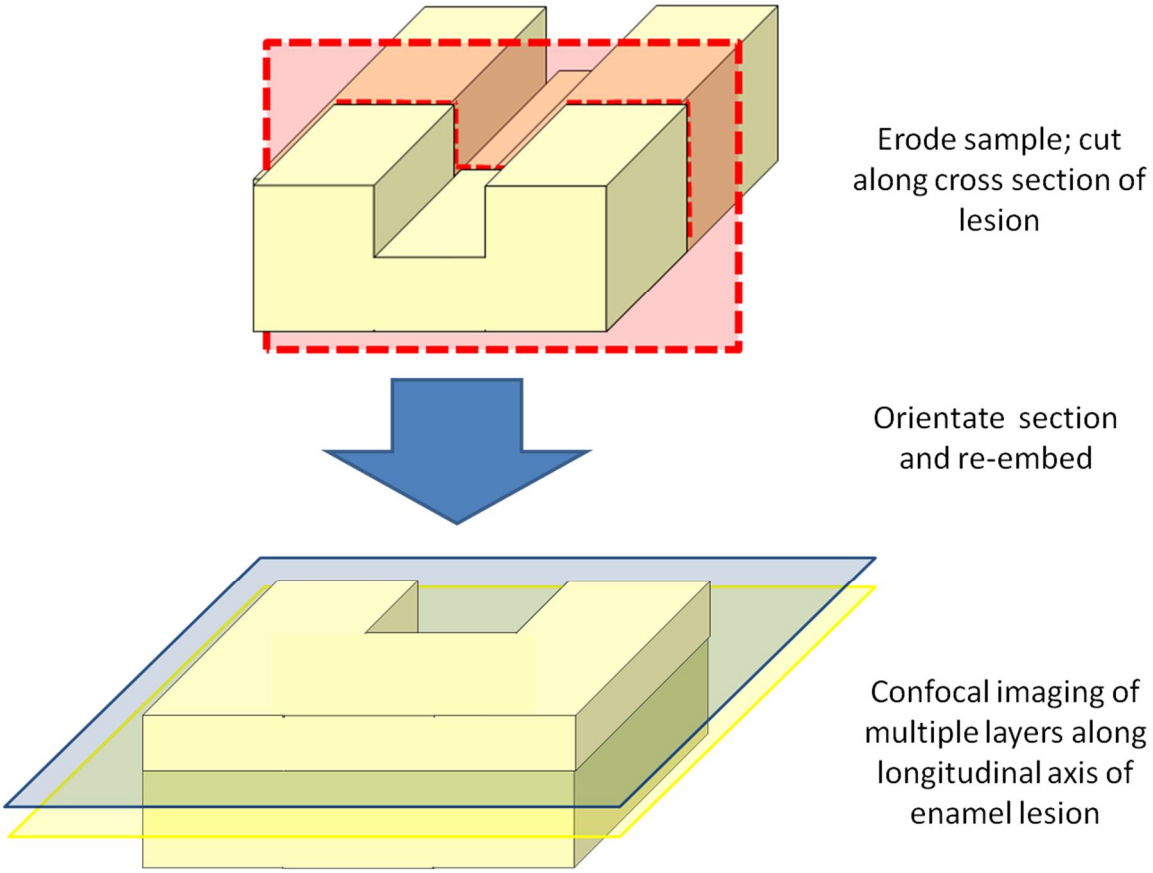

Figure 4.3-2: Schematic representation of the method of processing for obtaining cross section confocal images of an erosion lesion. In this example two areas are sampled, as illustrated below, represented by the blue cut for the superficial section and the yellow cut for a deeper section.

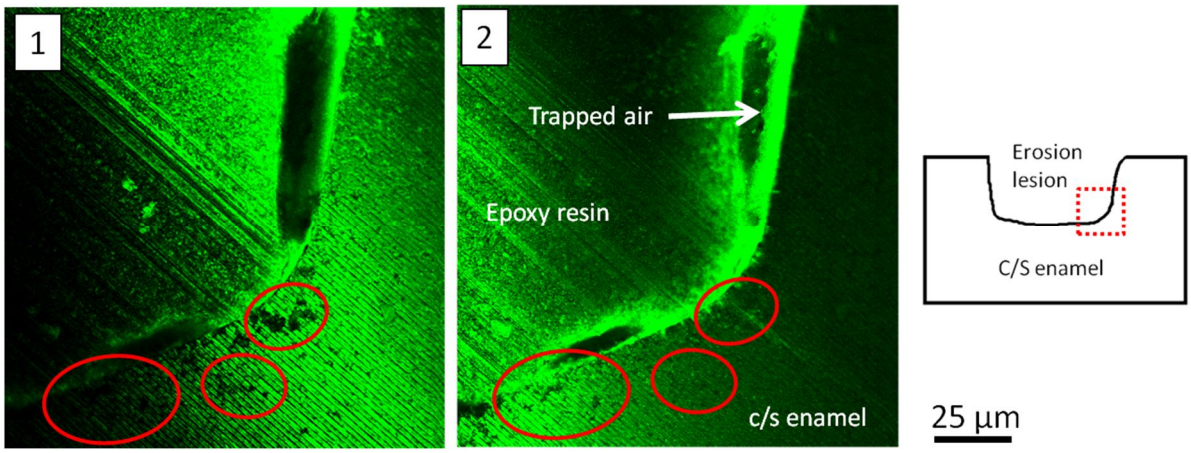

Figure 4.3-3: Sequential confocal images showing progressive increasing depth (image 1 is near the superficial surface; image 2 approximately 10 µm deeper) along the perpendicular axis of human enamel eroded with 0.05% phosphoric acid for 600 seconds. The area enclosed in the red circles appear to show mineral loss attributed to subsurface softening manifesting as microcavities (n = 8).

Two images taken in perpendicular sequence to the lesion are shown in Figure 4.3-3. Imaging of the lesion using confocal microscopy was difficult owing to the highly reflective nature of the mineral component. The epoxy resin is located at the top and right areas of the images, occupying approximately one half of the total image area. Two dark areas, between 25 and 50 µm, are present at the enamel:resin interface projecting into the epoxy resin. These are the remnants of trapped air pockets created when the sample was re-embedded into a second epoxy resin-filled mould. Scratch marks from polishing are present as diagonal lines running from the top right to lower left quadrants of the images. Dark, apparently cavitated areas, potentially representative of enamel softening, are present below the lesion basal surface (visible within the red circles in Image 1), but are not found further along the longitudinal axis of the lesion (Image 2), suggesting areas of isolated subsurface softening within the enamel lesion rather than the expected more uniform softening. It remains possible that these areas of apparent softening are the result of scratch artefact resulting from

polishing, however, should this have been the case it would have been expected that these darkened areas would have been mirrored on the lateral sides of the lesion, whereas they are absent from these images.

4.4. DISCUSSION OF CHAPTER 4

Optical profilometry continues to be useful as a tool for measuring early stage erosion events. The shape of the biphasic trend, initially reported in chapter 3 is supported by data using 0.05 % v/v solutions, however the optical profilometer is perhaps at the limit of its resolution and therefore susceptible to errors.

The body of work in this chapter has shown human enamel suffers significantly less erosion from 0.05 % acid challenges after 600 seconds than those produced using 1 $mol.L^{-1}$, as was expected. By contrast bovine enamel has been shown to be not significant from those lesions produced using a stronger 1 $mol.L^{-1}$ acid solution, thus the lesions are of comparable depth. The most likely explanation for this is the greater bulk tissue loss of bovine enamel compared to human enamel as found by Mellberg (1992) and Attin *et al.* (2007) which is attributed to morphological and mineral differences between the two materials, as discussed in Chapter 1.

The shape of the optical profilometry data largely appeared to corroborate the data found in Chapter 3 – an initial rapid lesion progression followed by a slowing of the bulk tissue loss. However, in some tests the rate data appeared to show static behaviour with respect to material loss of bulk tissue rather than the expected loss as would be attributed to erosion events. This apparently static behaviour observed during the rate calculations using optical profilometry may be explained by a number of factors including chelation, intrasample variability, experimental error and fluidics, the modelling of which is regrettably beyond the scope of this body of work.

The equilibrium reactions for apatite put forward by Patel & Brown (1975) – depicted below – provides a good framework for understanding the uncontrolled kinetics of enamel erosion, irrespective of species:

$$Ca_5(P0_4)_30H_{(s)} \leftrightarrow 5\ Ca(OH)_{2\ (aq)} + 3\ H_3PO_{4\ (aq)} + 9\ H_2O\ (aq)$$

(Patel & Brown, 1975)

Each of these reactants in the equation above may be further broken down to its ionic components, thus this equation simplifies the kinetics involved in hydroxyapatite dissolution but provides an indication of how the crystal would dissociate. Dissolution will be affected by whichever compounds may be present in the solvent, be it acid compound, such as phosphoric acid, or dissolution product such as brushite, octacalcium – or tricalcium phosphate and an increase in any of these compounds would drive dissolution in a particular direction. This is important to understand with respect to dissolution products, rate of dissolution and chelation.

The chelating effects of citric acid, for example, produces hydrated calcium citrate complexes, $Ca_3(citrate)_2.4H_2O$, which reduces the rate of acid action on enamel (Arbel *et al*, 1991). A linear relationship has been shown to exist between phosphates exchanged into solution and citrates exchanged into the matrix (as illustrated in the equation below using ionised citric acid at pH 4.3-4.8). However, as a note of caution in interpreting this data with respect to the work presented in this chapter, saturation of the solution by calcium citrates, which would reduce acid effectiveness along a concentration gradient is unaffected until well past the extent of this body of work:

$HCit^{2-} + 2H^{2+}$ (*interaction from solution to surface interface*) ↔ $H_2PO_4^{1-} + HPO_4^{2-} + 1.5$ Ca^{3+} (*interaction from surface interface to solution*) (Misra, 1996)

The above equation may be better explained in terms of hydroxyapatite dissolution by:

$2\ Ca_5(PO_4)_3OH + 4\ Citrate^{3-} + 12\ H^+ \leftrightarrow 2\ Ca_3(Citrate)_2^{4+} + 4\ Ca^{2+} + 2\ HPO_4^{2-} + 4\ H_2PO_4^- + 2H_20$ (Misra, 1996)

This equation shows the potential that acids, such as citric acid, have in affecting the outcome of dissolution kinetics, something poorly described when dealing with very low concentrations. The effect of chelated calcium has been shown to help reduce the effects of bulk tissue loss following erosion by acting as preferential interaction sites with acid compounds (Misra, 1996). Thus, where erosion occurs at such a low rate, these acid side-effects may play a greater role in enamel dissolution than previously thought. The effects of low acid concentrations on the enamel surface will be investigated in chapter 5.

EXPLAINING VARIATION WITHIN THE DATA

It has been found that the rate of bulk tissue loss increases with greater depth into the lesion. Thus the expected erosion rate would either increase exponentially with increased duration acid exposure (Eisenburger & Addy, 2001) or would increase uniformly about a linear trend as seems to be found more often (Barbour et al., 2005b; Shellis et al., 2005; Zheng et al., 2010). Our work appears to show that that there are two distinct asymptotes, which make up the continuous erosion trends: one for 10-60 seconds, the other between 60-600 seconds. Observed deviation about this trend may

be attributed to a distinct, yet not adequately modelled, erosion pattern or intrasample variability. Intrasample variability, such as chemical composition of the matrix or structural differences are perhaps the most likely cause for variation the results observed in some of these data. This hypothesis is substantiated by the statistical analysis of the rate data, expressed as the adjusted R^2 (R^2_a). As mentioned previously, R^2_a only increases if additional terms added to the equation improve the model more than may be encountered by chance. As there has been no modification of the model between the 1 $mol.L^{-1}$ and 0.05 % acid solution data and given that some expressions maintain an adequate to good R^2_a, while other datasets respond poorly, the most likely explanation is that of intrasample variability. This inter- and intrasample variability is also well documented in the literature (Shellis, 1984; Mellberg, 1992; Parkinson *et al*., 2010) and may play a further role in explaining the significance of results between QLF and optical profilometry.

It should be re-iterated that the work undertaken for this chapter used a number of instruments at the limit of their capabilities, such image resolution or limits of detection, including both the QLF machine and optical profilometer. Neither the available optical profilometer nor the QLF machine were developed for such low level bulk tissue loss measurement as was encountered for these erosion studies. Other machines, such as atomic force microscopy and stylus profilometers are available (the former was utilised during the work for this thesis) and are better suited for the measurement of bulk tissue loss at these low levels but most of the work undertaken in the literature has employed optical profilometry. Physical stylus profilometry, excluding techniques such as AFM, is limited by its inability to determine structures smaller than the probe diameter, typically to 100 - 500 μm (Rodriguez et al., 2008), and the predetermined load may damage or distort fragile topography created during the

erosion process (Heurich *et al.*, 2010). Furthermore, the much longer durations of exposure to acids employed by these other works resulted in comparatively deeper lesions which may be easily scanned and processed using optical profilometers.

Such low levels of mineral loss as were encountered during the 0.05 % acid erosion work means that any potential contamination will have a more noticeable effect on the sample variation (in the case of ion chromatography) and variation about the mean depth will be more pronounced in the overall results, as was observed in the optical profilometry results. However, QLF and optical profilometry exhibit significantly different results when directly compared. The optical profilometer was carefully calibrated using manufactured precision calibration grooves, ranging in depth from 1 - 30 μm and included multiple single spot sampling in order to obtain an average individual reading. The QLF machine was calibrated using manufacturer-supplied colour intensity *versus* corresponding depth grid, as presented in materials and methods, thus the variability attributed to detector sensitivity was minimised as much as possible.

The most likely reasons for this variability which remain are differences in the optical detection methods relating to light scattering and absorbance by enamel (Rodriguez *et al.*, 2008). In optical profilometry, broad spectrum light reflected was from the surface at different wavelengths corresponding to different heights and interpreted through interferometry[****]. By contrast, QLF employs a narrow wavelength (370 nm) light source to detect the natural autofluorescence of enamel, which is thought to be susceptible to erosion mediated light scattering. This will be discussed in greater detail later in this chapter.

[****] See Section 1.12.4, "Non-contact profilometry".

Eroded enamel consists of a crater shaped lesion and a superficial softened layer of enamel, as was found using μCT observed in Figure 4.3-1 and corroborated by the literature (Eisenburger *et al*., 2001). The softened superficial surface will not create a light scattering effect using QLF as this layer is considered too thin (Attin, 2006) whereas this may not be the situation for reflected light used in optical profilometry. As such, the erosion lesion measured using optical profilometry result may appear deeper than one measured using QLF.

The literature becomes more contradictory with respect to light absorbance as a cause for the significance of profilometry *vs*. QLF data. As mentioned previously, it is not clearly understood what drives autofluorescence change in human and bovine enamel although suggestions have been put forward, such as from Spitzer & Ten Bosch who found evidence of three distinct spectra at 350–360 nm, 405–410 nm, 440–450 nm and attributed it to the organic fraction of enamel, in particular the amino acid tryptophan (for emission spectra between 405 -450 nm). It was further found that an erosive challenge will cause a shift in autofluorescence, particularly at the 450 nm emission band and this was attributed to light scattering and wavelength dependent upon that scattering (Spitzer & Ten Bosch, 1976). Pretty *et al*. add alternative suggestions for this including the prevention of light entry and exit into underlying fluorescent tissue by light scattering and a change in the chromophore's molecular environment resulting in fluorescence decrease (Pretty *et al.*, 2004). However, consensus of the validity of QLF remains inconclusive. Pretty *et al*. found good correlation of ΔQ with change in sample height, ΔZ, r = 0.87, but increasing data variation with depth (Pretty *et al.*, 2004) while Elton *et al.* could not reproduce this and found a poor correlation of 0.25 for ΔQ against change in height (Pretty *et al.*, 2004). Furthermore, QLF software cannot differentiate between sound and partially eroded

enamel. This is achieved by use of luminescence threshold limits, typically set at 5% loss of fluorescence, whereupon a pixel is designated as eroded. In such early erosion events as the data presented in chapter 4, the subsurface lesion may be affected by an acid challenge sufficiently to record a 5 % loss of mineral thus giving an indication of a deeper lesion than was actually present.

Confocal microscopy, a technique commonly used in cell biology to generate 3-dimensional images of cells and their internal structures, may also be utilised to view internal structures of enamel, although the density of this mineral makes high resolution imaging at depths difficult. Radlanski (2001) employed this technique, coupled with serial grinding, to determine the pathway of a group of enamel rods from their point of origin at the DEJ to the surface of a tooth. A problem with confocal microscopy as an assessment lies in the flaring artefact and the serial grinding of samples: any grinding of softened enamel has the potential to destroy fragile surface/subsurface structures or features and is particularly dependent on variables such as grit-paper grade. Therefore the most accurate evidence of surface/subsurface events lies below the exposed surface at the point at which confocal microscopy becomes more limited unless the enamel is ground down.

From Figure 4.3-3 (the sequential confocal images of eroded enamel) it was possible to observe the potential effects of acid softening on enamel. The highlighted areas appeared to show pitting of the subsurface, while the surface interface remained intact. Such a phenomenon has been reported by Dowker *et al.* (2003), who identified areas of mineral softening in lesions following a cumulative 36-170 days acid exposure and Eisenburger *et al*., (2004) who found reported subsurface softening events exposed in association with ultrasonication. However, the observations described in Figure

4.3-3 may also be attributed to grinding and polishing artefact. While this is a distinct possibility it can also be seen from these images that the dark, pitted areas are not to be found within the walls of the lesion (at the bottom right) but seem to be more localised to the basal surface. This would suggest that the walls are less susceptible to the effects of acid, possibly as a result of the fluid dynamics described above, and that the bulk of the softening is occurred at the base, from where it would be possible for mineral to be displaced during polishing. The presence of air pockets may be ignored as these are post-erosion artefacts and thus would have no impact in affecting acid:surface interactions.

As a consequence of our observations regarding the lesion morphology and the results obtained from optical profilometry, which appear to show a biphasic trend of erosion, we hypothesised that a change in erosion dynamics may occur between 60-300 seconds. One hypothesis modelling this change in erosion rates involves the interaction of acid compounds and flow dynamics and is suggested below.

HYPOTHETICAL MODEL OF EARLY ENAMEL EROSION

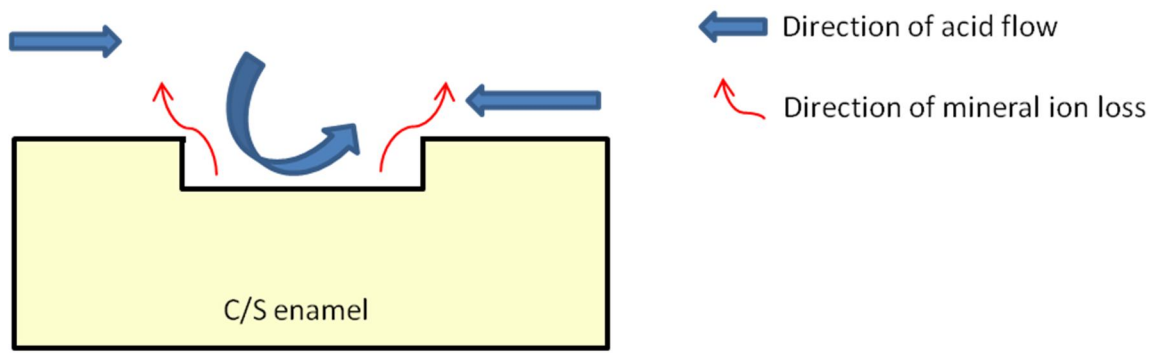

At the early stage of demineralisation (10-60 seconds, illustrated above) acid flow over the surface of the sample is continuous and uninterrupted, as illustrated by

Mazouchi & Homsy (2001), but progressively deepening the lesion. Mineral ions are released into the solution following a diffusion gradient. Saturation of the acid by mineral ions in solution is negligible owing to the evacuation of these ions into the greater volume of acid by flow refreshment as put forward by Christofferson (1981). In this paper it was postulated that crystal dissolution was a two-step process beginning with the dissolution of the solid:solution interface followed by clearance of that dissolved solid into the solution bulk. The two rates (dissolution of the solid:solution and subsequent clearance) determine the direction of dissolution. Voegel & Garnier (1979) found an initial rapid initial step of dissolution after 5 minutes, followed by a second stage, which released fewer quantities of calcium ions into solution. A significant loss of carbonate in the hydroxyl position of hydroxyapatite was lost during the first five minutes of dissolution, an ionic interaction which became reversed at 10 minutes whereupon phosphate was preferentially displaced. Wang & Nancollas (2009) further suggested that bulk tissue loss progression in a constant composition solution (such as affected during this and the preceding chapter) may be promoted dependant on whether or not dissolution pits are in excess of a certain size defined by the following equation:

$$r* = \frac{\gamma\Omega}{(\mathrm{k}T\ lnS)}$$

where r* denotes the critical size of the dissolution pit, γ the surface free energy and Ω the molecular volume, T represents temperature and *ln*S the natural log of supersaturation, which affects the stability of solids phases. Thus the dissolution of enamel crystallites is driven first by the physical criteria relating to the dissolution pit presence and size, as well as the presence or absence of crystallite impurities (such as

carbonate) affecting solubility, followed by the chemical interactions with the surface:solution interface and subsequent clearing.

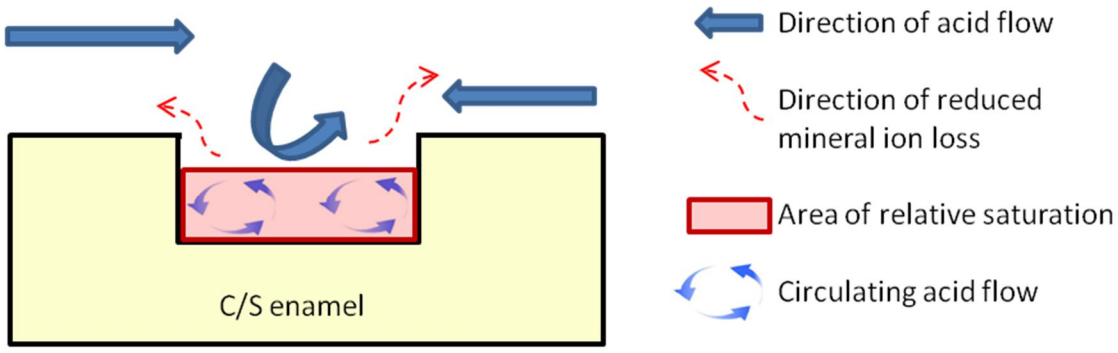

Figure 4.4-1: Hypothetical model to explain the reduction in erosion rate observed at later duration acid exposure, after 60 seconds.

As erosion progresses solid phase mineral is dissolved into solution and the lesion increases in depth. The refreshment rate of new acid solution declines relative to earlier events as trapped solution begins to circulate within the lesion, potentially as a result of pressure exerted by incoming fluid, as shown in Figure 4.4-1. This partially trapped solution, still undersaturated with respect to calcium phosphates, continues to erode the lesion but gradually increases in saturation reducing the erosion rate. Bulk mineral loss still occurs as ions in solution are exchanged at the circulating flow system:external flow system interface. However, this system is purely hypothetical, lacking any input from abrasion and or attrition, both of which would be common *in vivo*. As such, this hypothesis would benefit from additional work modelling the fluid flow within the erosion lesion.

Thus, the continuing presence of these biphasic rates of erosion is suggestive of greater surface and subsurface interactions. However, viewing of subsurface events, such as internal cavitation and mineral softening generally cannot be done unless the

sample is treated in some way, usually through serial grinding which could potentially destroy any structures. The use of penetrative visualisation, such as confocal microscopy or micro-computed tomography (μCT) was hampered by lack of penetrative depth and the presence of ring artefact, about which more will be said in a later chapter.

The next series of experiments sought to further investigate this subsurface phenomenon and its role in the biphasic trends of erosion.

CHAPTER 5

THE BIPHASIC TREND AND ITS RELATIONSHIP TO SUBSURFACE SOFTENING.

5.1. EFFECTS OF ACID ON THE SUBSURFACE MORPHOLOGY

The previous two chapters have confirmed the presence of the biphasic trend of early erosion using optical profilometry and ion chromatography. It has also been shown that comparing optical profilometry with an alternative technique of QLF is of limited use in obtaining definitive answers regarding the true erosion depth.

The reasons for these conflicting data may be attributable to surface and subsurface changes of the enamel. Such changes may be as a result of chelation (Misra, 1996), differential erosion capacity based on the acid used (Boyde *et al.*, 1978) or fluid:surface interactions (such as hypothesised in the previous chapter).

As such, this next body of work set out to look at the effects of acid challenges on the surface interface morphology of enamel.

The effects of acid on surface morphology may be assessed in two ways: visual representations, such as electron microscopy (Eisenburger *et al*, 2001; Ganss *et al*, 2004), optical/physical profilometry (Nekrashevych *et al.*, 2004 Kitchens & Owens, 2007) or atomic force microscopy (Barbour *et al*, 2005) and physical probing through micro- (Attin *et* al, 2003) and nanohardeness (Lippert *et al*, 2004c). This body of work will examine the effects of 0.05 % acid solution erosion on human and bovine enamel using atomic force microscopy and attempt to combine this data with information gathered using optical images to better elucidate surface events.

5.2. EROSION USING PHYSIOLOGICALLY TOLERATED SOLUTIONS ASSESSED USING AFM

The atomic force microscope has the capacity to not only image samples in 3-dimensions at a high magnification and resolution but also to perform hardness and material elasticity tests. Initial images were obtained from the surface of a sample of eroded human enamel (10 minutes in 0.05% phosphoric acid), in order to validate the observations with those of the scanning electron microscope and μCT in Chapters 3 and 4, respectively.

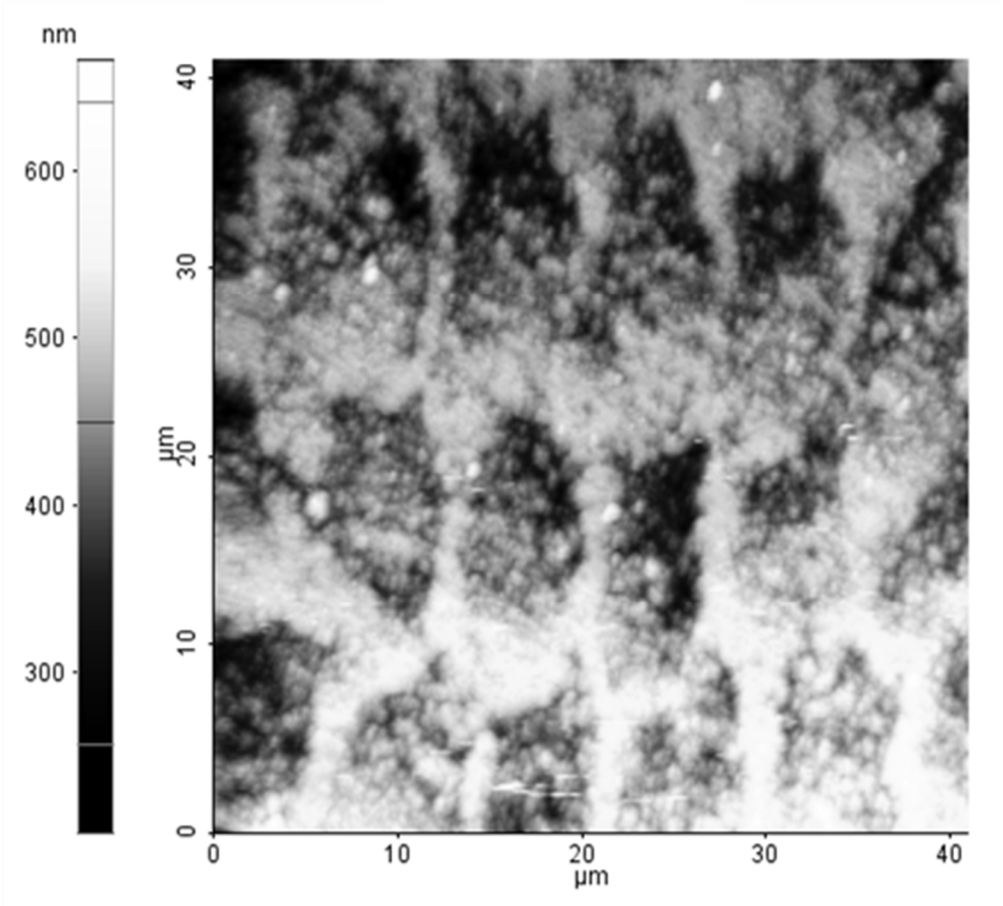

Figure 5.2-1: Atomic force micrograph of human enamel eroded using 0.05 % phosphoric acid for a cumulative total of 600 seconds. The darker aspect of the intra-rod enamel (toward the top of the image) indicates comparatively deeper erosion of the core than the opposing side. Hydroxyapatite crystallites are discernible within the rods as lighter, irregularly rounded areas.

The depth of erosion from the central, intra-rod enamel was 300 nm to the maximum height of the inter-rod enamel (illustrated in Figure 5.2-1), while the distance between the lip of the control area and the commencement of the erosion lesion was 500 nm (illustrated in Figure 5.2-2), which corroborates the bowl shape of the erosion lesion observed using µCT coupled to the deeper mean depth of 1.3 µm.

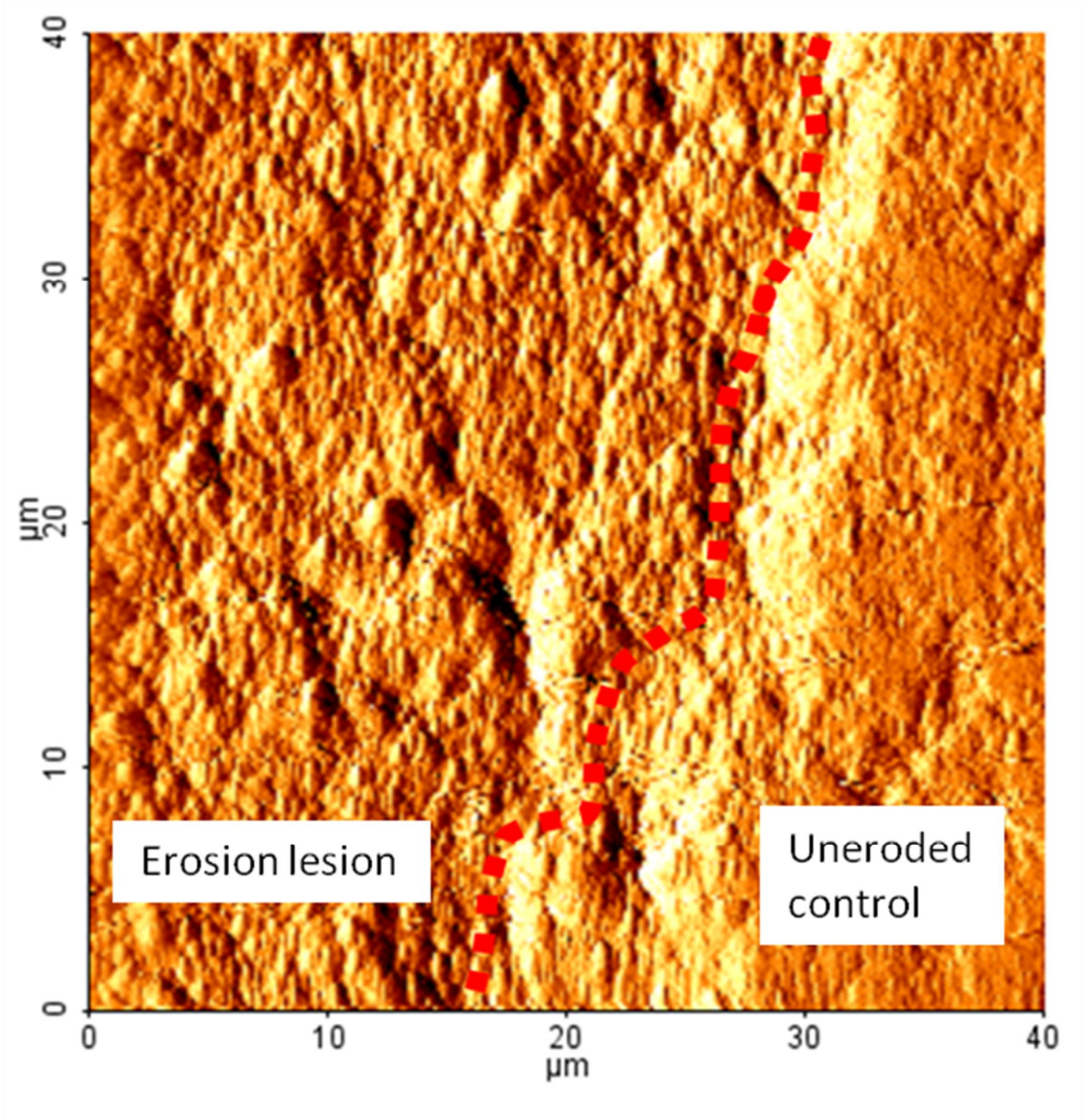

Figure 5.2-2: Atomic force micrograph of the above sample showing the border between eroded- and uneroded areas, with a step height of 500 nm.

5.2.1. THE ELASTIC PROPERTIES OF ERODED ENAMEL

Chapter 3 introduced the concept of material hardness and made use of microhardness to determine enamel material stiffness but found the technique unsuitable for more precise measurements. Atomic force microscopy has been

previously utilised in this body of work to obtain images of the enamel rods, however its uses extend to obtaining quantitative material stiffness measurements by means of force *versus* distance (FD) plots.

An atomic force microscope generated force *versus* distance plot employs a small, controlled load (or force) onto a microscope-designated area and provides information regarding superficial surface material characteristics and material stiffness. The loading force of the cantilever (F) is proportional to the deflection of the cantilever (d) as shown in the equation below:

$$F = -kd$$ (Morris *et al.,* 1997)

For hard materials such as enamel, the deflection of the cantilever (d) is directly proportional to the displacement of the sample (Morris *et al.,* 1997*)*.

The Oliver and Pharr method of indentation related the unloading stiffness of the tip-cantilever complex (S) and its geometry (where r is tip radius) to that of Young's modulus. This can be expressed mathematically, as shown below:

$$E^* = \frac{S}{2r}$$

This equation was used to determine the values of Young's modulus of the enamel samples under investigation during this chapter.

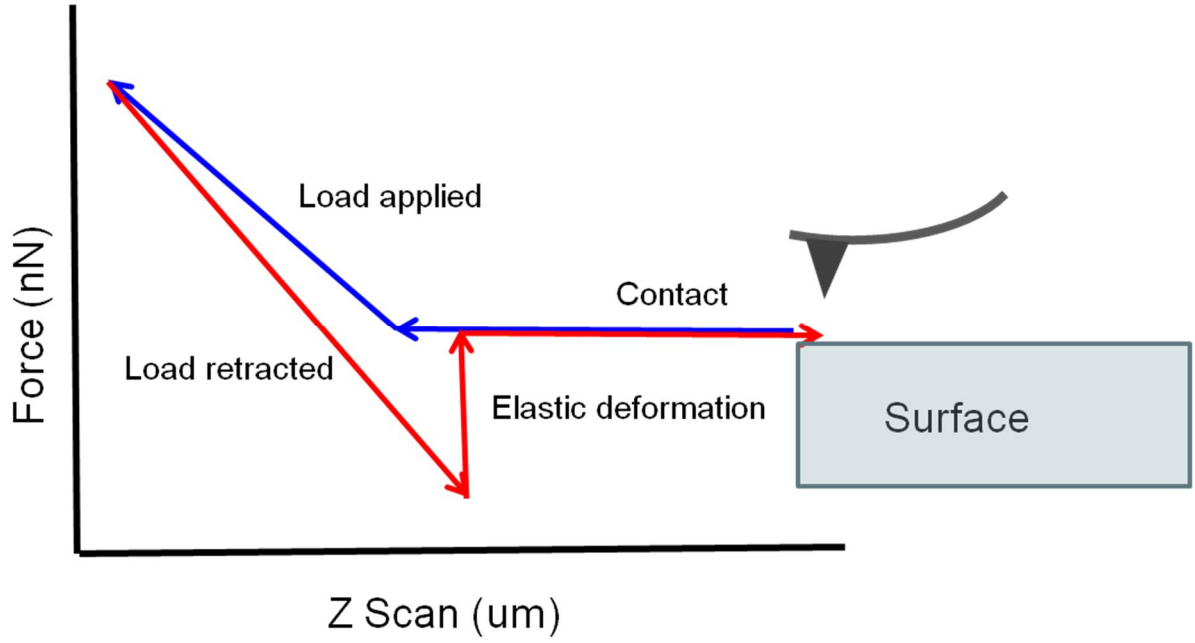

Figure 5.2-3: A schematic representation of a force *versus* distance curve generated using AFM.

Figure 5.2-3 shows an example of a force *versus* distance plot; The plot begins with contact of the AFM tip with the surface of the target material ("1: Contact"). Once the tip has contacted the surface a defined load is gradually applied ("2: Load applied") until a defined load is achieved, whereupon the tip is withdrawn ("3: Load retracted"). Any adherence of the tip to the surface is broken at ("4: Elastic deformation") as the retracting load on the tip is released.

Figure 5.2-4 shows an example of a force *versus* distance plot for a sample of silicon dioxide. As the probe approaches the surface ("1: Contact"), Van der Waal's forces rapidly attract the tip bringing it into contact with the surface, represented by the sudden drop of the deflection (indicating a sudden reduction of constant applied load) prior to the application of the load at 0.45 μm on the Z-scan axis. A load is then applied ("2: Load applied") forcing the probe tip into the material surface until either a predefined indentation depth or load is achieved at which point the probe is gradually

withdrawn ("2: Load retracted"). Adhesion of the probe to the surface, through material properties or the water double meniscus (Howland & Benatar, 2011), causes the continued contact with the material surface between 0.45-0.51 μm, which is released suddenly at 0.51 μm and the probe is fully withdrawn from surface contact ("Elastic deformation").

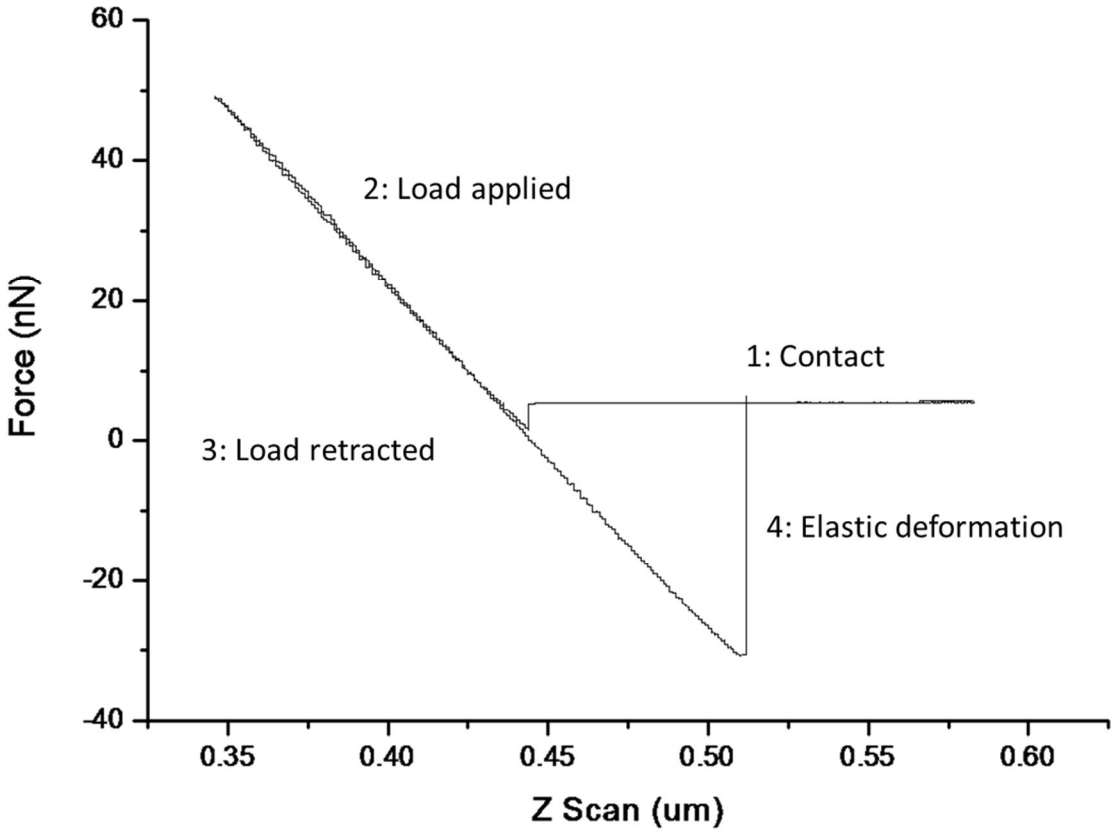

Figure 5.2-4: An AFM generated force *versus* distance plot of silicon dioxide (SiO_2)

Cantilevers with a spring constant of 0.6 $N.m^{-1}$ are more susceptible to vertical flexion, making them more suited to imaging than obtaining force *vs.* distance data. However, they are sometimes used in AFM FD data collection. This body of work aimed to compare the effects of cantilever spring constant on the accurate measuring of material hardness.

5.2.1.1. AFM PROBES - 0.6 N.M^{-1} CANTILEVERS

As mentioned above, AFM probes with a spring constant of 0.6 N.m^{-1} are preferentially designed for imaging purposes, being more flexible in the vertical plane, but are used as indenters in the literature. The plots were all similar in appearance to Figure 5.2-5, indicating a uniformly hard material was being probed. The graph below shows the results of using a 0.6 N.m^{-1} cantilever to obtain FD plots for human and bovine enamel:

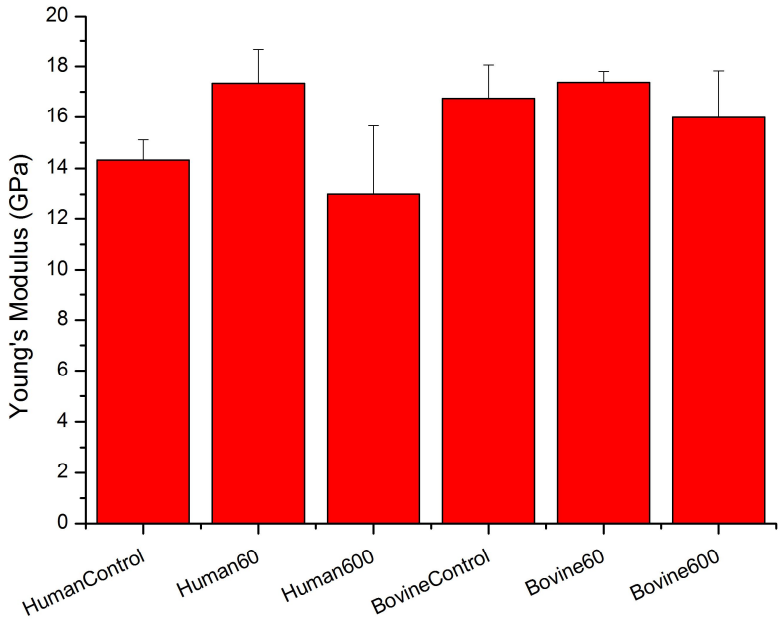

Figure 5.2-5: Results of human and bovine eroded and uneroded samples following a cumulative 600 second erosion protocol employing 0.05 % phosphoric acid. Suffixes of "60" indicate 60 seconds duration; those with "600" indicate 600 seconds duration (n = 8).

Uneroded control enamel for bovine enamel recorded a Young's modulus of 16.75 GPa (±1.31) and human enamel recorded a stiffness of 14.33 GPa (±0.79). After 60 seconds erosion, bovine enamel recorded a mean stiffness of 17.37 GPa (±0.44) and

human enamel 17.34 GPa (±1.33). After 600 seconds of erosion, bovine enamel recorded a stiffness of 15.99 GPa (±1.84), while human enamel recorded a stiffness of 13.01 GPa (±2.66). A Kruskal-Wallis ANOVA of the human data was not significant ($p = 0.43$), nor was the bovine data ($p = 0.42$). The results from a Mann-Whitney U-test of the control means of the human and bovine eroded enamel were significant ($p = >0.001$) as were the 600 second exposure means ($p = 0.002$). The 60 second means were not significant from each other.

5.2.1.2. AFM PROBES - 40 $N.M^{-1}$ CANTILEVERS

A 40 $N.m^{-1}$ probe possesses a much stiffer cantilever than its 0.6 $N.m^{-1}$ counterpart rendering it more resistant to vertical flexion. As such, the imaging properties are reduced (being less responsive to vertical deflection) but the tip is better suited to indentation work and FD curve generation, as will be explained later in this chapter.

FD plots of the erosion lesion using 40 $N.m^{-1}$ cantilevers produced a curve with two slopes, quasi-exponential in appearance. These were attributed to two separate changes in the hardness of the enamel material at two distinct depths: one at the surface and one below this in the subsurface. This was in contrast to the control slope, depicted in Figure 5.2-6:

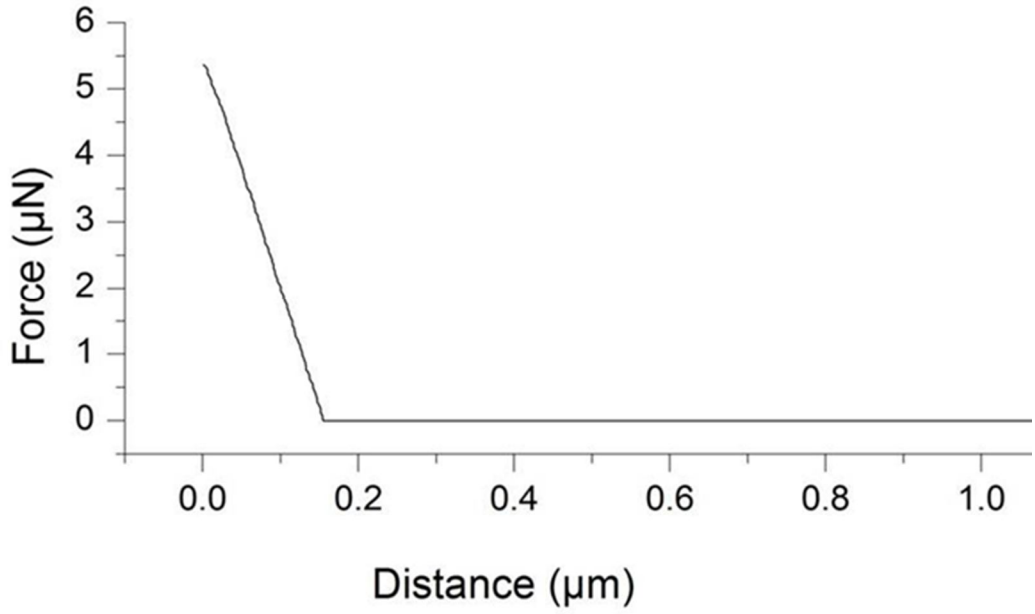

Figure 5.2-6: AFM Force vs. distance plot of human enamel control showing the retract slope of the probe relative to the enamel surface.

The control FD retract slope of human enamel is shown in Figure 5.2-6. The lack of deviation in the retract slope from that of the approach slope is indicative of an inelastic material. The abrupt upswing of the slope indicates a hard material, all of which would be expected from uneroded enamel (n = 8).

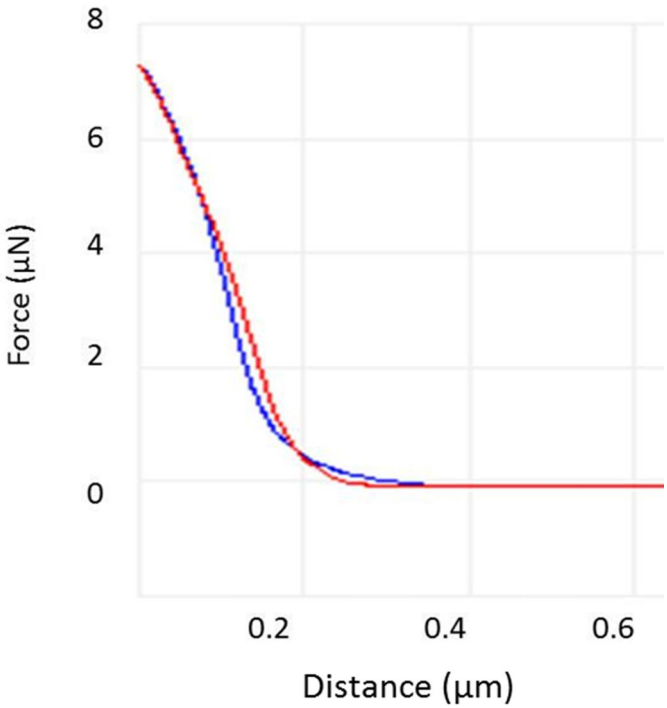

Figure 5.2-7: AFM Force vs. distance plot of human enamel following 600 seconds exposure to 0.05% phosphoric acid showing the approach slope (blue) and retract slope (red) of the probe relative to the enamel surface.

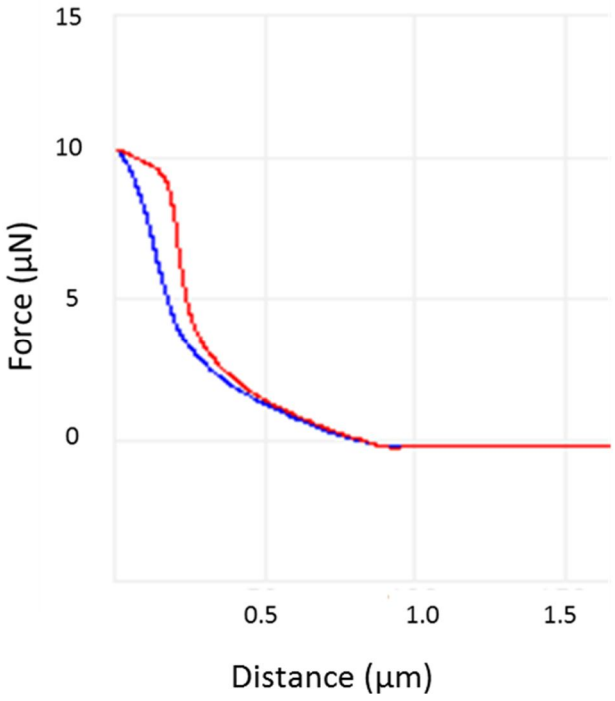

Figure 5.2-8: AFM Force vs. distance plot of human enamel following 600 seconds exposure to 0.05% acetic acid showing the approach slope (blue) and retract slope (red) of the probe relative to the enamel surface.

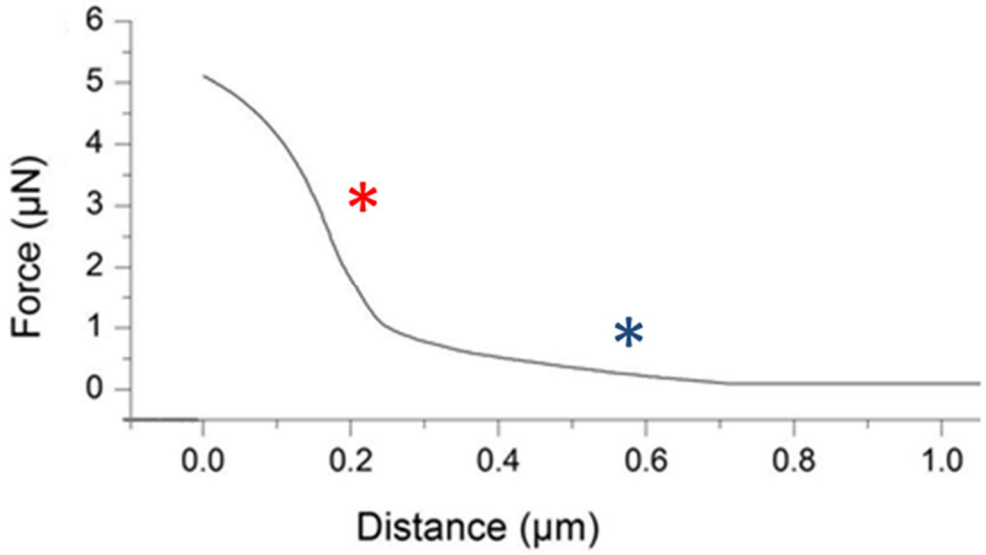

Figure 5.2-9: Retract slope from an AFM generated FD plot of human enamel eroded for 600 seconds using 0.05% phosphoric acid.

Comparing the eroded area slope (Figure 5.2-6 and Figure 5.2-8) to that of the control shows that the erosion lesion is a comparatively softer material. There was a gentle upswing of the approach slope, between 0.3 μm and 0.1 μm on the distance axis in Figure 5.2-7 and 0.7 μm and 0.2 μm on the distance axis in Figure 5.2-8. This indicates either a gradual indentation into the material meeting with increasing resistance at depth or contact with a charged enamel surface. The retract slope (as shown in detail in Figure 5.2-9) provides information regarding the material stiffness. The acute more angle of the slope at 0.1 μm (indicated by the red asterisk) shows an underlying material which is harder at depth than the enamel closer the surface (indicated by the blue asterisk). This can be seen by the shape of the trend, which appears to possess two distinct slopes.

In order to maintain experimental accuracy as much as possible, a new tip was used every four samples (for a total of 32 indentations) to prevent the tip becoming

blunt. This would minimise the risk of erroneous data attributed to apparent increasing sample material stiffness arising from an increase in the tip radius due to blunting.

The FD curves for human and bovine data were analysed as frequency distribution plots, in order to determine if any skewing was apparent in the data which would affect any statistical calculations, coupled with a Gaussian line fit to determine the most accurate mean and variation results. It was found that the control data for human and bovine was normally distributed (an example given by Figure 5.2-10) while the erosion lesion showed a degree of skewing to the right, meaning there were comparatively few higher values of the data (an example given by Figure 5.2-11) and the results could not be analysed using parametric statistics.

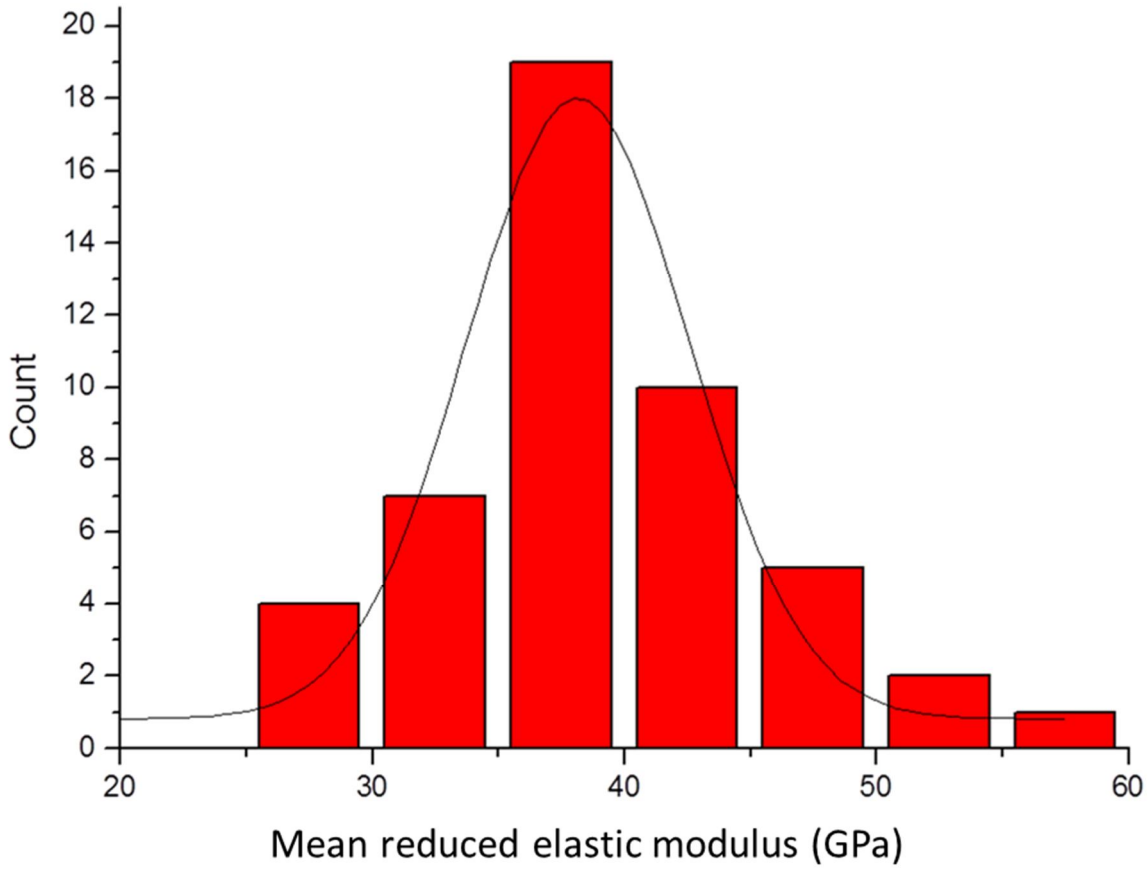

Figure 5.2-10: The frequency distribution plot of a single sample of uneroded human enamel together with a Gaussian curve fit.

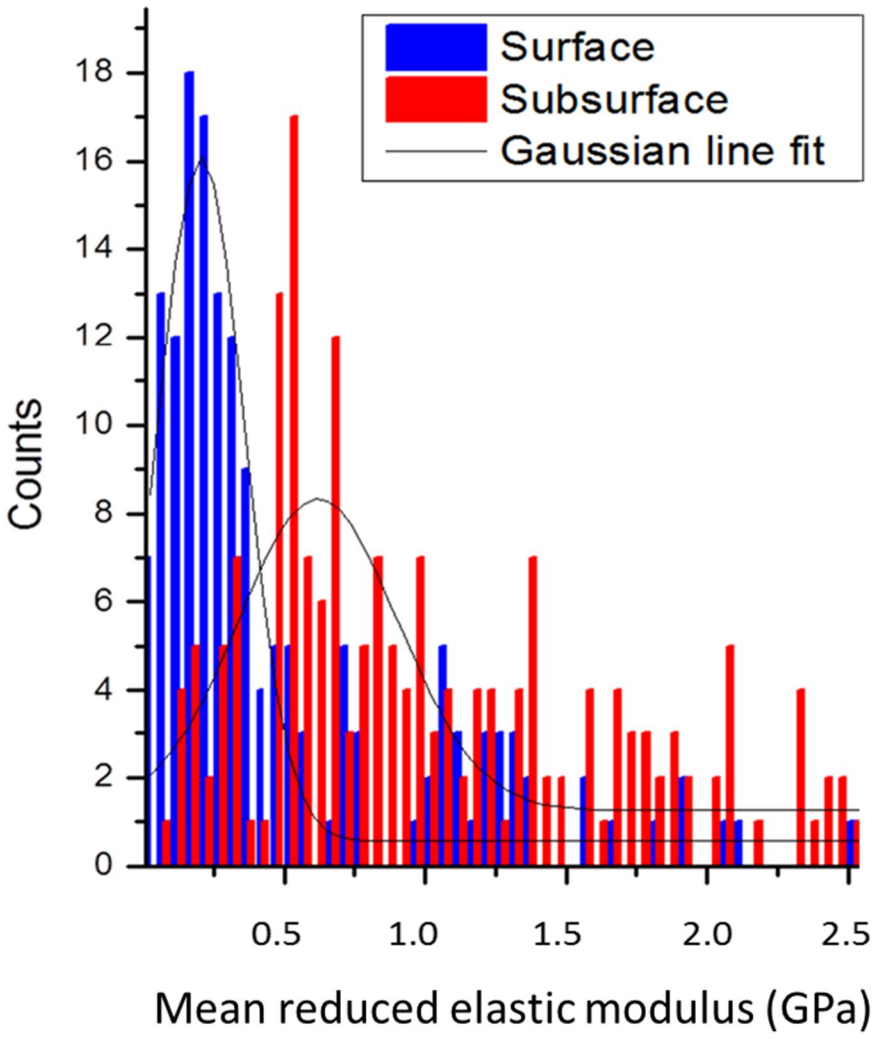

Figure 5.2-11: The frequency distribution plot of a single sample of bovine enamel eroded with 0.05 % citric acid together with a Gaussian curve fit for both surface and subsurface measurements.

The peak of each Gaussian line fit, for both the control and erosion lesion, represents the mean value of the frequency distributions, thus the true mean of the Young's modulus data. These mean values are recorded in the table below:

Reduced Elastic Modulus	Human		Bovine	
	Surface	Subsurface	Surface	Subsurface
	GPa	GPa	GPa	GPa
Control	20.91 (±0.73)		19.87 (±0.69)	
Acetic	4.29 (±0.07)	10.91 (±0.31)	4.01 (±0.22)	9.07 (±0.07)
Citric	0.23 (±0.02)	9.18 (±0.35)	2.05 (±0.09)	11.06 (±0.20)
Phosphoric	0.48 (±0.02)	8.93 (±0.16)	5.31 (±3.20)	15.76 (±6.99)

Table 5.2-1: The reduced elastic modulus values (GPa) for human and bovine enamel eroded with three commonly encountered, physiologically relevant 0.05 % acid solutions obtained using AFM force *vs.* distance plots (n = 8 for each category).

Uneroded human enamel had a Young's modulus of 20.91 (±0.73) GPa and uneroded bovine enamel control had a Young's modulus of 19.87 (±0.69) GPa, which represent the surface values as no subsurface softening was detected. These values were not significant from each other.

Human enamel treated with 0.05 % acetic acid had a Young's modulus of 4.29 (±0.07) GPa at the surface and 10.19 (±0.31) GPa for the subsurface reading. Bovine enamel treated with 0.05 % acetic acid had a Young's modulus of 4.01 (±0.22) GPa at the surface and 9.07 (±0.07) GPa at the subsurface. The difference between the surface and subsurface Young's modulus for both human and bovine enamel was statistically significant ($p = >0.001$).

Human enamel treated with 0.05 % citric acid had a Young's modulus of 0.23 (±0.02) GPa at the surface and 9.18 (±0.35) GPa in the subsurface. Bovine enamel treated with 0.05 % citric acid had a Young's modulus of 2.05 (±0.09) GPa at the surface and 11.06 (±0.20) GPa for the subsurface reading. The difference between the surface and subsurface Young's moduli for both human and bovine enamel was statistically significant ($p = >0.001$).

Human enamel treated with 0.05 % phosphoric acid had a Young's modulus of 0.48 (±0.02) GPa at the surface and 8.93 (±0.16) GPa for the subsurface reading. Bovine enamel treated with 0.05 % phosphoric acid had a Young's modulus of 5.31 (±3.20) GPa at the surface and 15.76 (±6.99) GPa for the subsurface. The difference between the surface and subsurface Young's moduli for both human and bovine enamel was statistically significant ($p = >0.001$). One way ANOVAs showed the Young's moduli of eroded surfaces and subsurface regions of bovine and human enamel to be significantly softer from that of the controls ($p = >0.001$).

Mann-Whitney U-tests of the results of the Young's moduli from uneroded human and bovine enamel control showed a significant difference between the 0.6 Nm^{-1} and 40 Nm^{-1} cantilevers ($p = > 0.001$). A significant difference was also apparent between the 0.6 Nm^{-1} and 40 Nm^{-1} cantilevers when the human enamel sample eroded with 0.05 % phosphoric acid for 600 second was compared ($p = 0.04$) but there was no significant difference for the eroded bovine sample ($p = 0.41$).

An additional piece of information granted by the AFM force *versus* distance measurement is the depth of indenter penetration recorded concomitant to the stiffness readings. Therefore, it is possible to determine the depth of each of these phases within the mineral matrix.

Erosion depth	Human		Bovine	
	Surface	Subsurface	Surface	Subsurface
	nm	nm	nm	nm
Control	39.12 (±6.77)		42.6 (±8.52)	
Acetic	102.83 (±73.11)	53.89 (±58.97)	54.97 (±22.92)	41.47 (±14.45)
Citric	120.49 (±82.67)	82.67 (±25.59)	80.97 (±65.86)	44.68 (±17.24)
Phosphoric	158.96 (±89.36)	78.1 (±91.71)	5.76 (±5.76)	95.28 (±22.47)

Table 5.2-2: The mean penetration of the cantilever tip into human and bovine enamel eroded with three commonly encountered, physiologically relevant 0.05 % acid solutions obtained using AFM force *vs* distance plots (n = 8 for each category).

Uneroded human enamel was indented to a median depth of 39 nm (±7) and uneroded bovine enamel was indented to a median depth of 43 nm (±9). There was no indication of subsurface softening events.

0.05 % acetic acid eroded human enamel indented to a median depth of 103 nm (±73) for the surface slope and to a median depth of 54 nm (±59) for the subsurface slope. Eroded bovine enamel recorded a median value of 55 nm (±23) for the surface slope penetration and 41 nm (±14) for the subsurface slope depth.

0.05 % citric acid eroded human enamel recorded a median indent depth of 120 nm (±83) for the surface slope and a median indent depth of 57nm (±26) for the subsurface slope. Eroded bovine enamel recorded a median value of 81 nm (±66) for the penetration relating to the surface slope and 45 nm (±17) for the median subsurface slope depth.

0.05 % phosphoric acid eroded human enamel recorded a median indent depth of 159 nm (±89) for the surface slope and an indent depth of 78 nm (±92) for the subsurface slope. Eroded bovine enamel recorded a median value of 19 nm (±6) for the penetration relating to the surface slope and 45 nm (±22) for the subsurface slope depth.

The medians for indentation depths of surface and subsurface slopes of human enamel subjected to acid challenges were then compared with each other using Mann-Whitney U-tests and were found to be significant from each other ($p = 0.02$ or below), as was the case with eroded surface and subsurface slope depths of bovine enamel – all indentation depths were found to be significant from each other ($p = >0.001$). When the surface and subsurface indentation depths of human samples were compared against the surface and subsurface slopes of eroded bovine samples using a Kruskall-Wallis ANOVA, these too were found to be significant ($p = 0.001$ or below).

Confirmation of the indentation was obtained using AFM in contact mode. Figure 5.2-12 shows one area of ready identification on a sample of bovine enamel selected as a site for confirming AFM indentation activity. A control image was obtained prior to indentation using a 0.6 Nm^{-1} cantilever. The test location was selected on the basis of readily identifiable morphology and noted using the *x-y* co-ordinates provided by the AFM software.

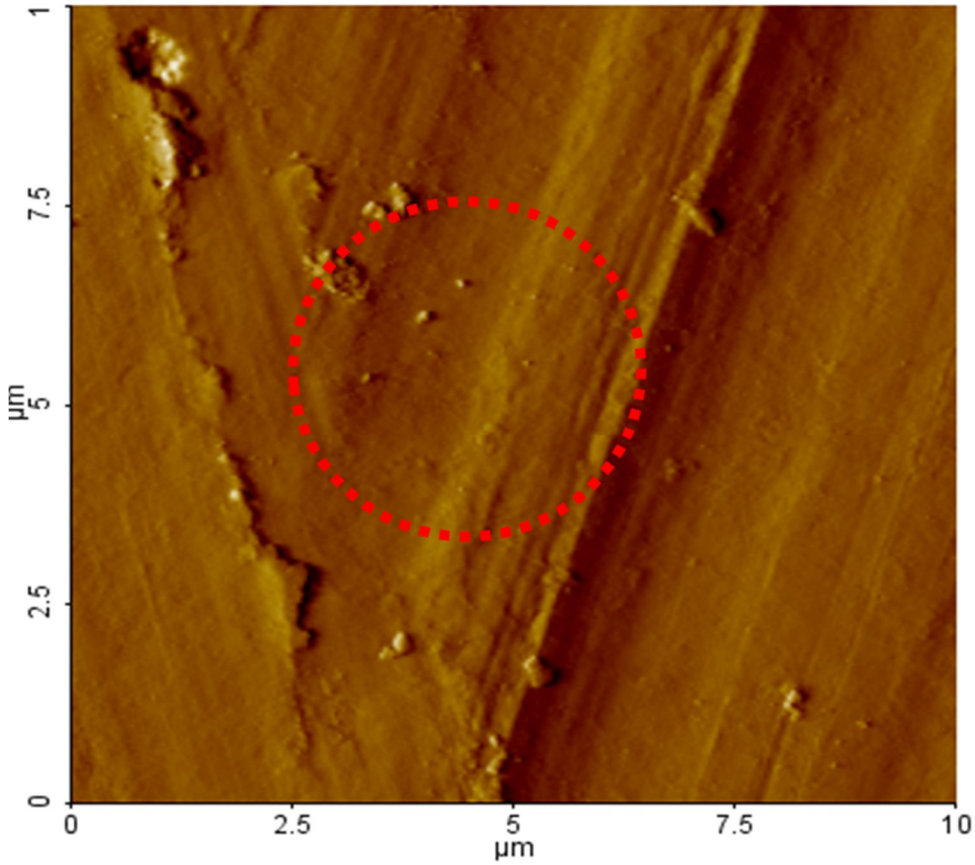

Figure 5.2-12: Topographic AFM image of uneroded bovine enamel surface following indentation using 40 $N.m^{-1}$ cantilever. The red circle represents the area in which the indentation occurred. The absence of any indent shows that the force applied is insufficient for the cantilever to penetrate sound enamel.

Once indentation was performed using a 40 Nm^{-1} cantilever, the tip was replaced for one better suited to imaging (a 0.6 Nm^{-1} cantilever) and the area imaged again. No evidence of indentation could be found in the uneroded control area. By contrast, indentations were detected in the acid eroded lesion, as depicted below:

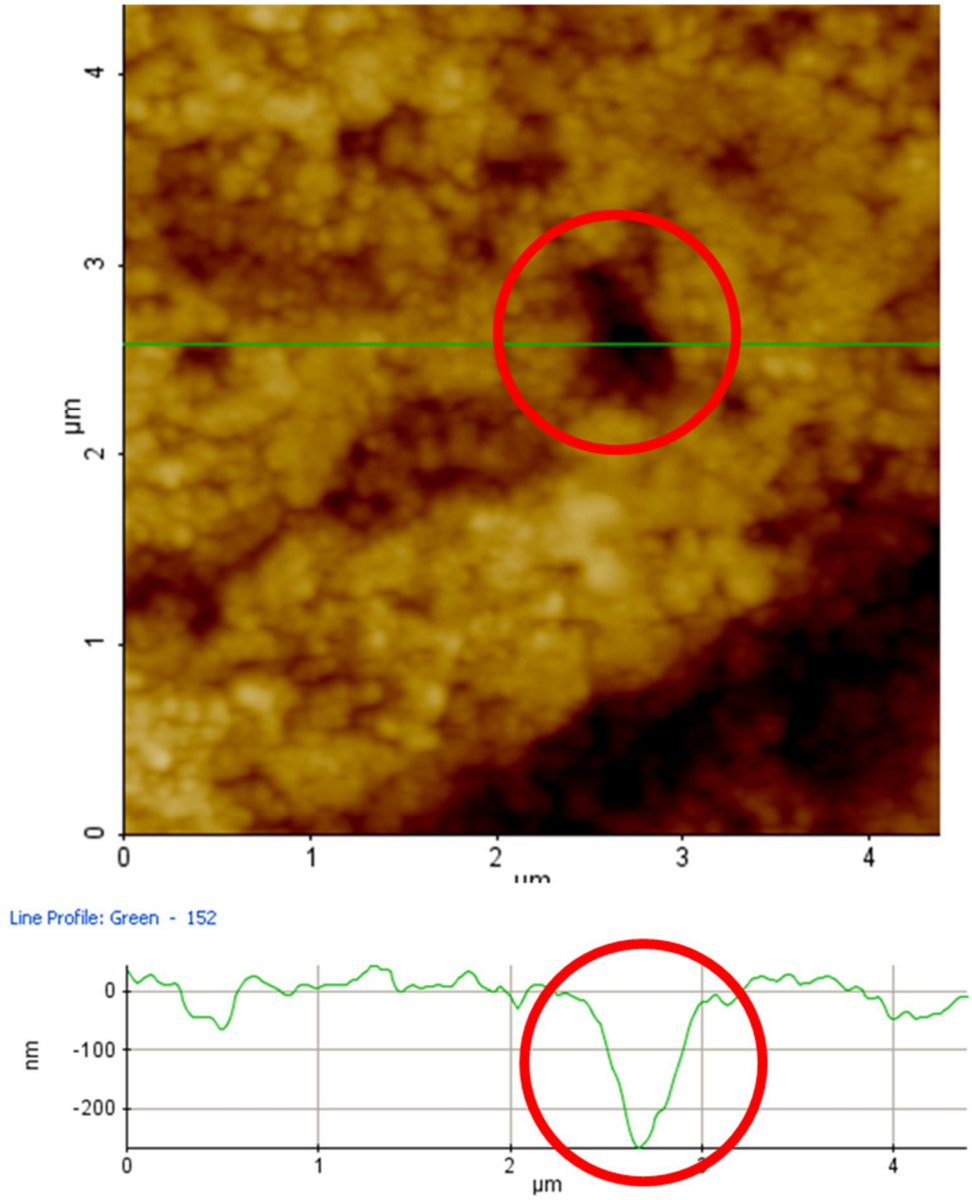

Figure 5.2-13: Deflection AFM image of site of indentation within bovine enamel erosion lesion. The transverse green line in the deflection image is a single line scan (bottom image) showing the penetration of the indenter into the enamel surface.

With the hypothesis that the enamel surface did not appear to be homogenously eroded, it was decided to investigate the subsurface morphology using focussed ion beam scanning electron microscopy. This hypothesis was formulated on the basis of observed surface topography (to be discussed in the next section), as well as the apparent biphasic trend seen in the optical profilometry data and corroborated by AFM FD work.

5.3. AREAS OF INITIAL ACID RESISTANCE EXPLORED USING SCANNING ELECTRON MICROSCOPY AND FIB-SEM

It was observed using optical profilometry during early stages of erosion that certain areas of variable dimensions within the lesion appeared to stand proud of its basal surface. These observations were corroborated using AFM (Figure 5.3-1) and SEM (Figure 5.3-2).

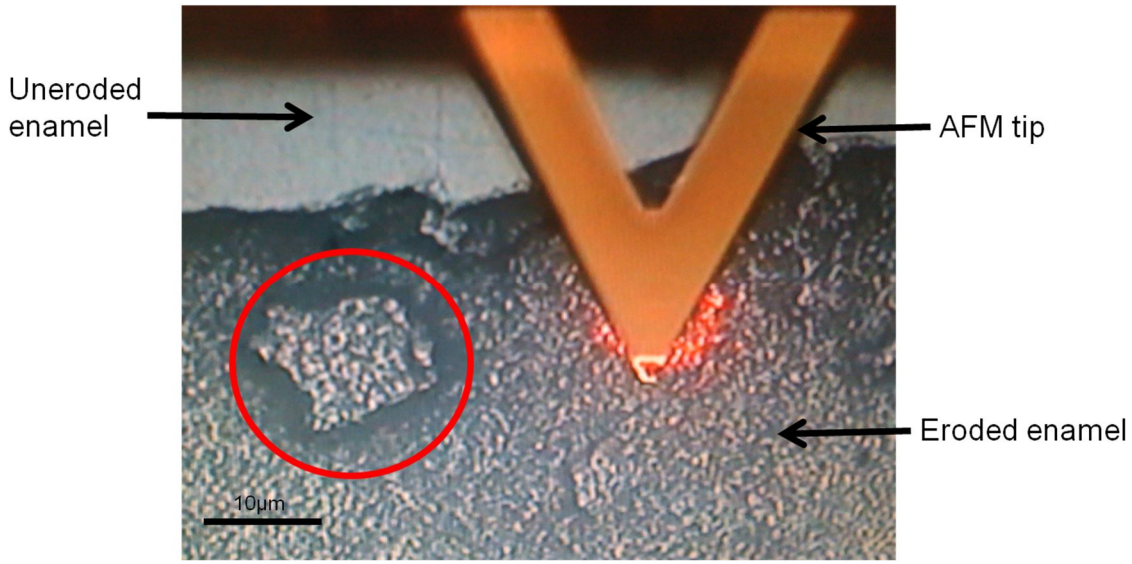

Figure 5.3-1: A sample of bovine enamel showing an area of apparent acid resistance (highlighted in red) in relation to an AFM probe.

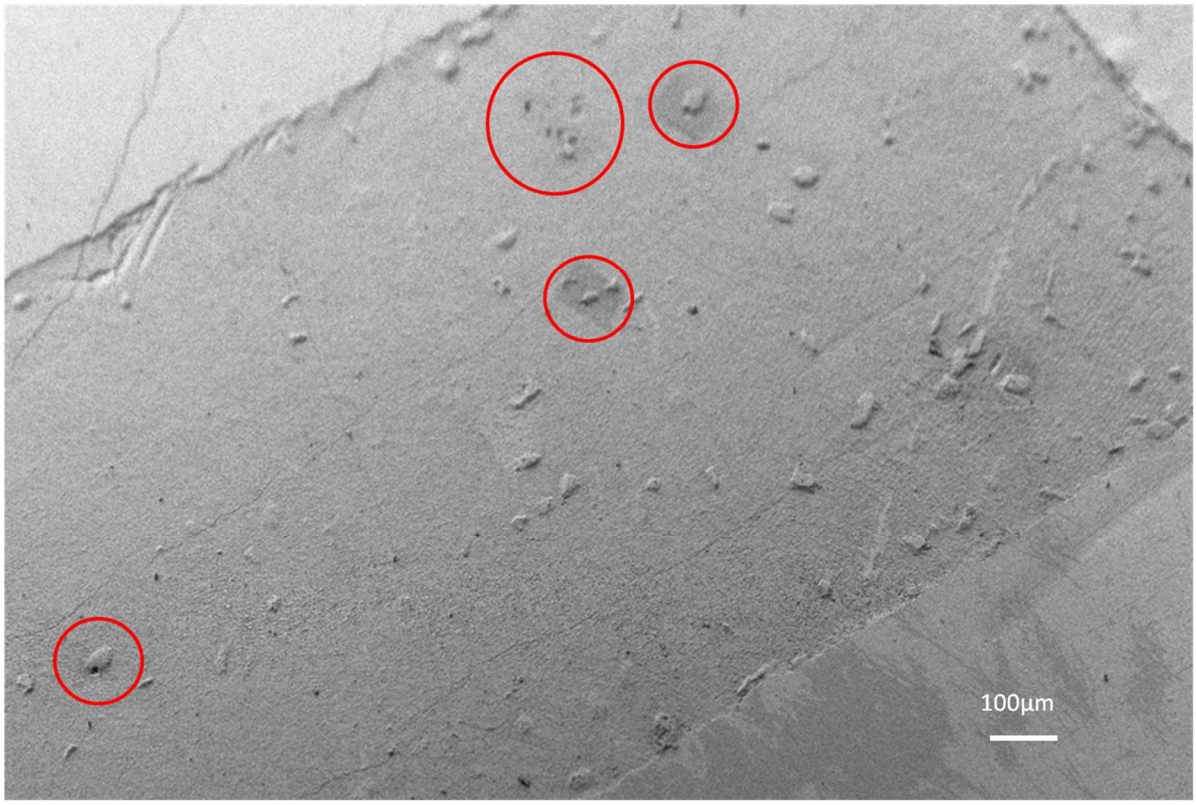

Figure 5.3-2: Scanning electron micrograph of human enamel subjected to 0.05 % phosphoric acid for a cumulative total of 600 seconds showing the erosion lesion bordered on either side by uneroded enamel. The lesion appears to show areas of apparent precipitate or acid resistance.

These areas of apparent initial acid resistance were present in all of the samples and progressively disappeared as acid exposure was prolonged (Figure 5.3-3).

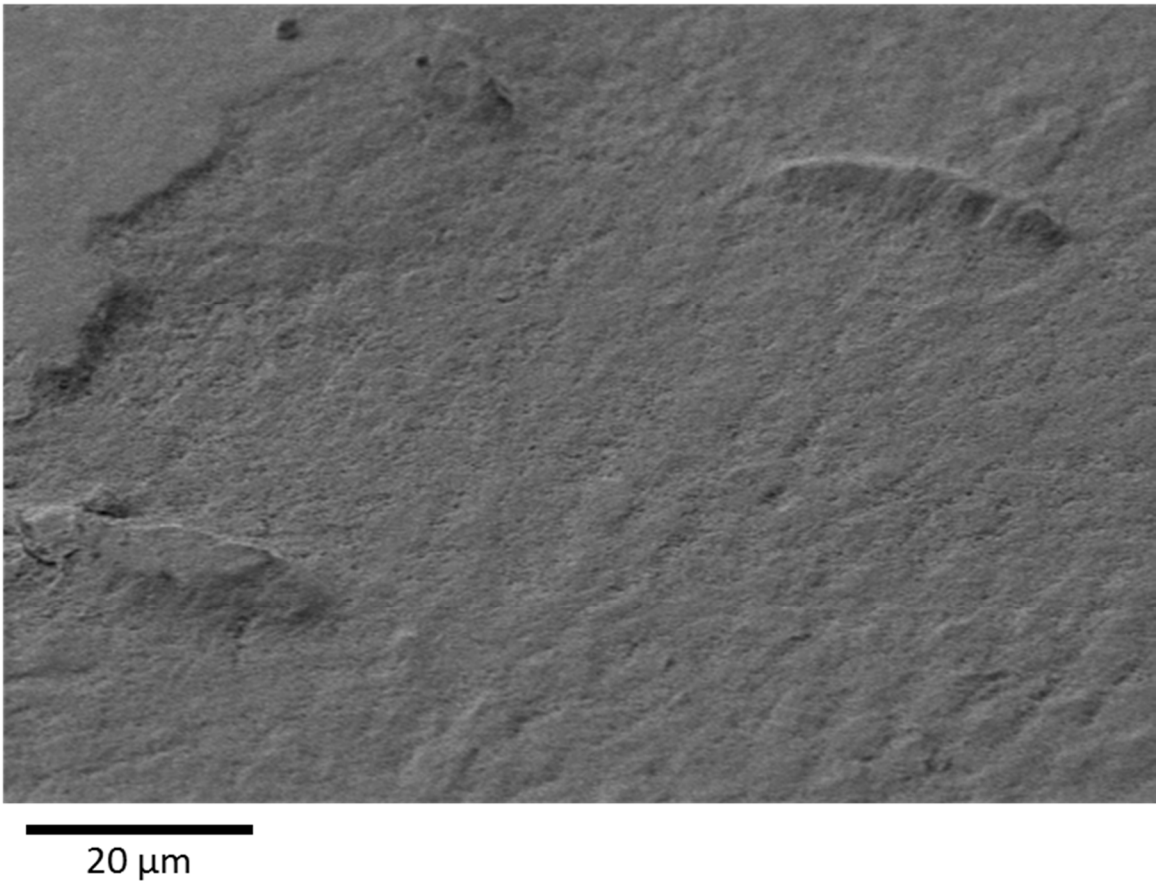

Figure 5.3-3: Scanning electron micrograph of the effects of 20 minute exposure of 0.05% phosphoric acid on human enamel. The raised areas of apparent acid resistance are reduced in dimensions, while smaller areas are erased altogether.

The areas of apparent initial acid resistance did not conform the expected structure of precipitated calcium phosphates, as shown in Figure 5.3-4, as calcium phosphate precipitate would exhibit a distinctive disorganised crystalline form.

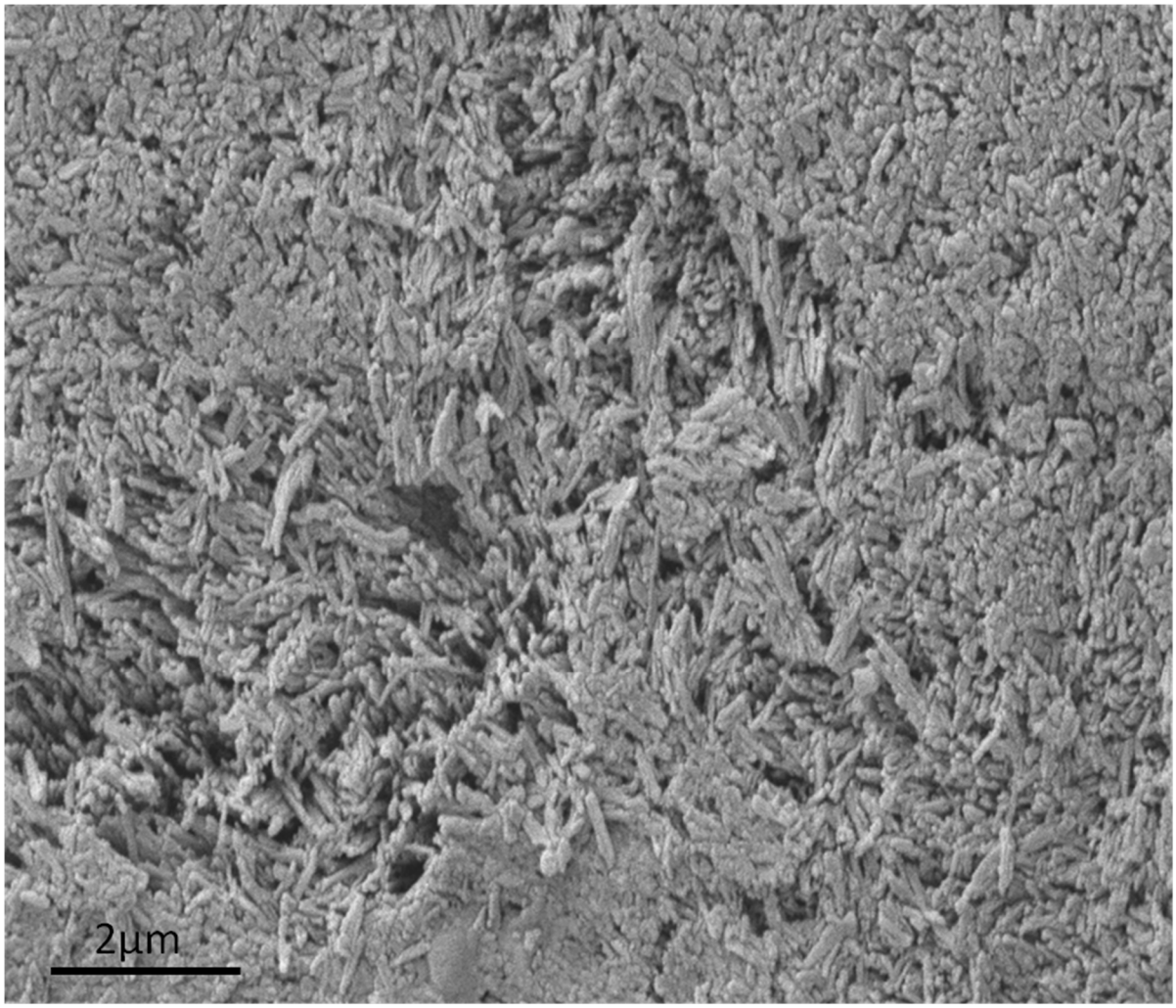

Figure 5.3-4: Example of calcium phosphate precipitate on the surface of bovine enamel, which is characterised by the presences of needle-like crystals in a random orientation.

This appeared to suggest that overall the erosion of enamel was not occurring at a uniform rate, a feature that could possibly be linked to the biphasic trends in erosion discussed in Chapter 4.

From the SEM observations alone it was difficult to determine if these raised areas were a result of some form of deposition - such as precipitate or contaminant - or part of the tooth morphology which was more resistant to acid attack than the surrounding material. Calcium and phosphorus EDX spectra were obtained (from 32 samples) of the control area, lesion and the unknown "resistant" morphology, all

standardised against synthetic sintered hydroxyapatite. An example of the results is seen in Figure 5.3-5.

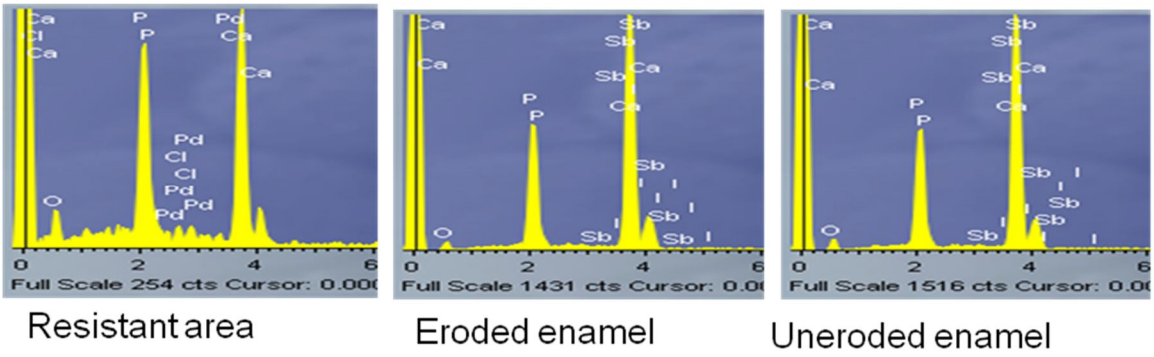

Figure 5.3-5: EDX spectra of human enamel showing the two predominant peaks associated with calcium (centre) and phosphorus (right).

The EDX spectra obtained were, as mentioned previously, standardised with respect to sintered, synthetic hydroxyapatite (BDH, UK) in terms of the calcium and phosphorus ratio. Figure 5.3-6 shows the results of the EDX analysis of human and bovine enamel with respect to sintered hydroxyapatite. Synthetic HAP had a phosphorus content of 69.60 % (0.37 %) and calcium content of 30.37 % (0.37 %). Uneroded enamel had a phosphorus content of 69.72 % (0.31 %) and calcium content of 30.38 % (0.26 %). The erosion lesion had a phosphorus content of 69.39 % (0.50 %) and calcium content of 30.61 % (0.50 %). The areas of apparent acid resistance had a phosphorus content of 69.45 % (0.17 %) and calcium content of 30.56 % (0.15 %). A one-way ANOVA of calcium and of phosphorus showed this data to be not significant.

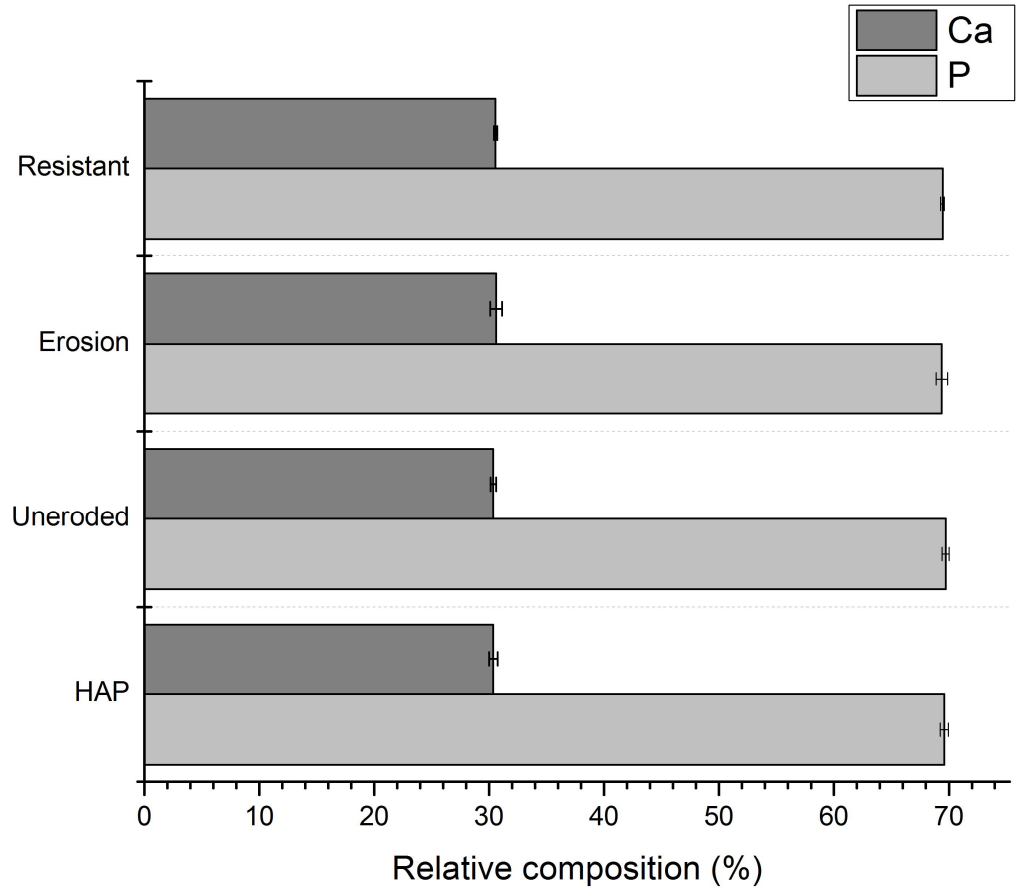

Figure 5.3-6: Relative composition (%) calculated from an excess of 5000 x-ray counts of calcium and phosphorus in synthetic HAP, uneroded control, erosion lesion and the areas of apparent acid "resistance".

A focussed ion beam attachment to the SEM (FIB-SEM) allowed progressive milling of the control enamel surfaces to expose the underlying morphology. Figure 5.3-7 shows a FIB-scanning electron micrograph of uneroded human enamel, which has been ground, polished and ultrasonicated for 30 seconds. The larger of the two images shows how the enamel has been milled using the focussed ion beam to be able to view the interior morphology by looking at the facing curtain wall. There is some evidence of slumping artefact at the base of the milled trench, a result of the high temperatures generated during milling.

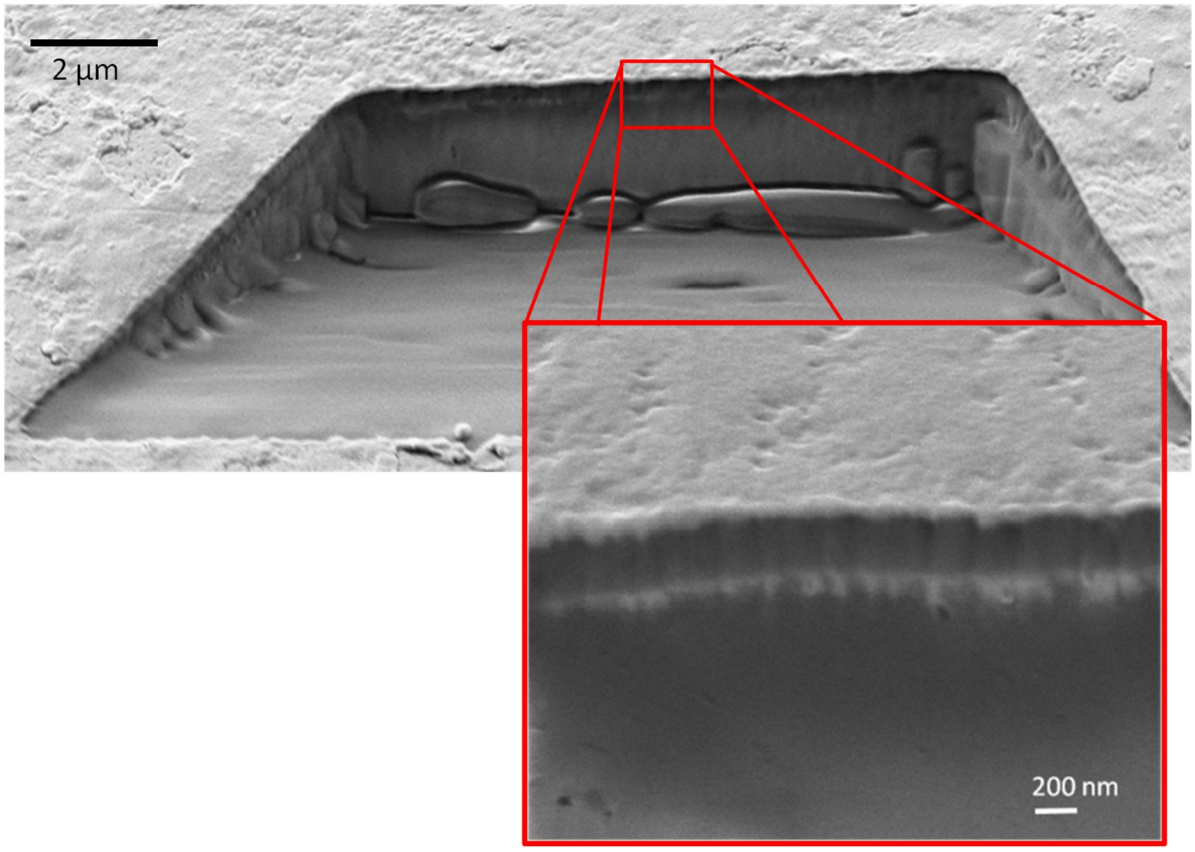

Figure 5.3-7: FIB-SEM images of uneroded human enamel. The surface is slightly pitted, most likely the result of grinding and polishing. The insert is a closer examination of the surface: curtain wall junction, which shows some flaring owing to the high magnification.

An examination of the curtain wall shows a homogenous surface with some evidence of random, submicron-sized cavitations, most likely inherent in the enamel structure as it was present for all samples. Some flaring artefact was present on the images owing to the high resolving power of the microscope being used.

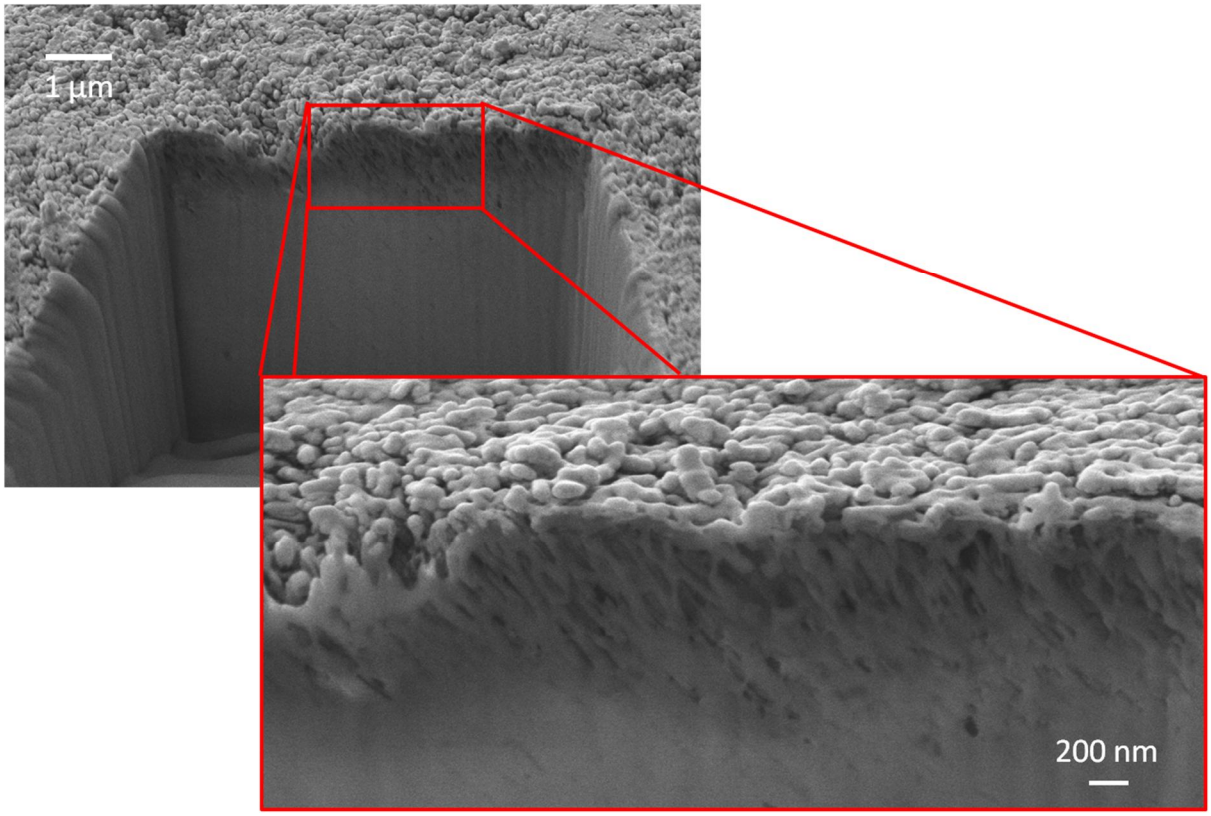

Figure 5.3-8: FIB-Scanning electron micrograph of human enamel eroded for a cumulative total of 600 seconds with 0.05 % phosphoric acid. The base of the lesion is roughened with individual, rounded crystallites of approximately 30nm being discernable. Examination of the curtain wall shows extensive cavitation to a depth of 200 – 500 nm, whereupon the enamel takes on a more solid appearance.

The effects of erosion on the enamel surface are shown in Figure 5.3-8 and show extensive microcavitation along the basal surface of the lesion to a maximum depth of 500 nm. Below this the enamel appears to be of a similar appearance to uneroded substrate. These images suggest the upper layer constitutes an area of reduced mineral content, where dissolution has leached calcium phosphate into the solution resulting in microcavitation of the enamel substrate.

Overall, these two areas can also be used as representative controls of uneroded and eroded enamel when examining the areas of apparent acid resistance.

Areas of apparent acid resistance were initially directly observed using AFM and SEM, as seen in Figure 5.3-2, a feature previously unreported in the literature. Using FIB-SEM it was possible to examine the internal morphology of these lesions to determine the origin of these structures.

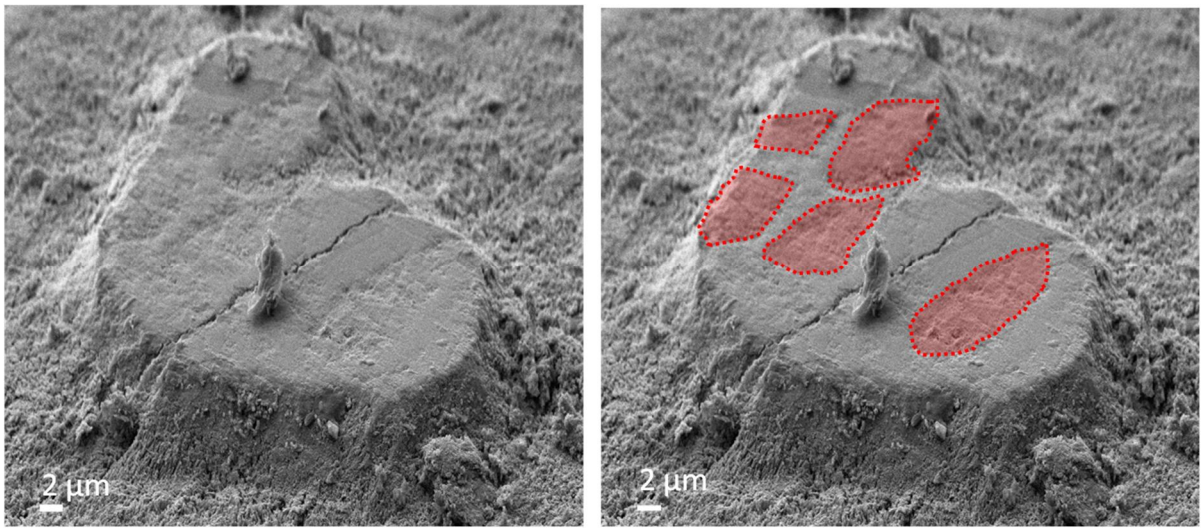

Figure 5.3-9: Scanning electron micrograph of an area of apparent acid resistance present within the erosion lesion of a sample of human enamel following a cumulative 600 second erosion challenge using 0.05 % phosphoric acid prior to milling. Enamel rods can be distinguished on the surface of the sample (highlighted in the copy image on the right).

Figure 5.3-9 shows a higher magnification image of one area of apparent acid resistance present within the erosion lesion. The sample shows trace evidence of enamel rods present on the superficial surface, highlighted in red on the right-side image. This is strongly suggestive that the area has resisted the cumulative acid challenge and maintained its surface and some degree of subsurface morphology resulting in a mesa-like structure.

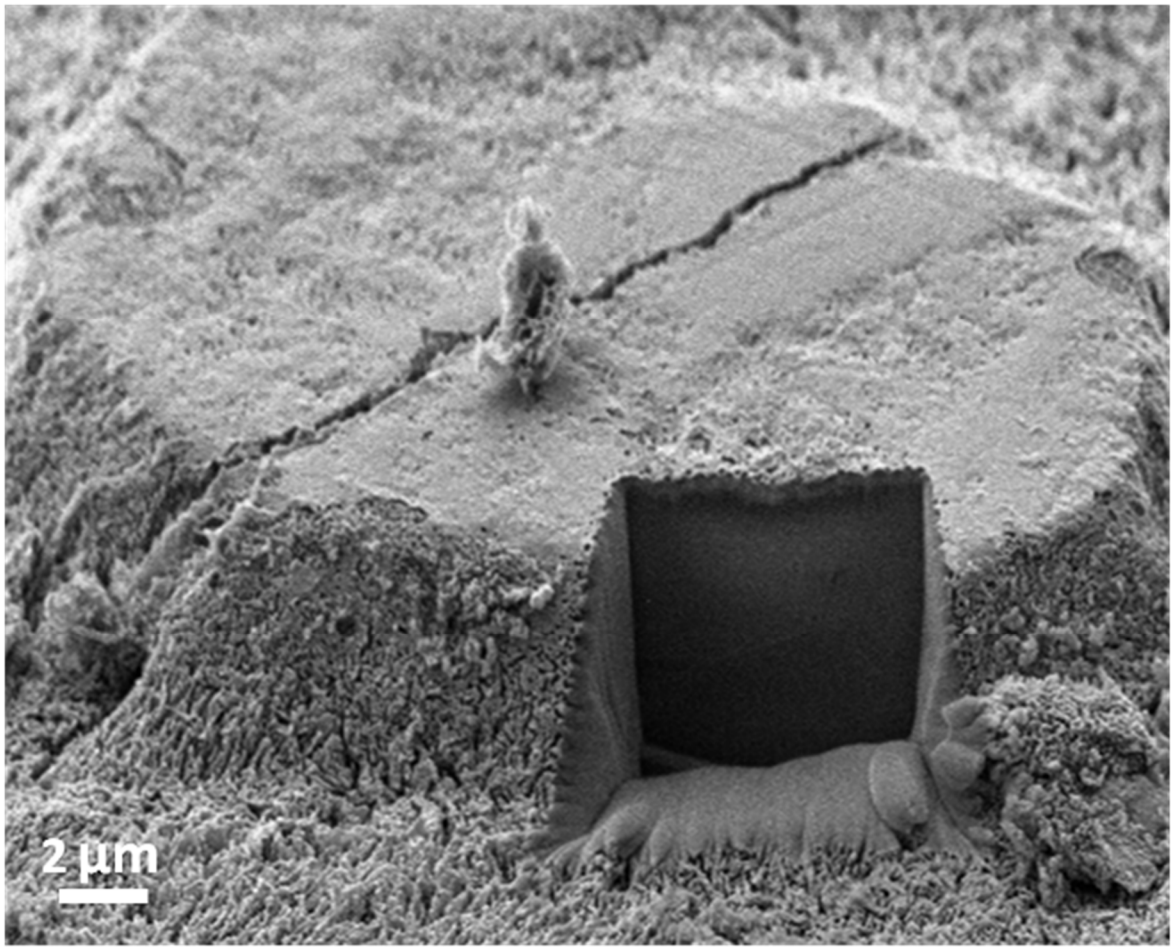

Figure 5.3-10: Scanning electron micrograph of an area of apparent acid resistance present within the erosion lesion of a sample of human enamel following a cumulative 600 second erosion challenge using 0.05 % phosphoric acid after milling.

Figure 5.3-10 shows the example of an area of apparent acid resistance described above following milling with a focussed ion beam. The internal morphology of the area of apparent acid resistance is revealed in the curtain wall, which most closely mirrors that of uneroded enamel seen in Figure 5.3-7. There is no superficial or subsurface microcavitation. A single microfracture propagates approximately 2 µm from the surface and extends out of the field of view at a depth of 4 µm: This is most likely related to drying artefact arising from the vacuum conditions within the electron microscope chamber. The internal morphology of the area of apparent acid resistance does not appear to have any visible demarcation between that of the basal surface of

the enamel lesion, suggestive that this mesa-like structure continuous and uninterrupted with the enamel and not the result of precipitation or artefact deposition.

An examination of another area of apparent acid resistance was undertaken with a view to looking at the junction between the basal surface of the lesion and the area of apparent acid resistance.

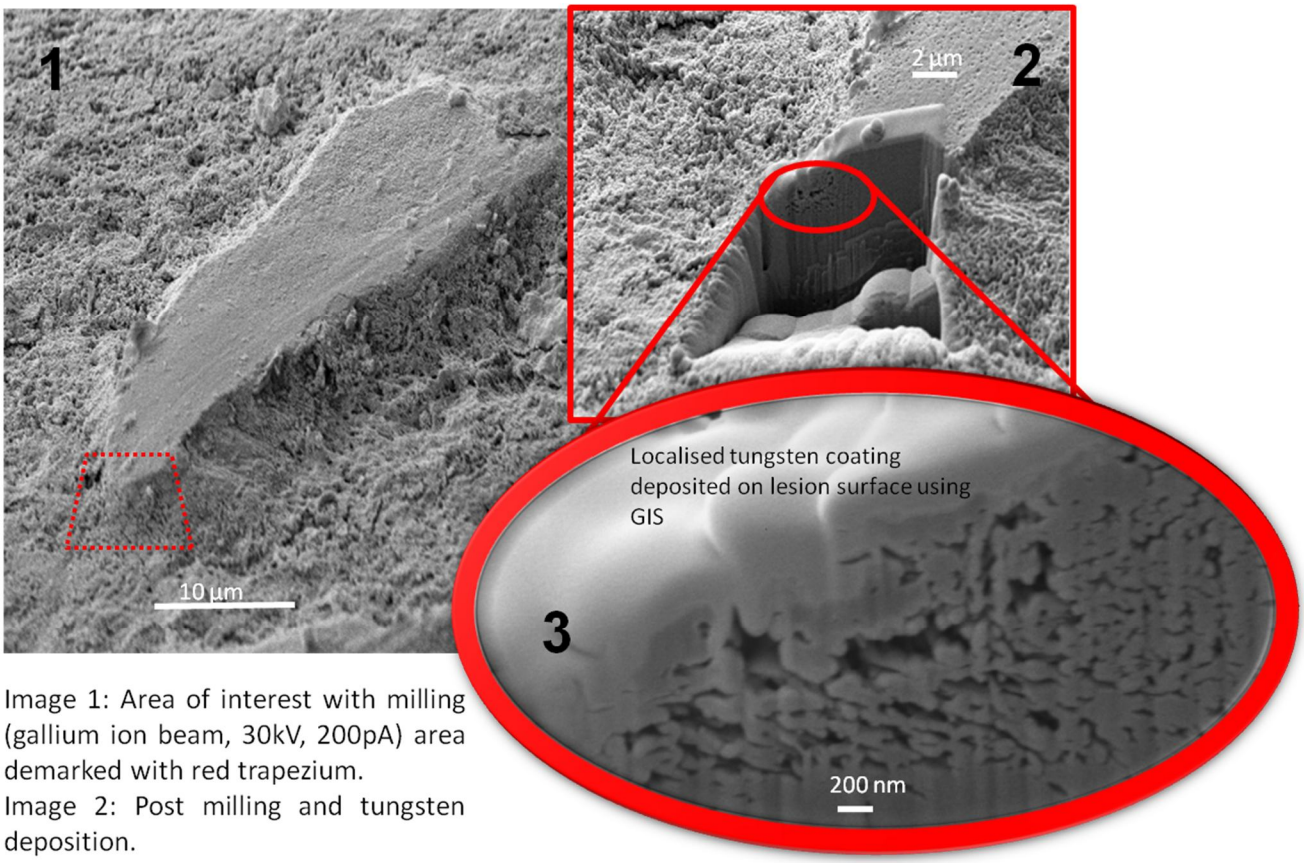

Image 1: Area of interest with milling (gallium ion beam, 30kV, 200pA) area demarked with red trapezium.
Image 2: Post milling and tungsten deposition.
Image 3: Highlight showing cavitation at lesion border.

Figure 5.3-11: Scanning electron micrographs of an area of apparent acid resistance within the erosion lesion following a cumulative 600 second 0.05 % phosphoric acid challenge. Image 1 shows the area of apparently acid resistant enamel in its native environment, with the area to be milled highlighted in red. Image 2 shows the results of milling and Image 3 is a close-up of the microcavitation present at the area of apparent acid resistance border.

Image 1 of Figure 5.3-11 shows another area of apparent acid resistance present with the erosion lesion. A notable feature of this example included the presence of

residual scratches from polishing present on the surface of the mesa-like feature. Milling of one peripheral edge of this structure revealed two morphologies: The first, more internal of the area of apparent acid resistance, is similar to that of uneroded enamel observed in Figure 5.3-7 and Figure 5.3-1, while the second, at the peripheral edge, is most similar to that of eroded enamel observed in Figure 5.3-8. Larger microcavities are present in greater quantities at the outermost edge of the periphery slope, closest the acid:enamel interface and reduce in dimensions closer to the internal morphology of the mesa. There is no evidence of cavitation development at the superficial surface of the area of apparent acid resistance.

5.4. DISCUSSION OF CHAPTER 5

NANOMECHANICAL PROPERTIES OF ENAMEL

In Chapter 3 use was made of microindentation in order to determine information regarding softened enamel. However, the effects of subsurface softening would potentially be missed or affected by microindentation for, as the name implies, the surface area and indentation depth of this technique is in the scale of micro- or tens of micrometers. The thickness of softened enamel following dissolution is thought to be between 2-5 μm (Barbour & Rees, 2004; Eisenburger *et al*., 2004) thus any measurement obtained by microindentation holds a real risk of being adversely influenced by uneroded, unaffected subsurface enamel. AFM FD curve generation permits better control over the applied load, better precision when determining the location of the indentation (a factor of considerable importance given the presence of areas of apparent acid resistance, about which more will be said later in this discussion) and finally, better control over the indentation depth.

The literature reports wide variation in reduced elastic moduli (Young's modulus) with respect to bovine and human enamel with values ranging from 114.8 GPa (±9.9) to 83.4 GPa (±2.2) recorded from the surface of uneroded enamel, which then decreased following an acid challenge (Habelitz *et al*., 2001; Lippert *et al*., 2004; Ge *et al*., 2005; He *et al.*, 2006). The results of published studies vary as a result of different preparation and erosion protocols, including variations in grinding and polishing, exposure time, acid concentration and applied indentation load, thus a direct comparison of elastic modulus data for identical erosion studies is comparatively rare.

Furthermore, some papers in the literature utilise an inappropriate cantilever with a spring constant of 0.6 $N.m^{-1}$ when obtaining AFM FD measurements. A 0.6 $N.m^{-1}$ cantilever is better suited to imaging than the indentation of hard materials as the comparatively low spring constant allows greater vertical flexibility, thus greater AFM deflection measurement than the stiffer 40 $N.m^{-1}$ cantilever. The experiments undertaken in section 5.2 compared measurements of eroded and uneroded enamel obtained using a 0.6 $N.m^{-1}$ and 40 $N.m^{-1}$ cantilever and, with the exception of eroded bovine enamel, found significant differences between the two cantilevers. The significantly lower result of the 0.6 $N.m^{-1}$ cantilever when probing uneroded human and bovine enamel suggests that there are external factors affecting the results. Should this be attributed to experimental error, this would most likely be attributed to the measurement of the probe stiffness of the 0.6 $N.m^{-1}$ cantilever as it preferentially yields instead of the sample. A caveat to this is the reported effect of the organic prism sheath on stress-strain behaviour, the orientation of the enamel prisms as well as differences observed using probes of different dimensions (He *et al*., 2006).

Chapter 4 suggested a biphasic trend of erosion was present during enamel dissolution. The use of the more appropriate, stiffer 40 $N.m^{-1}$ cantilever, together with a lower applied load were used to obtain reduced elastic modulus results which appeared to provide further evidence in support of this: The force *versus* distance curves for a large proportion of the samples appeared to show two trends, which indicated a soft superficial surface with underlying harder material. This would reflect a progressive loss of calcium phosphates from the mineral matrix: acid interface resulting in a softer composite at the superficial surface. As the acid penetrated into the enamel, possibly *via* the more organic inter-rod prism sheath, this resulted in subsurface softening, which is reflected in the frequency distribution plots such as that exemplified by Figure 5.2-11.

This biphasic trend in the reduced elastic modulus has not previously been reported in the literature, a fact that may be attributed to the lower applied load used to obtain the results. Loads for indentation purposes vary throughout the literature encompassing loads ranging from 50 μN to 5 mN (Lippert *et al*., 2004c; Barbour & Shellis, 2007; Cheng *et al*., 2009; Zheng *et al*., 2010), in order to obtain a sufficient indent. Barbour & Shellis (Barbour & Shellis, 2007) found a contact determining load of 1.8 μN to be largely insufficient to result in surface indentation most of the time. However, the load of 2.4 μN employed for this work proved sufficient for the purpose and was also shown to penetrate the erosion surface to a depth of 250 nm. However, consensus in the literature is that enamel has a reduced elastic modulus of between 70 - 125 GPa (Cuy *et al*., 2002; Barbour *et al*., 2005; Braley *et al*., 2007; Xue *et al*., 2009) compared to the value of 20.91 GPa for uneroded human enamel and 19.85 GPa for uneroded bovine enamel observed for these results. This discrepancy in results is most likely attributed to the low applied loads employed for this work, evidenced by the shallow penetration of the indenter into uneroded enamel, 39.12 nm (±6.77) for human enamel and 42.6 nm (±8.52) for bovine enamel. These control indentation depths were significantly different from the indentation depths at the superficial surface of both human and bovine eroded enamel irrespective of acid used, which supports the hypothesis of mineral loss at the surface: acid interface results in a layer of considerably softer material than that underlying it. At the deeper layer, represented by the subsurface category, the results show reduced indentation into the enamel but it should be remembered that these results represent cumulative data. The subsurface depth represents an additional penetration depth of the indenter into the material in excess of that previously created at the surface. This is depicted in Table 5.4-1, which represents the total indentation depths of the respective acids:

	Human (nm)	Bovine (nm)
Control	39.12	42.6
Acetic	156.72 (±66.04)	96.44 (±18.69)
Citric	203.16 (±54.13)	125.65 (±41.55)
Phosphoric	237.06 (±90.54)	101.04(±14.12)

Table 5.4-1: Mean indentation depths in human and bovine enamel resulting from exposure to three 0.05% acid concentrations

From this it can be seen how the softening of the bovine and human enamel through acid action affects the total indentation depth. A surprising finding was that eroded human enamel appears to suffer a greater softening effect compared to eroded bovine enamel, manifesting as a reduced relative elastic modulus and greater indentation depth. This was unexpected as the uneroded control suggested that human enamel would be more resilient to an enamel challenge based on the reduced elastic modulus and indentation depth. Furthermore, the significance of the indentation depths may be related to the variability of the samples as a result of differences in mineral composition (thus genetics) and sample preparation, such as depth of grinding and polishing.

However, it is uncertain whether or not the eroded bovine and human sample indentations completely penetrated through the softened layers and into unaffected enamel. Cheng *et al*. suggested this softened layer was 930 nm thick after 5 minutes erosion and 1390 nm in thickness following a 10 minute citric acid erosion challenge†††† and employing an applied maximum load of 1 mN (Cheng *et al.*, 2009). As may be seen from our work, the load applied did not penetrate beyond 237 nm deep.

†††† The concentration of the citric acid solution was not reported, however the pH was reported as 3.8.

Additional points to consider are the calibration of the tips and the potential for static charge artefact. The tips were not calibrated during any preliminary experiments as these were purchased pre-calibrated from the manufacturer. However, on this basis, it had to be accepted that the force constant values provided by the suppliers were accurate[‡‡‡‡]; therefore the data reported here may warrant careful interpretation owing to this given such tips may have an undetermined error. The effect of static charge artefact, common on organic samples, should also be considered, which may have adversely distorted the results of the FD curve (Morris *et al.*, 1997; Tolstikhina *et al.*, 2007). However, given the constant nature of the data obtained, the effect of charged enamel seems unlikely.

Despite this, the delicate nature of this work means that more needs to be done to better ascertain the full extent of subsurface softening without compromising any surface features.

AREAS OF APPARENT INITIAL ACID RESISTANCE

An interesting topographical feature observed using both AFM and SEM imaging was the presence of mesa-like areas of apparent acid resistance within the erosion lesion. As mentioned previously, these areas have been largely overlooked in the literature including in work whose duration of acid exposure most closely corresponds to that employed here (Sanches *et al.*, 2009). SEM observations alone were not sufficient to determine whether or not these mesa-like areas represented depositional artefact, precipitate or an area resistant to the effects of short term acid exposure. The lack of a carbon peak following EDX analysis was strongly suggestive that the potential

‡‡‡‡ The force constant was calibrated using the Sader method with an error up to 10% - Personal communication, MikroMasch UK.

artefact was not organic, thus eradicating the most likely source of potential depositional artefact (e.g.: skin or bacterial flora) while the majority of the elemental composition was a close match for that of hydroxyapatite, as illustrated in Figure 5.3-5. Given the small dimensions of the anomalous areas, including that of the height, the X-ray surface penetration during EDX had to be kept to a minimum. This was achieved using low voltage spot analysis with a penetration depth of approximately 2 μm which, based on the AFM step height measurements of 2.5 μm, was not sufficient to sample deeper enamel and therefore there was minimal risk of obtaining an erroneous result. The number of x-ray counts used to obtain the quantitative data, in excess of 5000 counts per sample, was further evidence that appreciable carbon quantities were not present within the sample area.

Having dismissed the mesa-like structures as depositional artefact it was hypothesised that these areas may reflect precipitation artefact as observed by Eisenburger (Eisenburger *et al*., 2004). However, the presence of surface topographical features, such as scratch marks and enamel rods on the surface of the mesa-like areas and the absence of observable needle-shaped seed crystallites or irregularly oriented, plate-like crystals (Sato *et al*., 2006; Wang & Nancollas, 2008; Fan *et al*., 2009) within these areas made calcium phosphate precipitate an unlikely cause for these mesa-like protuberances. Furthermore, there was no apparent demarcation of the different surfaces, i.e.: between mesa-like projection and the basal surface of the erosion lesion. This was suggestive that the mesa-like areas of apparent acid resistance formed a continuous surface with the basal surface of the enamel lesion and therefore were a reflection of actual enamel morphology and not a result of erosion mediated precipitation.

Conclusive evidence of the nature of the areas of apparent acid resistance could be obtained through a cross section of the mesa-like projection and the basal surface of the erosion lesion. Following on from the previous hypotheses, this would permit the finding of evidence of material demarcation – any artefact would lay on the basal surface of the erosion lesion – as well as cross sectional morphology. However, simply re-embedding the sample and implementing the standard cutting, grinding and polishing protocol to obtain a flat, polished cross section could potentially damage fine structures, while residue from these actions could potentially fill and obscure any evidence of demarcation. The use of a focussed gallium-ion beam to mill the enamel surface would result in a clean cut free from debris and was therefore best suited to this kind of work. Milling the control areas of uneroded and eroded human and bovine enamel showed differences in the morphology. The eroded enamel, whether bovine or human in origin, showed areas of apparent mineral loss manifesting as microcavities at the superficial surface of the lesion. There was no uniform depth of microcavitation, perhaps a reflection of the mineral composition or acid penetration into the deeper enamel *via* the organic prism sheath (Cheng *et al*., 2009). The uneroded enamel of both species showed no such microcavitation. When areas of apparent acid resistance were milled to a depth of 4 μm, thereby ensuring penetration into the deeper layers of enamel, there was no evidence of material demarcation which confirmed these mesa-like projections were an uninterrupted continuation of the enamel surface. Furthermore, the superficial surfaces most closely resembled that of uneroded enamel with no evidence of microcavity formation, in contrast to the control areas of the eroded enamel. A cross section of an area of apparent acid resistance and the basal surface, as observed in Figure 5.3-11, showed that the only evidence of microcavity formation to be

at the peripheral edges of the mesa-like projection and the basal surface of the erosion lesion.

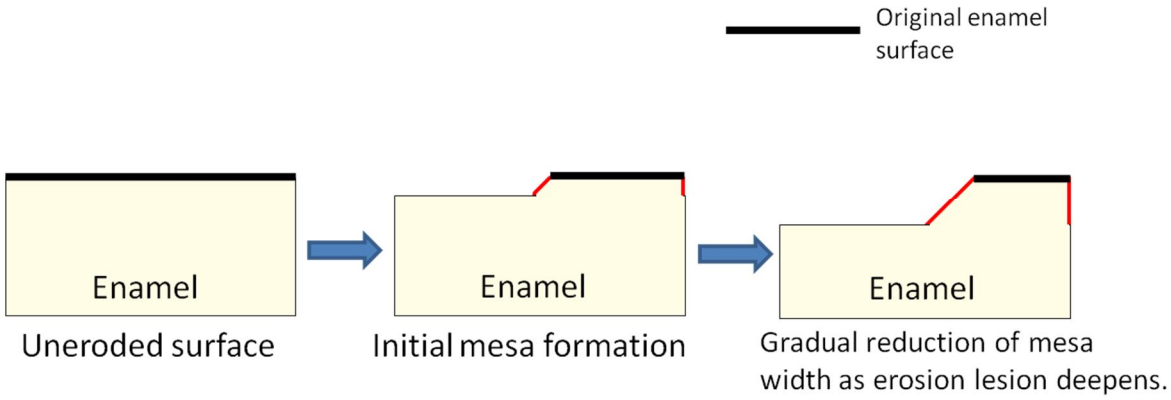

Figure 5.4-1: Schematic representation of the formation of an area of apparent acid resistance. The image on the left represents sound, uneroded enamel then which progresses' through initial mesa formation to deeper erosion lesion and smaller area of apparent acid resistance.

The figure above represents a hypothetical model of how an area of apparent acid resistance may emerge. The application of an acid solution results in the gradual erosion of the original enamel surface (depicted as a thick black line), while localised properties (such as rod orientation or chemical composition) within the enamel delay the effects of erosion. Mineral is initially lost from the developing lesion subsurface through diffusion as described in Chapter 4, forming cavities within the matrix. The coalescence of these microcavities forms the basis of bulk tissue loss. Continued acid exposure gradually affects the areas of apparent acid resistance, manifesting as microcavitation at the periphery of the mesa-like structure and the basal surface of the lesion with progressive reduction in resistant area dimensions.

The exact reason why these areas remain more resilient to acid exposure than the surrounding matrix remains unknown. There are no significant differences in terms of the calcium: phosphate ratio when compared to sound and eroded enamel as well as

synthetic hydroxyapatite; differences in enamel rod orientation remain indeterminate as there is no way as yet to predetermine where the enamel is more resilient and a more in depth compositional analysis was not possible owing to time and equipment constraints. Atomic force microscopy imaging showed that the erosion of the intra-rod enamel was deeper at one side of the core than at the other. This may potentially reflect the directionality of the emerging rod with associated changes in erosion susceptibility as opposed to the orientation of the image, a fact substantiated by the inter-rod enamel remaining at a constant height. The effects of depth of the behaviour of eroded enamel rods at depth have previously been correlated by Zheng *et al.*, a factor worth considering given the irregular path of the enamel rod within the matrix as observed by Radlanski *et al* (Zheng *et* al, 2010; Radlanski *et al*., 2001). Thus the irregularity of the enamel rods orientation in presenting a uniform surface perpendicular to the direction of travel may have a significant impact on the effect of erosion as recorded by hardness and reduced elastic (Young's) modulus after short durations of acid exposure (He *et al.*, 2006) but this is disputed by Braley *et al*., who found no significant difference between enamel prism orientation and hardness or elastic modulus although their sample size was limited to multiple measurements from one human molar (Braley *et al*., 2007).

It was observed that the heat generated by the focussed ion beam can detrimentally affect enamel over a wide area (typically the size of the viewing image) giving rise to progressive degenerative melting of surface features. However, this effect was only noted if the target area had been focussed upon for too long. Thus, the superficial appearance of the surface morphology of the erosion lesion may thus be affected by the beam giving a false indication of potential cavitation. However, this hypothesis is unlikely as such an effect was not observed in the sound enamel samples following milling.

In closing, the presence of the cavitated morphology corroborates well with information gained from AFM force vs. distance curves in terms of softened enamel depth, a fact which is also substantiated by the literature (Cheng et al., 2009). There remains potential for these areas to potentially aid in the remineralisation of enamel particularly in the presence of elevated levels of fluoride, calcium or phosphate.

CHAPTER 6

REMINERALISATION OF ENAMEL

6.1. THE EFFECT OF FLUORIDE IN REDUCING EROSION DAMAGE

Having previously established the effect of 1 mol.L^{-1} acid solutions on human and bovine enamel it was decided to examine the remineralisation of enamel using fluoride, a compound commonly employed as a remineralising agent in dentifrices and mouthrinses.

The dose response of fluoride on eroded bovine enamel was evaluated against a control for seven different concentrations of sodium fluoride added to a placebo dentifrice, which lacked any fluoride and subjected to a five day, cyclic erosion protocol[§§§§].

Figure 6.1-1 shows the results of increasing fluoride concentration on bulk tissue loss arising from an acid challenge, measured using optical profilometry and analysed using Mann-Whitney U-tests.

§§§§ See Section 2.10.2: "Assessment of the effect of fluoride on enamel remineralisation"

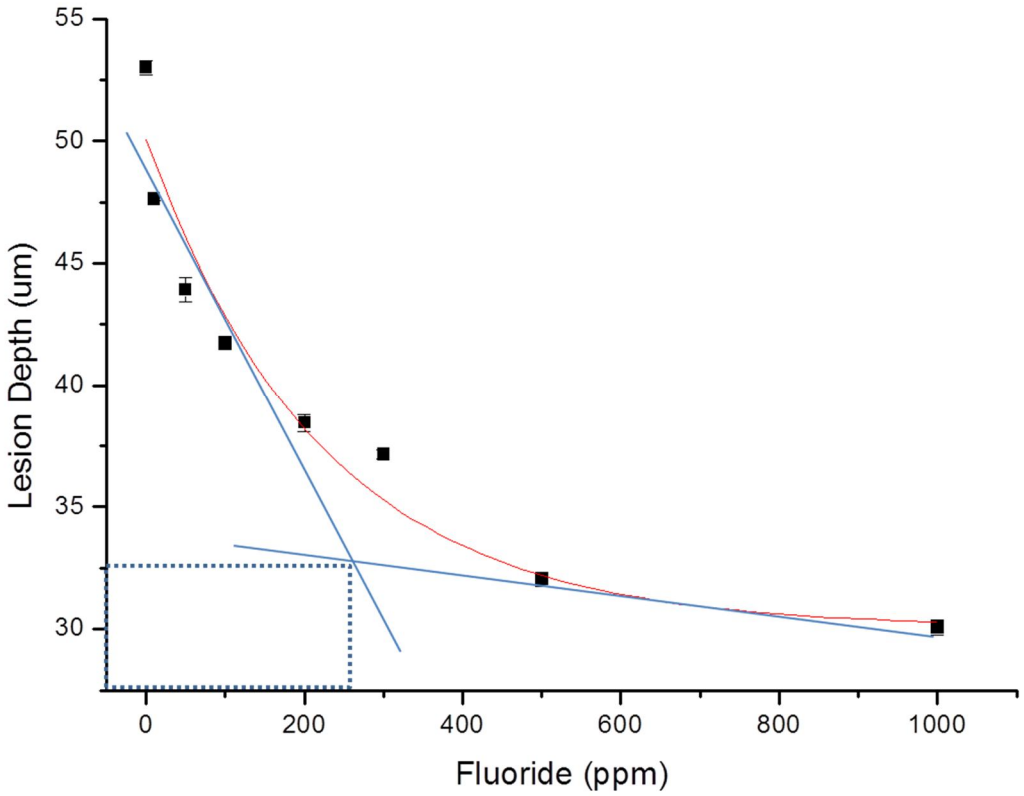

Figure 6.1-1: The dose response of fluoride in reducing bulk tissue loss of bovine enamel when exposed to a five day, cyclic erosion protocol.

The control sample showed the greatest erosion lesion depth at 72.76 µm (±1.14 SE). The addition of 10 ppm of sodium fluoride to the placebo dentifrice (lacking any fluoride) had a significant effect ($p = >0.001$) on the reduction the erosion depth to 51.60 µm (±1.42 SE). Increasing the fluoride dose to 50 ppm further reduced the lesion depth to 43.92 µm (±0.52 SE), which was significant from the 10 ppm dose ($p = 0.003$). Doubling the fluoride dose to 100 ppm again showed a significant ($p = 0.002$) reduction compared to the previous result, with the erosion lesion being 50.46 µm (±0.96 SE) deep. With the addition of 200 ppm fluoride to the placebo dentifrice the lesion was found to be 38.45 µm (±0.36 SE), a significant difference ($p = 0.001$) from that of 100 ppm fluoride. With the addition of 300 ppm fluoride the lesion was found to be 42.87 µm (±0.55 SE), which was significant ($p = 0.01$) from that of the previous result using 200 ppm fluoride. With the addition of 500 ppm fluoride to the placebo dentifrice the

lesion was found to be 32.05 μm (±0.29 SE), while 1000 ppm reduced the lesion depth to 30.06 μm (±0.31 SE).

Fitting two linear slopes to each terminal of the arc (represented on the figure by two blue slopes) and observing where they intersect allows for the determination of the point at which the slope of the data (represented by the red line in the figure) begins to reduce. This intersection at 250 ppm represents the point at which an increase in the concentration of fluoride begins to lessen.

6.2. ALTERNATIVE COMPOUNDS TO REDUCE EROSION

In addition to the fluoride tested in the previous section, two additional compounds were tested that are thought to have beneficial properties in minimizing dental erosion: sodium phosphate and calcium carbonate. The former provides an increase in the quantity of phosphates and the latter an increase in the quantity of calcium. Both of these reagents were evaluated against sodium fluoride.

The initial demineralisation of the enamel samples created a lesion with a median depth of 3.78 µm (±0.85) in the sodium phosphate samples, 2.03 µm (±1.87) for the sodium fluoride samples and 2.67 µm (±1.63) for the calcium carbonate samples. Treatment with the respective remineralisation compounds modified the lesion depths as follows: the sodium phosphate samples had a median lesion depth of 4.91 µm (±1.09), the sodium fluoride median sample depth was 2.16 µm (±2.29) and the calcium carbonate samples had a median depth of 0.98 µm (±1.92). There was a significant difference between the median of the sodium phosphate and calcium carbonate ($p = 0.003$ and 0.01, respectively) but not between those of the sodium fluoride.

A second demineralisation event and subsequent remineralisation with calcium, phosphate or fluoride ions further deepened the erosion lesion and produced lesions with the following depths: the sodium phosphate samples had a median lesion depth of 14.54 µm (±2.81), the sodium fluoride median sample depth was 12.25 µm (±1.78) and the calcium carbonate samples had a median depth of 15.75 µm (±2.42). All the more recent lesion depths were significantly deeper than those previously found ($p = .0.001$).

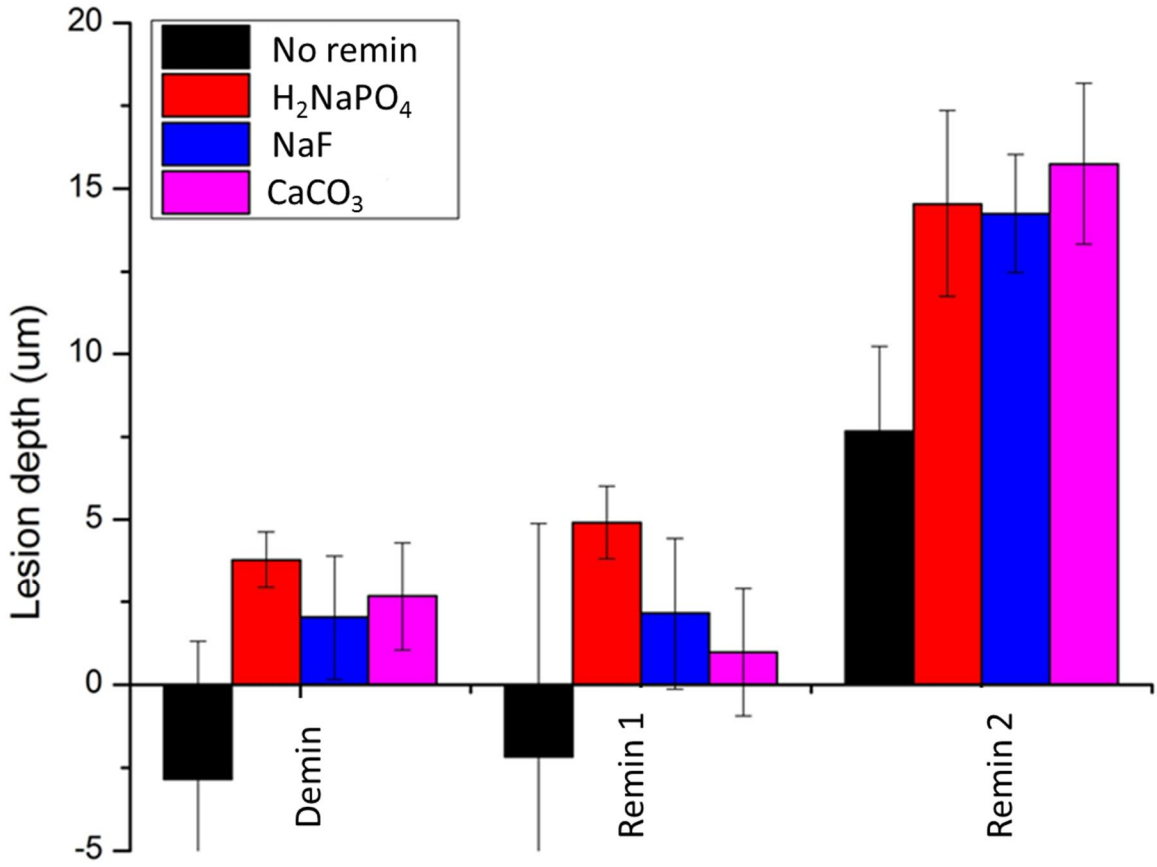

Figure 6.2-1: The median and IQR values of three remineralisation compounds on bulk tissue loss of human enamel. Result 1 represents demineralisation only, Result 2 represents Remineralisation 1 and Result 3 represents remineralisation 2.

A Kruskall-Wallis analysis of variance showed there was a significant difference between the means of the control (NoRemin), sodium phosphate, sodium fluoride and calcium carbonate following the first demineralisation event, the first remineralisation and the second remineralisation ($p = 0.04$; 0.05 and 0.02, respectively). The most likely cause for this was the control category. Further Kruskall-Wallis analysis, this time omitting the control category, showed there was no significant difference between the medians of sodium phosphate, sodium fluoride and calcium carbonate following the first demineralisation event and that of the second remineralisation event. This would appear to indicate that there is no significant difference between the remineralising capability of sodium phosphate an calcium carbonate when compared to that of

fluoride. However, the lesion depths of the first remineralisation event were found to be significantly different ($p = 0.03$). Moreover, there was no significant difference between the medians of the demineralisation and the first remineralisation for any of the test categories of control (NoRemin), sodium phosphate, sodium fluoride and calcium carbonate.

6.3. DISCUSSION OF CHAPTER 6

THE EFFECT OF FLUORIDE AS A REMINERALISING AGENT.

Many compounds have been shown to play a role in the reduction of enamel bulk tissue loss following a demineralisation challenge. Buonocore and Bibby evaluated several of these, including NaF and $SrCl_2$ and some which were cytotoxic and thus of limited pharmacological use, for example PbF_2 (Buonocore & Bibby, 1945).

Fluoride has been extensively tested in its capacity to improve dental health and has been shown to have a positive effect in the remineralisation of incipient lesions attributed to caries as well as its ability to minimise or prevent enamel demineralisation (Duckworth, 1993). Experiments with fluoridated buffer solutions have shown a decrease in fluoride ion concentration in the solution, which is indicative of ion substitution to form fluoroapatite on the surface of test samples (Wong *et al*, 1987). However, literature regarding the optimum minimum dose response of fluoride in order to initiate a cariostatic or remineralisation effect for enamel is scarce (Magalhães *et al*., 2007).

Norén *et al*. found that fluoride was localised to the superficial surfaces of enamel (Norén *et al*., 1983). Fluoride ions, from either fluoridated water supplies and/or fluoridated dentifrices, are incorporated into the hydroxyapatite crystal lattice in a substitution reaction for the hydroxyl (OH^-) ion of hydroxyapatite. Fluoridated hydroxyapatite is less soluble in an acid environment and, as a result of this reduced solubility, will precipitate at a faster rate when in contact with dissolved calcium and phosphate ions in solution (ten Cate, 1999) and, furthermore, has modified surface

electrochemical properties which will significantly interact with salivary proteins, promoting the adherence of these proteins to the tooth surface and so minimising surface damage to the tooth resulting from an erosive challenge (Moreno *et al*, 1974).

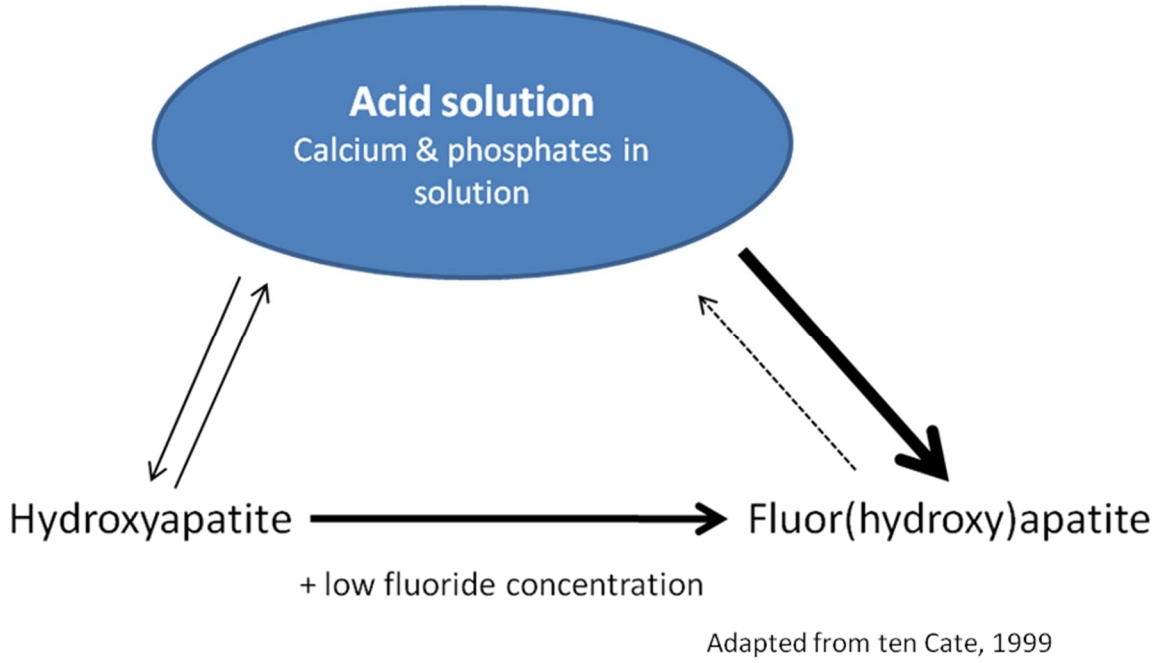

The data was tested using non-parametric analyses, which showed a significant declining trend in bulk tissue loss of bovine enamel following a cyclic, five day erosion study. The addition of 10 ppm of NaF to a placebo dentifrice with no previously added fluoride showed significant reduction in total lesion depth at the end of the study. Continuing to progressively increase the quantities of fluoride showed further significant reductions of bulk tissue loss but, as may be seen from Figure 6.1-1, the trend of decay begins to slow from the 200 ppm category meaning that the remineralising effect of fluoride, while still significant, begins to decline with increased concentration of fluoride. Plotting of the decay trend shows that the optimal minimal dose of fluoride for this work is approximately 260 ppm; any additional fluoride will not be as effective

in reducing demineralisation as the previous concentration, however the effect of additional fluoride remains significant.

THE EFFECTS OF ADDITIONAL COMPOUNDS ON REMINERALISATION

Despite fluoride being the predominant additive to dentifrice to reduce erosion, alternative compounds may also aid in enamel remineralisation. The addition of strontium, for example, has been suggested to significantly affect the remineralisation of enamel when used in conjunction with fluoride (Thuy *et al*., 2008). However this remains disputed and some groups maintain the protective effect of agents such as strontium chloride or potassium citrate are as effective as fluoride in reducing erosion (Kato *et al*., 2010).

Our second experiment exploring the remineralisation of enamel employed concentrations of sodium phosphate, sodium fluoride and calcium carbonate published previously (Buchalla *et al*., 2007; Magalhães *et al*., 2009) but modified to use an erosion protocol similar to those employed previously in this work***** and employing white light interferometry to obtain quantifiable data regarding the initial lesion depth and subsequent remineralisations. The results of this work were inconclusive: The control data was significantly different from all the test categories but not in the manner expected and there was no uniformity of significance between the remineralisation categories. A potential explanation for this could pertain to the tape used to demark the control and test areas. The variation of the tape was ±3.90 µm while the uneroded lesion depth was calculated to be between -3.62 to 6.52 µm, with a mean of 2.85 µm.

***** 0.05% acid solutions, section 2.8.2.

Thus, it is possible that the small lesion depth would be affected by the variation observed in the tape but this would also be dependent on other factors such as enamel susceptibility to erosion. As the data stands, use of the control data for comparative purposes is severely restricted as it suggests the samples with no remineralisation protocol implemented yielded the smallest lesion depth compared to those including a remineralising compound. Given that the previous section (Section 2) showed a significant decrease in bulk tissue loss with increasing fluoride concentration, this explanation is unlikely.

Omission of the control data in order to independently compare the results of the remineralisation compounds showed that the second remineralisation data does appear to support Kato *et al.* (2010) in that there appears to be no significant difference between the remineralising potential of fluoride against either phosphate or calcium. Thus an excess of calcium or phosphate appears to drive remineralisation as effectively as fluoride.

CHAPTER 7

CLOSING REMARKS & FUTURE WORK

There is a relative paucity of literature relating to early duration (under 10 minutes) acid exposure to enamel, as well as direct human and bovine enamel physicochemical behaviour comparisons. This body of work set out with the principal aims of determining the effect of a short term, repeated acid exposure on enamel and whether or not bovine enamel was a suitable substitute for human enamel for use in *in vitro* enamel erosion experiments.

Initial studies using three common but comparatively strong 1 $mol.L^{-1}$ acid solutions showed good correlation between human and bovine enamel during the first 600 seconds of erosion. This correlation was also observed using the same acids of a more physiologically relevant concentration and provided further evidence supporting the substitution of bovine enamel for human enamel for *in vitro* enamel erosion experimental work. A finding of particular interest was observed with respect to the rates of erosion for both 1 $mol.L^{-1}$ and 0.05 % acid solutions: the early phase of enamel erosion appeared to be biphasic when plotted as erosion rates between 10-60 and 60-600 seconds. This appeared to show the majority of enamel bulk tissue loss occurred during the first 60 seconds of acid erosion before the rate of bulk tissue loss began to decline. The close correlation between the species, both in terms of bulk tissue loss and the associated rates was strongly suggestive that bovine enamel is suitable as a human material substitute at these early durations. Additional work to confirm this was undertaken using an alternative method, such as QLF.

Correlating the optical profilometry findings with an alternative technique (QLF) supported the optical profilometry results, showing that there was good correlation between the two species in terms of bulk tissue loss. However, an attempt to directly

compare the readings from each protocol with each other showed significant differences between the results of QLF and optical profilometry. This is most likely attributed to the differences in mode of detection of height variation and light scattering. As a result of this and in conjunction with the apparently biphasic erosion trends observed from optical profilometry, it was hypothesised that a multi-layer erosion effect relating to the flow of acid could account for these results.

Surface hardness was the next phase of work in continuing the investigation of the behaviour of human and bovine enamel when exposed to a short duration acid exposure. Initially Vickers indentation was used to obtain readings regarding the hardness of the enamel lesion and its surrounding area. This is a commonly employed tool in enamel erosion evaluation but was found to be unsuitable for work of short duration acid exposure. Atomic force microscopy generated force *versus* distance plots were considered a more appropriate test as the load applied could be carefully controlled and there was less chance of undetected indenter penetration through the softened enamel. The results of the AFM FD appeared to substantiate our previous hypothesis regarding a multi-layer erosion effect by showing the presence of a softened enamel layer below that of the eroded superficial surface. This effect was present for both species.

Given the accumulating evidence for a biphasic model, it was decided to explore the morphological characteristics of early onset enamel erosion. An unusual finding was observed in the form of mesa-like areas at the basal surface of the lesion, which were initially resistant to enamel erosion. These were observed in all specimens, using both optical profilometry, AFM and SEM.

Cross sections through the control and eroded human and bovine enamel using focussed ion beam scanning electron microscopy (FIB-SEM) showed differential subsurface patterns between control and eroded human and bovine enamel: the uneroded control enamel presented a uniform curtain wall, while at the base of the erosion lesion, the curtain wall was found to be honeycombed with apparent microcavities. A FIB-SEM examination of the mesa-like structures observed on the basal surface of the lesion showed the superficial surface of these were more in keeping with the uneroded control enamel than that of the surrounding area. However, the lateral edges were more similar to the surrounding area and presented with variegated microcavities. This was suggestive that enamel loss progresses through coalescence of subsurface cavities.

From a clinical viewpoint, one of the best strategies to manage enamel erosion is through preventative measures, such as additives in the form of fluoride. Previous work in the literature has employed comparatively high fluoride concentrations (often in excess of 1000 ppm) and the effects of this on remineralisation are well documented. However, we aimed to determine at which minimum concentration do the effects of fluoride begin to decline. This was found to be at 250 ppm, whereupon adding more fluoride to the experimental system did continue to significantly affect remineralisation but the effects were less than the preceding dose. Two other compounds were then investigated, which provided additional calcium and phosphate to the erosion system, and evaluated against fluoride concentrations previously established in the literature. The addition of calcium and phosphate to the erosion system was shown to have a similar remineralising potential to that of fluoride, which may have benefits to

remineralisation strategies, especially in light of our findings regarding areas of apparent initial acid resistance.

We therefore assert that bovine enamel is a suitable substitute for human enamel for use in early stage enamel erosion studies and hypothesise that early stage superficial bulk enamel loss may progress as a result of coalescing subsurface cavitation in addition to enamel lost to the solution through diffusion. It may be possible that these areas of apparent initial acid resistance may have some part to play in acting as foci for remineralisation strategies.

FUTURE WORK

The development of the novel model of erosion was validated against a current *in vitro* protocol but it should be noted that this is a hypothetical representation of dental erosion. Future work of an *in vitro* or *in situ* nature exploring the effect of saliva and enamel adherent proteins as well as the oral biofilm in minimising the effects of early erosion under constant composition conditions is strongly recommended. However the difficulties in obtaining quantifiable data from such experimental work would probably necessitate the development of additional protocols or tools as the anticipated lesion dimensions from any future work would be smaller than those presented for this work.

Quantitative light fluorescence shows tremendous promise as a method of lesion measurement providing a greater understanding of the origins or autofluorescence can be fully elucidated and the adverse effects of light scattering suitably compensated.

Such a technique would prove beneficial for the rapid detection of early stage erosion in the clinical environment, permitting earlier prophylactic intervention.

The use of a focussed ion beam coupled to SEM has been shown to be successful in the examination of erosion lesion internal morphology. Future improvements in optical resolution may eventually permit a closer, more detailed examination of the internal cavitation of acid resistant lesions.

Finally, an expansion of the study described in this work to encompass an increased number of time points would permit a better description of the erosion trend, with a possibility of determining a more accurate description of the erosion kinetics, such as whether or not the initial erosion process is exclusively diffusion controlled. Furthermore, a repeat of the ion chromatography data, using more sensitive instrumentation and an improved method (such as automatic dispensing of 2 ml samples from a solution in continuous motion) might permit a more accurate determination of the loss of calcium ions into solution.

To close, this work puts forward a model for determining the chemical effects of a repeated, short duration acid exposure to enamel as well as a hypothetical explanatory model for the observed biphasic results of early dental erosion.

REFERENCES

Aas JA, Paster BJ, Stokes LN, Olsen I, Dewhirst FE, Defining the normal bacterial flora of the oral cavity, 2005, Journal of clinical microbiology, **43**:5721-5732.

Addy M, Hunter ML, Can tooth brushing damage your health? Effects on oral and dental tissues, 2003, International dental journal, **53**:177-186.

Addy M, Shellis PR, Interaction between attrition, abrasion and erosion in tooth wear, In: Lussi A, ed, 2006, Monograms in oral science, Basel, Karger, **20**:17–31

Aiello L, Dean C, An introduction to human evolutionary anatomy, 1990, Academic Press, pp 106-109.

Alben OA, 'Fourier transform infrared spectroscopy of enzyme systems', 1996; Infrared spectroscopy of biomolecules, Wiley-Liss Inc, 19-27.

Amaechi BT, Higham SM, In vitro remineralisation of eroded enamel lesions by saliva, 2001, Journal of dentistry, **29**:371-376.

Amaechi BT, Higham SM, Edgar WM, Use of transverse microradiography to quantify mineral loss by erosion in bovine enamel, 1998, Caries research, **32**:351-356.

Amaechi BT, Higham SM, Edgar WM, Factors influencing the development of dental erosion in vitro: enamel type, temperature and exposure time, 1999, Journal of oral rehabilitation, **26**:624-630.

Amaechi BT, Higham SM, Dental erosion: possible approaches to prevention and control, 2005, Journal of dentistry, **33**:243-252

Amerongen AVN, Oderkerk CH, Driessen AA, Role of mucins from human whole saliva in the protection of tooth enamel against demineralization in vitro, 1987, Caries research, **21**:297–309.

Aoba T, Moreno EC, The enamel fluid in the early secretory stage of porcine amelogenesis: Chemical composition and saturation with respect to enamel mineral , 1987, Calcified tissue international, **41**:86-94.

Aoba T, Moreno EC, Changes in the nature and composition of enamel mineral during porcine amelogenesis, 1989, Calcified tissue international, **45**:356-364.

Arbel A, Katz I, Sarig S, Dissolution of hydroxyapatite by calcium complexing agents, 1991, Journal of crystal growth, **110**:733-738.

Arends J; Ten Bosch, JJ, Demineralization and remineralization evaluation techniques, 1992, Journal of dental research, **71**:924-928.

Arends J, ten Cate, JM, Tooth enamel remineralisation, 1981, Journal of crystal growth, **53**:135-147.

Ashcroft AT, Joiner A, Tooth cleaning and tooth wear: A review, 2010, Proceedings of the institution of mechanical engineers, Part J: Journal of engineering tribology, 224: 539.

Atkins P, Jones L, Chemistry: Molecules matter and change (3rd edition), 1997, WH Freeman & company, New York.

Attin A, Meyer K, Hellwig E, Buchalla W, Lennon AM, Effect of mineral supplements to citric acid on enamel erosion, 2003, Archives of oral biology, **48**:753-759.

Attin T, Koidl U, Buchalla W, Schaller HG, Kielbassa AM, Hellwig E, Correlation of microhardness and wear in differently eroded bovine dental enamel, 1996, Archives of oral biology, **42**:243-250.

Attin T, Koidl U, Buchalla W, Schaller HG, Kielbassa AM, Hellwig E, Correlation of microhardness and wear in differently eroded bovine dental enamel, 1997, Archives of oral biology, **42**:243-250.

Attin T, Wegehaupt F, Gries D, Wiegand A, The potential of deciduous and permanent bovine enamel as substitute for deciduous and permanent human enamel: Erosion-abrasion experiments, 2007, Journal of dentistry, **35**:773-777.

Attin T, Becker K, Roos M, Attin R, Paqué F, Impact of storage conditions on profilometry of eroded dental hard tissue, 2009, Clinical oral investigations, 13:473-478.

Austin RS, Rodriguez JM, Dunne S, Moazzez R, Bartlett DW, The effect of increasing sodium fluoride concentrations on erosion and attrition of enamel and dentine in vitro, 2010, Journal of dentistry, **38**:782-787.

Azzopardi A, Bartlett DW, Watson TF, Sherriff M, The measurement and prevention of erosion and abrasion, 2001, Journal of dentistry, **29**:395-400.

Barbour ME, Parker DM, Allen GC, Jandt KD, Human enamel erosion in constant composition citric acid solutions as a function of degree of saturation with respect to hydroxyapatite, 2005a, Journal of oral rehabilitation, **32**:16-21.

Barbour ME, Finke M, Parker DM, Hughes JA, Allen GC, Addy M, The relationship between enamel softening and erosion caused by soft drinks at a range of temperatures, 2005b, Journal of dentistry, **34**:207-213.

Barbour ME, Rees JS, The laboratory assessment of enamel erosion, 2004, Journal of dentistry, **32**:591-602.

Barbour ME, Rees JS, The role of erosion, abrasion and attrition, 2006, Journal of clinical dentistry, **17**:88-93.

Barbour ME, Shellis RP, An investigation using atomic force microscopy nanoindentation of dental enamel demineralization as a function of undissociated acid concentration and differential buffer capacity, 2007, Physics in medicine and biology, **52**:899-910.

Bartlett DW, Evans DF, Smith BG, The relationship between gastro-oesphogeal reflux disease and dental erosion, 1996, Journal of oral rehabilitation, **23**:289-297.

Bartlett DW, Bureau GP, Anggiansah A. Evaluation of the pH of a new carbonated soft drink beverage: an in vivo investigation, 2003, Journal of prosthodontics, 12:21-25.

Bartlett DW, The role of erosion in tooth wear: aetiology, prevention and management, 2005, International dental journal, 55:277-284.

Bartlett DW, Shah P, A critical review of non-carious cervical (wear) lesions and the role of abfraction, erosion, and abrasion, 2006, Journal of dental research, 85:306-312.

Bassiouny MA, Yang J, Influence of drinking patterns of carbonated beverages on dental erosion, General dentistry, **53**:205-210.

Bergstöm J, Larvsedt S, An epidemiologic approach to toothbrushing and dental abrasion, 1978, Community dentistry and oral epidemiology, **7**:57-64.

Blunt RT, White Light Interferometry – a production worthy technique for measuring surface roughness on semiconductor wafers, 2006, CS Mantech conference, British Columbia, Canada, Accessed 25th November, 2010, http://www.csmantech.org/Digests/2006/2006%20Digests/4B.pdf

Blau PJ, A Comparison of four microindentation hardness test methods using copper, 52100 Steel, and an amorphous Pd-Cu-Si alloy, 1983, Metallography, **16**:1-18.

Bodier-Houllé P, Steuer P, Meyer JM, Bigeard L, Cuisinier FJG, High-resolution electron-microscopic study of the relationship between human enamel and dentin crystals at the dentinoenamel junction, 2000, Cell & tissue research, **301**:389–395.

Boehm TK, Scannapieco FA, The epidemiology, consequences and management of periodontal disease in older adults, 2007, Journal of the American dental association, **138**:26S-33S

Bollet-Quivogne FRG, Anderson P, Dowker SEP, Elliott JC, Scanning microradiographic study on the influence of diffusion in the external liquid on the rate of demineralization in hydroxyapatite aggregates, 2005, European journal of oral sciences, 113:53-59.

Boyde A, Dependence of rate of physical erosion on orientation and density in mineralised tissues, 1984, Anatomical embryology, **170**:57-62.

Boyde A, Jones SJ, Reynolds PS, Quantitative and qualitative studies of enamel etching with acid and EDTA, 1978, Scanning electron microscopy, **2**:991-1002.

Bozzola JJ, Russell LD, Electron microscopy: principles and techniques for biologists (2nd Ed.), 1998, Jones and Bartlett publishing.

Braley A, Darnell LA, Mann AB, Teaford MF, Weihs TP, The Effect of Prism Orientation in the Indentation Testing of Human Molar Enamel, 2007, Archives of oral biology, **52**:856-860.

British standards institution, Advanced technical ceramics – mechanical properties of monolithic ceramics at room temperature, 2005, BS EN 843-4:2005.

Britvic soft drinks report, 2010, accessed 9th August, 2010, http://ir.britvic.com/en/results-presentations/results-presentations/~/media/Files/B/Britvic/pdfs/britvic_soft_drink_report_2010.pdf

Buchalla W, Lennon ÁM, Becker K, Lucke T, Attin T, Smear layer and surface state affect dentin fluoride uptake, 2007, Archives of oral biology, **52**:932-937.

Buonocore MG, Bibby, BG, The effects of various ions on enamel solubility, 1945, Journal of dental research, **24**:103-108.

Buonocore MG, A simple method of increasing the adhesion of acrylic filling materials to enamel surfaces, 1955, Journal of dental research, **34**:849-853.

Buzalaf MAR, de Moraes Italiani F, Kato MT, Martinhon CCR, Magalhães AC, Effect of iron on inhibition of acid demineralisation of bovine dental enamel *in vitro*, 2006, Archives of Oral Biology, **51:**844-848.

Campbell AA, LoRe M, Nancollas GH, The influence of carbonate and magnesium ions on the growth of hydroxyapatite, carbonated apatite and human powdered enamel, 1991, Colloids and surfaces, **54**:25-31.

Carlson BM, Human embryology and developmental biology 2nd Edition, 1994, Mosby Publishing, pp 298-303.

Carmago MA, Marques MM, de Cara AA, Morphological analysis of human and bovine dentine by scanning electron microscope investigation, 2007, Archives of oral biology, **53**:105-108.

Caterina JJ, Skobe Z, Shi J, Ding YL, Simmer JP, Birkedal-Hansen H, Bartlett JD, Enamelysin (matrix metalloproteinase 20)-deficient mice display an amelogenesis imperfecta phenotype, 2002, Journal of biological chemistry, **277**:49598-49604.

Cheaib Z, Lussi A, Impact of acquired enamel pellicle modification on initial dental erosion, 2011, Caries research, **45**:107-112.

Cheng Z-J, Wang X-M, Cui F-Z, Ge J, The enamel softening and loss during early erosion studied by AFM, SEM and nanoindentation, 2009, Biomedical materials, **4**:1-7.

Christoffersen J, Dissolution of calcium hydroxyapatite, 1981, Calcified tissue international, **33**:557-560.

Cross SE, Kreth J, Wali RP, Sullivan R, Shi W, Gimzewski JK, Evaluation of bacteria-induced enamel demineralization using optical profilometry, 2009, Dental materials, **25**:1517-1526.

Cui F-Z, Cheng ZJ, Ge J, Nanomechanical properties of tooth and bone revealed by nanoindentation and AFM, 2007, Key engineering materials, p2263-2266.

Curzon ME, Crocker DC, Relationship of trace elements in human tooth enamel to dental caries, 1978, Archives of oral biology, **23**:647-653.

Cuy JL, Mann AB, Livi KJ, Teaford MF, Weihs TP, Nanoindentation mapping of the mechanical properties of human molar tooth enamel, 2002, Archives of oral biology, **47**:281-291.

Daculsi G, Kerebel B, Kerebel LM, Mitre D, High-resolution study by transmission electron microscopy of a microhypoplasia of the human enamel surface, 1984, Archives of oral biology, **29**:201-203.

Darling CL, Le John CQ, Featherstone JDB, Fried D, An automated digital microradiography system for assessing tooth demineralization (*poster*), 2009, Lasers in dentistry XV, 7192.

Deer, Howie, and Zussman, An introduction to rock-forming minerals, 1993, John Wiley and Sons publishing.

de Leew NH, Resisting the onset of hydroxyapatite dissolution through the incorporation of fluoride, 2004, Journal of physical chemistry B, **108**:1809-1811.

Devlin H, Bassiouny MA, Boston D. Hardness of enamel exposed to Coca-Cola® and artificial saliva, 2006, Journal of Oral Rehabilitation; **33**:26-30.

Dowker SEP, Elliott JC, Davis GR, Wassif HS, Longitudinal study of the three-dimensional development of subsurface enamel lesions during *in vitro* demineralisation, 2003, Caries research, **37**:237-245.

Drake RL, Vogl W, Mitchell AWM (editors), Gray's Anatomy for students, Elvisier Churchill Livingstone, 2005.

Duckworth RM, The science behind caries prevention, 1993, International dental journal, **43**:529-539.

Edgar M, Saliva: it's secretion, composition and functions, In: Harris M, Edgar M, Meghji S, Clinical oral science, 1998, Butterworth-Heinemann publishing.

Edgar WM, O'Mullane DM, Saliva and dental health, 1st Ed, 1990, British dental journal.

Edwards M, Creanor SL, Foye RH, Gilmour WH, Buffering capacities of soft drinks: the potential influence on dental erosion, 1999, Journal of oral rehabilitation, **26**:923-927.

Eisenburger M, Addy M, Evaluation of pH and erosion time on demineralisation, 2001, Journal of clinical investigation, **5**:108-111.

Eisenburger M, Addy M, Influence of temperature and liquid flow rate on erosion and enamel softening, 2003, Journal of oral rehabilitation, **30**:1076-1080.

Eisenburger M, Shellis RP, Addy M, Scanning electron microscopy of softened enamel, 2004, Caries research, **38**:67-74.

Eisenburger M, Degree of mineral loss in softened human enamel after acid erosion measured by chemical analysis, 2009, Journal of dentistry, **37**:491-494.

Elton V, Cooper L, Higham SM, Pender N, Validation of enamel erosion *in vitro*, 2009, Journal of dentistry, **37**:336-341.

Exterkate RAM, Damen JJM, ten Cate JM, Effect of fluoride-releasing filling materials on underlying dentinal lesions *in vitro*, 2005, Caries research, **39**:509-513.

Fan Y, Sun Z, Moradian-Oldak J, Effect of fluoride on the morphology of calcium phosphate crystals grown on acid-etched human enamel, 2009, Caries research, **42**:132-136.

Feagin, FF, Calcium, phosphate and fluoride deposition on enamel surfaces, 1971, Calcified tissue international, **8**:154-164.

Featherstone JD, Dental caries: a dynamic disease process, 2008, Australian dental journal, **3**:286-291.

Featherstone JD, Lussi A (ed), Understanding the chemistry of dental erosion, Dental Erosion: Monograms in Oral Science, 2006, Karger Publishing Basel, **20**:66-76.

Featherstone JD, Mellberg JR, Relative rates of progress of artificial carious lesions in bovine, ovine and human enamel, 1981, Caries research, **15**:109-14.

Fejerskov O, Manji F, Baelum V, 1990, The nature and mechanisms of dental fluorosis in man, Journal of dental research, **69**:692-700.

Field J, Waterhouse P, German M, Quantifying and qualifying surface changes on dental hard tissues *in vitro*, 2010, Journal of dentistry, **38**:182-190.

Fluoridation Facts, 2005, American Dental Association, p. 29. Accessed 17 June, 2009; http://web.archive.org/web/20070307065553/http://www.ada.org.au/media/Fluoridenow/Documents/AmDA+fluoridation_factsRO.pdf.

Fowler C, Gracia L, Edwards MI, Willson R, Brown A, Rees GD, Inhibition of enamel erosion and promotion of lesion rehardening by fluoride: a white light interferometry and microindentation study, 2009, Journal of clinical dentistry, **20**:178-185.

Frostell G, Larsson SJ, Lodding A, Odelius H, Petersson LG, SIMS study of element concentration profiles in enamel and dentin, 1977, Scandinavian journal of oral research, **85**:18-21.

Galil KA, Wright GZ, Effects of various acids on the buccal surface of human permanent teeth: a study using scanning electron microscopy, 1979, Pediatric dentistry, **1**:155–159.

Ganss C, Klimek J, Brune V, Schurmann A, Effects of two fluoridation measures on erosion progression in human enamel and dentine in situ, 2004, Caries research, **38**:561-566.

Ganss C, Lussi A, Scharmann I, Weigelt T, Hardt M, Klimek J, Schlueter N, Comparison of calcium analysis, longitudinal microradiography and profilometry for the quantitative assessment of erosion in dentine, 2009, Caries research, **43**:422-429.

Ge J, Cui FZ, Wang XM, Feng HL, Property variations in the prism and the organic sheath within enamel by nanoindentation, 2005, Biomaterials, **26**:3333-3339.

German M, Carrick TE, McCabe JF, Surface detail reproduction of elastomeric impression materials related to rheological properties, 2008, Dental materials, **24**:951-956.

Goldstein J, Newbury DE, Echlin P, Lyman CE, Joy DC, Lifshin E, Sawyer LC, Michael JR, Scanning electron microscopy and x-ray microanalysis 3rd Edition, 2003, Springer.

Gopakumar V, Gopakumar A, Stanley Drummond-Jackson: Pioneer of intravenous anaesthesia in dentistry, 2009, Proceedings of the history of anaesthesia society, **41**:94-100.

Gray JA, Kinetics of the dissolution of human dental enamel in acid, Journal of dental research, 1962, **41**:633-645.

Gray JA, Kinetics of enamel dissolution during formation of incipient caries-like lesions, 1966, Archives of oral biology, **11**:397-421.

Grippo JO, Abfractions: a new classification of hard tissue lesions of teeth, 1991, Journal of esthetic dentistry, **3**:14–9.

Grippo JO, Simring M, Schreiner S, Attrition, abrasion, corrosion and abfraction revisited: A new perspective on tooth surface lesions, Journal of the American Dental Association, 2004, 135:1109-1118.

Habelitz S, Marshall SJ, Marshall GW, Balooch M, Mechanical properties of human dental enamel on the nanometre scale, 2001, Archives of oral biology, **46**:173-183.

Hafner JH, Cheung C-L, Woolley AT, Lieber CM, Structural and functional imaging with carbon nanotube AFM probes, 2001, Progress in biophysics and molecular biology, **77**:73-110.

Hannig M, Balz M, Influence of *in vivo* formed pellicle on enamel erosion, 1999, Caries Research, **33**:372–79.

Hannig M, Hess NJ, Hoth-Hannig W, de Vrese M, Influence of salivary pellicle formation time on enamel demineralization – an in situ pilot study, 2003, Clinical oral investigations, **7**:158–161.

Hannig M, Fiebiger M, Güntzer M, Döbert A, Zimehl R, Nekrashevych Y, Protective effect of the in situ formed short-term salivary pellicle, 2004, Archives of oral biology, **49**:903-910.

Hannig C, Hamkens A, Becker K, Attin R, Attin T, Erosive effects of different acids on bovine enamel: release of calcium and phosphate in vitro, 2005, Archives of oral biology, **50**:541-552.

Hara AT, Zero DT, Analysis of the erosive potential of calcium-containing acidic beverages, 2008, European journal of oral science, **116**:60-65.

He LH, Fujisawa N, Swain MV, Elastic modulus and stress-strain response of human enamel by nano-indentation, *Biomaterials*, 2006, **27**: 4388-4398.

Hemingway, C, Tooth erosion, food proteins and salivary pellicle, PhD, University of Bristol

Heurich E, Beyer M, Jandt KD, Reichert J, Schnabelrauch M, Sigusch BW, Quantification of dental erosion—A comparison of stylus profilometry and confocal laser scanning microscopy (CLSM), 2010, Dental materials, **36**:326-336.

Hikita K, Van Meerbeek B, De Munck J, Ikeda T, Van Landuyt K, Maida T, Lambrechts P, Peumans M, Bonding effectiveness of adhesive luting agents to enamel and dentin, 2007, Dental materials, **23**:71-80.

Hoffman H, Hudgens PA,Head and Skull Base Features of Nine Egyptian Mummies: Evaluation with High-Resolution CT and Reformation Techniques, 2002, American journal of roentgenology, **178**:1367.

Holme B, Hove BH, Tveit AB, Using white light interferometry to measure etching of dental enamel, 2005, Measurement, **38**:137–147.

Hooper S, Hughes J, Parker D, Finke M, Newcombe RG, Addy M, West N, A clinical study in situ to assess the effect of a food approved polymer on the erosion potential of drinks, 2007, Journal of dentistry, **35**:541-546.

Howland R, Benatar L, A practical guide to scanning probe microscopy, Accessed 9th June, 2011;
http://www.mechmat.caltech.edu/~kaushik/park/contents.htm

Hughes JA, West NX, Addy M, The protective effect of fluoride treatments against enamel erosion in vitro, 2004, Journal of oral rehabilitation, **31**:357-363.

Human Tissue Authority (HTA), Fees and payments, accessed 4th August, 2010; http://www.hta.gov.uk/licensingandinspections/feesandpayments.cfm

Hunter ML, West NX, Hughes JA, Newcombe RG, Addy M, Relative susceptibility of deciduous and permanent dental hard tissues to erosion by a low pH fruit drink in vitro, 2000, Journal of dentistry, **28**:265-270.

Iijima M, Moradian-Oldak J, Control of apatite crystal growth in a fluoride containing amelogenin-rich matrix, 2004, Biomaterials, **26**:1595-1603.

Iijima Y, Takagi O, Ruben J, Arends J; In vitro remineralization of in vivo and in vitro formed enamel lesions; 1999, Caries Research; **33**:206-213.

Imfeld T, Dental erosion: definition, classification and links, 1996a, European journal of oral sciences, **104**:151-155.

Imfeld T, Prevention of progression of dental erosion by professional and individual prophylactic measures, 1996b, European journal of oral sciences, **104**:215-220.

Instron, Vickers test, accessed 23rd May, 2010: http://www.instron.us/wa/applications/test_types/hardness/vickers.aspx

Jaeggi T, Lussi A. Toothbrush abrasion of erosively altered enamel after intraoral exposure to saliva: An in situ study, 1999, Caries research, **33**:455-461.

Jälevik B, Odelius H, Dietz W, Norén JG, Secondary ion mass spectrometry and X-ray microanalysis of hypomineralized enamel in human permanent first molars, 2001, Archives of oral biology, **46**:239-247.

Jandt JD, Atomic force microscopy of biomaterials surfaces and interfaces, 2001, Surface science, **491**:303-332.

Joiner A, Pickles MJ, Tanner C, Weader E, Doyle P, An in situ model to study the toothpaste abrasion of enamel, Journal of clinical periodontology, 2004, **31**:434-438.

Kaneshiro NK, Zieve D, Tooth anatomy, [electronic image], Available from http://www.nlm.nih.gov/medlineplus/ency/imagepages/1121.htm (Accessed 11/04/2011)

Karlinsey RL, Mackey AC, Walker ER, Frederick KE, Fowler C, *In vitro* evaluation of eroded enamel treated with fluoride and a prospective tricalcium phosphate agent, 2009, Journal of dentistry and oral hygiene, **1**:52-58.

Kato MT, Lancia M, Sales-Peres SHC, Buzalaf MAR, Preventive effect of commercial desensitizing toothpastes on bovine enamel erosion *in vitro*, 2010, Caries research, **44**:85-89.

Kim J-Y, Cha Y-G, Cho S-W, Kim E-J, Lee J-M, Cai J, Ohshima H, Jung H-S, Inhibition of apoptosis in early tooth development alters tooth shape and size, 2006, Journal of dental research, **85**:530-535.

Kitchens M, Owens BM, Effect of carbonated beverages, coffee, sports and high energy drinks, and bottled water on the *in vitro* erosion characteristics of dental enamel, 2007, Journal of clinical pediatric dentistry, **31**:153-159.

Kosoric J, Williams RAD, Hector MP, Anderson P, A synthetic peptide based on a natural salivary protein reduces demineralisation in model systems for dental caries and erosion, 2007, International journal of peptide research and therapeutics, **13**:497-503.

Kosoric J, Hector MP, Anderson P, The influence of proteins on demineralization kinetics of hydroxyapatite aggregates, 2010, Journal of biomedical materials research (Part A), **94**:972-977.

Koutsi V, Noonan RG, Horner JA, Simpson MD, Matthews WG, Pashley DH, The effect of dentin depth on the permeability and ultrastructure of primary molars, 1994, Pediatric dentistry, **16**:29-35.

Krutchkoff DJ, Rowe NH, Chemical nature of remineralized flattened enamel surfaces, 1971, Journal of dental research, 50:1621-1627.

Kugel G, Ferrari M, The science of bonding: from first to sixth generation, 2000, Journal of the American dental association, **131** (supp):20S-25S.

Larsen MJ, Dissolution of enamel, 1973, Scandinavian journal of dental research, **81**:518-522.

Larsen MJ, Jensen SJ, The hydroxyapatite solubility product of human dental enamel as a function of pH in the range 4.6-7.6 at 20°C, 1989, Archives of oral biology, **34**:957-961.

Larsen MJ, Pearce EIF, Saturation of human saliva with respect to calcium salts, 2003, Archives of oral biology, **48**:317-322.

Larsen MJ, Nyvad B, Enamel erosion by some soft drinks and orange juices relative to their pH, buffering effect and contents of calcium phosphate, 1999, Caries research, **33**:81-87.

Laurance-Young P, Bozec L, Gracia L, Rees GD, Lippert F, Lynch RJM, Knowles JC, A review of the structure of human and bovine dental hard tissues and their physicochemical behaviour in relation to erosive challenge and remineralisation, 2011, Journal of dentistry, **39**: 266-272.

Lee KH, Kim HI, Kim KH, Kwon YH, Mineral loss from bovine enamel by a 30% hydrogen peroxide solution, 2006, Journal of oral rehabilitation, **33**:229-233.

Lee JJ-W, Kwon J-Y, Chai H, Lucas PW, Thompson VP, Lawn BR, Fracture modes in human teeth, 2009, Journal of dental research, **88**:224-228.

Legeros RZ, Miravite MA, Quirolgico GB, Curzon MEJ, The effect of some trace elements on the lattice parameters of human and synthetic apatites, 1976, Calcified tissue international, **22** (Supp 1):362-367.

Lindén LA, Björkman S, Hattab F, The diffusion in vitro of fluoride and chlorhexidine in the enamel of human deciduous and permanent teeth, 1986, Archives of oral biology, **31**:33-37.

Lippert F, Nanoindentation investigations of demineralisation and remineralisation of human tooth enamel surfaces, 2003, PhD, University of Bristol.

Lippert F, Parker DM, Jandt KD, Susceptibility of deciduous and permanent enamel to dietry acid-induced erosion studied with atomic force microscopy nanoindentation, 2004a, European journal of oral science, **112**:61-66.

Lippert F, Parker DM, Jandt KD, Toothbrush abrasion of surface softened enamel studied with tapping mode AFM and AFM nanoindentation, 2004b, Caries research, **38**:464-472.

Lippert F, Parker DM, Jandt KD, In vitro demineralization/demineralization cycles at human tooth enamel surfaces investigated by AFM and nanoindentation, 2004c, Journal of colloid and interface science, **280**:442-448.

Lussi A, Jaeggi T, Jaeggi-Scharer S, Prediction of the erosive potential of some beverages, 1995, Caries Research, **29**:349–354.

Lussi A, Jaeggi T, Gerber C, Megert B, Effect of amine/sodium fluoride rinsing on toothbrush abrasion of softened enamel *in situ*, 2004, Caries research, **38**:567-571.

Lussi A (editor), Dental Erosion: Monograms in Oral Science, 2006, Karger, **20**:152–172.

Lynch CD, O'Sullivan VR, McGillycuddy CT, Pierre Fauchard: the 'Father of Modern Dentistry', 2006, British dental journal, **201**:779-781.

Madigan MT, Martinko JM, Parker J, Brock Biology of microorganisms 8th Ed., 1997, Prentice Hall International, Inc.

Mantokoudis D, Joss A, Christensen MM, Meng HX, Suvan JE, Lang NP, Comparison of the clinical effects and gingival abrasion aspects of manual and electric toothbrushes, 2001, Journal of clinical periodontology, 289:65-72.

Magalhães AC, Rios D, Delbem ACB, Buzalaf MAR, Machado MAAM, Influence of fluoride dentifrice on brushing abrasion of eroded human enamel: An in situ/ex vivo study, 2003, Caries research, **41**:77-79.

Magalhães AC, Wiegand A, Rios D, Honório HM, Buzalaf MAR, Insights into preventive measures for dental erosion, 2009, Journal of applied oral science, **17**:75-86.

Malcolm D, Paul E, Erosion of the teeth due to sulphuric acid in the battery industry, 1961, British journal of industrial medicine, **18**:63-69.

Margolis HC, Beniash E, Fowler CE, Role of macromolecular assembly of enamel matrix proteins in enamel formation, 2006, Journal of dental research, **85**:775-793.

Margolis HC, Moreno EC, Kinetic and thermodynamic aspects of enamel demineralization, 1985, Caries Research, **19**:22-35.

Marshall AF, Lawless KR, TEM study of the central dark line in enamel crystallites, 1981, Journal of dental research, **60**:1773-1784.

Mason SC, Shirodaria S, Sufi F, Rees GD, Birkhed D, Evaluation of salivary fluoride retention from a new high fluoride mouthrinse, 2010, Journal of dentistry, **38**:S30-S36.

Mazouchi A, Homsy GM, Free surface Stokes flow over topography, 2001, Physics of fluids, **13**:2751-2762.

McCoy G, The etiology of gingival erosion, 1982, Journal of oral implantology, **10**:361–362.

Mehdawi I, Abou Neel EA, Valappil SP, Palmer G, Salih V, Pratten J, Spratt DA, Young AM, Development of remineralizing, antibacterial dental materials, 2009, Acta Biomaterialia, **5**:2525-2539.

Melcher AH, Holowka S, Pharoah M, Lewin PK, Non-invasive computed tomography and three-dimensional reconstruction of the dentition of a 2,800-year-old Egyptian mummy exhibiting extensive oral disease, 1997, American journal of physical anthropology, **103**:329-340.

Mellberg JR, Hard-tissue substrates for evaluation of cariogenic and anti-cariogenic activity in situ, 1992, Journal of dental research, **71**:913-919.

Meller C, Heyduck C, Tranæus S, Splieth C, A new in vivo method for measuring caries activity using quantitative light-induced fluorescence, 2006, Caries research, **40**:90-96.

Meredith N, Sherriff M, Setchell DV, Swanson SAV, Measurement of the microhardness and young's modulus of human enamel and dentine using an indentation technique, 1996, Archives of oral biology, 41: 539-545.

Meurman JH, Frank RM, Scanning electron microscopic study of the effect of salivary pellicle on enamel erosion, 1991, Caries research, **25**:1-6.

Meurman JH, ten Cate JM, Pathogenesis and modifying factors of dental erosion, 1996, European journal of oral sciences, **104**:199-206.

Miletich I, Sharpe PT, Normal and abnormal dental development, 2003, Human molecular genetics, **12**:R69-73.

Millward A, Shaw L, Smith AJ, *In vitro* techniques for erosive lesion formation and examination in dental enamel, 1995, Journal of oral rehabilitation, **22**:37-42.

Misra DN, Interaction of citric acid with hydroxyapatite: Surface exchange of ions and precipitation of calcium citrate, 1996, Journal of dental research, **75**:1418-1425.

Moreno EC, Kresak M, Zahradnik RT, Fluoridated hydroxyapatite solubility and caries formation, 1974, Nature, **247**:64-65.

Morris VJ, Kirby AR, Gunning AP, Atomic force microscopy for biologists, 1999, Imperial College Press.

Moss SJ, Dental erosion, *International dental journal*, 1998, **48**:529-539

Murray JJ, Rugg-Gunn AJ, Jenkins GN, Fluorides in caries prevention, 3rd edition, Wright, 1991

Nanci A, Ten Cate's Oral histology: Development, structure and function, 6th Edition, Mosby publishing, 2003.

Newbrun E, Timberlake P, Pigman W, Changes in microhardness of enamel following treatment with lactate buffer, 1959, *Journal of dental research*, **38**:293-300.

Nishino M, Yamashita S, Aoba T, Okazaki M, Moriwaki Y, The Laser-Raman spectroscopic studies on human enamel and precipitated carbonate-containing apatites, 1981, Journal of dental research, **60**:751-757.

Nekrashevych Y, Hannig M, Stösser L, Assessment of enamel erosion and protective effect of salivary pellicle by surface roughness analysis and scanning electron microscopy, 2004, Oral health & preventative dentistry, **2**:5-11.

Nelson DGA, Jongebloed WL, Arends J, Crystallographic structure of enamel surfaces treated with topical fluoride Agents: TEM and XRD considerations, 1984, Journal of dental research, **63**:6-12.

Norén JG, Lodding A, Odelius H, Linde H, Secondary ion mass spectrometry of human deciduous enamel. Distribution of Na, K, Mg, Sr, F and Cl., 1983, Caries Research, **17**:496-502.

Øgaard B, Fjeld M, The enamel surface and bonding in orthodontics, 2010, Seminars in Orthodontics, **16**:37-48.

Orellana MF, Nelson AE, Carey JPR, Heo G, Boychuk DG, Surface analysis of etched molar enamel by gas adsorption, 2008, Journal of dental research, **87**:532-536.

Padmanabhan SK, Balakrishnan A, Chu M-C, Kim TN, Cho SJ; Micro-indentation fracture behavior of human enamel; 2009; Dental materials; **26**:100-104.

Paice EM, Vowles RW, West NX, Hooper SM, The erosive effects of saliva following chewing gum on enamel and dentine: an *ex vivo* study, 2011, British dental journal, **210** (E3):1-5.

Parkinson CR, Shahzadand A, Rees GD, Initial stages of enamel erosion: An *in situ* atomic force microscopy study, 2010, Journal of structural biology, **171**:298-302.

Patel PR, Brown WR, Thermodynamic solubility product of human tooth enamel: Powdered sample, 1975, Journal of dental research, **54**:728-736.

Poole DFG, Johnson NW, The effects of different demineralizing agents on human enamel surfaces studied by scanning electron microscopy, 1967, Archives of oral biology, **12**:1621-1632.

Powers N, Archaeological evidence for dental innovation: an eighteenth century porcelain dental prosthesis belonging to Archbishop Arthur Richard Dillon, 2006, British dental journal, **201**:459-463.

Pretty IA, Edgar WM, Higham SM, The validation of quantitative light-induced fluorescence to quantify acid erosion of human enamel; 2004; Archives of oral biology, **49**: 285-94.

Pretty IA, Caries detection and diagnosis: novel technologies, 2006, Journal of dentistry, **34**:727-739.

Preston KP, Higham SM, Smith PW, The efficacy of techniques for the disinfection of artificial sub-surface dentinal caries lesions and their effect on demineralization and remineralization in vitro, 2007, Journal of dentistry, **35**:490-495.

Radlanski RJ, Renz H, Willersinn U, Cordis CA, Duschner H, Outline and arrangement of enamel rods in human deciduous and permanent enamel. 3D-reconstructions obtained from CLSM and SEM images based on serial ground sections, 2001, European journal of oral science, **109**:409-414.

Randall D, Burggren W, French K (editors), Eckert Animal Physiology: Mechanisms and adaptations, 4th Ed, 2000, Freeman publishing.

Rees JS, The biomechanics of abfraction, Proceedings of the institution of mechanical engineers, 2006, Part H: Journal of engineering in medicine, **220**:69-80.

Reis AF, Giannini M, Kavaguchi A, Soares CJ, Line SR, Comparison of microtensile bond strength to enamel and dentin of human, bovine, and porcine teeth, 2004, Journal of adhesive dentistry, **6**:117-121.

Rey, C, Shimizu M, Collins B, Glimcher MJ, Spectroscopy study of the environment of phosphate ion in the early deposits of a solid phase of calcium phosphate in bone and enamel and their evolution, 1991, Calcified tissue international, **49**:383-388.

Risnes S, Growth tracks in dental enamel, 1997, Journal of human evolution, **35**:331-350.

Rios D, Honório HM, Magalhães AC, da Silva SMB, Delbem ACB, de Andrade Moreira Machado MA, Buzalaf MAR, Scanning electron microscopic study of the *in situ* effect of salivary stimulation on erosion and abrasion in human and bovine enamel, 2007, Brazilian oral research, **22**:132-138.

Rios D, Magalhães AC, Polo ROB, Weigand A, Attin T, Buzalaf MAR, The efficacy of a highly concentrated fluoride dentifrice on bovine enamel subjected to erosion and abrasion, 2008, Journal of the American dental association, **139**:1652-1656.

Robinson C, Brookes SJ, Shore RC, Kirkham J, The developing enamel matrix: nature and function, 1998, European journal of oral science, **106**(Supp):282-291.

Robinson C, Connell S, Kirkham J, Brookes SJ, Shore RC, Smith A, The effect of fluoride on the developing tooth, 2004, Caries research, **38**:268–276.

Rodriguez JM, Curtis RV, Bartlett DW, Surface roughness of impression materials and dental stones scanned by non-contacting laser profilometry, 2009, Dental materials, **25**:500-505.

Rugg-Gunn AJ, Maguire A, Gordon PH, McCabe JF, Stephenson G, Comparison of erosion of dental enamel by four drinks using an intra-oral appliance, 1998, Caries research, **32**:337–343.

Sato Y, Sato T, Niwa M, Aoki H, Precipitation of octacalcium phosphates on artificial enamel in artificial saliva, 2006, Journal of material science: materials in medicine, **17**:1173-1177.

Sanches RP, Otani C, Damião AJ, Miyakawa W, AFM characterisation of bovine enamel and dentine after acid etching, 2009, Micron, **40**:502-506.

Sasaki LH, Lobo PDC, Moriyama Y, Watanabe I-S, Villaverde AB, Tanaka CS-I, Moriyama EH, Brugnera A, Tensile bond strength and SEM analysis of enamel etched with Er:YAG laser and phosphoric acid: a comparative study in vitro, 2008, Brazilian dental journal, **19**:57-61.

Schilke R, Lisson JA, Bauβ O, Geurtsen W, Comparison of the number and diameter of dentinal tubules in human and bovine dentine by scanning electron microscopic investigation, 2000, Archives of oral biology, **45**:355-361.

Schlueter N Ganss C, De Sanctis S, Klimek J, Evaluation of a profilometrical method for monitoring erosive tooth wear, 2005, European journal of oral science, **113**:505-511.

Sela M, Gedalia I, Shah L, Skobe Z, Kashket S, Lewinstein I, Enamel rehardening with cheese in irradiated patient, 1994, American journal of dentistry, **7**:134-136.

Seligman DA, Pullinger AJ, Solberg WK, The prevalence of dental attrition and its association with factors of age, gender, occlusion, and TMJ symptomatology, 1988, Journal of dental research, **67**:1323-1333.

Shellis RP, Relationship between human enamel structure and the formation of caries-like lesions in vitro, 1984, Archives of oral biology, **29**:975-981.

Shellis RP, Wahab FK, Heywood BR, The hydroxyapatite ion activity product in acid solutions equilibrated with human enamel at 37 degrees C, 1993, Caries research, **27**:365-372.

Shellis RP, Finke M, Eisenburger M, Parker DM, Addy M, Relationship between enamel erosion and liquid flow rate, 2005, European journal of oral science, **113**: 232–238.

Sijbers J, Postnov A, Reduction of ring artifacts in high resolution microCT reconstructs, 2004, Physics in medicine & biology, **49**:N247-N253.

Simmelink JW, Nygaard VK, Scott DB, Theory for the sequence of human and rat enamel dissolution by acid and by EDTA: A correlated scanning and transmission electron microscope study, 1974, Archives of oral biology, **19**:183-197.

Skobe Z, SEM evidence that one ameloblast secretes one keyhole-shaped enamel rod in monkey teeth, 2006, European journal of oral science, **114**:338–342.

Smith CE, Cellular and chemical events during enamel maturation, 1998, Critical reviews in oral biology and medicine, **9**:128-161.

Smith CE, Nanci A, Overview of morphological changes in enamel organ cells associated with major events in amelogenesis, 1995, International journal of developmental biology, **39**:153-161.

Smith G, Smith AJ, Shaw L, Shaw MJ, Artificial saliva substitutes and mineral dissolution, 2001, Journal of oral rehabilitation, **28**:728-731.

Spielman AI, The Birth of the Most Important 18th Century Dental Text: Pierre Fauchard's *Le Chirurgien Dentist*, 2007, Journal of dental research, **86**:922-926.

Spitzer D, Ten Bosch JJ, The total luminescence of bovine and human dental enamel, 1976, Calcified tissue research, **20**:201-208.

Standring S (editor), Gray's anatomy: the anatomical basis of clinical practice 39th Ed, 2005.

Stenhagen KR, Hove LH, Holme B, Taxt-Lamolle S, Tveit AB, Comparing different methods to assess erosive lesion depths and progression *in vitro*, 2010, Caries research, **44**:555-561.

Stookey GK, Optical methods-quantitative light fluorescence, 2004, Journal of dental research, **83**:C84-C88.

Suckling GW, Developmental defects of enamel - Historical and present-day perspectives of their pathogenesis, 1989, Advances in dental research, **3**:87-94.

Sydney-Zax M, Mayer I, Deutsch D, Carbonate content in developing human and bovine enamel, 1991, Journal of dental research, **70**:913-916.

Tang R, Orme CA, Nancollas GH, A new understanding of demineralization: The dynamics of brushite dissolution, 2003, The journal of physical chemistry B, **107**:10653–10657.

Taras HL, Frankowski BL, McGrath JW, Mears CJ, Murray RD, Young TL, Soft drinks in schools – policy statement, Committee on school health, 2004, Pediatrics, **113**:152-154.

ten Cate AR, The experimental investigation of odontogenesis, 1995, International journal of developmental biology, **39**:5-11.

ten Cate JM, Current concepts on the theories of the mechanism of action of fluoride, 1999, Acta Odontologica Scandinavia, **57**:329-329.

Thuy TT, Nakagaki H, Kato K, Hung PA, Inukai J, Tsuboi S, Nakagaki H, Hirose MN, Igarashi S, Robinson C, Effect of strontium in combination with fluoride on enamel remineralisation in vitro, 2008, Archives of oral biology, **53**:1017-1022.

Tolstikhina AL, Gaĭnutdinov RV, Zanaveskin ML, Sorokina KL, Belugina NV, Grishchenko Yu.V, Particular artefacts of topographic images of dielectrics in atomic-force microscopy, 2007, Crystallography Reports, **52**:925-931.

Van Houte J, Role of micro-organisms in caries etiology, 1994, Journal of dental research, **73**:672-681.

van Nieuw Amerongen A, Bolscher JGM, Veerman ECI, Salivary proteins: Protective and diagnostic values in cariology, 2004, Caries research, **38**:247-253.

Venasakulchai A, Williams NA, Gracia LH, Rees GD, A comparative evaluation of fluoridated and non-fluoridated mouthrinses using a 5-day cycling enamel erosion model, 2010, Journal of dentistry **38**:S21–S29.

Viera A, Lugtenborg M, Ruben JL, Huysmans MCDNMJ, Brushing abrasion of eroded bovine enamel pretreated with topical fluorides, 2006, Caries research, **40**:224-230.

Voegel JC, Garnier P, Biological apatite crystal dissolution, 1979, Journal of dental research, **58**(B):852-856.

Walker JC, Zaugg SE, Walker EB, Analysis of beverages by capillary electrophoresis, 1997, Journal of chromatography, **781**:481-485.

Wang LJ, Tang R, Bonstein T, Bush P, Nancollas GH, Enamel demineralization in primary and permanent teeth, 2006, Journal of dental research, **85**:359-363.

Wang L, Nancollas GH, Calcium orthophosphates: crystallization and dissolution, 2008, Chemical reviews, **108**:4628-4669.

Wang L, Nancollas GH, Pathways to biomineralization and biodemineralization of calcium phosphates: the thermodynamic and kinetic controls, 2009, Dalton transactions. **15**:2665-2672.

West NX, Hughes JA, Addy M, Erosion of dentine and enamel in vitro by dietary acids: the effect of temperature, acid character, concentration and exposure time, 2000, Journal of Oral Rehabilitation **27**, 875-880.

West NX, Maxwell A, Hughes JA, Parker DM, Newcombe RG, Addy M, A method to measure clinical erosion: the effect of orange juice consumption on erosion of enamel, 1998, Journal of dentistry, **26**:329-335.

West NX, Hughes JA, Parker D, Weaver LJ, Moohan M, De'Ath J, Addy M, Modification of soft drinks with xanthan gum to minimise erosion: a study *in situ*, 2004, British Dental Journal **196**: 478 – 481.

Wegehaupt F, Gries D, Wiegand A, Attin A, Is bovine dentine an appropriate substitute for human dentine in erosion/abrasion tests?, 2008, Journal of oral rehabilitation, **35**:390-394.

Wetton S, Hughes J, West N, Addy M, Exposure time of enamel and dentine to saliva for protection against erosion: A study *in vitro*, 2006, Caries research, **40**:213–217.

White W, Nancollas GH, Quantitative study of enamel dissolution under conditions of controlled hydrodynamics, 1977, Journal of dental research, **56**:524-30.

White AJ, Yorath C, Ten Hengel V, Leary SD, Huysmans MDNJM, Barbour ME, Human and bovine enamel erosion under 'single-drink' conditions, 2010, European journal of oral sciences, **118**:604-609.

Wiegand A, Begic M, Attin T, In vitro evaluation of abrasion of eroded enamel by different manual, power and sonic toothbrushes, 2006, Caries research, **40**:60-65.

Wiegand A, Stock A, Attin R, Werner C, Attin T, Impact of the acid flow rate on dentin erosion, 2007, Journal of dentistry, **35**:21-27.

Wong L, Cutress TW, Duncan JF, The influence of incorporated and adsorbed fluoride on the dissolution of powdered and pelletized hydroxyapatite in fluoridated and non-fluoridated acid buffers, 1987, Journal of dental research, **66**:1735-1741.

Wu W, Nancollas GH, The dissolution and growth of sparingly soluble inorganic salts: A kinetics and surface energy approach, 1998, Pure & applied chemistry, **70**:1867-1872.

Wyant JC, White Light Interferometry, 2010, accessed 25th November, 2010, http://www.optics.arizona.edu/jcwyant/pdf/meeting_papers/whitelightinterferometry.pdf

Xue J, Li W, Swain MV, In vitro demineralization of human enamel natural and abraded surfaces: A micromechanical and SEM investigation, 2009, Journal of dentistry, **37**:264-272.

Yoshida Y, Van Meerbeek B, Nakayama Y, Yoshioka M, Snauwaert J, Abe Y, Lambrechts P, Vanherle G, Okazaki M, Adhesion to and decalcification of hydroxyapatite by carboxylic acids, 2001, Journal of dental research, **80**:1565-1569.

Zero DT, Etiology of dental erosion – extrinsic factors, 1996, European journal of oral science, **104**:162-177.

Zhang XZ, Anderson P, Dowker SEP, Elliott JC, Optical profilometric study of changes in surface roughness of enamel during in vitro demineralisation, 2000, Caries research, **34**:164-17.

Zheng J, Xiao F, Zheng L, Qian LM, Zhou ZR, Erosion behaviors of human tooth enamel at different depth, 2010, Tribology international, , **43**:1262-1267.

Zipkin I, McClure FJ, Salivary citrate and dental erosion, 1949, Journal of dental research, **28**:613–626.

APPENDIX A – PATIENT SUPPLEMENTARY CONSENT FORM

Supplementary consent

I hereby consent to allow my dental specimen(s) to be stored as part of a tissue bank used exclusively for biomedical research purposes at the Eastman Dental Institute, 256 Gray's Inn Road, London.

This research will focus on characterising human (and bovine) dental structures and be conducted anonymously and in accordance with Health Professions Council and UCL ethics guidelines. At the end of the research all specimens pertaining to this work will be destroyed.

To be filled in by the patient:

Name (please print)……

Date of Birth……..

Date:…… Signature:……..

To be filled in by the clinician:

Name: ……..

Location:……..

APPENDIX B- WORK SUBMITTED FOR PUBLICATION OR PRESENTED AT CONFERENCES

Published papers:

"Laurance-Young P, Bozec L, Gracia L, Rees GD, Lippert F, Lynch RJM, Knowles JC, A review of the structure of human and bovine dental hard tissues and their physicochemical behaviour in relation to erosive challenge and remineralisation, 2011, Journal of dentistry, **39**: 266-272."

Titles of posters presented:

"Biphasic model of the mechanical properties of softened enamel" – SPM 2010.

"Behaviour of enamel following a short duration acid exposure" – IADR 2010.

Titles of presentations:

"Comparative morphology and behaviour of enamel: Bovine vs. Human." – GSK Science symposium 2010.

APPENDIX C – EXAMPLES OF RAW DATA

1. Optical profilometry

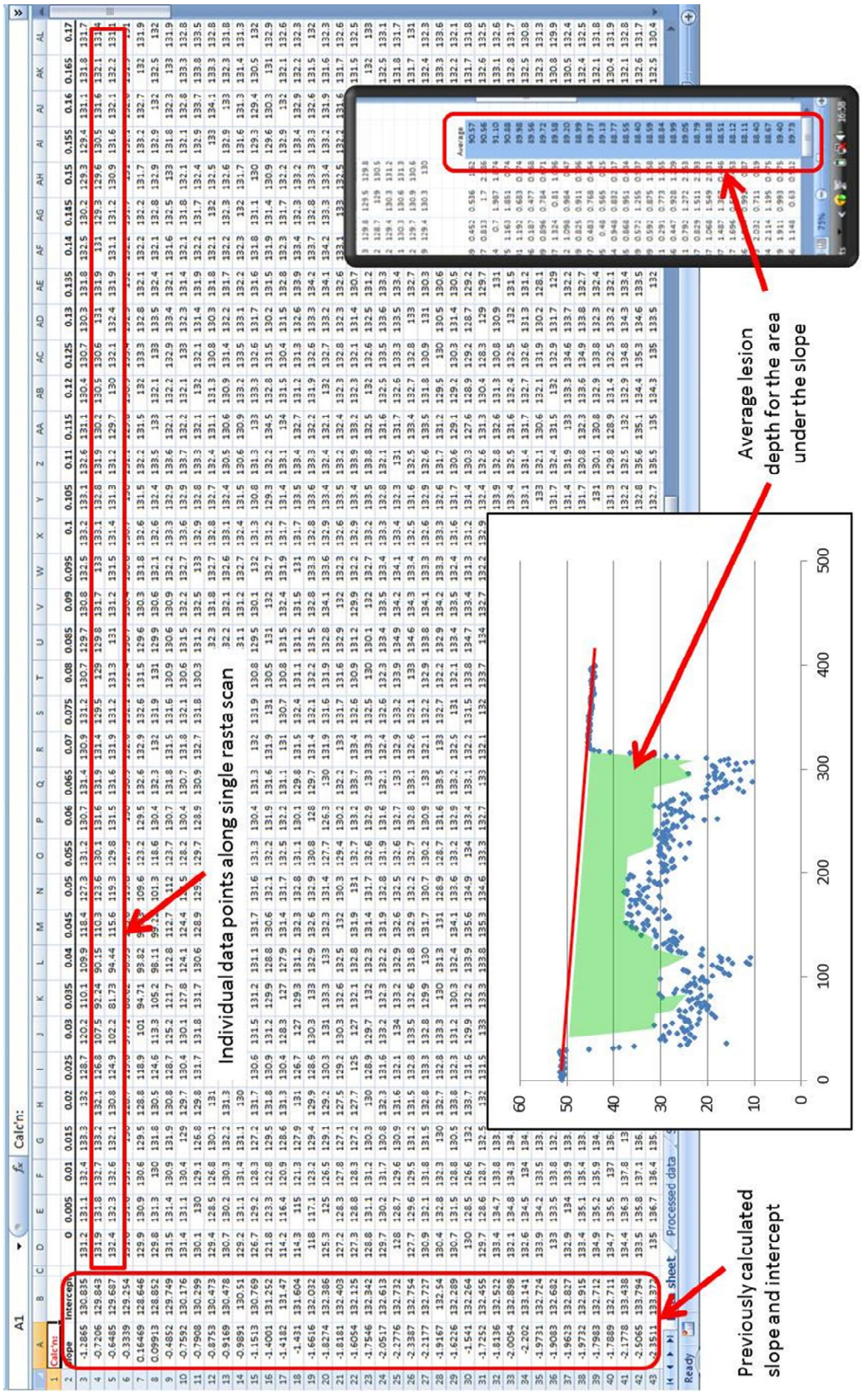

2. White light interferometry

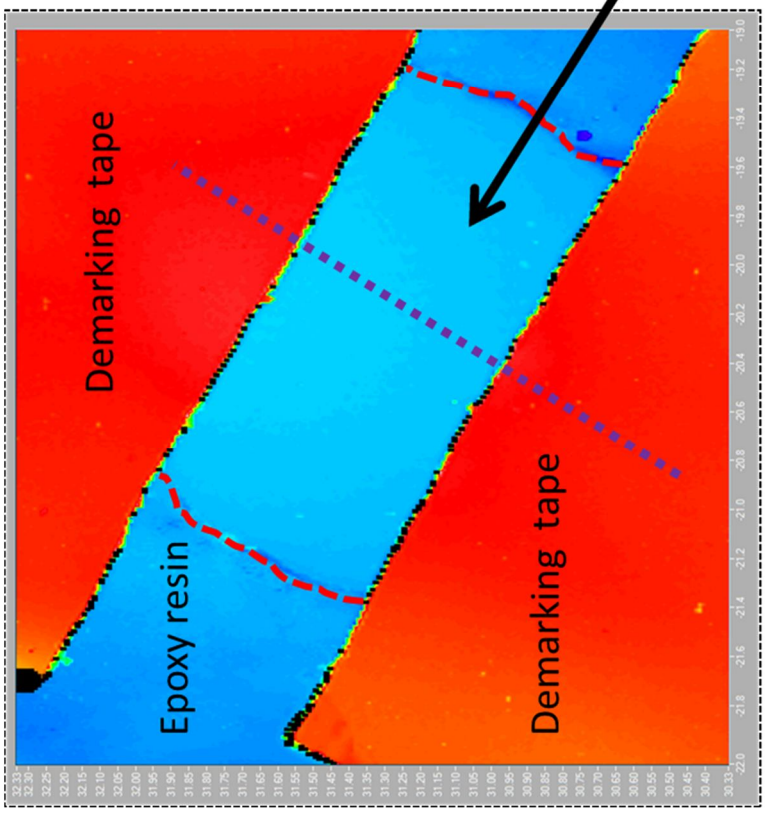

Line trace through erosion window and demarking tape, shown below.

Enamel window

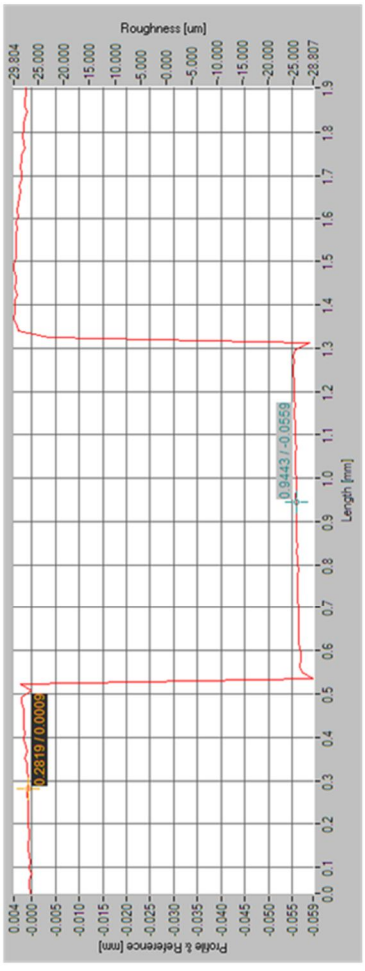

Line trace through erosion window and demarking tape as shown above

APPENDIX D – SUMMARY OF GALIL & WRIGHT, 1979 CLASSIFICATION

Type 1	Honeycomb appearance of eroded enamel resulting from dissolution of the central core.
Type 2	Multiple rounded protrution, appearance of cobblestones, resulting from the dissolution of the enamel prism periphery
Type 3	Poor coherence, a mixture of Type 1 and Type 2
Type 4	Pitting of the enamel surface, with random ingrained patterens respembling an irregular meshwork
Type 5	Unaffected surface, flat and smooth

Galil & Wright, 1979

APPENDIX E - ADDITIONAL EVALUATION TECHNIQUES

This appendix provides the results of experimental techniques attempted during this work but which, for various reasons, produced unsuitable data. The discussion at the end of this section explores reasons why this may be the case but it should be emphasised that these techniques remain in experimental use.

ION CHROMATOGRAPHY

Ion chromatography employs the electrical properties of ions to distinguish one from another, in the case of this work, calcium ion (Ca^{2+}) concentration was investigated. The ion chromatograph, a Dionex ICS-1000, uses four phases within the 25 µm sample loop to separate individual ions for characterisation: the eluent delivery, separation of individual ions, suppression of the eluent charge and detection of residual ions.

The eluent consisted of 20 mM methanesulfonic acid (Fluka, UK), which carried the sample fluid through the ion chromatograph and aided in ion separation. The sample itself was injected using an auto sampler, pumped into a 4x250 mm Ion Pac CS12A separation column (consisting of resin-materials inside an inert tube) which separated the sample into its constituent ions. Ion exchange occurred at specific sites on the separation column and, as the sample (plus eluent) flowed though the suppressor, the conductivity of the eluent would be suppressed while the sample

detection was enhanced. This was measured by means of a detection cell, the detection signal being based on the chemical and physical properties of the sample.

Prior to sample analysis, the ion chromatograph was calibrated from a stock solution of calcium chloride (BDH, UK) serially diluted to concentrations of 100, 50; 12.5; 6.25 and 3.12 ppm. As the separation column was sensitive to phosphate ions the sample fluids were run through an OnGuard IIA cartridge (Dionex, UK) to remove this species from the solution. These were changed for every sample. Computer software (Chromeleon) compares the data from the sample against the defined calibration samples. Specific ions are identified by their retention time in the column and quantified automatically.

VICKERS MICROHARDNESS

Eight specimens of human and bovine enamel were each employed for the time durations within this protocol. The time durations were in accordance with those used in section 2.7.1. Following the acid exposure for each sample it was loaded into a Vickers microhardness machine (Wallace, UK - Figure E-1) and the indenter applied under a 4.5 N load.

Figure E-1: The Vickers micro-indenter employed to determine the effects of acid erosion on human and bovine enamel.

7-10 indentation readings were made for each sample, for both the erosion lesion area and the control areas. The total results analysed using Origin statistical software. Owing to the results later described in chapters 3 and 4, which appeared to show superficial and subsurface nanostructural changes, Vickers indentation was replaced with the more sensitive and better resolution imaging technique of Atomic Force Microscopy, which also minimised damage to the superficial structures.

MICRO-COMPUTED TOMOGRAPHY

The micro-computed tomography work employed a Skyscan 1072 (Skyscan, Kontich, Belguim) capable of resolving to 4 μm. The epoxy resin embedded samples (n= 3) were loaded into the scanning chamber using adhesive putty attached to a stub and illuminated using a 50 kV x-ray source with aluminium filter and captured using a planar x-ray detector. Sequential 2-dimensional images were taken as the sample was rotated through 360° at 0.45° increments, and reconstructed from the image stack to provide a 3-dimensional image using automated software.

EFFECT OF ACIDS ON MATERIAL HARDNESS

The figure below (Figure E-2) shows the results of a preliminary study using eight samples of bovine enamel and Vickers indentation to determine the effects of 600 seconds erosion by 1 mol.L^{-1} of acetic, citric and phosphoric acid:

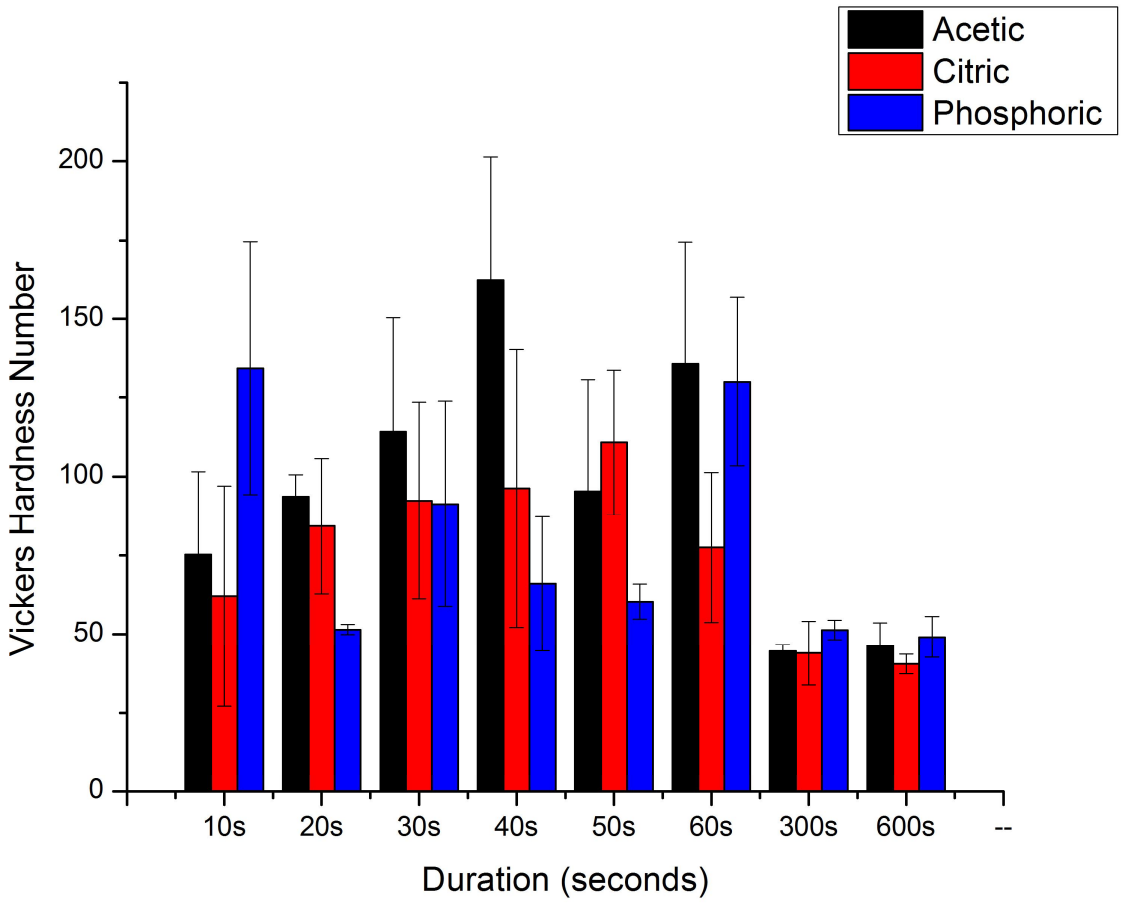

Figure E-2: Graph showing the median Vickers hardness for samples of bovine enamel eroded using 1 mol.L^{-1} acetic, citric and phosphoric acids.

The median Vickers hardness of the control enamel was 51.80 (57.00 Q1-Q3). The median Vickers hardness of the samples at 10 seconds was 83.60 (42.20 Q1-Q3) for acetic acid, 70.65 (55.40 Q1-Q3) for citric acid and 140.9 (50.2 Q1-Q3) for phosphoric acid. Following 60 seconds erosion the median hardness number was 136.10 (54.00 Q1-Q3) for acetic acid, 99.00 (50.10 Q1-Q3) for citric acid and 124.60 (43.60 Q1-Q3) for phosphoric acid. Acetic acid eroded samples at 60 seconds were significantly different from those at 10 seconds ($p = 0.03$). Citric and phosphoric acid eroded samples eroded for 60 were not significantly different from those eroded after 10 seconds.

At 300 seconds erosion the hardness value was 45.00 (1.00 Q1-Q3) for acetic acid, 39.00 (7.00 Q1-Q3) for citric acid and 51.00 (3.00 Q1-Q3) for phosphoric acid. At 600 seconds erosion the hardness value was 43.50 (13.00 Q1-Q3) for acetic acid, 41.00 (3.00 Q1-Q3) for citric acid and 50.00 (3.00 Q1-Q3) for phosphoric acid.

Samples from all acids at the 60 second erosion duration were significantly harder than the than their counterparts following 300 seconds duration ($p = 0.001$), analysed using Kruskall-Wallis ANOVA. There was a significant difference in the hardness of acetic acid eroded enamel at 10 seconds and 600 seconds ($p = 0.02$) but no significant difference was apparent between 10 seconds erosion and 600 seconds erosion for citric ($p = 0.20$) and phosphoric acids ($p = 0.83$), which is most likely a result of the data error attributed to sample variation.

In order to confirm the findings of a potential biphasic trend we undertook a trial study investigating the calcium ion loss from samples of human and bovine enamel into solution during a 0.05% phosphoric acid challenge. The initial results were indeterminate, most likely as the ion chromatography machine lacked the necessary sensitivity. As such, the standard variation within the three datasets limited interpretation of the results. An example of this is provided below (Figure E-3):

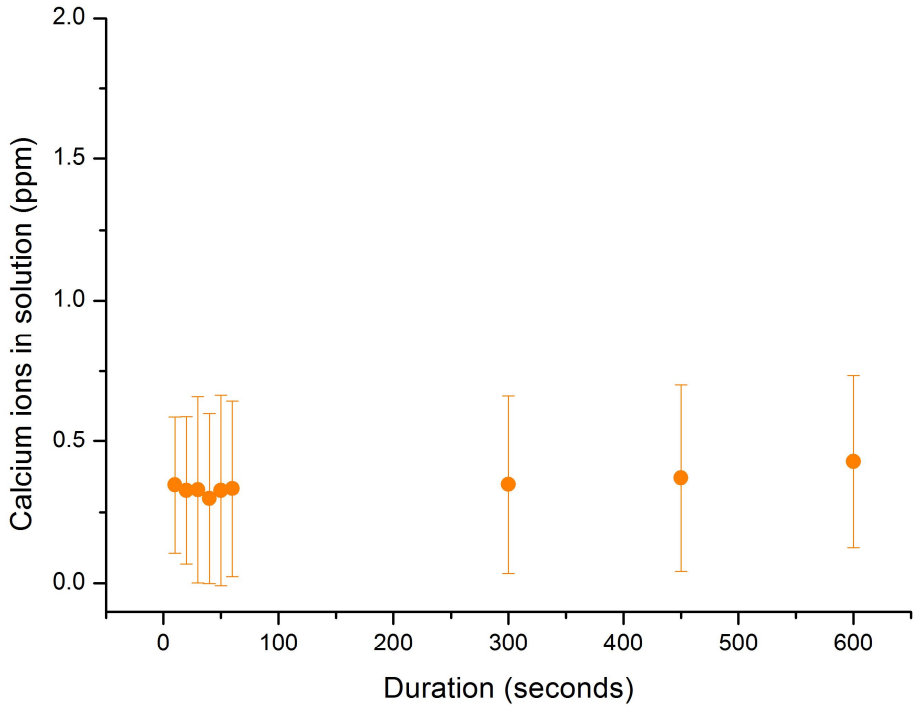

Figure E-3: Results of calcium ion loss into solution (ppm) from human enamel sample exposed to 0.05% phosphoric acid.

Examination of the data showed variation in the quantity of calcium ions in solution, including decreasing quantities of ions in solution from the previous result,

followed by an increase in the quantity of ions in the following result. Such a pattern was not consistent with continual increasing quantity of calcium ions resulting from a single sample undergoing repeated acid exposure.

Of the three samples from each category (human and bovine enamel) only one sample from each showed any pattern of progression consistent with a gradual release of calcium ions into an acid solution. This data is presented in Figure E-4.

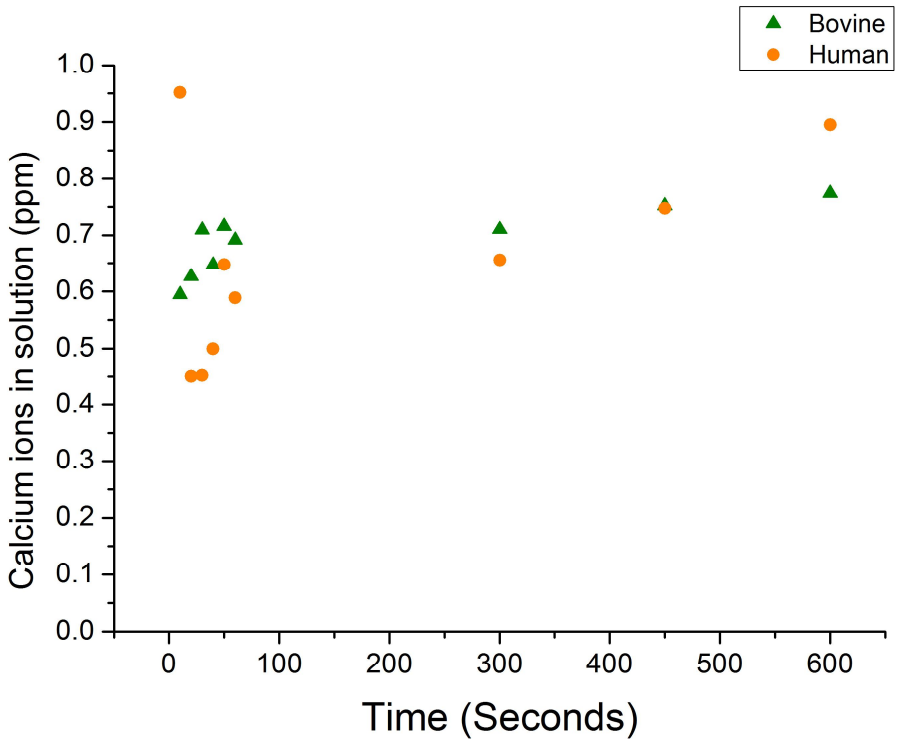

Figure E-4: Graph to show the loss of calcium ions into solution (ppm) from a single sample of human and bovine enamel following a cumulative 600 second erosion challenge using 0.05% phosphoric acid.

After 10 seconds 0.59 ppm Ca^{2+} were released into the acid solution from bovine enamel compared to 0.95 ppm Ca^{2+} for the human sample. However, by 20 seconds the human sample's free Ca^{2+} had fallen to 0.45 ppm, a possible indication of superficial surface contamination as later results did not show any evidence of this high concentration of calcium. These results then increased to 0.69 ppm Ca^{2+} for the bovine

sample after 60 seconds and 0.58 ppm Ca^{2+} for the human sample. By 300 seconds the amount of free Ca^{2+} in solution was 0.71 ppm Ca^{2+} for bovine and 0.66 ppm Ca^{2+} for human. At the end of the protocol bovine enamel had lost 0.77 ppm Ca^{2+} to the solvent and human enamel had lost 0.89 ppm Ca^{2+}.

Applying a division similar to that of the optical profilometry data to facilitate the rate calculation showed early stage erosion (10-60 seconds) bovine enamel lost Ca^{2+} ions to the solution at a rate of 1.97×10^{-3} ppm ($\pm 8.61 \times 10^{-4}$) while human enamel had a rate of 4.74×10^{-3} ppm ($\pm 16.6 \times 10^{-4}$). By contrast, later durations (60-600 seconds) showed results of 1.59×10^{-4} ppm ($\pm 2.76 \times 10^{-5}$) for bovine enamel and 5.51×10^{-4} ppm ($\pm 1.17 \times 10^{-4}$) for human enamel.

Although this technique showed promise, the lack of sensitivity at the low concentrations employed for this work severely restricted its use. This will be discussed in the next section.

ANALYSIS OF TECHNIQUES USED IN THE EXPERIMENTAL DEVELOPMENT

This subsection provides information regarding some of the techniques which did not provide suitable results. Despite the fact that these results did not form part of the final experimental protocols, they provided an insight into problems which occurred when attempting to obtain data, such as at low concentrations of acid or when attempting to investigate subsurface erosion events. The failure of Vickers indentation for example, prompted the adoption of an AFM-based strategy. Each technique and the limitations thereof will be examined in closer detail below.

SURFACE INDENTATION

The early work in Chapter 3 established a detectable erosion lesion was present at early durations of acid exposure and identified a potential biphasic trend in bulk tissue loss. A requirement was identified to examine the hardness of this softened surface in relation to uneroded material. Material hardness is a common method of measuring the effects of acid on enamel erosion, with the Vickers method being one of the most commonly employed (Attin *et al*, 1996, West *et al*, 1998, Devlin *et al*, 2006). The work described in section 0 was inconclusive and found no significant difference in the microhardness of samples after 600 seconds erosion. In addition to this, the results obtained from our control hardness studies - 51.80 (57.00 Q1-Q3) Vickers Hardness Number - do not correspond with values found in the literature, which average between 214.7 (±2.7) and 306.16 (±5.26) Vickers Hardness Number (Karlinsey *et al*, 1999; Attin *et al*, 1996). Attin *et al* (1996) reported Vickers Hardness Numbers of 272.5 (±8.6) VHN

at the 60 second mark using a commercial beverage as acid reagent compared to 136.10 (54.00 Q1-Q3) for acetic acid, 99.00 (50.10 Q1-Q3) for citric acid and 124.60 (43.60 Q1-Q3) VHN for phosphoric acid at 60 seconds in section 0. After 300 seconds Attin *et al* (1996) reported 256.6 (±9.4) VHN compared to 45.00 (1.00 Q1-Q3) for acetic acid, 39.00 (7.00 Q1-Q3) for citric acid and 51.00 (3.00 Q1-Q3) VHN for phosphoric acid in section 3.3.

The results obtained for section 7.1 may be attributed to an inappropriate load – 4.5N mass - obtained from the literature (Newbrun *et al*, 1959) or incorrect positioning of the indenter, an operation which had to be performed by eye, in which the indenter could unintentionally overlap the eroded area and the control shoulder. However, neither of these methods would result in the anomalous readings observed in section 0.

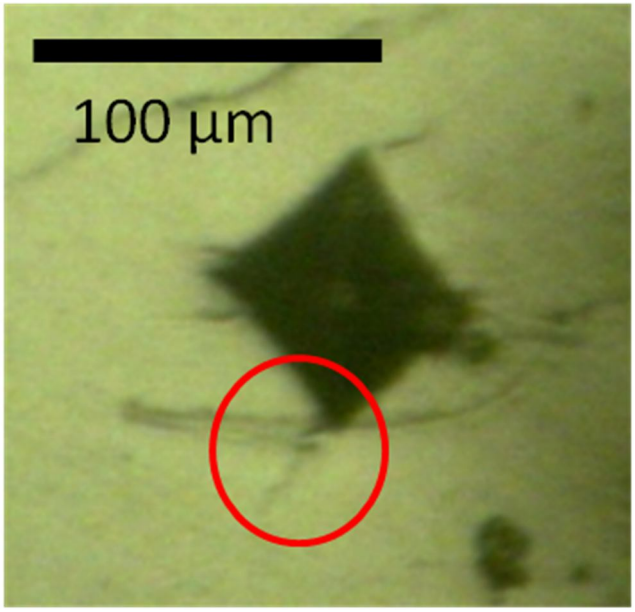

Figure E-5: Surface indentation in uneroded bovine control surface showing evidence of cracking at the pyramidal apex of the indentation (an example of which is highlighted in red).

Conclusions may be drawn from Figure , a photographic image of the indentation in uneroded control enamel. Palmqvist cracking, cracking of the sample originating at

the corners of the indent, is visible at all the apical edges. This suggests the load applied through the indenter is excessive although the directionality of enamel rods is also known to play a role in crack propagation and morphology (Lee *et al*, 2009; Padmanabhan *et al*, 2009). A possible hypothesis to explain the lack of any significant enamel softening following the early duration erosion is that the indenter penetrates through the softened surface layer and into the less acid-affected, therefore harder, layer beyond. However, given the observations in section 3.4 regarding a possible biphasic trend of erosion related to subsurface softening, it is further hypothesised that this softened subsurface will be considerably thinner - potentially in the region of 200+ nm - than would be readily detectable using a Vickers indenter. An alternative technique for measuring such a small anticipated changes in material hardness using controlled loads, and one which was adopted, is atomic force microscopy. This technique is capable of detecting not only material stiffness *via* Young's modulus but also of quantifying the depth of a softened area without the need to take numerous individual transverse pyramidal measurements from indentations using photomicrographs.

CALCIUM ION LOSS INTO SOLUTION

The preliminary ion chromatography results for enamel erosion using phosphoric acid appeared to substantiate the hypothesis regarding a biphasic trend of bulk mineral loss present between the early (10-60 second) and later (60-600 second) acid exposure. The cumulative quantity of calcium ions in solution showed an initial rapid trend of increasing bulk tissue loss up to one minute. Following this the rate of

tissue loss begins to decline although mineral continues to be lost into solution. There was some fluctuation in the results, most notably for the first exposure using a human sample. As the ion chromatography values are tending towards the limit of sensitivity of this method this also means that the technique is consequently extremely sensitive to contamination. This observation would potentially explain the anomalous results obtained for the sample repeats, resulting in a number of failures of this technique to investigate early calcium ion loss. Furthermore, this is the most likely explanation for the erroneous result seen at the start of the data presented in section 0, given the cumulative nature of the work and subsequent lower readings, none of which were in the region of this initial result. Overall however, the rate for this chromatography data showed the initial loss of calcium between 10-60 seconds to be an order of magnitude greater than that of the later durations, whether the enamel was bovine or human in origin.

Looking at a graphical depiction shown in Figure , optical profilometry rate and ion chromatography data, it is possible to see that a biphasic trend of erosion is present more often than not and as explained previously, where this trend is absent, the absence may be explained by intrasample variability.

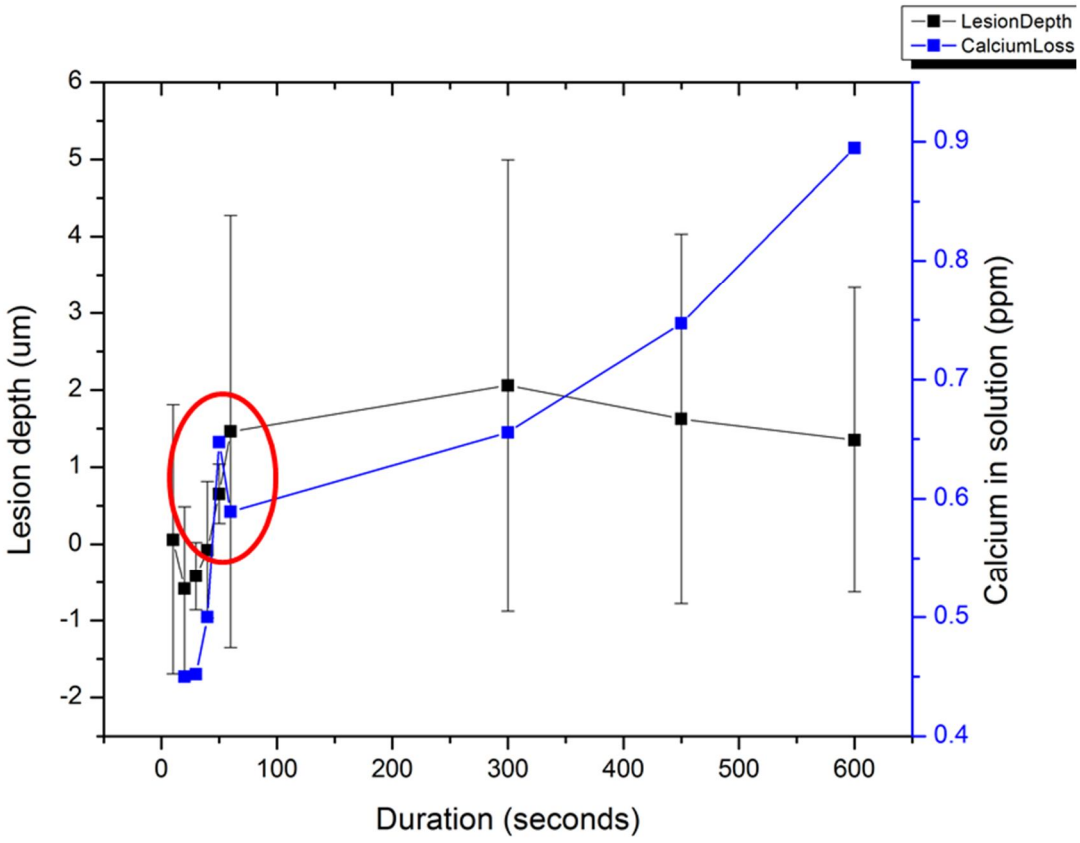

Figure E-6: Dual plot of optical profilometry and ion chromatography of Human enamel eroded with 0.05 % phosphoric acid solution for a cumulative total of 600 seconds. The encircled area represents a point at which there is a changeover between rate kinetics.

It should be reiterated that this technique was at the limit of its capacity to resolve the concentration of calcium in solution. Additional chemical tests may prove or refute these findings, however this is something to be undertaken in the future.

IMAGING THE EROSION LESION SUBSURFACE

µCT provided valuable information regarding the shape of the erosion lesion in section 4.3. However, the resolution was insufficient to do more than construct bulk 3D images. Individual serial slices, which make up the 3D construct, were unsuitable owing to the prevalence of ring artefact as illustrated below:

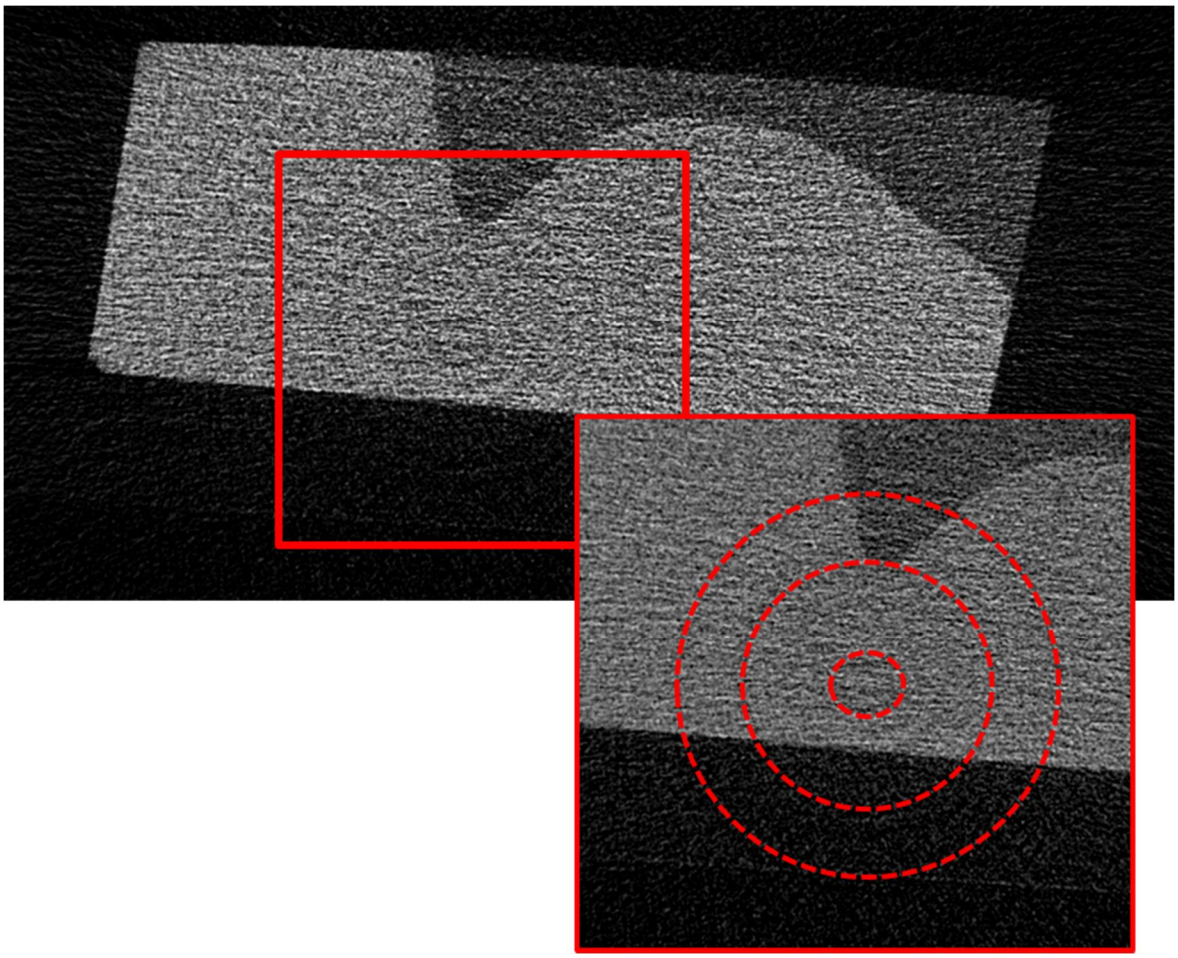

Figure E-7: Ring artefact present in serial section of human molar eroded with 0.05 % phosphoric acid for 600 seconds.

The above image shows a cross section through a human molar crown with ring artefact visible as concentric circles radiating out from the centre of the image, most likely a result of the heat variation from the epoxy resin. The ring artefact is caused by elements such as a gain error at a specific point in the image, beam hardening effects or uneven temperature fluctuations and makes quantitative analysis impossible as well as hampering any reconstructive processing such as noise reduction (Sijbers & Postnov, 2004). During the course of our work it was necessary to use a much higher voltage in order to obtain the required resolution (89kV, 112vA – any lower energy and the

resolution was affected), which had the negative effect of detrimentally overheating the epoxy resin.

Ring artefact is usually compensated for by using flat-field correction. This process is achieved by performing a scan with no sample present in the x-ray beam thereby effectively neutralising any background data using correctional software. However, correcting the artefact can result in loss of resolution which, when viewing at the maximum resolution, does not permit for accurate results. An alternative to 3D reconstruction was to simply view individual sections using confocal microscopy.

To close this chapter, it should again be re-iterated that although the results from these techniques were not suitable for this work, they remain a source of obtaining experimental data in dental studies to this day. The most probable reason for the unsuitability of these results had to do with the dimensions of the enamel erosion lesion ultrastructure, chemistry or the exploration of subsurface softening. All of these measurements were obtained at the limits or in excess of the machine capability. As such, for experiments involving greater erosion criteria (e.g.: a more prolonged erosion protocol), these techniques remain valid.